

Studies of EBV Infection of B Lymphocytes ex Vivo and in Vitro

by

Emily Heath

A thesis submitted to
The University of Birmingham
for the degree of
Doctor of Philosophy

CRUK School of Cancer Sciences
College of Medical and Dental Sciences
University of Birmingham
December 2010

UNIVERSITY OF
BIRMINGHAM

University of Birmingham Research Archive

e-theses repository

This unpublished thesis/dissertation is copyright of the author and/or third parties. The intellectual property rights of the author or third parties in respect of this work are as defined by The Copyright Designs and Patents Act 1988 or as modified by any successor legislation.

Any use made of information contained in this thesis/dissertation must be in accordance with that legislation and must be properly acknowledged. Further distribution or reproduction in any format is prohibited without the permission of the copyright holder.

Abstract

EBV is a lymphotropic herpesvirus that establishes lifelong persistence in the memory B cell compartment of the human host. It is still unclear, however, whether the virus infects memory B cells directly, or first targets naive B cells, driving them to differentiate into memory B cells via germinal centre (GC) transit. Using *ex vivo* analysis of sorted B cell subsets, we have found that whilst EBV preferentially colonises isotype-switched memory B cells, the virus was excluded from tonsillar GC B cells. Furthermore we found substantial viral loads in non-switched memory B cell populations, whose origins are likely to be germinal centre-independent. Using *in vitro* infection experiments, we showed that enzymes AID, UNG and pol- η , which are associated with the GC processes somatic hypermutation (SHM) and class switch recombination (CSR) were upregulated in EBV-infected B cells. Indeed following *in vitro* transformation, SHM of immunoglobulin (Ig) genes was induced in a proportion naive B cells. Whilst these cells did not undergo CSR following EBV infection alone, additional cytokine stimulation together with CD40L was able to induce isotype switching. EBV infection *in vitro* together with the provision of appropriate signals was therefore able to induce genotypic and phenotypic memory B cell characteristics in naive B cells, in a non-GC environment. Taken together our findings suggest that GC transit is not an essential requirement for EBV colonisation of the memory B cell population.

Acknowledgments

I would like to thank my supervisors Dr Andrew Bell and Professor Martin Rowe for their sustained support and encouragement throughout this study. I would also like to thank Professor Alan Rickinson as his enthusiasm and supervision contributed greatly to the project. In addition I extend my gratitude to all members of the B cell group, in particular Debbie Croom-Carter for her extensive help with IgH sequencing, Dr Claire Shannon-Lowe for her help with *in vitro* infection experiments, Dr Sridhar Chaganti who guided me during the initial weeks of the PhD and Dr Christopher Fox for supplying me with tonsillar B cells. Thanks are also due to Wendy Thomas, who advised me during flow cytometry analysis and Roger Bird for his help with FACS sorting, and Laine Wallace and Dr Jonathan James, who were always helpful regarding the plasmid to profile sequencing facility. Other people I wish to thank include Dr David Lissauer for supplying fresh cord blood, Dr Martina Vockerodt for supplying fresh tonsillar UMs and Dr Dieter Kube who kindly carried out CDR3 spectratype analysis on a selection of DNA samples. Finally I would like to thank Cancer Research UK for their sponsorship.

Table of Contents

1	INTRODUCTION	1
1.1	Introduction to Epstein Barr Virus	1
1.1.1	EBV is a Member of the Herpesvirus Family.....	2
1.1.2	EBV Subtypes	4
1.1.3	EBV Genome	5
1.1.4	Alternative Forms of EBV Latent Infection	6
1.1.5	EBV Lytic Infection	17
1.2	B cell Development	18
1.2.1	Antibody Structure.....	20
1.2.2	B cell Receptor	21
1.2.3	Organisation of Immunoglobulin Genes.....	22
1.2.4	B cell Maturation.....	23
1.2.5	T cell-Dependent B cell Activation.....	27
1.2.6	T cell-Independent (TI) B cell Activation.....	32
1.2.7	Non-Switched Memory B cells	33
1.2.8	Activation-Induced Cytidine Deaminase (AID)	38
1.3	EBV Colonisation in Vivo	40
1.3.1	Primary Infection	40
1.3.2	Establishment of Persistent Infection	42
1.3.3	Persistent Infection.....	47
1.4	Immune Response to EBV Infection	49
1.4.1	Antibody Response against EBV Infection.....	49
1.4.2	Cell-Mediated Responses to EBV Infection	50

1.5	EBV-Associated Diseases	52
1.5.1	Infectious Mononucleosis	52
1.5.2	X-Linked Lymphoproliferative Disease	54
1.5.3	Post-Transplant Lymphoproliferative Disease.....	55
1.5.4	Hodgkin's Lymphoma.....	57
1.5.5	Burkitt's Lymphoma.....	60
1.6	Aims of Current Work	63
2	MATERIALS AND METHODS	65
2.1	Standard Cell Culture	65
2.2	Biological Samples	65
2.3	Isolation of Blood B cell Subsets	67
2.3.1	Isolation of Peripheral Blood Mononuclear cells (PBMCs)	67
2.3.2	Isolation of B cells from PBMCs	67
2.3.3	FACS Sorting of Healthy Adult B Cell Subsets	69
2.4	Isolation of Tonsillar B cell Subsets	71
2.4.1	Isolation of B Cells by CD3-Depletion of Tonsillar UMs	71
2.4.2	FACS Sorting of Tonsillar B cell Subsets	72
2.5	Isolation of Lymphocytes from Umbilical Cord Blood	73
2.6	B cell Transformation	73
2.6.1	Preparation of B95.8 Virus Supernatant.....	73
2.6.2	Establishment of Bulk LCLs from Purified B cells	74
2.6.3	Establishment of Limiting Dilution LCL Cultures from Naive Peripheral Blood B cells	75

2.6.4	Establishment of Bulk LCLs from Purified Cord Blood Lymphocytes	75
2.7	Transformation Assays	76
2.8	Generation of CD40 Blasts	77
2.9	Induction of Lytic Replication in AKBM cells	78
2.10	Induction of Ig Isotype Switching	78
2.11	Analysis of Ig Phenotype by Flow Cytometry	78
2.12	Analysis of IgVH Genotype	79
2.12.1	DNA Extraction	79
2.12.2	IgH PCR	79
2.12.3	Identification and Recovery of the PCR Product	80
2.12.4	Cloning the IgH PCR Product.....	82
2.12.5	Preparation of Competent Cells	84
2.12.6	Sequencing IgH Products.....	85
2.12.7	Analysis of IgH Sequences	85
2.13	Taqman qPCR to Estimate EBV DNA Load	86
2.13.1	Introduction.....	86
2.13.2	Preparation of Namalwa Standards	87
2.13.3	Setting up qPCR Reactions.....	88
2.13.4	qPCR Data Analysis.....	89
2.13.5	Limiting Dilution EBV POL qPCR Assays	89

2.14	Taqman qPCR to Measure AID Transcripts	91
2.14.1	Conventional RT-PCR to amplify AID Transcripts in Akata-BL.....	92
2.14.2	Sequencing of AID variant transcripts	93
2.14.3	AID Variant qPCR primer design.....	94
2.14.4	AID Variant Plasmid Standards.....	94
2.14.5	AID variant qPCR Assays	96
2.15	Taqman qPCR to Measure UNG and Polη Transcripts	96
3	<i>EX VIVO</i> STUDIES OF EBV COLONISATION WITHIN	
	DISTINCT B CELL SUBSETS	98
3.1	Isolation of Peripheral Blood B cell Subsets	98
3.2	Isolation of Tonsillar B cell Populations	99
3.3	Total EBV Genome Load in B cell Populations	100
3.3.1	Healthy Carrier Peripheral Blood B cell Populations.....	100
3.3.2	Healthy Carrier Tonsillar B cell Populations	101
3.3.3	Infectious Mononucleosis Tonsillar B cell Populations	102
3.4	Frequency of EBV-Infected cells	103
3.4.1	Validation of the Limiting Dilution Method Using Namalwa-BL Cell Line.....	103
3.4.2	Frequency of Infected Cells in Peripheral Blood B cell Subsets Derived from Healthy Carrier Donors.....	104
3.4.3	Frequency of Infected Cells in <i>Ex Vivo</i> IM Tonsillar B cells	105
3.4.4	Genome Copies in Lytic and Latent AKBM Cells	106
3.5	Discussion	107
3.5.1	EBV Colonisation of Non-Switched Memory B cells	108

3.5.2	EBV Colonisation of Germinal Centre B cells.....	111
3.5.3	Frequency of EBV-Infected Cells and Genome Copies in Individual Cells .	114

4 EBV INFECTION OF B CELL SUBSETS *IN VITRO*: EFFECTS ON IGH GENOTYPE AND CELLULAR PHENOTYPE **118**

4.1 Isolation of Peripheral Blood B cell Subsets **120**

4.2 Establishment and Analysis of EBV-Infected Naive LCLs and CD40L/IL-4 B Blasts **120**

4.2.1 Experimental Outline..... 120

4.2.2 IgH Analysis of Bulk Naive CD40 Blasts 122

4.2.3 IgH Analysis of Bulk Naive LCL1..... 124

4.2.4 IgH Analysis of Bulk CD40 Blast and Bulk LCL Cultures Established from a Single Donor 125

4.2.5 Detailed Studies of Clonal Evolution in Three LCLs Established from a Single Donor 128

4.2.6 Analysis of IgH Mutations in Bulk LCLs and LCLs Established by Limiting Dilution..... 134

4.2.7 Phenotype of Naive LCLs 138

4.3 Transformation Assays Comparing EBV Infection of Peripheral Blood B cell Subsets **140**

4.4 Tonsillar Naïve B Cell Transformation **141**

4.4.1 Phenotype of the Bulk Tonsillar Naive LCL 143

4.5 Umbilical Cord B cell Transformation **143**

4.5.1 Bulk Cord Blood LCL1 144

4.7	AID Variant Expression in Peripheral Blood B cell Cultures	147
4.7.1	Validation of AID qPCR Assays	148
4.7.2	AID Upregulation in Peripheral Blood B cells Following EBV Infection <i>in Vitro</i>	148
4.7.3	AID Expression in Tonsillar B cells.....	149
4.7.4	AID expression in Naive LCLs and CD40 blasts	149
4.7.5	Expression of SHM molecules Polymerase- η and Uracil DNA Glycosylase	150
4.8	Discussion	151
4.8.1	EBV Infection of Naive B cells Induces IgH Mutations <i>in Vitro</i>	151
4.8.2	AID is Upregulated Following EBV Infection <i>in Vitro</i>	154
4.8.3	SHM was detected in BN-LCLs but not BN-blasts	156
4.8.4	EBV Infection does not Induce Isotype-Switching in Vitro.....	161
4.8.5	LCLs are Characterised by Outgrowth of Dominant Clones.....	162
5	CONCLUSIONS AND FUTURE WORK.....	166
6	REFERENCES	169

Appendix

follows page 221

List of Figures

<i>Figure</i>	<i>follows page</i>
Figure 1. Structure of the Herpesvirus	2
Figure 2. Schematic diagram of the EBV genome	5
Figure 3. Patterns of EBV latent gene expression in different forms of latency	6
Figure 4. Structure of an antibody molecule.....	20
Figure 5. B cell receptor complex.....	21
Figure 6. Ig gene rearrangement.....	22
Figure 7. B cell maturation in the bone marrow.....	23
Figure 8. T-dependent B cell activation and differentiation	27
Figure 9. Class switch recombination.....	30
Figure 10. functional domains of AID isoforms.....	38
Figure 11. Selective colonisation of the memory B cell compartment during primary EBV infection.....	43
Figure 12 - Taqman primers and probes targetting in AID variant qPCRs	94
Figure 13. CD20 staining of CD19-selected peripheral blood B cells.....	99
Figure 14. Isolation of peripheral blood B cell subsets	99
Figure 15. Isolation of tonsillar B cell subsets	100
Figure 16. EBV load distribution in PB B cell subsets	101
Figure 17. EBV load distribution in healthy carrier tonsil B cell subsets	101
Figure 18. EBV load distribution in IM tonsil B cell subsets.....	102
Figure 19. Validation of limiting dilution analysis using the Namalwa-BL cell line	103

Figure 20. EBV distribution in sorted peripheral blood B cell populations from healthy carriers.....	104
Figure 21. EBV genome copies in individual GFP+ and GFP- AKBM cells...	107
Figure 22. Generation of bulk naive CD40 blasts and LCLs	121
Figure 23. Examples of mutated and unmutated IgH sequences.....	121
Figure 24. BN-LCL1 family 1 germline sequences were detected at 6, 9 and 12 weeks.....	125
Figure 25. BN-LCL1-family 1 related and unrelated mutations	125
Figure 26. CDR3 spectratyping analysis of BN-blast 3 and BN-LCL3.....	126
Figure 27. BN-LCL3 family 4.....	128
Figure 28. BN-LCL3 family 5.....	128
Figure 29. Establishment of three separate LCLs from one donor (BN-LCL4a, b and c)	128
Figure 30. CDR3 spectratyping analysis of BN-LCL4b	130
Figure 31. BN-LCL4a family 2 tree.....	133
Figure 32. BN-LCL4a family 2 branch 1	133
Figure 33. BN-LCL4a family 2 branch 2	133
Figure 34. BN-LCL4a family 2 branch 3	133
Figure 35. BN-LCL4b family 3 tree.....	134
Figure 36. BN-LCL4b family 3 alignment	134
Figure 37. Establishment of limiting dilution naive LCL clones and bulk naive LCLs from one donor	135
Figure 38. Naive LCL5 limiting dilution culture 23 (CN-LCL3/c23)	137
Figure 39. Phenotypic analysis of BN-LCL3 and BN-LCL5	139
Figure 40. Phenotypic analysis of two representative CN-LCL5 cultures.....	139

Figure 41. transformation assays comparing EBV-transformation in naive B cells to non-switched B cells from five separate peripheral blood donors	141
Figure 42. BTN-LCL1-family 2 mutation distribution.....	142
Figure 43. percentage of mutated and unmutated clonal families in BTN-LCLs over time	142
Figure 44. BTN-LCL1 phenotype	143
Figure 45. BN-LCL treated with CD40L, IL-4 and IL-21	146
Figure 46. AID plasmid standards	148
Figure 47. AID upregulation in PB B cells following EBV infection or CD40L/IL-4 stimulation	148
Figure 48. AID expression in tonsillar B cells	149
Figure 49. AID expression in established naive LCLs and CD40 blasts.....	149
Figure 50. Pol-η and UNG expression in established LCLs and CD40 blasts	150
Figure 51. Frequency of mutations in resting B cell populations	152
Figure 52. High numbers of mutations in naive LCL cultures accumulate in AID hotspots	155
Figure 53. Mutation frequencies in PB BN-blast and BN-LCL cultures over time	156
Figure 54. Proposed models of EBV colonisation of the memory B cell reservoir	166

List of Tables

<i>Table</i>	<i>follows page</i>
Table 1. List of antibodies used to isolate B cell subsets and for phenoytpe analysis	70
Table 2. AID-FL, AID- Δ E4 and AID- Δ E3E4 Taqman assay primers	94
Table 3. Summary of peripheral blood FACS-sorted B cell populations for virus load assays	99
Table 4. Summary of FACS-sorted tonsillar B cell populations for virus load assays.....	100
Table 5. EBV load distribution in peripheral blood B cell subsets.....	100
Table 6. EBV load in tonsillar B cell subsets	101
Table 7. EBV distribution in sorted peripheral blood B cell populations from healthy carriers.....	104
Table 8. Frequency of infected cells in unfractionated B cells derived from 4 IM tonsils.....	106
Table 9. EBV genome copies in individual GFP+ and GFP- AKBM cells	106
Table 10. Summary of peripheral blood FACS–sorted B cell populations used in in vitro experiments	120
Table 11. BN-blast 1	122
Table 12. BN-blast 2	122
Table 13. BN-LCL1	124
Table 14. Resting naive B cells used for BN-blast 3 and BN-LCL3.....	126
Table 15. BN-blast3	126
Table 16. BN-LCL3	126

Table 17. Two week IgH data from BN-LCL4a, b and c	129
Table 18. BN-LCL4a	129
Table 19. BN-LCL 4b	130
Table 20. BN-LCL 4c.....	131
Table 21. BN-LCL5	135
Table 22. Naive LCL5 limiting dilution cultures.....	136
Table 23. BN-LCL6	137
Table 24. Naive LCL6 limiting dilution cultures.....	137
Table 25. Summary of Ig phenotypes of PB bulk naive LCLs	139
Table 26. Summary of limiting dilution culture phenotypes	139
Table 27. BTN-LCL1	142
Table 28. BCB-LCL1	144
Table 29. BCB-LCL2.....	144
Table 30. Summary of isotype-switching experiments.....	146

Abbreviations

Ab-MLV	Abelson murine leukemia virus
AID	activation-induced cytidine deaminase
AIDS	acquired immunodeficiency syndrome
Ab	antibody
β2M	beta-2-microglobulin
BCR	B cell receptor
BL	Burkitt's lymphoma
BN-LCL	bulk naive LCL
BCB-LCL	bulk cord blood LCL
Bp	base pair
BTN-LCL	bulk tonsillar naive LCL
C	constant region
CD40L	CD40 ligand
cDNA	complementary deoxyribonucleic acid
CDR	complementarity determining region
CN-LCL	clonal naive LCL
CSR	class-switch recombination
D	diversity region
DNA	deoxyribonucleic acid
DSB	double-stranded breaks
EA	early antigen
EBER	EBV encoded RNA
EBNA	EBV nuclear antigen
EBNA-LP	EBNA leader protein
EBV	Epstein Barr virus
FACS	fluorescence activated cell sorter
FCS	foetal calf serum
FISH	fluorescent in situ hybridisation

FITC	fluorescein isothiocyanate
FR	framework region
GAPDH	glyceraldehydes 3-phosphate dehydrogenase
GC	germinal centre
GFP	green fluorescent protein
Gln	glutamine
HCV	hepatitis C virus
HL	Hodgkin's lymphoma
HIV	human immunodeficiency virus
HRS	Hodgkin and Reed-Sternberg
IE	immediate early
Ig	immunoglobulin
IgH	Ig heavy chain
IL-4	interleukin 4
IL-21	interleukin 21
IM	infectious mononucleosis
IPTG	isopropyl- β -D-thiogalactoside
ITAM	immunoreceptor tyrosine-based activation motif
J	joining region
JNK	cJun N-terminal kinase
KSHV	Kaposi's sarcoma-associated herpesvirus
kbp	kilobase pair
L	leader protein
LCL	lymphoblastoid cell line
LCV	lymphocryptovirus
LMP	latent membrane protein
MAPK	mitogen-activated protein kinase
MgCl ₂	magnesium chloride
MHC	major histocompatibility complex

MOI	multiplicity of infection
mRNA	messenger RNA
N	naive
NF- κ B	nuclear factor kappa B
NK	natural killer
N-LCL	naive LCL
NPC	nasopharyngeal carcinoma
NSM	non-switched memory
OriP	origin of plasmid replication
PAMP	pattern-associated molecular pattern
PB	peripheral blood
PBMC	peripheral blood mononuclear cells
PBS	phosphate buffered saline
PCR	polymerase chain reaction
pol	EBV DNA polymerase
Pol η	polymerase eta
PS	pencillin and streptomycin
PTK	protein tyrosine kinase
PTL	post-transplant lymphoproliferation
PTLD	post-transplant lymphoproliferative disease
RAG	recombination-activating gene
RF-LCL	rheumatoid factor-producing lymphoblastoid cell line
RNA	ribonucleic acid
R-PE	R-phycoerythrin
rpm	rotations per minute
RPMI	Roswell Park Memorial Institute
RT	reverse transcription
RT-PCR	reverse transcription polymerase chain reaction
SAP	SLAM-associated protein

SHM	somatic hypermutation
SLAM	Signaling lymphocytic activation molecule
SM	switched memory
S region	switch region
TA	transformation assay
TEMED	N,N,N',N',-tetramethylenediamine
TNF	tumour necrosis factor
TRADD	TNF receptor-associated death domain
TRAFs	TNF receptor associated factors
Trp	Tryptophan
UM	unfractionated mononuclear
UNG	uracil-N-glycosylase
V	variable region
VCA	viral capsid antigen
VDJ	variable-diversity-joining
X-Gal	5-bromo-4-chloro-3-indoyl- β -D-galactoside
XLA	X-linked agammaglobulinemia
XLP	X-linked lymphoproliferative disease

1 Introduction

1.1 Introduction to Epstein Barr Virus

Epstein Barr virus (EBV) is a gamma subfamily member of the herpes virus family. Within the human host population, infection with EBV is widespread, with >90% of individuals carrying the virus. EBV is a lymphotropic virus, targeting B cells for colonisation, whereby it has the capacity to establish latent infection and persist within the host indefinitely. As is the case with typical herpes viruses, the life cycle of EBV can be broadly divided into two stages; the dormant or latent stage of infection characterised by downregulation of most viral genes, and a reactivation or lytic stage which enables the production of new infectious virus and is required to maintain B cell infection within the host, and spread within the host population (Rickinson and Kieff, 2007, White and Fenner, 1994).

Infectious virus is manufactured and released within the oropharynx, and is spread through saliva. In the developing world, most infants acquire subclinical EBV infections via interactions with family members. Conversely, in developed countries it is often the case that such contact is delayed until adolescence when amorous encounters lead to contraction of the virus. In such instances infection may manifest as the self-limiting lymphoproliferative disease, infectious mononucleosis (IM), otherwise known as glandular fever (Rickinson and Kieff, 2007, White and Fenner, 1994).

Although in most instances EBV is a harmless passenger within the host, the virus is associated with a number of diseases in addition to IM. When infection is left unchecked by the immune response in immunosuppressed individuals, severe lymphoproliferative diseases can ensue which may prove fatal.

Furthermore, EBV is associated with a number of malignancies, the most notorious of which are Burkitt's lymphoma, Hodgkin's lymphoma, and nasopharyngeal carcinoma (Rowe et al., 2009, Kuppers, 2009, Kapatai and Murray, 2007, Shah and Young, 2009).

1.1.1 EBV is a Member of the Herpesvirus Family

Although EBV is classified as a unique virus species with individual properties, it is ultimately a member of the *Herpesviridae* family, sharing many characteristics with other family members, and therefore it is important to consider the virus within this setting (White and Fenner, 1994, Davis-Poynter and Farrell, 1996, Davison et al., 2009).

The name of this virus family *herpes* derives from the Greek word meaning "creeping". All herpes viruses have the capacity to persist within their hosts indefinitely. Most vertebrate species examined have been found to support at least one species of herpes virus which has co-evolved with its host for millennia. Additionally, different subfamilies can co-exist within a single host non-competitively since each occupies a distinct ecological niche (cell type). Structurally, the virion consists of several concentric layers (Figure 1). The double-stranded (ds) DNA genome is at the centre of the particle, and is associated with a protein core. This inner core is surrounded by an icosohedral capsid of approximately 100nm in diameter. The capsid is encased in an

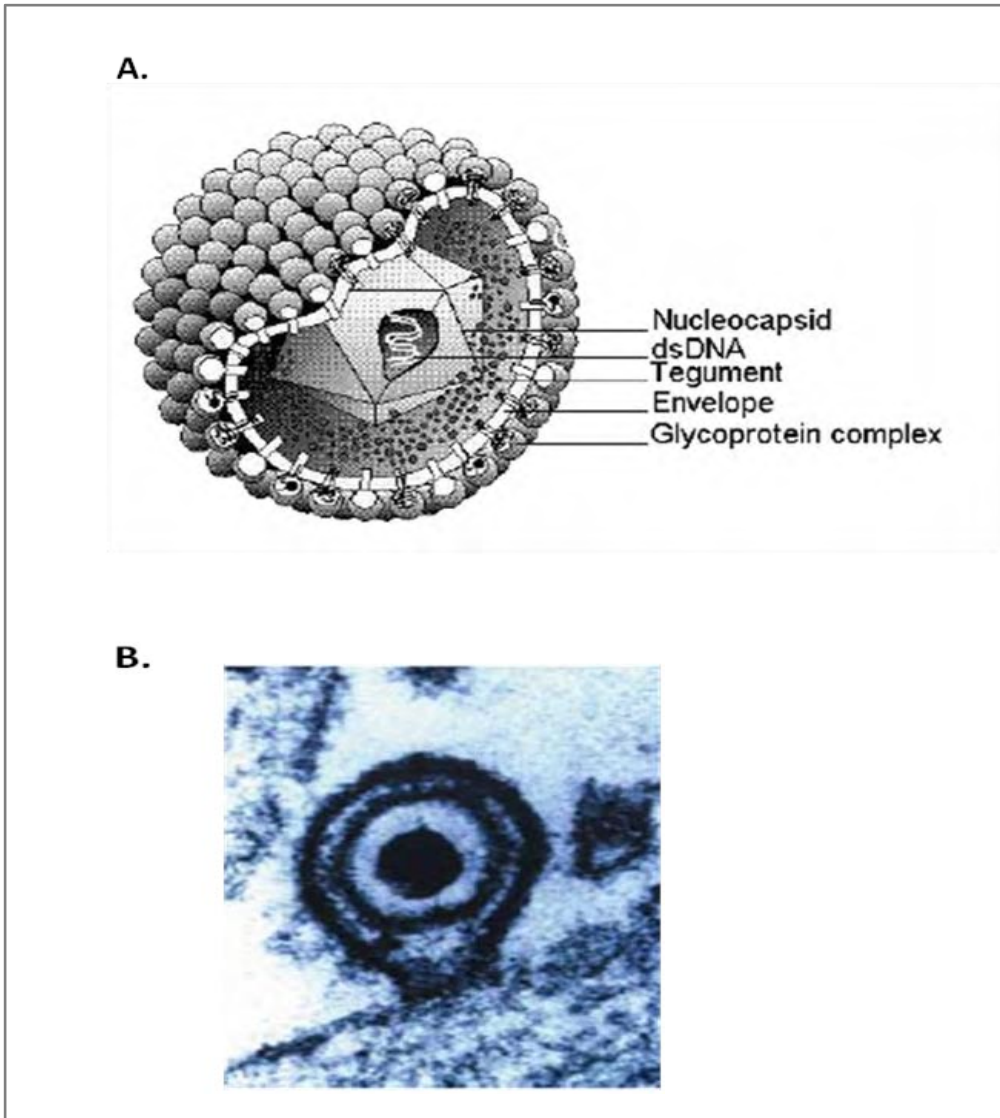


Figure 1. Structure of the Herpesvirus

A. Schematic representation of the composition and structure of a typical herpesvirus.

Taken from The Big Picture Book of Viruses

(http://www.virology.net/Big_Virology/BVDNAherpes.html). **B.** Electron micrograph of the EBV virion. Taken from Young and Rickinson, 2004.

amorphous tegument composed of globular material, and an outer lipoprotein envelope, which is obtained via budding through the nuclear envelope of the host cell. The virion ranges from 120-200nm, but is typically around 150nm in diameter (White and Fenner, 1994, Davison et al., 2009).

Latent genomes persist within the virus-specific target cell (typically neurons or lymphocytes) until reactivation triggers lytic replication, usually within the process of continuous virus shedding or due to a disruption in the host immunity. Reactivation of herpes viruses are almost always seen in cases of severe immunosuppression, for example in AIDS patients. Viral replication takes place in the cell nucleus and usually involves sequential expression of immediate early (IE), early (E) and late (L) genes, the earlier of which regulate transcription of the later genes (White and Fenner, 1994).

The herpesvirus family is subdivided into three subfamilies based on biological properties, *Alphaherpesvirinae*, *Betaherpesvirinae* and *Gammaherpesvirinae*. The *Alphaherpesvirinae* includes herpes simplex virus types 1 and 2, and Varicella-Zoster Virus, which persist latently within sensory nerve ganglia. The *Betaherpesvirinae* includes cytomegalovirus and human herpesvirus 6, whose infection produces characteristic large, multinucleate cells (cytomeglia), and which establish latency in lymphoreticular tissue. Finally, the *Gammaherpesvirinae* include Kaposi's sarcoma-associated herpesvirus (KSHV), and EBV, which is the only human member of the genus *Lymphocryptovirus* (LCV). Non-human LCVs, however, are known to infect both old world primates such as chimpanzees, gorillas and orang-utans, and new world primates such as black spider monkeys, black-pencilled marmosets and common marmosets. Gammaherpesviruses are distinguished from other

herpesvirus members by their ability to establish persistence in lymphoid cells (White and Fenner, 1994, Ehlers et al., 2010).

1.1.2 EBV Subtypes

EBV is divided into two subtypes; type 1 and type 2, distinguishable by allelic polymorphisms within the latent antigen genes EBNA2, 3A, 3B and 3C (Dambaugh et al., 1984, Sample et al., 1990). Within types 1 and 2, numerous further strains are identifiable predominantly by small sequence variations within latent genes EBNA1, EBNA2 and LMP1 (Aitken et al., 1994, Habeshaw et al., 1999, Miller et al., 1994, Schuster et al., 1996, Sung et al., 1998, Wraitham et al., 1995).

In order to study the prevalence of different types and strains within the human population, both *in vitro* and *ex vivo* techniques have been employed; the results of which have led to conflicting conclusions regarding the number of strains present within individuals. *In vitro* assays generating LCLs from throat washings have suggested that within European populations, individual immunocompetent hosts have a tendency to carry a single dominant strain, which in 90% of cases is type 1 (Gratama et al., 1994, Yao et al., 1991). By contrast, examination of viral DNA sequences in *ex vivo* blood and throat samples using polymerase chain reaction (PCR) assays, has revealed co-infection with types 1 and 2 within healthy individuals (Apolloni and Sculley, 1994), and multiple strains in IM patients (Plaza et al., 2003). Furthermore heteroduplex tracking assays (HTAs) mapping co-resident LMP1 sequences have demonstrated the presence of multiple strains in both asymptomatic carriers and IM patients (Sitki-Green et al., 2003, Sitki-Green et al., 2004).

These findings were supported by a study using HTAs mapping both LMP1 and EBNA2 in IM patients, which also found multiple strains in both blood and throat within *ex vivo* samples from these individuals. Possible explanations for these contradictory findings are firstly that one strain may have dominant transforming properties *in vitro*, producing an outgrowth of infected cells, or secondly that particular strains may harbour transformation deficiencies. The latter possibility is particularly significant since if this were the case, it would suggest that transformation is not a prerequisite for virus colonisation and persistence *in vivo* (Tierney et al., 2006).

1.1.3 EBV Genome

During latent infection, the EBV genome exists as an extrachromosomal circular plasmid, or episome, within the nucleus of the infected cell. The genome is replicated once during S phase (Adams, 1987) along with the host DNA, and is partitioned equally into the two daughter cells at the end of mitosis (Kirchmaier and Sugden, 1995). This maintenance of the viral genome appears to require only the cis element, OriP, and EBV nuclear antigen (EBNA) 1 (Yates et al., 1984, Yates et al., 1985). The EBV genome, which is approximately 172 kilobase pairs (kbp) long, has been fully sequenced (Baer et al., 1984) (Figure 2). Since initial mapping was carried out by digesting the genome into smaller fragments using the *Bam*HI enzyme, open reading frames encoding the various genes were designated *Bam*HI regions and named in order of size, with A being the largest and Z the smallest (Young and Murray, 2003). The EBV genome also contains a series of 0.5kbp terminal repeats (TRs) of variable number, together with internal repeats (IRs), which serve to divide the genome into short and long domains (Young and Murray, 2003).

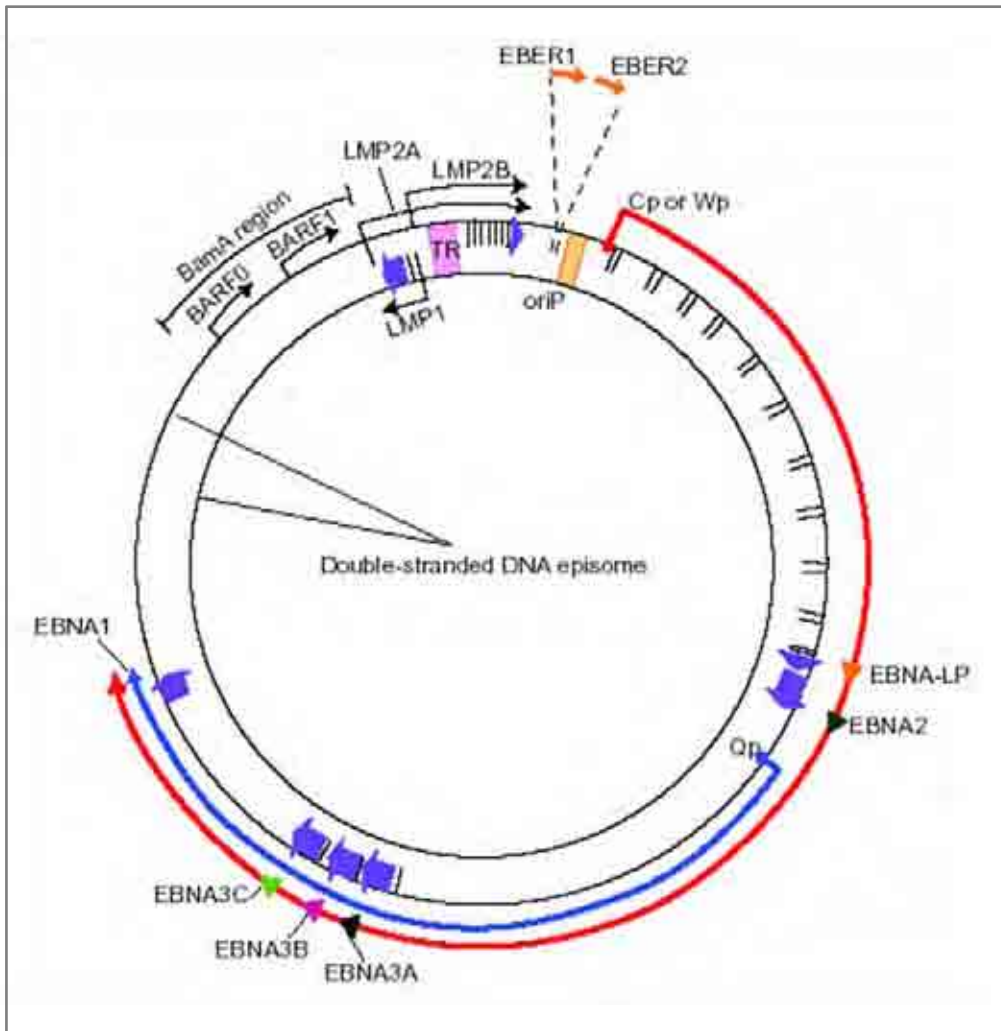


Figure 2. Schematic diagram of the EBV genome

Location and transcription of the EBV latent genes on the dsDNA episome. The large blue solid arrows represent exons encoding each of the latent proteins and the direction in which they are transcribed. The long outer red arrow represents EBV transcription in the latency III program, where all the EBV nuclear antigens (EBNAs) are transcribed from either the *Cp* or *Wp* promoter. The inner shorter blue arrow represents the EBNA1 transcript originating from the *Qp* promoter during Latencies I and II. Taken from Murray and Young, 2001.

1.1.4 Alternative Forms of EBV Latent Infection

Latent infection is the term used to describe the stage in the virus life cycle where a limited number of viral genes are expressed, but no infectious virus is actively produced. Since an assortment of different viral gene expression patterns have been observed during latent EBV infections, latency has been divided into four separate types; Latency I, Latency II, Latency III and Latency 0 (Figure 3).

Latency III

The most readily available *in vitro* model to study EBV latent infection is lymphoblastoid cell lines (LCLs). Lymphoblastoid cell lines are produced by the infection of resting B cells using supernatant containing EBV, which has been harvested from virus-infected cell lines. In contrast to resting B cells, LCLs are transformed, activated, continuously proliferating cells, in which each cell contains multiple copies of the EBV genome. LCLs characteristically express six nuclear antigens (EBNAs1, 2, 3A, 3B, 3C and –LP), and three latent membrane proteins (LMP1, 2A and 2B), the coordinate expression of which facilitates cell growth and transformation. In addition these cells also express a number of non-coding transcripts including those derived from the *Bam*HI A region (BART) transcripts, and EBV-encoded RNAs (EBERs) 1 and 2 (Rickinson and Kieff, 2007). This form of latent infection established in resting B cells *in vitro* is known as Latency III (see Figure 3).

Events during B cell Infection in Vitro

The process of EBV infection of resting B cells *in vitro* is defined by a specific series of events. Initial attachment and internalisation of the EBV particle into

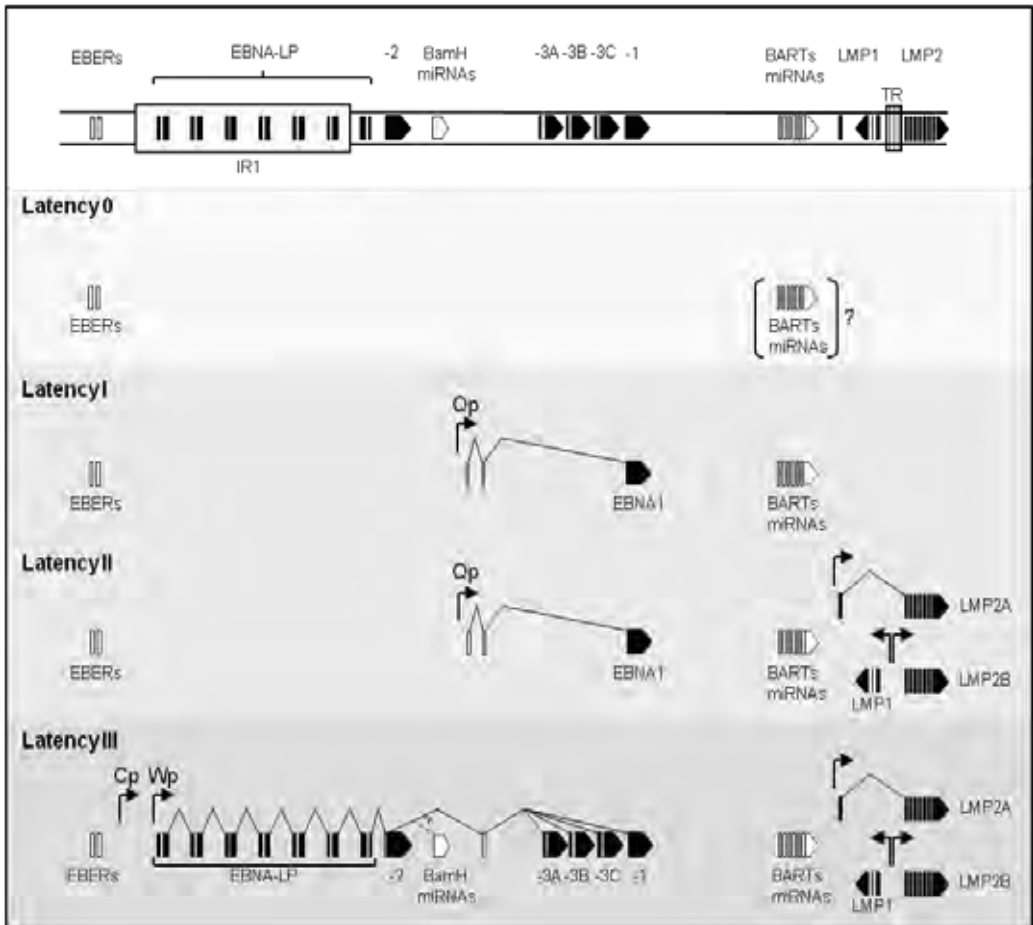


Figure 3. Patterns of EBV latent gene expression in different forms of latency

The top panel is a schematic illustration of the linear EBV genome, showing the location of the BamHI W internal repeat (IR1) and indicating the genomic location of latent cycle genes. Note that the genome is circularised in latently infected cells through the terminal repeats (TR). Shown below are the transcripts expressed in each form of latency with promoters (arrowheads) and splicing patterns as shown; coding exons (EBNA and LMP mRNAs) are shaded solid, while non-coding exons (EBER RNAs, BART RNAs, BamH miRNAs and BART miRNAs) are unfilled. Adapted from Kelly et al. 2009.

the cell is facilitated by interaction between the viral protein gp350 and the B cell surface receptor CD21 (otherwise known as complement receptor 1 (CR1)), and by interaction of the viral coreceptor gp42 with HLA II on the B cell surface (Nemerow et al., 1987, Tanner et al., 1987). The first detectable viral transcripts are initiated from Wp promoters situated within the *Bam*HI W repeat regions (Alfieri et al., 1991, Sample et al., 1986, Woisetschlaeger et al., 1990).

Whilst Wp-derived transcripts have the capacity to encode each EBNA protein, during the early stage of infection only EBNA2 and EBNA-LP are expressed (Alfieri et al., 1991). Subsequently EBNA2 alone or EBNA2 together with EBNA-LP go on to activate both viral and cellular promoters that are involved in the transformation process. These include the viral promoters Cp, located upstream in the *Bam*HI C region (Rooney et al., 1992, Sung et al., 1991, Woisetschlaeger et al., 1991), and the LMP promoters (Abbot et al., 1990, Fahraeus et al., 1990, Nitsche et al., 1997, Wang et al., 1990, Zimmer-Strobl et al., 1991), and promoters for cellular genes CD21, CD23 and cyclin D2 (Cordier et al., 1990, Sinclair et al., 1994, Wang et al., 1987). At the same time as Cp is activated, expression of all six EBNA proteins begins and transcription from Wp declines (Woisetschlaeger et al., 1991). The different EBNA proteins are translated from distinct mRNA splice products derived from a single long primary transcript (Woisetschlaeger et al., 1989). The LMPs are expressed from separate promoters in the *Bam*HI N region. Whereas transcription of both LMP 1 and 2B is initiated at the same promoter, the process occurs in a bidirectional fashion, with LMP1 transcribed leftward and LMP2B transcribed rightward (Rickinson and Kieff, 2007) (see Figure 3).

Although Latency III is the classic gene expression program exhibited following infection of resting B cells *in vitro*, B cells expressing this profile are seldom seen *in vivo* in the context of non-malignant infection. In circumstances where rare latency III infected cells have been detected during primary infection (Tierney et al., 1994), it has been proposed that this programme drives host cell proliferation in the initial stages of infection, but viral gene expression is downregulated to a more restricted pattern thereafter. In the context of EBV-driven lymphoproliferations in immunocompromised individuals, latency III expression can be readily detected in infected cells (Young et al., 1989). This may be due to the absence of an efficient CD8⁺ T cell response, which under normal conditions would facilitate the removal of B cells expressing the full complement of EBV antigens (see PTLD section later).

Latency I and II

Other forms of latent infection, in which there is a more restricted pattern of gene expression, have also been described. The latency I form of infection is typically found in Burkitt's lymphoma (BL) tumours cells, and BL-derived cell lines. In these cells EBNA1 transcripts are driven by the Qp promoter located in the BamHI Q region of the genome (Schaefer et al., 1995, Nonkwelo et al., 1996). No other viral proteins are expressed as Cp/Wp and LMP promoters are all silent, however the non-coding EBERs and BART transcripts can be detected (Rowe et al., 2009).

The Latency II programme was originally identified in undifferentiated nasopharyngeal carcinoma (NPC) (Fahraeus et al., 1988, Young et al., 1988, Gilligan et al., 1990), and has since been found in EBV-associated gastric

carcinomas (Imai et al., 1994, Sugiura et al., 1996), Hodgkin's lymphoma (Niedobitek et al., 1991, Pallesen et al., 1991b) and T-cell lymphomas (Chiang et al., 1996). Similarly to Latency I, in Latency II EBNA1 transcription is driven by the Qp promoter in the absence of the other EBNAs. In addition LMP1, LMP2A and LMP2B are also expressed (Fahraeus et al., 1988, Young et al., 1988, Gilligan et al., 1990, Niedobitek et al., 1991, Pallesen et al., 1991a, Pallesen et al., 1991b). As with Latency I, EBERs and BARTs can also be detected in Latency II (Rowe et al., 2009).

A further form of latency where expression of all viral proteins is switched off has also been described. It has been proposed that the virus uses this program, termed Latency 0, in order to avoid detection by the host immune system, thereby achieving long term persistence within resting memory B cells. In this scenario EBV infection is identified by the presence of EBER transcripts (Miyashita et al., 1995).

Individual transcripts and proteins expressed during EBV latent infection are discussed in further detail below.

EBNA1

EBNA1 is a DNA-binding phosphoprotein that is expressed in all EBV-associated tumours. It localises to the nucleus of the host cell where it is able to interact with host chromosomes (Shire et al., 1999), and plays an essential role in viral genome replication and maintenance (Lee et al., 1999). EBNA1 binds to specific sequences with the plasmid origin of replication (OriP), including those from within the OriP dyad symmetry (DS) element, and the family of repeats (FR) (Rawlins et al., 1985). EBNA1 tethers the replicated EBV

genome to metaphase host cell chromosomes via the amino (N) terminal of the protein, ensuring equal numbers of EBV genomes are acquired by the daughter cells (Reedman and Klein, 1973, Ohno et al., 1977, Petti et al., 1990, Mackey et al., 1995, Mackey and Sugden, 1999). In addition to its role in genome maintenance, EBNA1 also acts as a transcriptional regulator, mediating expression of other viral genes. EBNA1 binds specific sites immediately downstream of the Qp promoter, and is able to negatively regulate its own expression (Sample et al., 1992, Nonkwelo et al., 1996). The protein can also function as a transcriptional activator of the Cp promoter (Yates et al., 1984, Altmann et al., 2006), and the LMP1 promoter (Gahn and Sugden, 1995). Furthermore, the use of chromatin immunoprecipitation and microassays has revealed that EBNA1 can bind to and regulate various cellular genes and promoters, and has identified several binding sites within the human genome (Dresang et al., 2009, Canaan et al., 2009, Lu et al., 2010).

Although EBNA1's primary function still appears to be the propagation of the EBV genome, EBNA1 expression may also be necessary for B cell transformation (Lee et al., 1999), and the resultant development of B cell lymphomas within transgenic mice following EBNA expression suggests the protein plays a role in tumorigenesis (Wilson et al., 1996).

EBNA2

EBNA2 is a transcriptional activator protein which is the first viral antigen to be expressed following B cell infection (Young and Rickinson, 2004, Thompson and Kurzrock, 2004). EBNA2 transactivates the Cp promoter during the early stages of infection, producing a switch from Wp to Cp transcription

(Woisetschlaeger et al., 1991). The protein upregulates expression of viral genes including LMPs, and various cellular genes including CD21, CD23 and c-myc (Wang et al., 1987, Wang et al., 1990, Kaiser et al., 1999). Although it contains a transcription activation domain, it does not bind DNA directly, but rather binds cellular proteins including RBP-Jk, PU.1 and AP2, which mediate interactions with other promoter regions (Grossman et al., 1994, Hsieh and Hayward, 1995).

EBNA2 has a key function in growth transformation of the host cell since the P3HR-1 EBV strain, which carries an EBNA2 deletion, is unable to transform B cells in vitro (Cohen et al., 1989). Indeed EBNA2 expression has been linked to transformation of non-B cells; specifically the rat fibroblast cell line F2408 (Shimakage et al., 1995). *In vitro* studies have demonstrated that EBNA2 is important for the continuous proliferation characteristic of LCLs since the EREB2.5 LCL, which has been engineered to express an oestrogen receptor-EBNA2 fusion protein, requires oestrogen in order for cell survival and proliferation to occur (Kempkes et al., 1995). EBNA2 may also have a role in tumorigenicity since transgenic mice carrying the EBNA2 gene have been shown to develop multiple tumour foci (Tornell et al., 1996).

EBNA3 Family

The EBNA3 latent protein family comprises three related nuclear proteins, 3A, 3B and 3C. All three have activation and repression functions on viral promoters (Cludts and Farrell, 1998, Lin et al., 2002, Marshall and Sample, 1995, Radkov et al., 1997, Zhao and Sample, 2000), and interact with cellular corepressor proteins (Cotter and Robertson, 2000, Hickabottom et al., 2002,

Knight et al., 2003, Radkov et al., 1999, Touitou et al., 2001). They associate with RBP-Jk, disrupting its binding to cognate Jk sequences and to EBNA2, resulting in repression of EBNA2-mediated transactivation. This mechanism enables the EBNA3 proteins, together with EBNA2, to control RBP-Jk activity and consequently to regulate expression of viral and cellular proteins that contain Jk sequences (Young and Murray, 2003). In addition to their transcriptional regulatory functions, further studies have revealed the EBNA3 family of proteins are involved in disruption of the host cell cycle; specifically at the G2/M checkpoint (Krauer et al., 2004).

Whereas EBNA3A and 3C have been shown to be essential for *in vitro* growth transformation of B cells, EBNA3B is dispensable (Tomkinson et al., 1993, Tomkinson and Kieff, 1992, Chen et al., 2005). Since 3B is, however, conserved in lymphocryptoviruses infecting Old World primates (Jiang et al., 2000), it is likely to be an important component of infection *in vivo*.

EBNA-LP

EBNA-leader protein (LP) is encoded by the leader of each of the EBNA mRNAs, and varies in size according to the number of BamHI W repeats contained within the specific EBV isolate (Rickinson and Kieff, 2007). In recently infected B cells, a range of EBNA-LP isoforms are expressed, but this number decreases over time spent in culture (Finke et al., 1987, Dillner et al., 1986). EBNA-LP appears to be required (but is not essential) for effective outgrowth of LCLs since infection with mutant viruses expressing defective EBNA-LP results in reduced transformation efficiencies (Hammerschmidt and Sugden, 1989, Mannick et al., 1991, Allan et al., 1992). The protein also

functions as a coactivator of EBNA2, preferentially enhancing expression of LMP1 (Fahraeus et al., 1990, Harada and Kieff, 1997, Nitsche et al., 1997, Peng et al., 2005).

LMP1

Latent membrane protein 1 (LMP1) is expressed in all EBV-positive tumours except BL, and due to its critical role in B cell transformation is considered to be a classical viral oncogene (Kaye et al., 1993, Izumi and Kieff, 1997, Middeldorp and Pegtel, 2008). The LMP1 protein contains a transmembrane domain containing six loops, an amino (N) terminal cytoplasmic portion which fixes the protein to the membrane of the infected cell, and a long cytoplasmic tail which is able to interact with cellular signalling molecules. The cytoplasmic portion contains carboxy (C) terminal activation regions (CTARs) which are functionally homologous to the cytoplasmic tail of human CD40 as they interact with tumour necrosis factor (TNF) receptor associated factors (TRAFs) and TNF receptor-1 associated death domain protein (TRADD) (Luftig et al., 2003, Devergne et al., 1998, Schneider et al., 2008). Interactions between CTARs and TRAFs/TRADDs lead to activation of various intracellular signalling molecules including MAP kinases. Indeed CTARs 1 and 2 were identified based on their capacity to activate the NF- κ B signalling pathway (Huen et al., 1995). Deletion of the LMP1 C-terminal signalling domain was shown not to ablate B-cell transforming capabilities (Kaye et al., 1999), indicating that the transmembrane domains of the protein are also important for activation of signalling pathways and other critical roles of LMP1. Further studies have revealed the lipid microdomains or “rafts” within this section of the protein to be involved in

intracellular signalling processes which ultimately lead to NF- κ B activation (Kaykas et al., 2001, Kaykas et al., 2002, Soni et al., 2006, Yasui et al., 2004).

The homology of LMP1 with CD40 is an important consideration within the context of *in vivo* B cell infection. One of the most widely believed models of EBV colonisation of the B cell compartment is based in part on the ability of LMP1 to mimic the CD40-CD40 ligand (L) interaction usually provided by T cell help (Uchida et al., 1999). The infected cell subsequently participates in a germinal centre (GC) reaction, resulting in differentiation to a memory B cell.

LMP1 expression in healthy tissue is rarely seen; approximately 20% of EBER-positive cells in healthy tonsil tissue were found to express low levels by immunohistochemistry in one study (Hudnall et al., 2005). By comparison, LMP1 expression in EBV-positive tumours including post-transplant lymphoproliferative disease (PTLD) (Liebowitz, 1998), Hodgkin's Lymphoma (HL) (Dukers et al., 2000) and subsets of nasopharyngeal carcinoma (NPC) (Khabir et al., 2005) is relatively high, and in immunocompromised individuals evidence of abundant LMP1 expression has been observed in healthy tonsils preceding the onset of PTLD (Mowry et al., 2008).

LMP2

The LMPs 2A and 2B share a similar structure, comprising a transmembrane domain made up of 12 membrane-spanning loops, with a C-terminal cytoplasmic tail. Additionally, LMP2A has an N-terminal cytoplasmic portion that comprises eight tyrosine residues, two of which form an immunoreceptor tyrosine-based activation motif (ITAM) (Longnecker, 2000). Upon phosphorylation, the ITAM is able to recruit various cellular tyrosine kinase

proteins, ultimately leading to the disruption of B cell receptor (BCR) signalling (Longnecker, 2000, Dykstra et al., 2001).

LMP1 and LMP2A together have the potential to mimic antigen-driven activation of B cells, and provide survival signals. BCR-negative pre-cursor cells observed in the periphery of LMP2A transgenic mice first lead to the suggestion that the protein promotes survival of defective B cells, which would otherwise be selected for apoptosis (Caldwell et al., 1998). The ability of EBV infection to rescue BCR⁻ B cells was further highlighted by subsequent *in vitro* infection studies using GC B cells. In one study, infection of human tonsillar GC B cells yielded a small proportion of LCL cultures containing BCR⁻ cells (Chaganti et al., 2005), and in a second, BCR⁻ GC B cells were selected based on lack of Ig expression, and successfully transformed by EBV (Mancao et al., 2005). The link between LMP2A expression and cell survival was firmly established when a recombinant EBV encoding a conditional, floxed LMP2A allele was able to transform both BCR⁺ and BCR⁻ GC B cells effectively *in vitro*. The same study confirmed that cell survival and proliferation were absolutely dependent on LMP2A (Mancao and Hammerschmidt, 2007).

Within the context of B cell colonisation during primary infection *in vivo*, it has been proposed that LMP2A's capacity to imitate BCR signalling may act in conjunction with LMP1's surrogate T cell help in order to drive infected cells through GC reactions. When considering this hypothesis however, the prevailing BCR⁺ phenotype of the EBV-infected memory B cell reservoir is an important counter-argument.

EBERs

EBV also encodes a pair of non-coding RNAs, EBERs1 and 2, which can be detected in all forms of latent infection. Neither of the two gene products appear to be essential for B cell transformation, however EBER2 may increase the efficiency of this process (Wu et al., 2007). A contribution to malignancy has been suggested by various studies in which EBERs have been shown to increase tumourigenicity, promote cell survival and induce the upregulation of cytokines such as IL-10 (Ruf et al., 2000, Takada and Nanbo, 2001). EBERs can bind directly to the ds RNA-activated protein kinase, PKR, which contributes to the antiviral effects of interferon (IFN), suggesting that EBER-mediated inhibition of this molecule could promote viral resistance (Clarke et al., 1991, Nanbo et al., 2002). In addition, EBERs also interact with the autoantigen La (Lerner et al., 1981) and the ribosomal protein L22 (Fok et al., 2006, Toczyski et al., 1994, Houmani et al., 2009), and have been shown to induce expression of IL-10 in BL (Takada and Nanbo, 2001, Ruf et al., 2000, Kitagawa et al., 2000), IL-9 in EBV-infected T cells (Yang et al., 2004) and insulin-like growth factor in epithelial cells (Iwakiri et al., 2003, Iwakiri et al., 2005). Stable expression of EBERs in immortalized nasopharyngeal epithelial cells confers resistance to apoptosis (Wong et al., 2005).

BHRF1

*Bam*HI fragment H rightward open reading frame 1 (BHRF1), which encodes a gene homologous to cellular Bcl2 (Vaux et al., 1988), was initially classified as an early lytic cycle protein since it was never detected in tightly latent LCLs and is expressed from its own lytic cycle promoter (Pearson et al., 1987, Austin et

al., 1988). Recent studies, however, have highlighted an anti-apoptotic role for BHRF1 during latent infection in a subset of BL and growth transformation of B cells (Altmann and Hammerschmidt, 2005, Kelly et al., 2009). An investigation into the anti-apoptotic activity of EBV in BL focussing on EBNA2-deleted Wp-restricted BL cell lines revealed that deletions within certain tumours had placed a copy of the Wp promoter immediately upstream from BHRF1 (Kelly et al., 2009). Expression of BHRF1 was also detected in these lines at both the mRNA and protein levels. Furthermore, the study used a dox-inducible vector expressing BHRF1 in BL lines to show that BHRF1 conveyed anti-apoptotic properties on the infected cells even at low levels of expression. In addition to the role of BHRF1 in BL, BHRF1 was also found to be constitutively expressed in long term LCL cultures; a finding which was consistent with the observed burst of BHRF1 expression correlating with resistance from apoptosis immediately following B cell EBV infection (Altmann and Hammerschmidt, 2005).

1.1.5 EBV Lytic Infection

EBV lytic infection occurs *in vivo* during primary infection, where the virus replicates in epithelial cells that have acquired the virus either directly, or, as suggested by *in vitro* experiments (Shannon-Lowe et al., 2006), indirectly from the surface of adjacent B cells. Reactivation of the lytic cycle also occurs sporadically during persistent infection, probably when memory B cells are induced to differentiate into plasma cells (Laichalk and Thorley-Lawson, 2005). Lytic infection in the oropharynx leads to high levels of infectious virus shed into the throat, which ensures transmission to new hosts and maintains infection of the current host (Fafi-Kremer et al., 2005, Balfour et al., 2005). *In vitro*,

approximately 5% of cells in LCL cultures undergo spontaneous lytic replication, and Akata-BL cell lines stably transfected with reporter plasmids can be induced into lytic cycle by cross-linking of the BCR with anti-Ig (Binne et al., 2002, Rensing et al., 2005).

Lytic replication involves the sequential expression of lytic viral antigens. The process is initiated by immediate early genes BZLF1 and BRLF1, which transactivate expression of early genes such as BALF2, BHRF1 and BMRF1. Whilst the latter antigens are involved in viral DNA synthesis, further late lytic antigens are involved in synthesis of viral structural proteins. Specifically, late antigen BLLF1 encodes the envelope glycoproteins gp350 and gp220, BCRF1 encodes a viral protein that closely resembles IL-10, and BALF4 encodes the glycoprotein gp110 (Rickinson and Kieff, 2007).

The process of viral replication imposes significant nuclear and cytoplasmic changes within the infected cell, which ultimately leads to cell lysis. The initial stages take part in the nucleus and involve synthesis of viral DNA, which is subsequently packaged into the capsid. Capsids bud through the nuclear membrane, forming cytoplasmic vesicles which contain the enveloped virus. The vesicles fuse with the plasma membrane of the host cell, and the new virus particle is released via exocytosis, followed by death of the host cell (Rickinson and Kieff, 2007).

1.2 B cell Development

Before discussing what is known about EBV persistence in the B cell system, it is first necessary to provide an introduction to the normal pathways of B cell development. The main purpose of a B cell is to produce immunoglobulin (Ig).

Immunoglobulin when expressed on the B cell surface is the essential component of the B cell receptor (BCR) complex and is also termed “antibody” when in secreted form. The primary role of Ig is to recognize and bind to specific pathogenic antigens, which it has been primed to do via a series of diversification processes starting with VDJ recombination in the immature B cell, and finishing with somatic hypermutation in the activated mature B cell. As a result of these mechanisms the B cell pool is collectively capable of recognizing almost infinite numbers of unique antigens. Different effector functions are determined by both the class of Ig expressed by the individual B cell, and the B cell sub-type (see below). As a result of Ig production, B cells function within the immune system to bind pathogens such as bacteria and viruses. This can result in neutralization, when sites on the pathogen necessary for replication are blocked by antibodies, and opsonisation, which promotes complement-driven phagocytosis by other immune cells. B cells also function as antigen-presenting cells, presenting MHC class II-restricted antigens to T cells, and can produce immunomodulatory cytokines that influence different components of the immune response, for example T cell differentiation, dendritic cell regulation, transplant rejection, tumour immunity and lymphoid organogenesis.

Importantly, B cells not only carry out these effector functions during the first encounter of pathogenic antigen within the context of a primary response, but subsequently confer lifelong protection against that pathogen via production of highly specific, rapidly-responding memory cells that can persist within the individual for life (LeBien and Tedder, 2008, Parham, 2000).

1.2.1 Antibody Structure

The function of antibodies in host defence is to recognise and bind to specific antigens in order to facilitate clearance of that antigen from the body either by direct neutralization or targeting to other components of the immune system. Antigen and/or immune system constituents interact with different parts of the antibody molecule (Figure 4). The antigen-binding portion is highly variable between each molecule, accounting for the vast diversification in antibody specificities. The remaining parts of the antibody molecule are more conserved and as such are used to distinguish the five different classes of antibody, which have distinct effector functions; IgD, IgM, IgG, IgA and IgE. Since IgG is the most abundant antibody found in human beings, it usually serves as the example to describe antibody structure (LeBien and Tedder, 2008, Litman et al., 1993, Parham, 2000, Market and Papavasiliou, 2003).

Antibodies are glycoproteins comprised of two identical heavy chains and two identical light chains. Each heavy chain is covalently linked to a light chain via a disulphide bond, and together the two heavy and light chain pairs resemble a Y-shaped structure with two arms and a stem. Most of the antibody molecule consists of amino acid sequences of limited diversity known as the constant regions (CH in the heavy chain, CL in the light chain). The light chains contain a single C domain, whereas the heavy chains consist of three or four, depending on isotype. The configuration of the CH domains determines whether the antibody is IgM, IgD, IgG, IgA or IgE. The amino terminal at the end of each chain is made up of a single variable domain (VH in the heavy chain, VL in the light chain) containing highly variable amino acid sequences. Two different classes of light chain are found in humans, κ and λ . Both types

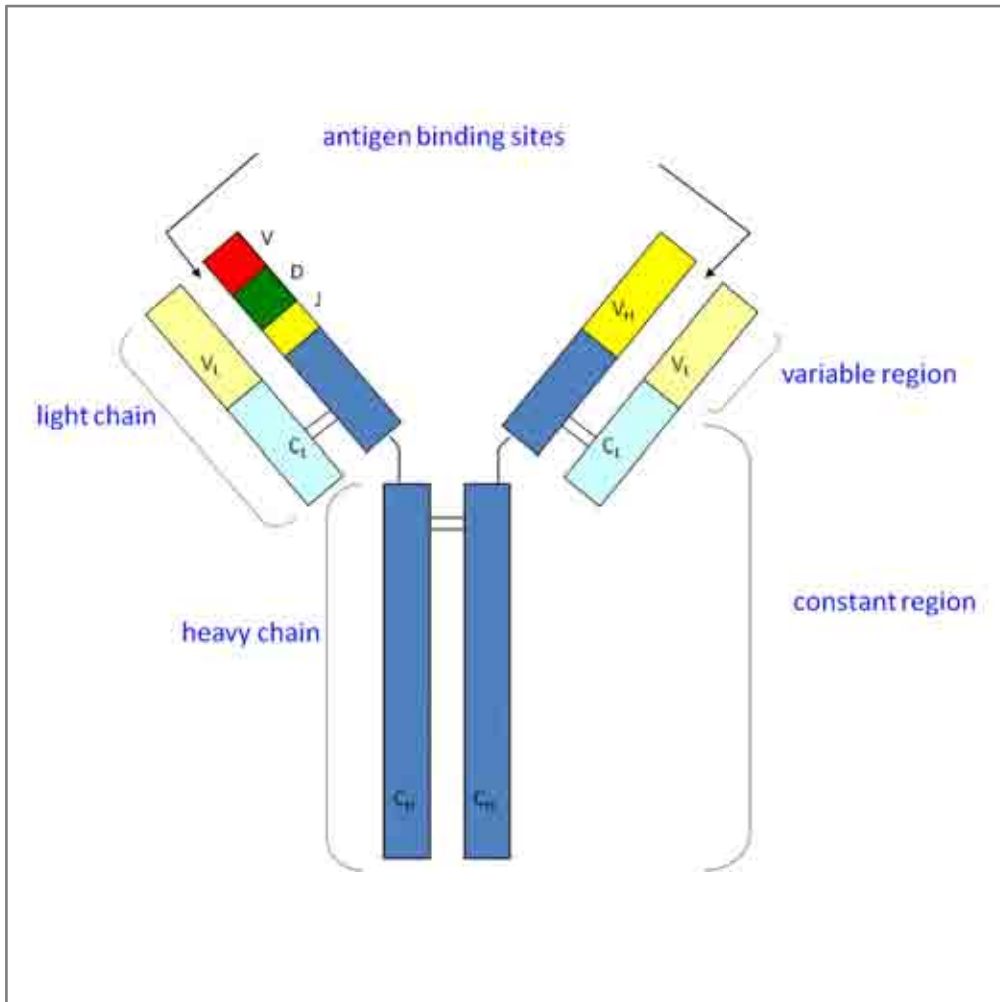


Figure 4. Structure of an antibody molecule

The diagram shows the structure and locations of functional domains within an IgG molecule. The constant (C) regions are shown in blue and the variable (V) regions are in yellow. Both the heavy (H) and light (L) chains are highlighted. The basic positions of the V, D and J segments within the variable region are shown on the left arm of the H chain. Adapted from Janeway et. al. 2001.

are associated with each class of antibody, although the κ chain is more abundant, being present in two thirds of antibody molecules. The pairing of the VH and VL segments produces the antigen binding site at the amino-terminal of the molecule. Within each V domain, three regions of highly diverse amino acid sequences known as complementarity-determining regions (CDRs) together form the hypervariable regions of the binding site. The less diverse regions, known as the framework regions provide structural stability for the V domain (LeBien and Tedder, 2008, Litman et al., 1993, Parham, 2000, Market and Papavasiliou, 2003).

1.2.2 B cell Receptor

Antibodies that are membrane-bound to the B cell surface are referred to as Immunoglobulin (Ig) molecules (Figure 5). Although surface Ig is able to bind specific antigen, this interaction alone is not sufficient to stimulate the B cell, but requires two transmembrane proteins, $Ig\alpha$ and $Ig\beta$ (CD79). These possess long cytoplasmic tails containing intracellular tyrosine-based activation motifs (ITAMs), which can interact with signalling molecules such as Src family kinases following antigen-binding (Reth, 1989). This complex of Ig, $Ig\alpha$ and $Ig\beta$ forms the functional B cell receptor (BCR).

B cell activation is achieved by binding of the BCR to protein or carbohydrate epitopes. Following specific binding in a naive B cell, IgM molecules become cross-linked with each other on the cell surface and cluster in a localised area. This assemblage provides a signal to the cell nucleus from the BCR complex, which is communicated via $Ig\alpha$ and $Ig\beta$. In addition to Ig cross-linking, other signals are required to activate the B cell. In particular the B cell co-receptor

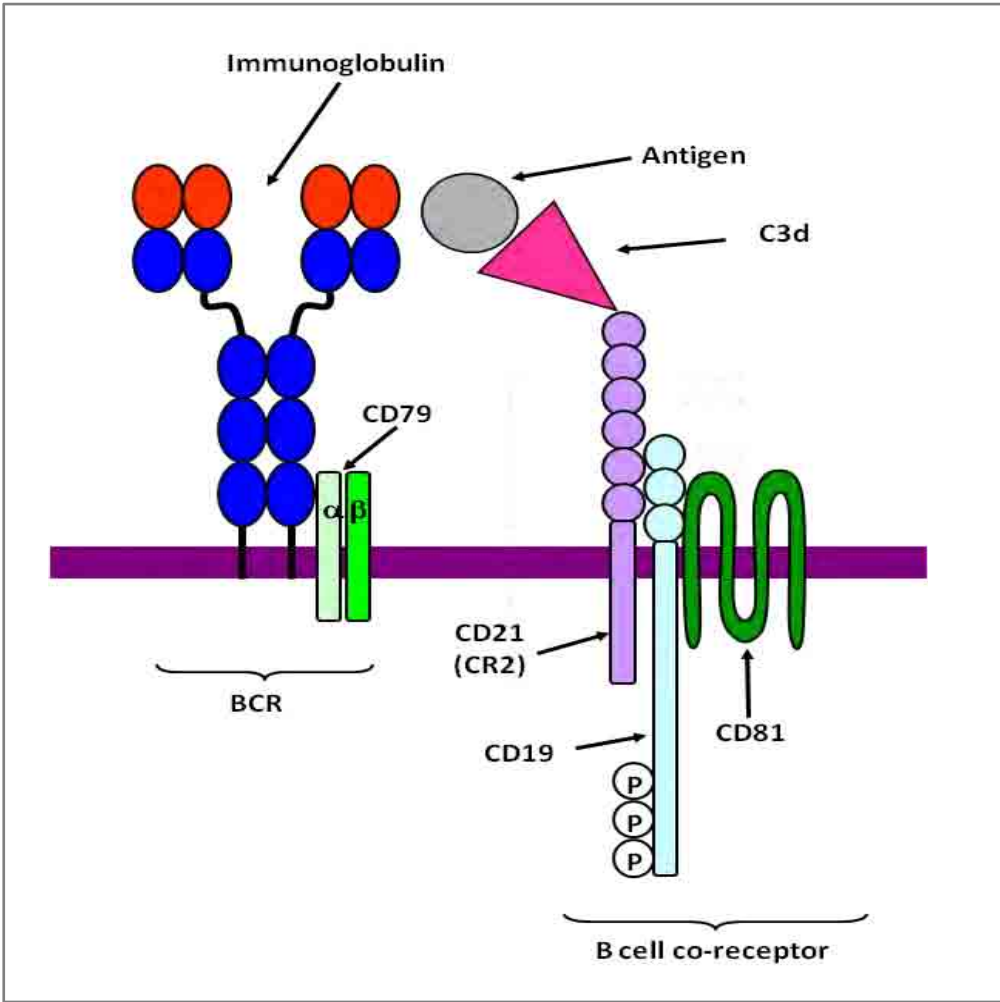


Figure 5. B cell receptor complex

Binding of CD21 (CR2) to C3d bound antigen enables the co-receptor complex to cluster with the BCR complex. This allows receptor-associated kinases to phosphorylate CD19, which in turn binds the Src-family tyrosine kinases and PI3 Kinase, thus activating downstream signalling pathway. Adapted from Janeway et al., 2001.

complex which is made of several proteins including; complement receptor CR2 (also known as CD21), CD19 and CD81. CR2 binds complement 3d-bound antigen, enabling the co-receptor complex to cluster to the BCR complex. Receptor-associated kinases are then able to phosphorylate CD19, which then binds Src family tyrosine kinases and P13 kinases, in order to activate the downstream signalling pathway (Figure 5). This simultaneous ligation of the BCR and B cell co-receptor is able to increase the activation signal 1000-10,000-fold. When the B cell is stimulated by T-dependent antigens, CD4 T cell help is also required for proliferation and differentiation of the B cell (see later) (LeBien and Tedder, 2008, Parham, 2000, Litman et al., 1993).

1.2.3 Organisation of Immunoglobulin Genes

In humans the organisation of Ig loci differs to that of other genes elsewhere in the genome. In non-B cells, the germline Ig genes are in a fragmented form that cannot be expressed (Figure 6a). Rather than containing a single gene, Ig heavy and light chain loci contain different sets of gene segments corresponding to the major components of the variable domain. In humans, Ig genes are found at three separate chromosomal locations; chromosome 14 (heavy chain locus), chromosome 2 (κ light chain locus) and chromosome 22 (λ light chain locus). In both the light and heavy chains, different gene segments encode the leader peptide (L), the variable region (V) and the constant region (C). In order to express the V region genes, rearrangements to form functional sequences are first necessary. The light chain variable domain is encoded by two gene segments; one variable (V) region segment and one joining (J) region segment. The heavy chain variable domain is also encoded by one V segment and one J region segment, and an additional diversity (D) segment encoding an

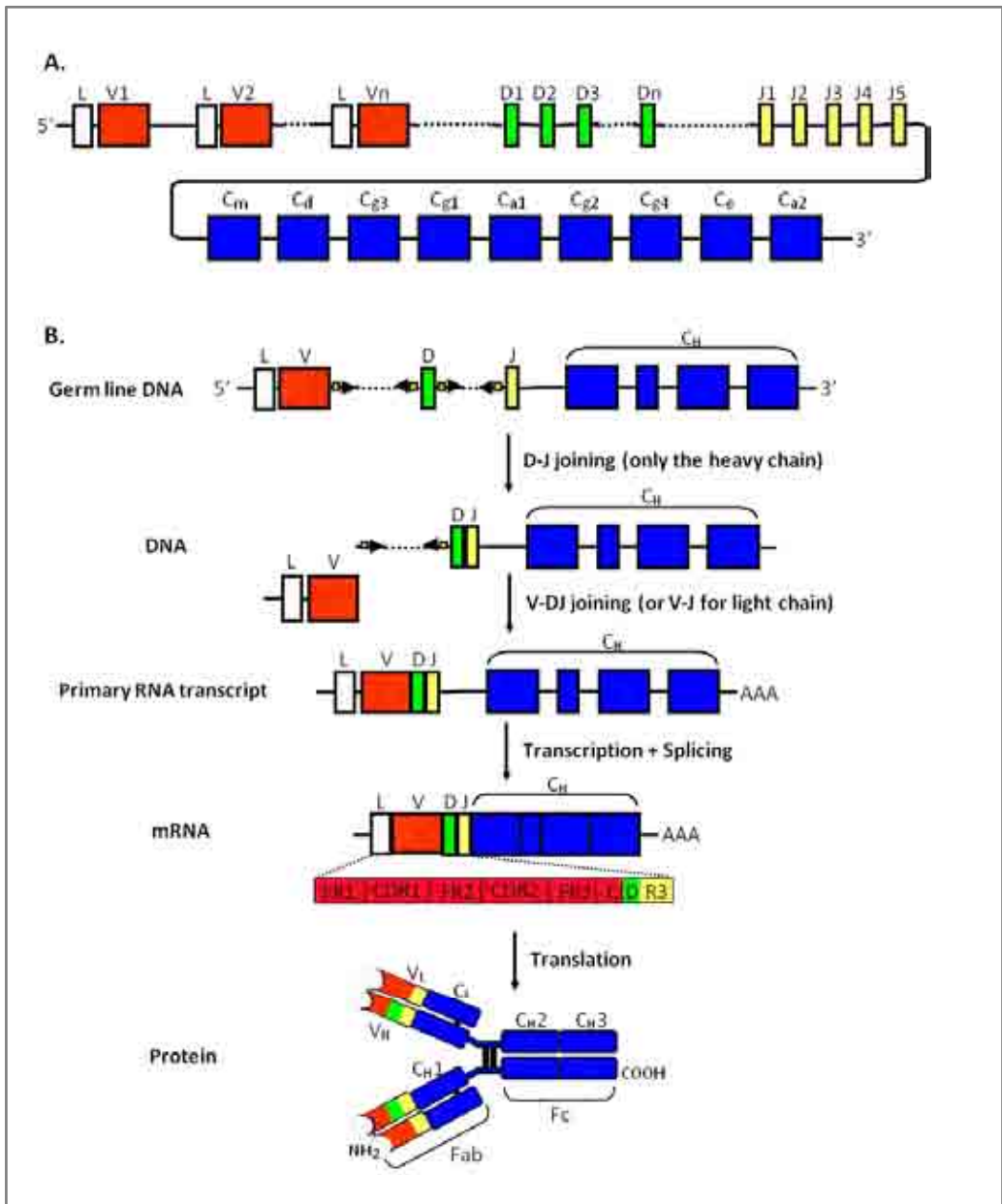


Figure 6. Ig gene rearrangement

A. Germline distribution of genes on the heavy chain locus situated on chromosome 14.
B. Sequence of the gene rearrangement for the heavy chain and assembly of both heavy and light chains to form a functional polypeptide. Disulphide bonds are shown as solid black bars. Adapted from Janeway et al., 2001.

extra region situated between the V and J regions. Approximately 65 V, 27 D and 6 J regions are available for Heavy chain rearrangement. CDR1 and CDR2 represent regions of diversity with the V gene in both heavy and light chains. The CDR3 region is determined by the junction between the V and J segments in the light chains, but in the heavy chain includes the junctions between the V, D and J regions (Market and Papavasiliou, 2003, Parham, 2000).

1.2.4 B cell Maturation

B cells develop in the bone marrow throughout adult life, from hematopoietic stems carrying germline Ig genes. B cell development occurs in successive stages (Figure 7) distinguished by molecular changes accompanying Ig gene rearrangements, where V, D and J segments are recombined to form functional BCRs (Figure 6b) (Li et al., 1993, Rajewsky, 1996). The heavy chain is the first to be rearranged in the earliest identifiable B cell, known as the progenitor B cell (pro-B cell). In order to generate the heavy chain, two recombination events take place. The first brings together a D and a J segment in the early pro-B cell, and the second event adds a V segment to the recombined DJ segment in the late pro-B cell. The multiple V, D and J segments that are available ensure that thousands of different VDJ combinations are possible; hence the rearrangement mechanism is very important for the generation of a diverse repertoire of Ig variable regions. Once the cell is able to express a functional heavy chain, it is known as a large pre-B cell. In the early phase of the pre-B cell stage, a μ heavy chain is transiently expressed on the cell surface. The chain is joined by two surrogate light chains to form the pre-B-cell receptor which, upon stimulation, induces cell division mechanisms to yield small pre-B cells. In these cells, most μ heavy chains remain in the cell cytoplasm, whereas a small

proportion is expressed on the cell surface. Small pre-B cells then initiate rearrangement of the light chain during which another recombination event is needed to bring together a V and a J segment (Wang et al., 1998). The cutting and joining together of the gene segments is carried out by enzymes encoded by recombination activating genes 1 and 2 (RAG 1 and 2) (Schatz et al., 1989), and during this process further V region diversity is provided to the antibody molecule via the introduction of additional N nucleotides at V, D and J junctions (since the accumulation of these nucleotides is specific to each individual B cell, distinct junction CDR3 sequence provide a means to identify clonally related B cells).

B cell development can only continue to the next phase following a productive VDJ rearrangement. Since every cell carries two copies of each Ig loci (one inherited from each parent) rearrangements can take place on either of the homologous chromosomes, affording the cell two attempts to make a productive rearrangement. If this is successful, subsequent rearrangements are prevented, ensuring that the cell carries a heavy or light chain of single specificity whereas B cells unable to generate productive rearrangements are eliminated by apoptosis. This process is known as allelic exclusion (Mostoslavsky et al., 2004).

After the heavy and light chains have been successfully rearranged and expressed, they are able to assemble with the μ heavy chains into functional IgM molecules. In this final stage, however, the immature B cells are not yet fully released into the periphery. Due to the random nature of the rearrangement process, some B cell receptors may be reactive towards self antigen. In order to prevent potential targeting of the body's own constituents,

which may lead to autoimmune disorders, the immature B cells are therefore selected for self-tolerance (Nemazee et al., 1991).

Release from the bone marrow into the peripheral blood coincides with alternative mRNA splicing of the heavy chain to yield IgD as well as IgM transcripts. The assembled VDJ sequence lies upstream from the C region genes. The closest C region gene on the 3' side of the VDJ sequence is C μ (encoding IgM), followed by C δ (encoding IgD). In mature, naive B cells transcription of the complete Ig heavy chain begins at the V gene segment and continues through the μ and δ genes before terminating. The primary transcript is processed to remove introns between the C region genes, and alternatively spliced to yield either IgM or IgD mRNA. The resultant naive B cell is therefore identifiable by co-expression of IgM and IgD on the cell surface (Geisberger et al., 2006).

Immature B cells exiting the bone marrow are referred to as transitional B cells. They express the B cell marker CD21, with IgD and CD22 (LeBien and Tedder, 2008), and are associated with TI responses (Coutinho and Moller, 1975).

Following entrance to the periphery, B cells circulate between the blood and lymphoid tissues, including the lymph nodes, spleen and mucosa-associated lymphoid tissue. B cells are also particularly enriched in areas of gut-associated lymphoid tissue (GALT), including Peyer's patches, the appendix and the tonsils, where high numbers of IgA-secreting B cells congregate. Within lymphoid tissue, B cells gather in organised structures known as follicles. As billions of mature B cells leave the bone marrow every day however, competition exists for a limited number of follicular sites. B cells which are unable to gain access to lymphoid follicles only survive for a few days, whereas

those that are able to enter and receive survival signals survive between three and eight weeks, or until they encounter antigen (LeBien and Tedder, 2008).

Mature B cells circulating in the peripheral blood can be divided into three main subsets (Klein et al., 1998); (i) antigen-inexperienced IgD+CD27- naive B cells carrying germline IgH genes, which make up ~60% of the peripheral blood B cell population, (ii) antigen-selected IgD-CD27+ switched memory B cells that have differentiated via a germinal centre reaction, where clonal B cell expansion occurs alongside IgH mutation and isotype switching and (iii) IgD+CD27+ non-switched memory B cells whose origins are controversial. Although these cells carry mutated IgH genes, their presence in GC-deficient individuals suggests SHM arises in a GC-independent manner (Weller et al., 2001, Weller et al., 2005, Agematsu et al., 1998). The switched memory and non-switched memory subsets each comprise ~15-20% of the peripheral blood B cell population.

In addition to the three largest circulating B cell subpopulations described above, CD27+IgM+IgD- B cells, also known as IgM-only B cells, represent a small fraction (~1%) of the B cell pool. The origins of IgM-only B cells are not fully understood, but there is evidence to suggest that these cells are products of a GC reaction since they can be detected in elevated numbers in individuals who are able to form GCs, but are unable to carry out CSR or SHM, due to a deficiency of the enzyme vital to these processes, activation-induced cytidine deaminase (AID) (Weill et al., 2009).

1.2.5 T cell-Dependent B cell Activation

Naive B cells pass through the T cell zone of secondary lymphoid tissue until they encounter their specific antigen. Upon binding antigen, the B cell receptor complex not only sends signals to the cell nucleus (as described previously), but internalises the antigen via receptor-mediated endocytosis before processing the fragments that will be presented to a specific CD4 T cell. The B cell presents the antigenic peptide to a CD4 T cell via a complex with the MHC class II molecule on its surface. This contact prompts binding between CD40 ligand (CD40L) on the T cell surface with CD40 on the B cell. The CD40L-CD40 interaction induces increased expression of the adhesion molecule ICAM-1 on the cell surface, which in turn strengthens the interaction between the B cell and T cell, and also induces the CD4 T cell to express cytokines such as IL-4, further inciting B cell proliferation (Parker, 1993).

Upon activation with specific antigen, clonal expansion of the activated B cell occurs, leading either to the transient production of plasmablasts and short-lived extrafollicular plasma cells, which secrete unmutated antibodies, or to germinal centre (GC) formation in nearby lymphoid follicles (Figure 8) (McHeyzer-Williams and McHeyzer-Williams, 2005). Upregulation of Bcl6 and AID expression is a hallmark of GC B cells (Allman et al., 1996, Muramatsu et al., 1999), which can broadly be divided into two cell types; centroblasts and centrocytes. Centroblasts are highly proliferating GC B cells that are present within the dark zone of the GC and are identifiable by surface expression of CD38 and CD77. Centroblasts give rise to centrocytes, which undergo lower rates of proliferation, also express CD38, but lack CD77 expression (Ma and Staudt, 2001). The purpose of the GC reaction is to enable BCR affinity

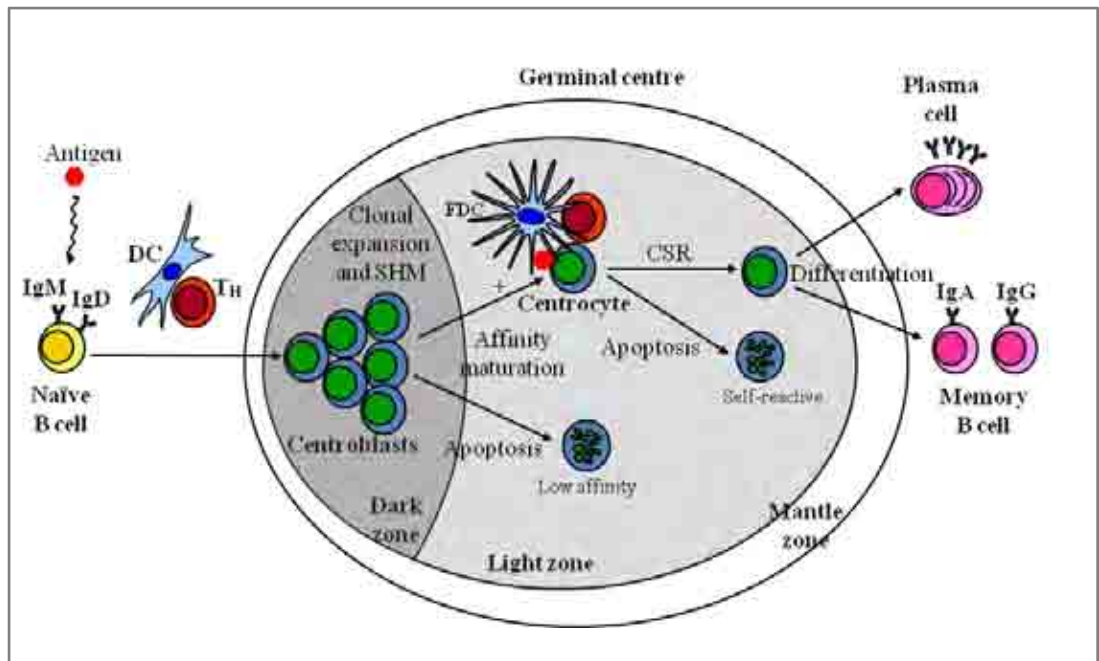


Figure 8. T-dependent B cell activation and differentiation

Upon encounter with antigen in lymphoid tissues, naïve B cells proliferate to form a germinal centre, undergoing SHM and CSR in order to differentiate into memory B cells or antibody secreting plasma cells. GC cells that acquire deleterious mutations or fail to achieve affinity maturation are eliminated by apoptosis. Adapted from Kuppens, 2003.

maturation via somatic hypermutation (SHM) and class switch recombination (CSR). Following the successful completion of these processes B cells are able to leave the secondary lymphoid organ and differentiate into either antibody-secreting terminally differentiated plasma cells, or long-lived resting memory B cells, both of which express highly specific isotype-switched antibodies. Memory B cells are also capable of terminally differentiating into plasma cells upon re-encounter with antigen in secondary immune responses. Antigen-specific antibody titres, which persist within individuals for sustained periods, typically derive from long-lived plasma cells which reside within the bone marrow (McHeyzer-Williams and McHeyzer-Williams, 2005, LeBien and Tedder, 2008, Parker, 1993).

Somatic Hypermutation

Somatic hypermutation (SHM) in humans is a hallmark of the GC affinity maturity process, occurring at the centroblast stage. SHM is dependent on the enzyme, activation-induced cytidine deaminase (AID), which is expressed by centroblasts and initiates mutation by targeting cytidine nucleotide residues for deamination (Muramatsu et al., 1999, Muramatsu et al., 2000). Point mutations introduced during SHM may ultimately lead to amino acid replacements within the heavy and light chain variable regions of the Ig molecule, which in turn impacts on the affinity of the BCR for binding specific antigen. Favourable changes resulting in an increased capacity to bind antigen are subsequently positively selected for, whilst cells bearing unfavourable mutations are eliminated (Peled et al., 2008, McHeyzer-Williams and McHeyzer-Williams, 2005).

Most mutations are single nucleotide changes starting 100-200bp from the transcription initiation site and ending 1.5-2.0 kb downstream. The highest frequency of SHM is found primarily within the V, D and J coding regions of the rearranged Ig locus, with a much lower frequency in unrearranged Ig VDJ segments or the Ig constant region. Compared to the basal rate of mutation in the eukaryotic genome, the rates of IgV region mutation during SHM are estimated to be 10,000 – 1,000,000 times higher (Peled et al., 2008).

At the molecular level, the first step of SHM involves an AID-mediated deamination event converting a cytosine residue to a uracil residue. This base change may be interpreted as a thymidine residue during DNA replication, resulting in a C-T transition mutation in the daughter cell. Alternatively, uracil DNA glycosylase, UNG, may remove the uracil residue to yield an abasic site, which is subsequently subject to DNA repair mechanisms (Schrader et al., 2005). Under normal circumstances, point mutations introduced into the genome are repaired efficiently by high fidelity repair enzymes, such as Pol β (Beard and Wilson, 2006). Within the context of a germinal centre reaction, however, normal repair mechanisms are replaced with error-prone enzymes, such as Pol η and θ , which have the capacity to incorporate further mutations into the afflicted segment during their attempts to repair the AID-induced damage (Delbos et al., 2007, Masuda et al., 2005). Specifically, the processes of base excision repair (BER) and mismatch repair (MMR), normally employed to maintain genome integrity, induce significant diversification of the Ig locus during SHM. Whereas short-patch BER involves repair of the abasic site using any of the four available nucleotides, long-patch BER and MMR ultimately lead to excision of a section of the uracil-bearing strand comprising several

nucleotides, which is then “repaired” by error-prone polymerases which add a mixture of bases to the site, forming a sequence of DNA containing multiple mutations (Di Noia and Neuberger, 2007).

The classic SHM scenario occurs within the context of a germinal centre reaction where antigen-activated naive B cells acquire Ig mutations in a T cell-dependent manner. Various studies have found instances of SHM outside of this familiar setting; both in terms of SHM in non-Ig genes following EBV infection (Epeldegui et al., 2007), and in the absence of germinal centres in non-switched memory cells (Weller et al., 2001) (see below).

Class-Switch Recombination

Whereas SHM of the Ig variable region is important for generating antibody diversity, class-switch recombination (CSR) involves the Ig constant (C) region and determines the effector function of the molecule (Figure 9). This portion of the Ig not only interacts and is bound by other immune cells, epithelial cells and complement, but determines whether antibodies are able to pass through epithelial membranes at mucosal surfaces, tissues, or polymerise for increased avidity. In naive B cells, constant heavy region C μ and C δ genes are transcribed resulting in expression of IgM and IgD. During CSR, double-stranded breaks (DSB) are introduced into switch (S) regions, and the intervening DNA strands removed by an intrachromosomal deletional recombination event (Stavnezer et al., 2008).

S regions are located downstream of each of the CH regions except C δ and consist of tandem repeats of short G-rich sequences (20-80bp). In order for CSR to occur, DSBs must be created in two S regions; the S μ region upstream

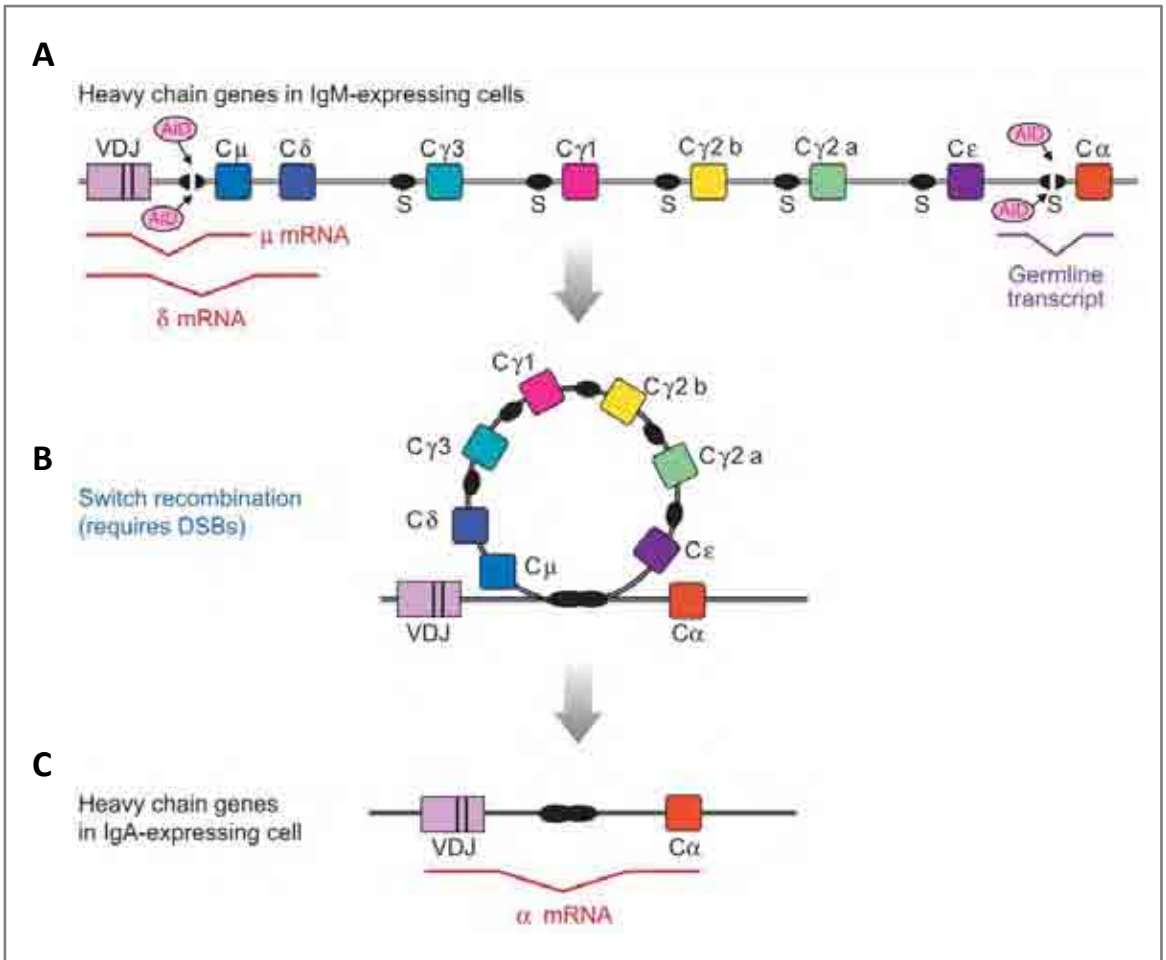


Figure 9. Events during class switch recombination

A B cell expressing IgM and IgD undergoes CSR to IgA. **A.** AID deaminates dC residues in transcriptionally active S regions (S μ and S α in the diagram). **B.** Double-strand breaks in each region enable CSR by intrachromosomal deletion. **C.** The IgH locus after CSR to IgA. Adapted from Stavnezer et al. 2008.

of the C μ gene and any other S region further downstream (denoted S x). The overall length of S regions varies with each isotype (~1kb-12kb), and CSR can occur anywhere within or near to these regions (Dunnick et al., 1993, Min et al., 2005). As with SHM, the enzyme AID is essential for the process of CSR (Muramatsu et al., 2000). AID deaminates dC nucleotides to uracil within transcriptionally active S regions, which subsequently leads to an abasic site following removal of the uracil residue by UNG. Error-prone DNA repair mechanisms generate DSBs at the AID-targeted sites (Schrader et al., 2005). Overhanging strands at the DSBs are either repaired by translesion polymerases, or removed by exonucleases to produce blunt ends, which are then joined by end-joining recombination (Stavnezer et al., 2008). IgG1-4, IgA or IgE isotypes are then expressed.

Every naive B cell has the potential to switch to any of these classes (Jefferis and Kumararatne, 1990, Smith, 1992); however, isotype switching *in vivo* largely depends on the infection instigating the response. Factors involved in isotype switching to particular classes include various cytokines expressed by T cells and dendritic cells (Banchereau and Rousset, 1992, Geha et al., 2003, Toellner et al., 1996). Class switching has been demonstrated in *in vitro* systems using mouse splenic B cells and human naive B cells in numerous studies. In these techniques, CD40 ligation is typically used, together with the addition of cytokines such as IL-4, IL-10, IL-13, IL-21 and TGF β , each of which has been shown to induce CSR (Gascan et al., 1991, Pene et al., 1988, Jabara et al., 1990, Punnonen et al., 1993, Briere et al., 1994, Defrance et al., 1992, Kitani and Strober, 1994, Fayette et al., 1997, Pene et al., 2004, Nagumo et al., 2002, Servet-Delprat et al., 1995). Controversy still remains, however, as to

which isotype expression results from particular cytokines. A recent study exploring stimulation of peripheral blood naive B cells with different cytokine combinations demonstrated that CD40L/IL-4/IL-21 upregulated IgG1 expression, whereas treatment with CD40L and IL-21 alone yielded IgG3 or IgA expression (Avery et al., 2008).

As with somatic hypermutation, CSR is predominantly found in centroblast cells during a germinal centre reaction. However, recent evidence suggests the process may occur at low levels prior to germinal centre formation (Cunningham et al., 2007), or outside the context of the germinal centre. Thus in one study almost normal levels of gut IgA were detected in CD40^{-/-} mice lacking germinal centres (Bergqvist et al., 2006), whilst other studies found evidence of switching in pre-B and immature B cells isolated from bone marrow (Han et al., 2007, Ueda et al., 2007).

1.2.6 T cell-Independent (TI) B cell Activation

In addition to the classical T cell-dependent mechanism, distinct subtypes of B cells, B-1 cells and marginal zone B cells may be activated independently of interaction with T cells (Martin et al., 2001, Zandvoort and Timens, 2002).

Relatively little is known about the function and origins of B-1 cells in humans, and whether they derive from the same progenitors as conventional B cells or have a distinct lineage remains controversial (Martin and Kearney, 2001, Dorshkind and Montecino-Rodriguez, 2007, LeBien and Tedder, 2008). B-1 cells can be further subdivided based on CD5 expression into B-1a (CD5⁺) and B-1b (CD5⁻). While it is believed that both are involved in T-independent (TI) responses, B-1a cells may contribute towards innate immunity, whilst B-1b cells

may be associated with the adaptive response (Haas et al., 2005). Marginal zone B cells, which may be synonymous with circulating IgD+IgM+CD27+ non-switched memory B cells (Weller et al., 2004), have similarly controversial origins and diversification methods (discussed in further detail below). These B cell types may become activated upon contact with pathogens without the necessity for T cell help. TI responses involve recognition of conserved pathogen-associated molecular patterns (PAMPs) such as lipopolysaccharide on gram-negative bacteria, and bacterial or viral unmethylated CpG DNA (Ademokun et al., 2010, Janeway and Medzhitov, 2002). In TI type I responses, non-BCR receptors are utilised, whereas TI type II responses involve direct BCR engagement of pathogen-derived antigens (Ademokun et al., 2010). T-independent B cell activation results in the rapid differentiation into low affinity IgM-secreting polyclonal plasmablasts of a collectively broad specificity for antigen. Although these cells are short-lived and offer no immunological memory upon re-infection, the speed at which they are generated ensures an effective first line of defence against pathogens such as encapsulated bacteria, and as such the TI-independent response is deemed part of innate immunity. TI-independent immunity is not present in humans at birth, but rather develops later in childhood (Ademokun et al., 2010, Parham, 2000).

1.2.7 Non-Switched Memory B cells

Memory B cells (both switched and non-switched) are identifiable on the basis on several criteria; larger cell size with abundant cytoplasm, the ability to induce Ig secretion following appropriate stimulation *in vitro*, mutated Ig genes and, crucially, expression of the TNF-receptor superfamily molecule CD27 (Klein et

al., 1998). Indeed since the majority of B cells displaying these characteristics were all found to express CD27, this molecule is now universally used as the definitive memory B cell marker by most researchers. Subsequently, however, the acceptance that CD27 is an unequivocal marker for memory B cells has been challenged by several findings including; the identification of a subset of CD27+ precursor B cells in the bone marrow (Vaskova et al., 2008), and the isolation of CD27- class-switched B cells within the peripheral blood (Fecteau et al., 2006, Wei et al., 2007). Furthermore the ongoing debate as to the origins of NS memory B cells also brings into question the validity of CD27 as a marker of memory, as it has been suggested that these CD27-expressing cells undergo prediversification independently of antigen-driven activation, and therefore should not be classified as memory B cells at all.

The NS memory subset is identifiable by its IgM+IgD+CD27+ phenotype and mutated Ig genotype, which is highly similar to that of marginal zone B cells. Indeed NS memory B cells are often referred to as marginal zone B cells, regardless of their anatomical location. Since the cells express a mutated BCR, which would normally be indicative of GC-associated SHM, yet appear not to have completed a typical GC reaction since CSR has not taken place; their method of diversification is unclear.

Three main theories have been proposed describing the development of IgM+IgD+CD27+ subset; (i) the cells are products of abortive germinal centre reactions following TD antigen stimulation, (ii) the cells have a role in TI responses and diversify their BCR in extrafollicular sites and (iii) the cells are neither the products of TD nor TI antigen-driven activation and are instead prediversified prior to participating in an immune response.

T-dependent Diversification

NS memory B cells may be activated in a T-dependent manner yet only go through a partial GC reaction, exiting the GC before CSR is initiated. This hypothesis was initially put forward due to the morphological and genotypic similarities between non-switched and conventional memory B cell types (Klein et al., 1998). Recent work to support this view found mutations within the Bcl6 locus of IgM+IgD+CD27+ B cells, an event restricted to the confines of a GC reaction where Bcl6 is predominantly expressed, together with evidence for clonally related NS and S memory B cells sharing the same Ig mutations, presumably acquired by a common ancestor GC B cell within the reaction (Seifert and Kuppers, 2009). Fascinatingly, although this study provides solid evidence to support the hypothesis of a TD route for the development of NS memory B cells, recent, equally compelling findings from a separate investigation, directly contradict the work carried out by Seifert and Kuppers. Comparisons of IgVH gene usage from different B cell subsets concluded not only that switched and non-switched memory B cells carry significantly distinct IgVH repertoires, indicating separate diversification pathways for each, but that within this pool of >1500 IgG and IgM memory B cell Ig genes studied, no clonally related cells were isolated (Wu et al., 2010).

T-independent Diversification

The original argument for T-independent (TI) IgM+IgD+CD27+ B cell development comes from studies of X-linked hyper-IgM (HIGM) patients (Agematsu et al., 1998, Weller et al., 2001). Defects within CD40 or CD40L prevent the interaction between the two molecules which normally follows

antigen activation, leading to a lack of T-B collaboration in these patients. As such, germinal centre reactions cannot occur, resulting in a lack of isotype-switched memory B cells. Intriguingly these patients have high levels of circulating IgM+IgD+CD27+ memory B cells, which express BCRs carrying mutations, albeit at lower rates than age-matched donor controls (Agematsu et al., 1998, Weller et al., 2001). The presence of an IgM+IgD+CD27+ subset in HIGM patients suggests an alternative role for these cells, leading to the proposal that NS memory B cells may be involved in TI responses. The theory that peripheral blood IgM+IgD+CD27+ B cells are essentially circulating marginal zone B cells supports this argument (Weller et al., 2004). Studies of B cell subsets in asplenic individuals revealed little or no NS memory B cells within the peripheral blood, a finding which correlated with increased occurrence of infections with encapsulated bacteria such as *Streptococcus pneumoniae* (Kruetzmann et al., 2003). Regarding the diversification of these cells during TI responses, Kruetzmann et al. suggested possible SHM within extrafollicular sites of the spleen. Alternatively, evidence of low levels of hypermutation within GCs of transgenic mice formed in response to TI antigens such as NP-ficolI, suggests that GC-dependent SHM is possible in the absence of a classical TD response (de Vinuesa et al., 2000, Toellner et al., 2002).

Prediversification Prior to an Immune Response

In the scenarios described above, the involvement of IgM+IgD+CD27+ NS memory B cells in either TD responses or TI responses, assume that these cells are true memory B cells that are derived from antigen-activated IgM+IgD+CD27- naive B cells. There are, however, several convincing studies indicating that the NS memory B cell subset is not formed as a result of a typical

immune response, but rather represents a prediversified cell population that is formed via a separate developmental route to conventional mature B cells. Several factors support this notion, primarily the existence of a somatically mutated IgM+IgD+CD27+ memory B cell population in the blood and spleen of young infants and in cord blood and foetal tissues. Such evidence indicates that these cells are already diversified prior to pathogenic contact, although their number and IgH mutation frequency increases with age (Weller et al., 2008, Weller et al., 2001, Scheeren et al., 2008, Weller et al., 2004). In addition, an examination of B cell subsets in children under the age of two years was carried out by Weller et al. to look for evidence of antigen-driven clonal expansion within the different populations. This investigation took advantage of the fact that children of this age group have not yet fully developed TI responses, yet undergo childhood vaccinations which engage TD responses. IgH spectratyping was carried out to analyse lengths of CDR3 regions within B cell populations; a technique based on the premise that clonally unrelated B cells bear unique CDR3 sequences and therefore a collection of diverse cells will present a range of different CDR3 lengths. As expected naive B cell populations revealed an extremely diverse CDR3 repertoire, whereas conventional memory B cell populations displayed a very restricted repertoire of CDR3 lengths, indicative of antigen-driven clonal expansion as a result of TD responses generated by the vaccinations. By contrast, the IgM+IgD+CD27+ NS memory B cells examined showed a diverse repertoire similar to that of naive B cells, indicating a lack of clonal expansion. Furthermore, these diverse IgM+IgD+CD27+ B cells, which were isolated from individuals who were incapable of mounting TI immune responses, carried mutated Ig genes, strongly

suggesting the process of SHM occurred in these cells in the absence of either a TD or a TI response (Weller et al., 2008).

Although the debate concerning the development and diversification processes of the IgM+IgD+CD27+ memory B cell subset remains ongoing, with convincing arguments presented from each viewpoint, a fourth possibility may be that these cells do indeed undergo pre-diversification, but then go on to participate in TD or TI responses, which may account for the increase in cell number and mutations with age.

1.2.8 Activation-Induced Cytidine Deaminase (AID)

The enzyme activation-induced cytidine deaminase (AID) is a 24kDa protein which shuttles back and forth between the cytoplasm and nucleus. Structurally the carboxy (C) terminal of the protein is involved in CSR, whereas the amino (N) terminal facilitates SHM (Bransteitter et al., 2004). AID is highly expressed in centroblast B cells; however, lower expression has been detected elsewhere in immature and transitional B cells from human cord blood and foetal tissues (Kuraoka et al., 2009), plasmablast-like cells in mouse spleens during TI responses (Han et al., 2007), in small numbers of peripheral blood memory B cells (Wu et al., 2008), and in B cells stimulated with IL-4 *in vitro* (Zhou et al., 2003).

Five separate AID variants have been identified (Figure 10). The most prevalent transcript in healthy cells is known as AID full-length (AID-FL) (Revy et al., 2000, Greeve et al., 2003), and contains five exons. The second variant, AID- Δ E4a carries a 30bp deletion in exon 4 (Noguchi et al., 2001, Oppezso et al., 2005, Oppezso et al., 2003, Greeve et al., 2003), whilst a third variant, AID-

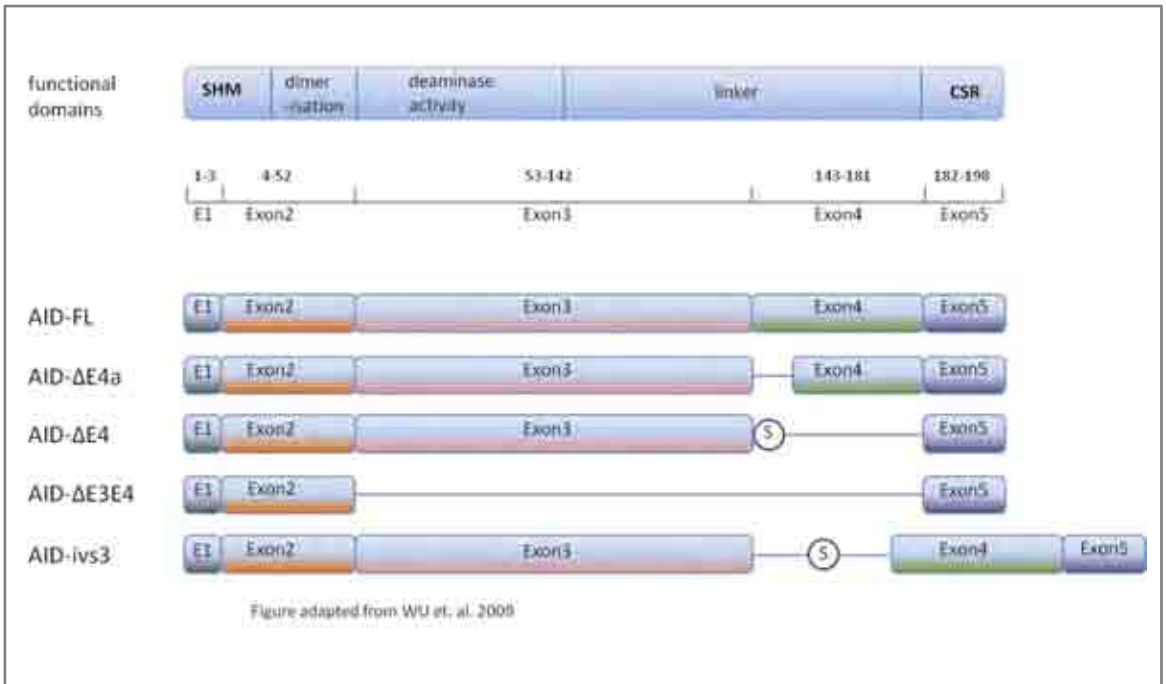


Figure 10. Functional domains of AID isoforms

The upper diagram highlights the functional domains of the full-length molecule, including the somatic hypermutation (SHM) and class switch recombination (CSR) domains. The lengths of the corresponding exons are given below. Exon arrangements of five distinct AID variants; AID-FL, AID-ΔE4a, AID-ΔE4, AID-ΔE3E4 and AID-ivs3 are shown. Adapted from (Wu et al., 2008).

$\Delta E4$, is missing all of exon 4 (Noguchi et al., 2001, Oppezzo et al., 2003). The fourth AID- $\Delta E3E4$ transcript lacks both exon 3 and exon 4 (Greeve et al., 2003), whereas in the AID-ivs3 transcript the intronic sequence between exons 3 and 4 is retained (Greeve et al., 2003, McCarthy et al., 2003, Albesiano et al., 2003). Alternative transcript expression has been reported in asthmatic patients (Noguchi et al., 2001), cases of non-Hodgkin's lymphoma (Greeve et al., 2003), chronic lymphocytic leukaemia (McCarthy et al., 2003), and in B cells stimulated with CD40L and IL-4 (Oppezzo et al., 2003).

Recent work examining AID variant transcripts in detail suggests not only that expression by single B cell chronic lymphocytic leukemia (B-CLL) cells is restricted to one variant type, but that splicing results in specific impairment of the AID function, depending on which exon is missing. Specifically, in relation to SHM activity the authors suggest the variant AID- $\Delta E3E4$ does not support SHM, whereas the variants AID- $\Delta E4a$ and AID- $\Delta E4$ showed increased levels of SHM. Class-switch recombination was defective in all splice variants (Wu et al., 2008).

In vitro studies have revealed that within cell-free systems AID only targets single-stranded (ss) DNA, however C in double-stranded (ds) DNA is deaminated *in vivo*. Strong evidence suggests that this is due to the availability of ssDNA within transcription bubbles of genes that are being actively transcribed (Bransteitter et al., 2003), and therefore transcription itself is essential for AID activity. As hypermutation occurs at the highest rates within Ig genes, much speculation exists as to the mechanisms employed in AID targeting. It is clear that gene transcription is not the only factor required for AID action since not all genes undergoing transcription in centroblasts are

mutated (Shen et al., 2000). Possible explanations include targeting of AID to the Ig locus either via increased accessibility to this part of the genome, or by active recruitment of the enzyme by additional proteins or cis-acting sequences. Alternatively, error-prone repair mechanisms may be selectively employed to deal with AID-induced deaminations within the Ig, whereas those inflicted elsewhere in the genome may be repaired in an error-free fashion (Peled et al., 2008). Another aspect to this puzzle is that SHM has been discovered within non-Ig genes in normal individuals (Bcl6, CD79 and CD95) (Shen et al., 1998, Muschen et al., 2000, Gordon et al., 2003), as well as in malignant B cells (Bcl6, Pim1, Myc, RhoH/TTF and Pax5) (Pasqualucci et al., 2001, Pasqualucci et al., 1998), albeit at much lower levels than within the Ig locus. Of particular relevance to this study are the reports not only of AID upregulation following EBV infection of B cells *in vitro* (He et al., 2003), but also the discovery that this EBV-induced AID expression, together with an upregulation of pol- η corresponds to SHM within the proto-oncogenes, Bcl6 and p53 (Epeldegui et al., 2007). Work published by others has shown that whilst splenic naive B cells induced to express AID in short-term culture undergo CSR, no SHM was seen (Petersen et al., 2001). However, at the time of writing no other studies have focussed on SHM in naive B cells induced to express AID following EBV infection *in vitro*.

1.3 *EBV Colonisation in Vivo*

1.3.1 Primary Infection

EBV is transmitted orally during exchange of saliva. Typically individuals become infected in an asymptomatic manner during infancy via close familial

contacts. In some instances however, usually in societies of the developed world, when the virus is acquired later in life during adolescence or adulthood, infection can produce the self-limiting disease known as infectious mononucleosis (IM) (Gratama et al., 1990, Crawford et al., 2006). Although it is known that EBV enters the host via the oropharynx, the initial target cell infected by EBV is still a matter of debate. The two principal candidates include (i) epithelial cells and (ii) B cells.

Epithelial cells in Primary EBV Infection

Early studies of EBV primary infection described high titres of virus recorded from the saliva and throat washings of IM patients (Gerber et al., 1972). More specifically, EBV DNA and lytic transcripts were detected in epithelial cells that had been shed into throat washings, suggesting that they were not only permissive for EBV infection, but also for the lytic production of new infectious virus (Sixbey et al., 1984). Although both these investigations point to the oropharyngeal epithelium as an important reservoir for EBV infection during IM, subsequent studies using post-mortem tongue biopsies from a range of non-IM patients only found evidence of epithelial cell lytic infection in a very small proportion (1.3%) of tongue mucosal samples (Frangou et al., 2005), or in conjunction with an impaired immune response either as a result of immunosuppressive therapy or terminal cancer (Herrmann et al., 2002).

B cells in Primary EBV Infection

In contrast several separate studies provide evidence that B cells are the principal target for EBV during primary infection. More than one investigation failed to find evidence of EBV replication within the epithelium, but instead

found that infection was confined to B cells, with lytic antigens identified within plasmacytoid B cells located proximally to epithelial crypts (Anagnostopoulos et al., 1995, Niedobitek et al., 1997). These observations are supported by *in vitro* epithelial cell infection experiments. While infection with cell-free virus is extremely difficult to achieve *in vitro*, co-culture of epithelial cells with infected B cells increases the efficiency of epithelial cell infection up to 1000-fold (Shannon-Lowe et al., 2006), suggesting that B cell-mediated delivery of the virus is a prerequisite for epithelial cell infection. Examination of patients with the rare hereditary disorder XLA also favours the hypothesis that B cells are the initial target for EBV colonisation. Since this disease is characterised by a lack of circulating mature B cells, it is reasonable to assume that these individuals are unlikely to support persistent long term EBV infection. Indeed no evidence of the virus was detected either in throat washings or peripheral blood. More importantly no EBV-specific T cells could be found in these patients, suggesting not only a lack of persistent infection, but also an inhibition of primary infection in the absence of mature B cells (Faulkner et al., 1999), supporting the hypothesis that B cells are required for epithelial cell infection. Considering all the evidence described above, it is likely that that EBV first infects B cells, not least since the virus ultimately establishes stable persistence within the B cell population.

1.3.2 Establishment of Persistent Infection

Assuming EBV primarily targets oropharyngeal B cells for infection, there is further dispute as to the exact order of events and B cell subtypes involved in early stages of infection leading to persistent colonisation. In order to identify the predominant B cell types infected with EBV, investigators have focussed on

phenotypic expression of B cell markers, and genotypic differences in Ig sequences. Such investigations have revealed that latent EBV infection is largely restricted to the IgD-CD27+ switched memory B cell population within the peripheral blood of both healthy carriers and IM patients, and is excluded from the IgD+CD27- naive B cell population (Babcock et al., 1998, Hochberg et al., 2004). This finding has been further substantiated by Ig analysis of individual EBV-infected cells, which were found to contain mutated IgV regions, consistent with a memory B cell genotype (Souza et al., 2005). Although the outcome of primary EBV infection is the persistent infection of the switched memory B cell compartment, the mechanisms the virus employs to achieve this goal remain controversial. More than one model has been proposed to describe these events, with the key disparity between the hypotheses resting on whether or not the process is dependent on germinal transit (Figure 11).

Germinal Centre-Dependent Colonisation of Memory B cells

Perhaps the most popular explanation for memory B cell colonisation, put forward by Thorley-Lawson and colleagues, suggests that the virus uses a Latency III pattern of gene expression to mimic physiological antigen-driven naive B cell activation, followed by subsequent germinal centre-mediated differentiation into a memory cell (Thorley-Lawson and Gross, 2004). This hypothesis is based on the findings that EBV expresses different forms of latency in different B cell types *in vivo*. In this model, initial infection is proposed to occur in naive B cells since these are the only cell type within the oropharynx where Latency III infection has been detected (Babcock et al., 2000, Joseph et al., 2000a). A subsequent switch from Latency III to Latency II then pushes the infected naive B cell to become a GC B blast (Thorley-Lawson, 2001, Babcock

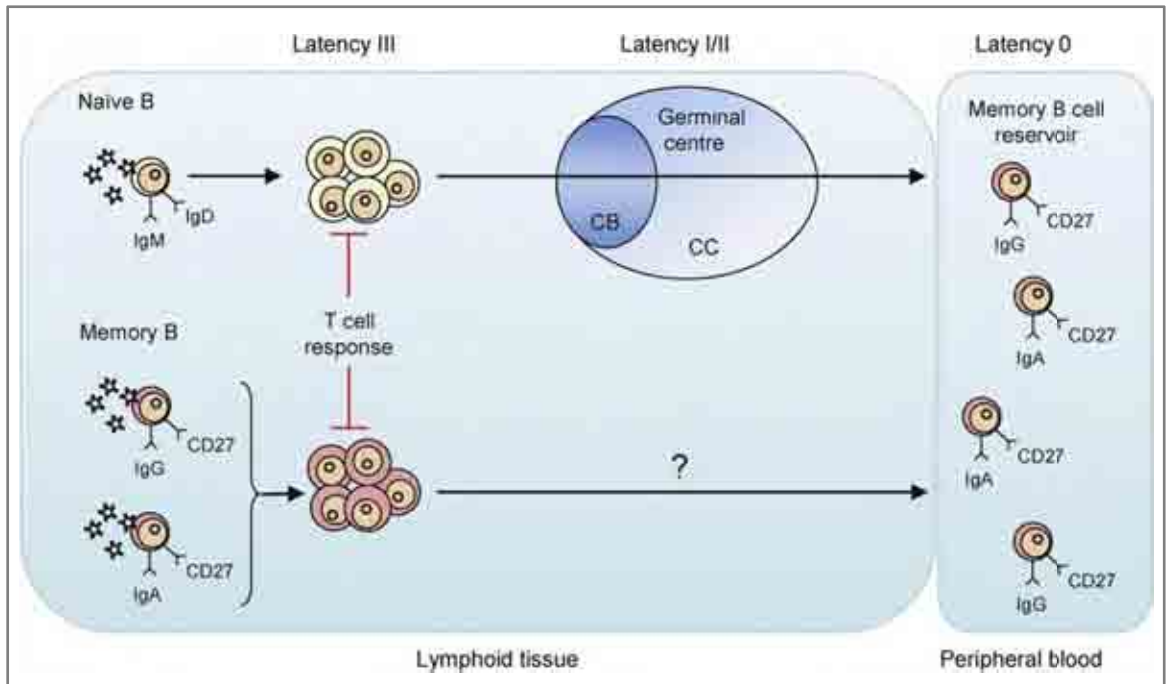


Figure 11. Selective colonization of the memory B cell compartment during primary EBV infection

Two theories describing EBV colonisation of the memory B cell population. One hypothesis proposes that the virus preferentially infects IgM⁺IgD⁺ naïve B cells, transiently expressing latency III genes, of which LMP1 and LMP2 are able to mimic antigen stimulation and drive the cell through a germinal centre (GC) reaction. Thereafter the physiological processes of SHM and CSR take place and deliver latently infected IgG⁺CD27⁺ or IgA⁺CD27⁺ progeny cells into the long-lived memory compartment. An alternative hypothesis, based on histochemical studies of individual cells micro-dissected from IM tonsillar tissue, questions the involvement of GC transit and instead proposes the preferential infection and/or survival of memory cells post-infection, compared to their naïve counterparts. Taken from Rowe et al. 2009.

and Thorley-Lawson, 2000) via the expression of LMP1 and LMP2, which are able to substitute for the T cell help and BCR signals normally required following antigen activation (Kilger et al., 1998, Caldwell et al., 1998). The infected cell is then presumed to transit through the GC processes of SHM and CSR, simultaneously carrying the virus, until completion of the differentiation process yields an infected memory B cell (Thorley-Lawson and Gross, 2004). All viral gene expression is then switched off by the time the infected cell has acquired its memory characteristics.

Germinal Centre-Independent Colonisation of Memory B cells

Alternative models have also been suggested to explain the selective colonisation of memory B cells. One of the principal arguments against the GC model is the difficulty to detect EBV-positive GC B cells. The virus has been detected within tonsillar CD10+ B cells (Babcock et al., 2000), and although the reliability of this phenotypic molecule as a GC marker is debatable since immature B cells also express CD10 (Kalled et al., 1995), a very recent study attempted to validate these EBV-infected CD10+ B cells as GC derived since they co-express the characteristic GC proteins AID and Bcl6 (Roughan and Thorley-Lawson, 2009). Immunohistochemical evidence for the presence of EBV within tonsillar GCs is, however, unconvincing and is more consistent with the second model of EBV persistence; the direct infection of memory B cells (Kurth et al., 2000, Kuppers, 2003). Thus, in immunohistochemical examinations of IM tonsillar tissue, EBV-positive cells have been consistently identified in extrafollicular areas, but only rarely in follicles or germinal centres (Anagnostopoulos et al., 1995, Niedobitek et al., 1997, Kurth et al., 2000, Kurth et al., 2003). In these studies, significant variation has been found regarding

both the type of infected cell, and the viral proteins expressed therein. The following is a summary of morphological descriptions of infected cells, together with viral expression: (a) small cells expressing EBNA2 but not LMP1, which may reflect recent infection, (b) slightly larger lymphoblastoid cells expressing EBNA2 and LMP1, possibly reflecting a Latency III type infection, (c) large blast-like cells, which morphologically resemble HRS cells and express LMP1 in the absence of EBNA2, (d) a small population of small cells expressing neither EBNA2 nor LMP1, which resemble peripheral blood memory B cells.

Interestingly, morphologically distinct EBV-infected cells belonging to the same clone have been isolated in these investigations (Kurth et al., 2000), suggesting that the cell morphology and EBNA1/LMP1 expression patterns described above may represent sequential stages of virus infection. Based on these findings, it has been suggested that the Latency III program is expressed immediately upon infection of the host B cell, as evidenced by the EBNA2+/LMP1+ lymphoblastoid cells, followed either by downregulation of EBNA2 as seen in the blast-like cells, or by downregulation of both proteins, as seen in the small resting cells. Taken together, the studies by Anagnostopoulos et al., Niedobitek et al. and Kurth et al. provide convincing evidence that infection occurs within tonsillar extrafollicular areas, and argue against obligatory GC transit of infected cells. Instead, the direct infection and preferential expansion of memory B cells within the tonsil is a more likely explanation for these observations. This is further supported by studies analysing the mutational status of the Ig V region of individual EBV-infected B cell clones from IM tonsils (Kurth et al., 2003). While the virus was detected in both unmutated, genotypically naive B cells and mutated B cell clones, there

was no evidence of EBV infection within cell clones that were actively undergoing SHM (identifiable by intraclonally diverse IgV sequences), i.e. cells that were, by definition, true GC B cells. Instead, infection was confined to memory B cell clones with identical IgV mutations, suggesting expansion of infected cells occurred following completion of the GC reaction.

Susceptibility of B cell Subsets to EBV Infection

The susceptibility of different B cell subsets to EBV infection *in vitro* have yielded results that collectively suggest no significant difference exists between naive or switched memory tonsillar B cells. In one experiment where total tonsillar B cells were infected, the relative proportions of IgM+, IgA+ or IgG+ transformed cells were comparable to the starting population (Ehlin-Henriksson et al., 2003). A separate examination of tonsillar B cell populations that were separated based on expression of CD19 and CD27, found that whilst both CD27- naive and CD27+ memory B cells were equally susceptible to infection *in vitro*, when CD19+CD27+ B cells were further separated into IgA or IgM switched, or IgM non-switched tonsillar memory B cells, the switched population produced a higher frequency of infection (Dorner et al., 2008). A more recent study has compared infectibility of B cells from nasopharyngeal-associated tissue (NALT) with B cells from peripheral blood or other lymphoid locations (Dorner et al., 2010). This investigation concluded that whilst naive and memory B cells from NALT are equally susceptible to EBV infection, memory B cells from NALT are significantly more infectable than those from remote lymphatic organs. In addition the investigators have proposed that the surface molecule beta-1 ($\beta 1$) integrin expressed by NALT B cells, is a marker for increased susceptibility to EBV infection (Dorner et al., 2010). When non-NALT

peripheral blood memory B cells were stimulated with CD40, together with BCR cross-linking in the same study, an increased susceptibility to EBV infection was observed. Based on their results, this group has suggested that EBV may take advantage of the activation status of NALT memory B cells in order to establish persistence directly via the colonisation of memory B cells (Dorner et al., 2010).

1.3.3 Persistent Infection

In the weeks following IM presentation, the EBV DNA load within peripheral blood mononuclear cells (PBMCs) falls significantly, whereas high viral loads persist in saliva for up to 34 weeks (Balfour et al., 2005, Fafi-Kremer et al., 2005). It appears from these studies that IM patients remain highly infectious during convalescence and the length of time it takes for them to acquire viral loads comparable to long-term carriers remains unknown. The majority of healthy EBV carriers shed virus intermittently (Balfour et al., 2005, Yao et al., 1985) as a result of viral replication with the oropharyngeal epithelium.

Detection of lytic cycle transcripts within plasmacytoid cells located close to the crypt epithelium suggests the virus lytic cycle may be reactivated in B cells during their terminal differentiation to plasma B cells (Anagnostopoulos et al., 1995, Thorley-Lawson and Babcock, 1999). It has thus been suggested that following reactivation in infected B cells virus is transferred to oropharyngeal epithelial cells, where lytic replication occurs (Rickinson and Kieff, 2007).

In chronic EBV carriers, the frequency of infected B cells within the peripheral blood is approximately 1-50 per 10^6 ; a value which is around 1000-fold lower than that estimated for IM patients (Miyashita et al., 1995, Khan et al., 1996). Within the B cell population, persistent infection is reportedly limited to the

switched memory subgroup (Babcock et al., 1998), and in such cells, all viral gene expression is silenced with the exception of EBERs and BARTs (Tierney et al., 1994, Chen et al., 1999). Indeed it is likely that restricted pattern of latency, characterised by downregulation of immunogenic viral proteins, facilitates evasion of cytotoxic T cell-mediated clearance of infected cells, thereby ensuring long term persistence of the virus.

The frequency of EBV-infected cells estimated within tonsils is comparable to peripheral blood values. In lymph nodes located elsewhere such as the spleen and mesenteric lymphoid tissue, the frequency of infected B cells is approximately 20-fold lower than in the tonsils (Laichalk et al., 2002). It has been suggested that these cells are oropharyngeal-derived circulating B cells performing surveillance of more distal lymphoid tissue before returning to the oropharynx (Laichalk et al., 2002).

Histological examination of chronic carrier tonsils revealed the presence of low numbers of EBER-positive cells which do not express either EBNA2 or LMP1. The cells, which morphologically resemble small lymphocytes consistent with memory B cells, are located in extrafollicular regions (Niedobitek et al., 1992). Some studies have also isolated low numbers of EBV-positive naive B cells (Babcock et al., 2000, Joseph et al., 2000a, Laichalk et al., 2002), and the detection of lytic replication in these cases could indicate they are examples of *de novo* infection (Babcock et al., 1998, Babcock et al., 2000, Joseph et al., 2000a). In addition, investigations employing RT-PCR techniques to examine viral load in tonsillar B cell subsets have found Latency III transcripts within the naive B cell subset (Babcock et al., 2000, Joseph et al., 2000a). In parallel, GC and memory B cells populations were found to express LMP1, LMP2A and Qp-

initiated EBNA1 transcripts, characteristic of a Latency II gene expression pattern.

1.4 Immune Response to EBV Infection

Herpesviruses have co-evolved with their hosts and ancestors for millions of years, and as such a fine balance has been struck between viral infection and persistence, and the ability to mount an effective immune response. Although EBV is widespread within the human population with up to 90% of individuals infected, virus-associated disease is relatively rare. The virus is never fully cleared from the host due to adaptive mechanisms employed to evade detection from immunity. One such strategy is the ability to downregulate expression of viral antigens and exist in a silent state within resting memory B cells, which effectively function in the same way as their uninfected counterparts.

1.4.1 Antibody Response against EBV Infection

The presentation of IM is typically characterised by increased levels of heterophile antibodies within the serum, which may persist for up to one year (Blake et al., 1976). Consequently one of the most established diagnostic tools for the detection of IM, the monospot test, is designed to detect the presence of these antibodies via their ability to agglutinate sheep and horse erythrocytes. Although the monospot test is arguably the most traditional assay used for IM diagnosis, its tendency to yield false positive results has ultimately led to the development of more specific methods (Sumaya and Ench, 1985). Enzyme immunoassays are commonly used to detect IgG and IgM antibodies that are reactive against viral capsid antigen (VCA) and EBNA1. EBV-specific proteins

can also be used to estimate the stage of infection. For example IgG reactivity against early antigen (EA) can be detected at all stages of infection, whereas IgG anti-p23 is prevalent early on, and EBNA1 antibodies which are detectable between four to eight weeks during illness are reportedly an indicator of past infection (Bauer, 2001). In addition, EBV infections are generally characterised by a transition from an increase in IgG avidity over time; in one particular study, anti-VCA IgG was found to be low in patients with recent infections, but higher in patients with past infections (Gray, 1995, Robertson et al., 2003). This persistent antibody response against a lytic cycle antigen is consistent with the suggestion that EBV infection undergoes intermittent lytic reactivation throughout the host's lifetime.

1.4.2 Cell-Mediated Responses to EBV Infection

The most extensively studied and possibly most important component of the cellular immune response against EBV is the CD8+ T cell response. Acute IM is marked by an expansion of CD8+ T cell populations of oligoclonal T cell receptor (TCR) usage (Annels et al., 2000). Remarkably, during IM individual epitope responses are accountable for 1%-40% of the total CD8+ T cell population, with reactivities to immediate early (IE) or early (E) lytic proteins being dominant. Responses to latent proteins are smaller, accounting for 0.1%-5% of CD8+ T cells, and are usually reactive against the EBNA3 family of proteins (Hislop et al., 2007). Antigen-stimulation of EBV-specific CD8+ T cells isolated from IM blood is required to prolong survival *in vitro* (Callan et al., 2000, Dunne et al., 2002, Tamaru et al., 1993), perhaps explaining why EBV-specific CD8+ populations decline rapidly *in vivo*, following the limited availability of viral antigen upon entrance into latency (Hislop et al., 2007). In the months following

IM, the surviving low numbers of EBV epitope-specific CD8+ T cells lose expression of activation markers such as CD38 and Ki-67, indicating that they are no longer in an activated state (Catalina et al., 2001, Hislop et al., 2005).

Investigations focussing on long-term virus carriers with no history of IM have revealed that memory CD8+ T cells are maintained in the presence of low level antigenic stimulation, most of which display a resting phenotype and lack activation markers such as CD38 and CD69 (Catalina et al., 2002, Hislop et al., 2001). Individual epitope-specific populations account for 0.2%-2% of the CD8+ T cell population in the case of lytic epitopes (Benninger-Doring et al., 1999, Saulquin et al., 2000, Bihl et al., 2006), and 0.05%-1% in the case of latent epitopes (Bihl et al., 2006). Although fluctuations in the frequency of memory CD8+ T cells can be seen over time, levels remain more or less stable (Crough et al., 2005) until later on in life when an increase is observed; 60+ year old individuals may harbour up to 14% CD8+ T cells against individual EBV epitopes (Ouyang et al., 2003, Khan et al., 2004).

Significantly less is known about the CD4+ T cell response during primary EBV infection. The CD4+ T cell pool does undergo an expansion such as that seen in the CD8+ T cell population, but no marked oligoclonality can be observed (Maini et al., 2000). The frequencies of EBV-specific CD4+ T cells are very low relative to their CD8+ counterparts, but are nonetheless comparable to CD4+ responses to other pathogens (Gamadia et al., 2003). Responses to several latent and lytic antigens have been studied, with the most common CD4+ T cell response being to the immediate early (IE) protein BZLF1, less common responses observed against BMFL1 or the latent protein EBNA3A, and the least frequent against EBNA1 (Woodberry et al., 2005, Precopio et al., 2003). As

with the CD8 response, EBV-specific CD4+ T cell numbers peak during acute IM and decline rapidly thereafter (Precopio et al., 2003).

There is conflicting evidence for and against the involvement of the natural killer (NK) cell response during EBV infection. The NK response is an important component of the early innate immune response, and has been shown to play a role in the early response against CMV infections in mice and humans (Braud et al., 2002, Vidal and Lanier, 2006). Expansions of NK cells have been observed in the blood of acute IM patients (Williams et al., 2005), and NK cells have been found to inhibit resting B cell transformation by EBV *in vitro* via IFN γ production (Lotz et al., 1985). Clinical evidence, however, conflicts with these studies since, in recipients of T-depleted stem cell transplants, EBV-driven lymphoproliferative disease (LPD) is most common during the 3-6 months following transplantation, the time period in which the NK cell, but not the T cell population has recovered (O'Reilly et al., 1997).

1.5 *EBV-Associated Diseases*

1.5.1 **Infectious Mononucleosis**

Infectious mononucleosis (IM) most commonly affects individuals within the second decade of life, and is the result of primary EBV infection that has been delayed until adolescence as a result of the improved economic and sanitation standards of the developed world (Takeuchi et al., 2006, Luzuriaga and Sullivan, 2010). Studies carried out in the U.S. using cohorts of university students have revealed the incidence of I.M. to be approximately 500 cases per 100,000 individuals per year. The highest incidence occurs in the 15 to 24 year age group, with between 30 to 50% of primary infections manifesting as IM

(Crawford et al., 2006). The virus is transmitted through saliva, and in IM cases predominantly via kissing (Thorley-Lawson, 2001). Although the delay between infection and the onset of symptoms means many of the initial events in infection have already taken place by the time patients present at clinic, the incubation period has been estimated to be between 30 and 50 days (Luzuriaga and Sullivan, 2010).

During IM, lytic replication at oropharyngeal sites results in high levels of virus being shed into saliva (Balfour et al., 2005, Hadinoto et al., 2008). Such shedding decreases over the first year following IM presentation, but thereafter persists at lower levels for life (Hadinoto et al., 2009). In addition to high virus loads in saliva, levels of detectable virus are also significantly increased within the B cell reservoir of both the peripheral blood and tonsils. IM is also characterized by lymphocytosis, including a large expansion of T cells (Callan et al., 1998, Catalina et al., 2001, Precopio et al., 2003), with evidence to suggest that this response not only limits primary infection and controls chronic infection, but that it may also contribute to the symptoms of IM (Hadinoto et al., 2008, Clute et al., 2005). Although the vast majority of IM cases make full recoveries, a history of IM is associated with an increase risk of developing both multiple sclerosis (Thacker et al., 2006) and HL (Hjalgrim et al., 2003, Lunemann and Munz, 2009).

Various risk factors have been suggested for the development of IM during primary EBV infection. These include; (i) age-related alterations in host immunity, for example the exaggerated CD8⁺ T cell response observed in IM may be a result of cross-reactivity of the memory T cell repertoire with earlier infection (Clute et al., 2005), (ii) polymorphisms in the HLA class I locus

(McAulay et al., 2007), (iii) sexual behavior (Crawford et al., 2006), and (iv) infection with EBV type 1 (Crawford et al., 2006).

1.5.2 X-Linked Lymphoproliferative Disease

X-linked lymphoproliferative disease (XLP) is an extremely rare disorder inherited on the X chromosome. It was first identified in 1975 when three maternally related boys succumbed to fatal IM (Purtilo et al., 1975), and is characterized by extreme sensitivity to EBV infection (Seemayer et al., 1995, Nagy and Klein, 2010). Primary EBV infection in these patients leads to fulminant, often fatal IM in approximately 50% of cases, the development of malignant tumours in 30%, and dys-gammaglobulinemia in 30%. Around 53% of XLP patients develop lymphomas (which are not always EBV-associated), and the risk of lymphoma development has been estimated to be 200-fold (Nagy et al., 2009).

The causative factor of this disease is the inheritance of mutations within the SH2D1A gene, which encodes the signaling lymphocytic activation molecule (SLAM)-associated protein (SAP) (Coffey et al., 1998, Nichols et al., 1998, Sayos et al., 1998, Veillette, 2006). Expression of SAP has been detected in NK cells, T cells and thymocytes (Nichols et al., 1998, Liu et al., 2002, Sayos et al., 2000), and is upregulated in activated T cells *in vitro* (Nagy et al., 2009), and elevated numbers of SAP-expressing T cells have been observed at the time of IM presentation in non-XLP patients (Williams et al., 2004). SAP deficiency interferes with the CD4+ T cell help required by B cells in order to produce competent GCs and GC activities (Crotty et al., 2003, Ma et al., 2005, Cannons et al., 2006). XLP patients can therefore present with hypogammaglobulinemia

even in the absence of EBV infection, together with an impaired IgG or IgA antibody response, which is mostly likely a result of the poor GC formation observed in these cases (Ma et al., 2006).

Recent studies have described pro-apoptotic function for the SAP protein in BL cell lines (Nagy et al., 2004, Nagy et al., 2009). Since the marked reduction of white cells occurring 3 to 16 days following IM presentation is reportedly a result of T-cell-mediated apoptosis, a link has been suggested between the clearance of EBV-infected B cells and the role of SAP, whose expression is upregulated in the T cells of IM patients (Nagy and Klein, 2010, Nagy et al., 2009). This hypothesis is indeed consistent with the extreme sensitivity to EBV infection observed in SAP-deficient XLP patients, who are unable to eliminate lymphocyte expansions. Furthermore, these investigators suggest that in XLP, which is also characterized by increased levels of lymphoma, DNA-damaged B cells that would be removed by apoptosis in healthy individuals, are able to survive in and go on to acquire mutations which ultimately result in lymphoma development (Nagy and Klein, 2010).

1.5.3 Post-Transplant Lymphoproliferative Disease

Immunocompromised individuals with depleted T cell numbers are at high risk of developing B cell lymphomas. Perhaps the most extensively studied example of these EBV-associated lymphomas is the condition known as post-transplant lymphoproliferative diseases (PTLD), which arises in transplant recipients who are undergoing immunosuppressive therapy. PTLD encompasses a range of morphologically distinct tumours, which are usually B cell-derived, and mostly EBV-positive (Krams and Martinez, 2008). According

to the World Health Organization (WHO), PTLD tumours can be divided into three main subtypes (Harris et al., 2000): (i) early lesions, which arise during the first year after graft transplantation and are polyclonal, IM-like proliferations which regress following the withdrawal of immune suppression, (ii) polymorphic PTLD, which is the most commonly occurring, can manifest at any time following transplantation, includes tumours derived from B cells at various stages of differentiation, and can be either polyclonal or monoclonal, and (iii) monomorphic PTLD lesions, which arise later following transplantation, are mostly monoclonal and comprise a range of different subtypes including diffuse large B cell lymphomas, BL-like lesions and plasma cell myeloma (Harris et al., 2000, Krams and Martinez, 2008).

Early-onset tumours are almost exclusively EBV-positive, and express both EBNA2 and LMP1, indicative of a Latency III gene expression program. Consequently, these lesions have been identified as virus-transformed B cells that have been able to grow out in the absence of T cell control (Young et al., 1989). EBV-positive PTLD tumours arising later on have been found to exhibit a range of viral gene expression profiles, including latency III expression similar to early lesions, lack of EBNA2 and LMP1, and LMP1 expression in the absence of EBNA2 (Young et al., 1989, Timms et al., 2003, Capello et al., 2003).

Although the pathogenesis of PTLD has traditionally been attributed to diminished EBV-specific CD8+ T cell responses, recent studies have shown that these circulating cells are both readily detectable in transplant recipients, and comparable to those present in healthy individuals (Macedo et al., 2005, Guppy et al., 2007). Interestingly, these investigations have further shown that

the functional activity of EBV-specific CD8+ T cells (defined by IFN- γ production) is impaired in these cases, suggesting that T cell functional capacity, rather than absolute numbers, may be more important in the pathogenesis of PTLD. The observation that the proportion of function EBV-specific CD8+ T cells increases following withdrawal of immune suppression, supports this hypothesis (Guppy et al., 2007).

1.5.4 Hodgkin's Lymphoma

The first cases of Hodgkin's Lymphoma (HL) were originally identified by Thomas Hodgkin in 1832 (Hodgkin, 1832). The trademark mononucleated Hodgkin's cell and multinucleated Reed-Sternberg, collectively known as HRS cells, were subsequently described in 1900 (Kuppers, 2009). Distinct subtypes of HL are distinguished on the basis of cell morphology and phenotype, and the composition of the cellular infiltrate of the tumour tissue; the two main types are classified as classical HL and nodular lymphocyte-predominant HL (NLPHL) (Kapatai and Murray, 2007, Kuppers, 2009). Since NLPHL only accounts for 5% of HL cases, with EBV-association rarely seen (Anagnostopoulos et al., 2000, Chang et al., 2005), this HL type will not be discussed in any further detail. Classical HL is further subdivided into nodular sclerosis (60%), mixed cellularity (30%) and the rarer lymphocyte depletion and lymphocyte-rich forms (Kapatai and Murray, 2007, Kuppers, 2009).

The HRS cells in classical HL comprise roughly 1% of the tumour, with the remaining portion made up of an infiltrate of mixed immune cells including T cells, B cells, plasma cells, neutrophils, eosinophils and mast cells.

Remarkably, there is evidence to suggest the HRS cells themselves actively

attract many of these cells via secretion of a range of chemokines such as CCL5, CCL17, CCL22 and IL-8 (Skinnider and Mak, 2002, Aldinucci et al., 2008, Fischer et al., 2003). Although HRS cells exhibit a very unique phenotype which has proven difficult to assign to any particular cell type, most researchers have concluded they are derived from mature B cells of germinal centre origin (Kapatai and Murray, 2007, Kuppers, 2009). The Ig genes in HRS cells are both rearranged and somatically hypermutated, consistent with antigen-driven germinal centre activity and up to a quarter of cases carry disruptive mutations that confer a non-functional BCR (Kuppers et al., 1994, Kanzler et al., 1996, Brauninger et al., 2003). Whereas other lymphomas retain phenotypic and functional features of the original cell type (Kuppers, 2005), HRS cells display a dramatic loss in B cell phenotype (Schwering et al., 2003), which has been attributed to a complex deregulation of multiple signalling pathways and transcription factor networks, for example NF- κ B, Jak-Stat, P13K-Akt, Notch 1 and receptor tyrosine kinases (Kuppers, 2009). In addition, HRS cells often express markers associated with cells of other haematopoietic lineages (Mathas et al., 2006, Takahashi et al., 1995, Drexler, 1992, van den Berg et al., 1999).

Approximately 40% of cases of classical HL reported in the developed world are EBV-associated. Most instances of EBV-positive HL are of the mixed cellularity or lymphocyte-depleted subtype, with fewer being nodular sclerosis HL or lymphocyte rich HL (Anagnostopoulos et al., 2000, Chang et al., 2005). In cases of paediatric HL in Central and South America, up to 90% of cases are EBV-associated, and HL in AIDS patients is almost always EBV-positive (Dolcetti et al., 2001, Kutok and Wang, 2006). HRS cells infected with EBV

express three viral proteins, EBNA1, LMP1 and LMP2A, along with the EBERs and BARTs. In addition to its role in viral genome maintenance, EBNA1 has also been shown to have a direct role in HL pathogenesis by facilitating downregulation of the putative tumour suppressor gene, protein tyrosine kinase κ (Flavell et al., 2008). LMP1 and LMP2A can mimic physiologic CD40 and BCR signalling respectively (Kilger et al., 1998, Alber et al., 1993), both of which are instrumental in instigating the GC reaction following antigen-activation of B cells (Liu et al., 1989). It has therefore been suggested that via expression of LMP1 and LMP2A EBV is able to promote survival of infected B cells within the GC. Interestingly, both of these viral proteins have been linked to the downregulation of the B cell phenotype in EBV+ HRS cells (Portis et al., 2003, Vockerodt et al., 2008).

Despite the significant association of EBV with many cases of HL, the pathogenic contribution of the virus is still questioned by some investigators since approximately 60% of tumours do not harbour EBV-infected HRS cells. More recent studies have, however, provided evidence to support the role of EBV in the pathogenesis of HL. For example, a number of *in vitro* investigations have unequivocally demonstrated the ability of the virus to rescue B cells harbouring crippled BCRs (Bechtel et al., 2005, Mancao et al., 2005, Chaganti et al., 2005, Mancao and Hammerschmidt, 2007); findings which are consistent with the observation that the majority of HRS cells with non-functional BCRs are EBV-infected (Brauninger et al., 2006).

1.5.5 Burkitt's Lymphoma

Burkitt's lymphoma (BL) was first described by Dennis Burkitt in 1956 as a tumour affecting children in equatorial Africa. Following its discovery, a transmissible pathogen such as an insect-borne vector was initially proposed to be the causative agent of BL (Burkitt, 1958, Burkitt, 1962). Research carried out by Epstein and colleagues later revealed that cells in a BL-derived line were infected with a hitherto unidentified herpesvirus, which was subsequently named EBV (Epstein et al., 1964). The three distinct forms of BL which are now recognised (endemic BL, sporadic BL and HIV-associated BL) are distinguished on the basis of geographical and anthropological distribution (Rickinson and Kieff, 2007), rather than on discrepancies within the tumours themselves. Endemic BL arises in children within equatorial Africa and Papua New Guinea, where the incidence of the disease is high. In these areas, where malaria is holoendemic, there is a 100%-association between BL and EBV. Sporadic BL cases occur in the rest of the world, with incidence and EBV association correlating with certain areas. The lowest incidence is recorded in developed countries, where EBV association is also lowest (15-20% of tumours), whereas some developing countries such as equatorial Brazil and north Africa present an intermediate incidence of BL, with up to 85% of tumours being EBV+ (Kelly and Rickinson, 2007). Unlike endemic and sporadic BL which primarily afflicts children, HIV-associated BL, which displays a 30-40% association with EBV, arises in adults infected with HIV. Development of the lymphoma commonly precedes the onset of AIDs, arising in HIV+ individuals who are often still relatively immunocompetent up until that point (Carbone, 2003, Kelly and Rickinson, 2007).

The BL tumour itself usually affects the jaw or abdomen. Histological characteristics include collections of malignant, round, monomorphic cells that are interspersed with macrophages (Rickinson and Kieff, 2007). The highly proliferative malignant cells phenotypically resemble GC B cells (Gregory et al., 1988), expressing GC markers such as Bcl6, CD10 and CD38 (Dogan et al., 2000, Pajic et al., 2001). The primary tumourigenic event in the pathogenesis of all cases of BL is the deregulation of the cellular oncogene c-myc, which occurs as a result of chromosomal translocation of the c-myc gene located on chromosome (c) 8, onto an Ig locus on either c14, c22 or c2 (Dalla-Favera et al., 1982, Lenoir et al., 1982, Taub et al., 1982). All BL tumours carry the c-myc translocation, regardless of whether they are EBV+ or EBV-.

The c-myc protein is a transcription factor that has been estimated to bind around 15% of cellular gene promoters (Li et al., 2003). It influences various cellular functions including proliferation and apoptosis, and its expression is usually very tightly regulated. For example, promotion of cellular proliferation is counterbalanced by c-myc-induced apoptotic checkpoints which include the p53 pathway (Adhikary and Eilers, 2005). The translocation of the c-myc gene that occurs in BL places the c-myc under the control of promoters within Ig gene loci, resulting in a deregulation of expression and therefore of c-myc-mediated control of growth and apoptosis. Although over-expression of c-myc is also a common feature in many other lymphomas, precisely how it drives tumourigenesis is still an unresolved issue.

In EBV-associated BL, the viral expression program is more restricted than that seen elsewhere, for example in LCLs (Rowe et al., 1986, Rowe et al., 1987, Masucci et al., 1987). Most BL tumours only express EBNA1, reflecting a

latency I type of infection, in which the Qp, rather than the Wp or Cp promoter is used to generate the EBNA transcript (Rowe et al., 2009, Schaefer et al., 1995, Nonkwelo et al., 1996). In addition, 15% of endemic BL cases also display a unique type of latency in which expression of the EBNA2 is activated from Wp, rather than Qp for reasons that are still not fully understood. In this program, termed Wp-restricted latency, all EBNA2s except for EBNA2 are expressed, together with LMP1 and LMP2A (Kelly et al., 2002, Kelly et al., 2006). The absence of EBNA2 is attributable to a deleted sequence within the viral genome which has removed the EBNA2 gene (Kelly et al., 2005). Interestingly, the viral protein BHRF1, which was not previously associated with latent infection, has recently been identified in Wp-restricted latency and shown to provide a survival advantage to infected BL cells (Kelly et al., 2009).

Although c-myc translocation is the key event in the pathogenesis of BL, the association of EBV is also believed to be an important contributing factor. The exact involvement of the virus in tumourigenesis is still an issue of extensive research, however, one intriguing hypothesis has been put forward, based on the link between the GC-like characteristics of the BL cells, and the malarial co-factor in endemic BL cases (Rowe et al., 2009). Immunosuppression of EBV-specific CD8+ T cells has been described in individuals suffering from acute malarial infections (Moss et al., 1983, Whittle et al., 1984, Njie et al., 2009, Moormann et al., 2007), a phenomenon which may lead to the increase in viral load which has been observed in the peripheral blood in such cases (Moormann et al., 2005, Rasti et al., 2005, Yone et al., 2006). In addition, it has been found that malaria infection produces a mitogenic effect on B cells (Greenwood and Vick, 1975, Chene et al., 2007), and based on these findings, it has been

suggested that the two factors together may lead to elevated activation of B cells, producing increased GC activity. Since the GC environment is conducive to AID-mediated mutations and DNA-breaks, it is reasonable to assume that increased GC activity may lead to an increase in the likelihood of c-myc translocations taking place. DNA damaged cells, which would usually be eliminated via apoptosis may be rescued by EBV infection (Rowe et al., 2009). Although only 30-40% of cases are EBV-associated, a similar theory has been suggested for EBV+ cases of HIV-associated BL, since HIV infection also activates the B cell system (Ioachim et al., 1990).

1.6 Aims of Current Work

It is widely acknowledged that EBV selectively colonises switched memory B cells *in vivo*. The mechanisms involved in this process, however, are controversial and the involvement of the GC reaction is at the heart of this debate. The aim of the present study is, therefore, to improve our understanding of how the virus establishes persistence in the memory B cell compartment via a combination of *ex vivo*, and *in vitro* investigations.

Both the *ex vivo* and *in vitro* sections of this PhD project involved ongoing work carried out within the B cell group. The focus of both chapters was a continuation of the PhD project previously carried out by Dr Sridhar Chaganti, and as such the initial part of the *ex vivo* investigation was carried out in collaboration between myself and Dr Chaganti, and was subsequently published (Chaganti et al., 2009).

The following questions were the primary focus of this project:

- (i) Examination of EBV colonisation in distinct B cell subpopulations isolated *ex vivo* from the peripheral blood and tonsil on the basis of phenotypic markers. Of particular interest is the colonisation firstly of non-switched memory B cells, whose origins are likely GC-independent, and secondly on GC cells themselves (chapter 3).
- (ii) Examination of EBV transformation of IgD+CD27- naive B cells *in vitro*, focusing on EBV-induced alterations to cell IgH genotype, and Ig phenotype. The aim of these experiments is to ask whether EBV infection alone is capable of conferring memory characteristics on an infected naive B cell, thus colonising a “memory” cell (Chapter 4).
- (iii) Analysis of expression of AID, UNG and pol- η (molecules involved in the SHM and CSR) in EBV-infected B cells (Chapter 4).

2 Materials and Methods

2.1 Standard Cell Culture

All cell lines were grown in cell culture medium (RPMI1640 medium (Gibco or Sigma) supplemented with 10% v/v selected foetal calf serum (FCS), 6mM glutamine (Gibco) and 8µg/mL gentamycin) at 37°C, 5% CO₂, in 25cm flasks. Cells were passaged twice weekly by replacement of 80% or 50% (LCLs and CD40 blasts) of cell culture medium/cell mix with fresh cell culture medium. Human fibroblast cells and mouse L cell fibroblasts were grown in DMEM medium (Gibco) supplemented with 10% v/v FCS, 6mM glutamine (Gibco) and 8µg/mL gentamycin at 37°C, 5% CO₂, in 75cm flasks. In order to passage fibroblasts, medium was removed and cells washed in 1x PBS to remove serum. Adherent cells were dislodged by the addition of 5mL 0.5% w/v trypsin (Gibco) and 5 minutes incubation at 37°C. Any remaining cells were washed off with warm medium and cells were pelleted by centrifugation at 1,400 RPM for 4 minutes in a large benchtop centrifuge before resuspension in supplemented DMEM medium.

2.2 Biological Samples

The following biological samples were included in this study; peripheral blood from healthy adult EBV carriers, umbilical cord blood from healthy neonates, tonsillar tissue from chronic EBV carriers, and tonsillar tissue from IM patients.

Adult peripheral blood was supplied by the National Blood Service (Birmingham, UK) as either plasma-depleted buffy coats (between 45-65ml), or plasma-depleted leukocyte cones (approximately 15ml).

Tonsillar tissue was obtained following informed consent from patients undergoing tonsillectomy at the Queen Elizabeth Hospital, Birmingham, or the Birmingham Children's Hospital. This material was supplied via collaboration between Dr Michael Kuo (consultant ENT Surgeon, University Hospital Birmingham and Birmingham Children's Hospital) and Dr Sridhar Chaganti. Tonsil lymphocyte suspensions were processed by Dr Sridhar Chaganti and stored in liquid nitrogen prior to being used in this project.

The B cell group was able to acquire a rare collection of frozen tonsillar cell suspensions from adult IM patients undergoing tonsillectomy. This material was donated by Professor WF Berglar (Pathology Institute, University of Heidelberg, Germany)

Umbilical cord blood samples (10-75ml) were obtained from healthy neonates following delivery by women undergoing elective caesarean section at the Birmingham Women's Hospital and were kindly collected after informed consent by Dr David Lissauer (Clinical Research Fellow, Birmingham Women's Foundation Trust and School of Clinical and Experimental Medicine).

All investigations using the above samples were approved by the South Birmingham Research Ethics Committee, UK.

2.3 Isolation of Blood B cell Subsets

2.3.1 Isolation of Peripheral Blood Mononuclear cells (PBMCs)

Adult peripheral blood samples from buffy coats or leukocyte cones were diluted 1:1 in 1x phosphate buffered saline (PBS). 45ml diluted blood was then carefully overlaid onto 15ml Lymphoprep™ (Axis-Shield) in 50ml Falcon tubes (Corning™). To fractionate the different leukocytes, the samples were centrifuged at 1800rpm (without brake) for 30 minutes at room temperature. The top layer containing serum and platelets was first removed with a 25ml pipette and discarded, in order to provide easier access to the lymphocyte-rich interface. Lymphocytes were carefully collected using a 5ml plastic Pasteur pipette, and deposited into two 50ml tubes. In order to remove any residual Lymphoprep, the cells were washed in PBS, by increasing the cell suspension total volume to 50ml, and then centrifuged at 1600rpm (with brake) for 10 minutes at room temperature. The cells were washed twice more by removing the supernatant, resuspending the cells in 50ml PBS and centrifuging at 1200rpm for the second wash, followed by 1000rpm for the third wash. The PBMC pellet was then resuspended in wash buffer (RPMI supplemented with 1% foetal calf serum (FCS, PAA Laboratories), 2mM glutamine (Gibco), and 50units/ml penicillin and 50µg/ml streptomycin (PS) (Gibco)) prior to being counted.

2.3.2 Isolation of B cells from PBMCs

CD19-expressing B cells were positively selected from the PBMC suspension using M-450 CD19 Dynabeads® (Dyna). The pan-B cell marker CD19 is expressed on the cell surface of most members of the B cell lineage, with

exception of terminally differentiated plasma cells, and as such is an excellent target to distinguish B cells from other lymphocytes. The beads themselves are coated with monoclonal antibody (mAb) specific for the CD19 antigen. The amount of Dynabeads[®] used in each B cell preparation was calculated as per the manufacturer's instructions; at a ratio of four beads to every B cell, assuming B cells comprise 5% of PBMCs. The Dynabeads were first washed in 2ml cold wash buffer (supplemented RPMI described above) to remove residual preservatives, before addition to the PBMC sample. The total volume of the PBMC/bead suspension was adjusted to give a concentration of 1×10^7 beads/ml, before being transferred to appropriate number of 15ml tubes and incubated in a laboratory cold room (4°C) for 30 minutes whilst undergoing gentle rotation on a sample mixer (DYNAL[®] sample-mixer) to ensure maximum contact between the beads and the cells. Bead-bound cells were then collected by allowing Dynabeads[®] to attach to a Dynal MPC magnet (Dynal) for two minutes. A high purity of isolated CD19+ B cells was achieved by washing the bead-bound cells in 10ml wash buffer a further five times.

The Dynabeads[®] were detached from the CD19+ cells using DETACHaBEAD[®] CD19 (Dynal). Since DETACHaBEAD[®] CD19 contains polyclonal anti-Fab antibodies targeting the CD19 mAb on the Dynabeads[®], detachment of the latter from the B cell surface is accomplished by successful competition between the DETACHaBEAD[®] abs and the CD19 antigen for Dynabead CD19 mAb binding sites. The DETACHaBEAD[®] reagent was added according to the manufacturer's instructions; using 10µl for every 25µl of Dynabeads[®] used with the bead-bound cell/DETACHaBEAD mixture resuspended in 1000µl wash buffer in a 15ml tube. The tube was then placed on a sample mixer and gently

mixed for 45 minutes at room temperature. Upon completion of the incubation period, the mixture was made up to 10ml with wash buffer and the detached beads allowed to adhere to the magnet for 2 minutes. At this stage the CD19+ B cells were free in the supernatant, which was removed and placed in a fresh 50ml tube. The Dynabeads[®]/ DETACHaBEAD[®] complexes were washed and added to the magnet twice more in wash buffer in order to achieve maximal recovery of CD19+ cells. Approximately 100µl of the remaining bead mixture was placed on a haemocytometer and viewed under the microscope in order to ascertain that all cells had been detached and collected from the beads. The CD19+ B cells were then centrifuged at 1400rpm for 4 minutes, resuspended in B cell complete medium (RPMI supplemented with 10% FCS, glutamine and PS), and stored at 4°C until required (no longer than 24 hours).

2.3.3 FACS Sorting of Healthy Adult B cell Subsets

Cell surface antigens IgD and CD27 were used as targets for FACS sorting the purified B cells into 3 different subsets; IgD⁺CD27⁻ naïve B cells, IgD⁻CD27⁺ switched memory B cells and IgD⁺CD27⁺ non-switched memory B cells.

Purified B cells were centrifuged at 1400rpm for 4 minutes at room temperature, washed once in 10ml FACS wash buffer (1x PBS supplemented with 2% FCS, PS), and the pellet resuspended in 4ml FACS wash buffer. The resuspended cells were added directly into a 5ml polypropylene FACS tube (BD Biosciences) via a sterile 50micron filter to eliminate cell clumps or other material that may cause blockages in the FACS apparatus during sorting. 50µl of cell suspension was then added to each of four control FACS tubes, and the remaining cells were pelleted, the supernatant poured off and the pellet resuspended in 50µl

FACS wash buffer for every 5×10^6 cells. During the course of the study, several combinations of dual staining were employed with the ultimate goal to produce the purest sorted B cells populations possible. Three different strategies were eventually explored before the conclusion of the project (see Table 1 for antibody details).

(1) B cells were costained with FITC-labelled anti-IgD and PE-labelled anti-CD27.

(2) B cells were costained with FITC-labelled anti-IgD and APC-labelled anti-CD27.

(3) B cells were costained with PE-labelled anti-IgD and FITC-labelled anti-CD27.

No antibody was added to the unstained control tube. The isotype control was dual stained with appropriate antibodies, 2 of either; FITC control (1:20, Dako), PE control (1:20, Dako) or APC control (1:20, SEROTEC). Two samples were included for compensation controls using anti-IgD and anti-CD27 single stains with the same fluorescence-labelled antibodies used to stain the sorting sample. The sorting sample was dual stained with both anti-IgD and anti-CD27, with volume of antibody calculated according to cell number. All 5 tubes were incubated at 4°C for 15-30 minutes before being washed once with FACS wash buffer and resuspended in $500\mu\text{l}$ FACS wash buffer. Collection tubes were prepared prior to cell sorting, each containing $500\mu\text{l}$ FACS wash buffer. As described above, three B cell fractions were collected during a single FACS sorting session on a MoFlo cell sorter (Dako Cytomation); (1) $\text{IgD}^+\text{CD27}^-$ naïve B cells, (2) $\text{IgD}^-\text{CD27}^+$ switched memory B cells and (3) $\text{IgD}^+\text{CD27}^+$ non-

antibody	conjugate	dilution	manufacturer
anti-CD20	RPE	1:40	Dako
anti-IgD	FITC	1:40	Dako
anti-IgD	RPE	1:40	Dako
anti-CD27	FITC	1:20	BD Pharmingen
anti-CD27	RPE	1:20	BD Pharmingen
anti-CD27	APC	1:20	BD Pharmingen
anti-CD38	PE-Cy5	1:40	BD Pharmingen
anti-IgG	FITC	1:20	Dako
anti-IgA	FITC	1:20	Dako
anti-M	FITC	1:20	Dako

Table 1 – List of antibodies used to isolate B cell subsets and for phenoytpe analysis

switched memory B cells. Small volumes of the three sorted subsets were used to analyse population purity.

2.4 Isolation of Tonsillar B cell Subsets

All tonsillar tissue used in this study was provided in the form of unfractionated mononuclear cells (UMs). UMs used for virus load studies were either recovered from liquid nitrogen storage (previously prepared by Dr Sridhar Chaganti, or Professor WF Berglar), or provided as fresh UMs by Dr Martina Vockerdot (University of Birmingham). In some cases, tonsillar B cells were provided by Dr Claire Shannon-Lowe (for the generation of BTN-LCL1), and by Dr Christopher Fox (for frequency of infected cell assays).

2.4.1 Isolation of B cells by CD3-Depletion of Tonsillar UMs

Since tonsillar UM cells comprise a high proportion (30-80%) of B cells, with the remainder being mostly T cells, it can be more desirable to deplete the T cells using CD3 Dynabeads, rather than to positively select B cells. This strategy has the added benefit of skipping. Starting numbers of tonsillar UMs varied as cells were inevitably lost upon recovery from liquid nitrogen, but the majority of aliquots were stored at 200×10^6 UM cells per vial. The vials were transferred from liquid nitrogen to the tissue culture lab on ice before being thawed briefly at 37°C , and added to complete B cell medium. The cells were then pelleted by centrifugation and resuspended in wash buffer. The UMs were counted in order to calculate the number of magnetic beads to use. A total count of 200×10^6 will be used in the following example calculation. It was assumed that B cells represented 50% of the UM sample; therefore 100×10^6 T cells would be contained in one frozen vial. The manufacturer advises 4 beads per target cell,

therefore with the beads at a concentration of 4×10^8 /ml, 1ml of beads is required to deplete 100×10^6 T cells. The Dynabeads were washed once with 1ml wash buffer before being added to the cell suspension. The final volume was then adjusted according to number of beads used, aiming for 1ml for every 50 μ l beads, which in this example is 20ml. The mixture was then divided between two 15ml tubes and incubated with gentle rotation on a sample mixer for 30 minutes at 4°C. The tubes were then placed on a Dynal MPC for 2 minutes in order for the bead-bound T cells to adhere to the magnet, and the supernatant removed to a fresh 50ml container. The beads were washed once more with 10ml wash buffer to ensure all B cells were collected. The B cells were then pelleted and resuspended in 20ml complete B cell medium and stored at 4°C until used (no longer than 24 hours).

2.4.2 FACS Sorting of Tonsillar B cell Subsets

The purified B cells were counted in order to determine what quantity of antibodies to use during staining. A triple staining procedure was employed in order to isolate four distinct B cell subsets; CD38+ germinal centre B cells, and three CD38- non-germinal centre populations, namely IgD+CD27- naïve B cells, IgD-CD27+ switched memory B cells and IgD+CD27+ non-switched B cells. As with the blood B cell staining procedure, two slightly different protocols were used at various times during the study (see Table 1 for antibody details):

1. B cells were costained with PE-Cy5-labelled anti-CD38, FITC-labelled anti-IgD and PE-labelled anti-CD27.
2. B cells were costained with PE-Cy5-labelled anti-CD38 (, PE-labelled anti-IgD and FITC-labelled anti-CD27.

Steps involving FACS staining were as described above in the blood B cell FACS staining procedure. Five control tubes were set up; (1) unstained, no antibody added, (2) isotype control, triple staining for PE-Cy5, FITC and PE antibodies, (3) CD38-PE-Cy5 only, (4) IgD-FITC or IgD-PE only, and (5) CD27-PE or CD27-FITC only. B cells to be sorted were triple stained in accordance with one of the above protocols, and the subsets were isolated to high purity using a MoFlo cell sorter. Small volumes of sorted subsets were used to analyse the purity of each population. The cells were stored at 4°C prior to use.

2.5 Isolation of Lymphocytes from Umbilical Cord Blood

Cord blood was diluted 1:1 with sterile 1x PBS. 35ml diluted blood was gently overlaid onto 15ml Lymphoprep in 50ml Falcon tubes. The tubes were then centrifuged at 1800rpm for 30 minutes with no brake at room temperature in order to fractionate the blood. The lymphocyte-rich interface was carefully removed with a transfer pipette and transferred to a new 50ml tube. 1x PBS was added to the cells to a volume of 50ml. The suspension was then centrifuged at 1600rpm to remove any residual Lymphoprep. The pellet was then washed twice more in 50ml 1x PBS before being resuspended in 20ml B cell complete medium. The suspended cord blood lymphocytes were stored at 4°C until used.

2.6 B cell Transformation

2.6.1 Preparation of B95.8 Virus Supernatant

B95.8 virus supernatant was harvested from B95.8 cell cultures typically containing 5-10% cells in lytic cycle. The supernatant was filtered (using a

0.45µm Supor[®] membrane filter) before being stored at -80°C in 1ml aliquots. A small aliquot was reserved for genome quantitation by qPCR. 20µl of the filtered supernatant was incubated with 20µl 2x lysis buffer (2x PCR buffer, 2% TWEEN[®] 20, and 0.2mg/ml Proteinase K) in an Eppendorf Thermocycler at 55 °C for 1 hour, followed by 95°C for 5 minutes in order to inactivate the Proteinase K. Small aliquots of the lysate were then used in an EBV load qPCR assay (see qPCR for EBV load section below). The 2089 supernatant used in this study contained 3×10^8 virus genomes/ ml, and the B95.8 supernatant contained 2.5×10^8 virus genomes/ml.

2.6.2 Establishment of Bulk LCLs from Purified B cells

Freshly isolated B cells were used to generate LCLs. Cell types used to generate bulk infections included; unsorted CD19+ peripheral blood B cells, purified IgD+CD27- peripheral blood naive B cells, purified CD38-IgD+CD27- tonsillar naive B cells, and umbilical cord B cells (see establishment of bulk LCLs from umbilical cord lymphocytes section below). Between 0.5×10^6 and 3×10^6 B cells were incubated with virus supernatant at 50 MOI (multiplicity of infection = the ratio of virus particles to target cells) for a minimum of 1 hour at 37°C. The cells were then centrifuged in a microcentrifuge at 8000rpm for 3 minutes or until a cell pellet was visible, resuspended in 200µl complete B cell medium, and added to a single well of round-bottomed 96-well plate. When higher cell numbers were used, the volume of media and well size was adjusted appropriately. Cultures were expanded until enough cells were present to seed a T25 tissue culture flask (usually around 4 weeks after infection), at which point cell pellets were collected every week and stored at -80°C for DNA and/or RNA. The cultures were routinely split 1:1 every 3-4 days.

2.6.3 Establishment of Limiting Dilution LCL Cultures from Naive Peripheral Blood B cells

In order to establish clonal LCLs from purified naive peripheral blood cells, a limiting dilution technique was employed whereby cells were seeded in 96-well plates in decreasingly low numbers. Irradiated human fibroblasts were used as a feeder layer to support transformation of low cell numbers. To allow time to adhere to the plates, these feeder cells were seeded into round-bottomed 96-well plates, typically at 1000-2000 cells in 100µl complete B cell medium per well, 24 hours before the addition of naive B cells. In order to eventually seed three 96-well plates, at 1000 cells/well, 500 cells/well and 200 cells/well, appropriate numbers of naive B cells were divided into three 1.5ml microfuge tubes. Each sample was incubated in 200µl of complete B cell medium plus virus supernatant, and incubated at 37°C overnight. The following day, the cells were mixed thoroughly by pipetting up and down, and added to 5ml RPMI 10%. The 5ml containing the cells was mixed thoroughly and added to a 10cm dish. A multichannel pipette was used to seed 100µl of the cell mixture per well into 48 wells. The cells were then expanded separately, and pellets collected for DNA and RNA at 14 weeks.

Other naive LCL clones were generated from transformation assays (see Transformation Assays section below).

2.6.4 Establishment of Bulk LCLs from Purified Cord Blood Lymphocytes

Umbilical cord blood lymphocytes were counted (average yield 30-50 x 10⁶ from one cord bleed), and number of B cells estimated by assuming they accounted

for 5% of the lymphocyte pool. 10×10^6 lymphocytes (or 0.5×10^6 estimated B cells) were set aside for bulk infections. The quantity of virus supernatant was calculated based on estimated number of B cells, aiming for an MOI of 50. The cells were pelleted and resuspended in 2ml complete B cell complete medium plus B95.8 supernatant in a 15ml tube, then incubated at 37°C for 1 hour. Following incubation, the lymphocytes were centrifuged again at 1400rpm, resuspended in 3ml B cell complete medium supplemented with 1ug/ml cyclosporin A (CSA) and added to 1 well of 6-well plate. The cells were cultured in CSA-supplemented media for 2 weeks in order to prevent T-cell killing of B cells, after which time standard B cell complete medium was used. The LCLs were expanded and pellets collected when enough cells were available to seed a T25 flask. Thereafter the cultures were split 1:1 every 3-4 days.

2.7 Transformation Assays

In order to compare the transformation efficiency of different peripheral blood B cell subsets (IgD+CD27- naïve, IgD-CD27+ switched memory and IgD+CD27+ non-switched memory), cells were infected with B95.8 supernatant at a range of different MOIs, typically either 50, 25, 12.5 and 6.25, or 25, 12.5, 5 and 1. The cells were collected by FACS to high purity (as described above), and counted using a haemocytometer. Since the number of sorted non-switched memory cells collected was usually the lowest of the 3 subsets, this population determined the number of cells used in the assay; typically four 96-well plates were set up (containing 800-1000 B cells per well), each plate being infected at a different MOI. On occasions where non-switched memory numbers were extremely limited, 48 wells of a 96-well plate were used at each MOI.

Four infections were set up using different MOIs for each of the three B cell populations. Aliquots containing 80,000-100,000 cells were added to four tubes, centrifuged and resuspended in the correct volume of B95.8 supernatant. Each infection was then incubated at 37°C for a minimum of 1 hour. The supernatant and cells were then diluted in 10ml complete B cell medium and 100µl of the mixture was pipetted onto human fibroblast feeders (see establishment of clonal LCLs from PB naive B cells above). The plates were scored at 5-6 weeks post-infection, and in one experiment wells established from the naive subset were selected for expansion to clonal LCLs cultures.

2.8 Generation of CD40 Blasts

Activated CD40 blasts were generated from primary CD19+ B cells or FACS sorted IgD+CD27+ naive B cells by culturing with irradiated CD40 ligand-expressing mouse L cells in the presence of interleukin-4 (IL-4) (Fecteau and Neron, 2003). For primary B cell stimulation, irradiated L cells were plated into 6-well tissue culture plates at 0.5×10^6 per well, and allowed to adhere overnight before the addition of $2-4 \times 10^6$ B cells in 3ml CD40 blast medium (Iscove's Medium supplemented with 10% human serum and 100 U/ml IL-4) (Fecteau and Neron, 2003). In the case of sorted naive B cells, irradiated L cells were plated into 24-well plates at 0.2×10^6 per well and allowed to adhere overnight before the addition of $0.5-1.5 \times 10^6$ naive B cells. Cultures were maintained for 8-10 weeks or until the CD40 blasts stopped proliferating. Cell pellets were collected for DNA every 7 days from approximately 6 weeks in culture.

2.9 Induction of Lytic Replication in AKBM cells

2×10^6 AKBM cells were pelleted by centrifugation and washed once in 1ml Optimem media. The cells were then resuspended in 100ul of Optimem, containing F(ab')₂ goat anti-human IgG antibody (Cappel: 55049) at 1% of sterile stock solution. The mixture was incubated for 30 minutes to 1 hr at 37°C in a CO₂ gassed incubator. Following incubation, the cell suspension was transferred to fresh cell culture media and grown for 3 days before GFP-positive and GFP-negative cells were sorted by FACS.

2.10 Induction of Ig Isotype Switching

Naive B cell-derived LCLs were cultured with irradiated CD40 ligand-expressing mouse L cells in IL-4/IL-21-supplemented complete B cell medium. L cells were added to 12-well tissue culture plates at 0.2×10^6 per well prior to addition of 2×10^6 LCLs in 1.5ml CD40 blast medium supplemented with either 100 U/ml IL-4 alone, or IL-4 plus 50ng/ml IL-21 (Avery et al., 2008). The cells were split after 3-4 days in culture, and harvested after 7 days for Ig phenotype staining.

2.11 Analysis of Ig Phenotype by Flow Cytometry

Surface immunoglobulin (sIg) expression was determined by flow cytometry. Briefly, between 0.2×10^6 and 1×10^6 cells were added to a FACS tube and pelleted by centrifugation at 1400rpm for 4 minutes. The cells were washed once in FACS wash buffer before being resuspended in 100ul FACS wash buffer containing fluorochrome-conjugated antibodies (against IgD, IgM, IgG and IgA) diluted to the appropriate concentration; isotype controls were set up in parallel for each antibody. The samples were then incubated at 4°C for 30 minutes, in the dark. Following incubation the cells were pelleted and

resuspended in 1ml FACS washing buffer (or fixed in 1ml 1% formaldehyde/PBS solution). The samples were stored at 4°C in the dark until analysed on a Coulter® Epics® XL-MCL flow cytometer. FACS data were analysed using FloJo software.

Cells were also analysed for intra-cytoplasmic immunoglobulin (Ig) using fluorochrome-labelled isotype-specific mAbs to IgD, IgM, IgG and IgA (Dako), together with commercial fixing and permeabilisation kit (Caltag). The staining protocol was followed as per the manufacturer's instructions, and FACS analysis was performed as detailed above.

2.12 Analysis of IgVH Genotype

2.12.1 DNA Extraction

Genomic DNA was extracted from cell pellets (typically $1-2 \times 10^6$ cells) using a Qiagen® DNeasy Blood and Tissue Kit. The procedure was carried out according to the manufacturer's instructions, and the DNA eluted in 50-100µl PCR grade water (Ambion), depending on initial cell input. DNA quality and concentration was determined using a NanoDrop™ spectrophotometer, and the DNA stored at -20°C.

2.12.2 IgH PCR

PCR amplification of the Ig heavy chain variable region (IgH PCR) was performed using published primers (Aubin et al., 1995, Timms et al., 2003), and a high fidelity Taq polymerase. Note that the Expand High Fidelity System includes a 3'→5' exonuclease proofreading activity, and is reported to be 3-fold more accurate compared to standard Taq DNA polymerase (estimated error

rate 8×10^{-6} per bp/doubling (Cline et al., 1996)). The forward primer corresponded to a consensus sequence for the framework 1 (FR1c) region (5'-AGG TGC AGC TGS WGS AGT CDG G-3'), and the reverse primer consisted of a combination of a consensus primer for JH1, 2, 4 and 5 (5'-ACC TGA GGA GAC GGT GAC CAG GGT-3'), plus JH3 (5'-TAC CTG AAG AGA CGG TGA CCA TTG T-3') and JH6 (5'-ACC TGA GGA GAC GGT GAC CGT GGT-3') specific primers. Each PCR assay contained a water-only negative control, and a Namalwa DNA positive control. The DNA and PCR reagents were added to thin-walled 0.5ml PCR tubes in a PCR set-up room. Every PCR reaction contained a final concentration of 1x Expand High Fidelity reaction buffer (with 1.5mM MgCl₂), (Roche), 3.5 units of Expand High Fidelity enzyme mix (Roche), 200μM each of dATP, dGTP, dTTP and dCTP, 0.8μM FR1c primer and 0.26μM each of JH primer (JH1245, JH3 and JH6). The assembled PCR reactions were placed in an Eppendorf™ Thermocycler and amplified using the following conditions; initial denaturation at 94°C for 5 minutes, followed by 29 cycles of 94°C for 30 seconds (denaturation), 61°C for 1 minute (annealing) and 72°C for 1 minute (extension), plus a final 10 minute extension at 72°C. Completed PCR reactions were stored at 8°C until analysis.

The Expand High Fidelity enzyme mix contains thermostable Taq DNA polymerase together with a polymerase with a 3'-5' exonuclease proofreading activity. The polymerase mixture provides a higher fidelity of DNA synthesis (3-fold compared to Taq DNA polymerase alone), and generates a mixture of blunt-ended products and 3' overhang products suitable for TA cloning.

2.12.3 Identification and Recovery of the PCR Product

Since analysis of the PCR products demanded better resolution than that provided by an agarose gel, non-denaturing polyacrylamide gels were used. 13µl of gel loading dye (1.25 mg/ml bromophenol blue, 1.25 mg/ml xylene cyanol, 30% v/v glycerol) was added to 50µl of PCR product. Aliquots of 5µl and 50µl of sample were loaded in adjacent wells of a gel comprised of 8% acrylamide solution (BioRad), 5x TBE buffer (50mM Tris base, 50mM boric acid, 2mM EDTA), 0.07% w/v ammonium persulphate and 0.02% v/v N, N, N, N tetramethylethylenediamine (TEMED, Sigma) in 1x TBE running buffer. The 5µl aliquot was used to improve discrimination of the bands of interest. The size of the expected PCR products (~360bp) was determined by comparison to a 1kb DNA ladder (Invitrogen), which was run in parallel to the samples. Electrophoresis was carried out at 180V for ~2 hours. The gel was stained with ethidium bromide, and the bands were visualised by UV light using a transilluminator.

The desired bands were sliced from the gel using a scalpel blade and placed in a 1.5ml microfuge tube. The gel fragments were mashed using a 1000µl filter tip, and 350µl 2.5M ammonium acetate added. The mixture was left shaking overnight at 37°C. The following day, the eluate was transferred to a fresh 1.5ml tube and the DNA precipitated by addition of 2.5 volumes of 99% ethanol together with 2µg glycogen DNA carrier (Roche) in order to help visualise the pellet. The sample was incubated for 30 minutes at -70°C, and then pelleted by centrifugation at 13000 rpm for 30 minutes at 4°C. The DNA pellet was washed twice more in 70% v/v ethanol, air-dried and resuspended in 25µl PCR grade water. To estimate the quantity of the PCR product, a 3µl aliquot of DNA was

analysed on a 2% agarose gel (1x TBE as running buffer), with comparison against a 1kb DNA ladder.

2.12.4 Cloning the IgH PCR Product

For sequencing purposes, the IgH PCR product was ligated into a plasmid vector and transformed into competent *E.coli*. To achieve this, the TA cloning system chosen was the pGEM[®] Easy Vector System I (Promega).

During IgH PCR, Expand High Fidelity Taq polymerase adds a non-template directed nucleotide, invariably deoxyadenosine, to the 3' end of the PCR product. Since the linearised pGEM-T vector contains a single deoxythymidine at each 3' end, the PCR product can be cloned directly into the vector without prior enzymatic manipulation.

The pGEMT plasmid harbours an ampicillin resistance gene, enabling transformed bacteria to be selected on agar plates or in broth containing ampicillin. The plasmid also carries an α -peptide coding region for β -galactosidase (*lacZ* gene), which complements a deletion in the α region of the *LacZ* gene in the host DH5 α cells. Transformed cells containing the empty plasmid vector are therefore able to produce β -galactosidase and can be screened on X-gal indicator plates. Successful insertion of the PCR product, within the α -peptide region results in insertional inactivation of the β -galactosidase enzyme. Recognition sites for the restriction enzyme *EcoRI* flanking the pGEM-T vector cloning site provide a means by which clones containing the insert can be readily identified. *EcoRI* digestion followed by agarose gel electrophoresis allows both confirmation of the insertion of a PCR product insertion and estimation of insert size (see below). The pGEM-T vector

also contains an M13 primer sequence adjacent to the cloning site, which is used to sequence the IgH inserts.

PCR product ligation

For each IgH PCR product, 3.5µl DNA was added to 0.5µl pGEM[®]-T Easy vector, 5µl 2x Rapid Ligation Buffer and 1µl T4 DNA Ligase (all supplied in the Promega kit) in a 1.5ml microfuge tube and incubated for 1 hour at room temperature. A positive control using control insert DNA (supplied) and a background vector-only control were set up in parallel.

E.coli transformation

Ligation reactions were transformed into DH5α competent cells and plated out onto X-Gal/IPTG/ampicillin L-broth agar plates, enabling blue/white colony screening. 100µl of DH5α competent cells (for preparation of competent cells see below) were added to the ligation products and left on ice for at least 5 minutes. The cells were then heat shocked at 42°C for 2 minutes, and returned to ice for 1 minute. 1ml L-broth (no ampicillin) was added to the tubes, and the mixture incubated in a shaker for 1 hour at 37°C. The cells were then pelleted by centrifugation at 6000rpm for 3 minutes in a microcentrifuge. All but approximately 150µl of supernatant was discarded, and the cells resuspended by gentle pipetting up and down. Each suspension was spread on a freshly prepared indicator plate containing; LB agar, 100µg/ml ampicillin, 80µl 2% X-gal (Calbiochem[®]) and 20µl 100mM IPTG (Promega). The plates were incubated overnight at 37°C. IPTG induces β-galactosidase production, which breaks down the X-gal on the plates, giving a blue colour to those colonies containing DH5α transformed with plasmid alone (no DNA inserts). Those cells

which are transformed with the recombination plasmid carrying PCR products cannot synthesise β -galactosidase and therefore produce white colonies.

The plates were inspected the next day and up to 24 colonies picked for analysis. The selected colonies were inoculated into 2ml L-broth containing 100 μ g/ml ampicillin in 15ml tubes, and incubated overnight in a shaker at 37°C.

Analysis of recombinant plasmids

Plasmid DNA was extracted using a QIAGEN[®] Spin Miniprep Kit, following the manufacturer's instructions. DNA was eluted from the column in 50 μ l PCR-grade water. In order to determine whether the DNA contained a PCR product of expected size, an aliquot was digested with the restriction endonuclease *EcoRI* (Roche). 3 μ l DNA was added to 2 μ l 10x Buffer H (supplied with the enzyme), 14.5 μ l PCR-grade water, and 0.5 μ l *EcoRI* enzyme. The mixture was incubated at 37°C for 1 hour and the digested fragments were separated using electrophoresis on a 2% agarose gel. The samples were mixed with 5 μ l 5x gel loading dye and loaded on the gel, which was then run in 1x TBE buffer. The gel was stained in a solution of 1x TBE containing 0.5mg/ml ethidium bromide, and was visualised under UV. Plasmid clones containing DNA inserts of the predicted size (300-360bp) were analysed by DNA sequencing.

2.12.5 Preparation of Competent Cells

Competent DH5 α cells were prepared using the following protocol (Inoue et al., 1990); 250ml SOB medium (containing per 1 litre; 20 g bacto-tryptone, 5 g yeast extract, 10 ml 250 mM KCl, 0.5 g NaCl, pH 7, plus 20mM Mg⁺ salts), was added to a sterile 2 litre flask. Approximately 10-12 DH5 α colonies were added to the broth. The cells were grown at room temperature with gentle shaking,

until the culture reached a density of $A_{600} = 0.6$. The flask was then incubated on ice for 10 minutes. The culture was then divided and centrifuged at 2500xg (3000rpm in Beckmann J-6B) for 10 minutes at 4°C. The supernatant was discarded and the DH5 α pellet resuspended in 80ml ice-cold TB (containing 10mM Pipes, 15mM CaCl₂, 260mM KCl adjusted to pH 6.7 with KOH, before addition of 55mM MnCl₂). The resuspended cells were incubated on ice for 10 minutes before being centrifuged again for 10 minutes at 2500xg. The pellet was resuspended in 20ml ice-cold TB, and 1.5ml DMSO added and gently mixed in. The cells were incubated on ice for a further 10 minutes before being aliquoted in volumes of 200ul into sterile 1.5ml microcentrifuge tubes. The aliquots were flash-frozen by dunking in liquid nitrogen and stored at -80°C.

2.12.6 Sequencing IgH Products

For each PCR product derived from bulk LCL time points, at least 20 plasmid clones were sequenced, whereas in the case of clonal LCLs cultures, 3-5 samples were analysed. 200-500ng plasmid DNA was added to a thin-walled 0.5ml PCR tubes together with 3.2 pmol M13 forward primer, and the volume adjusted to 10 μ l with PCR-grade water. The sequencing reaction was prepared and performed using the plasmid to profile DNA sequencing service at the Functional Genomics Laboratory, University of Birmingham, UK.

2.12.7 Analysis of IgH Sequences

Raw sequence data were interpreted using the Chromas Lite (version 2.01) software package and corrected if required by manual checking of each chromatogram trace. Corrected sequences were further characterised using

BioEdit software version 7.0.5 (created by Tom Hall, Ibis Therapeutics, A division of Isis Pharmaceuticals, 1891 Rutherford Road, Carlsbad, CA, USA).

The *EcoRI* restriction sites (GAATTC) flanking the inserted DNA sequence was identified first, allowing the intervening sequence to be copied into a new datafile. The trimmed sequence was then analysed using V-BASE (MRC Centre for Protein Engineering, The University of Cambridge, UK) to confirm the IgV status (in some cases it was necessary to reverse and complement the sequence as the insert may be ligated in the opposite direction relative to the M13 primer site). V-BASE is a comprehensive database of >1000 published Ig variable germline sequences. Each IgVH sequence was aligned with the nearest germline sequence and identified by V-BASE. The number of mutations (single nucleotide changes compared to corresponding germline sequence), together with the matched V, D and J region alignments, and the first 10 amino acids of the junction translation were noted and added to an Excel spreadsheet. Confirmation of the V-BASE alignments was carried out using a separate database, IMGT/V-QUEST (Brochet et al., 2008) in a selection of sequences. Sequence alignment figures highlighting differences to germline were produced with GeneDoc (Karl Nicholas, Pittsburgh Supercomputing Center, USA).

2.13 Taqman qPCR to Estimate EBV DNA Load

2.13.1 Introduction

Real-time quantitative PCR (qPCR) is an invaluable tool to measure quantities of both DNA and RNA (Heid et al., 1996). Unlike standard PCR assays, which provide a measurement of endpoint PCR products, qPCR measurements are

made at the optimal phase of DNA amplification, before the reaction reaches plateau (ref). In this study, dual-labelled TaqMan probes specific for the gene of interest (DNA or RNA) were used (ref). TaqMan probes are labelled at the 5' end with a fluorescent reporter (usually FAM or VIC), and at the 3' end with a fluorescent quencher (TAMRA or BHQ). Close proximity of the quencher to the reporter ensures that an intact probe emits minimal fluorescence. During the PCR reaction, primer extension during amplification of the target sequence leads to displacement and cleavage of the probe by the 5'-3' exonuclease activity of Taq polymerase. Resultant release of the reporter produces an increase of fluorescence intensity during the reaction, levels of which are continuously monitored and the data collected throughout the PCR reaction. Accumulation of the PCR product is therefore measured in real-time. An additional advantage of using real-time PCR is the ability to simultaneously detect more than one PCR product (multiplex PCR) using separate probes labelled with dyes emitting fluorescence on different spectra. In much of this study, PCR amplification of the gene of interest (DNA POL, encoded by BALF5) was multiplexed with PCR amplification of the cellular gene beta-2-microglobulin (β 2M). BALF5/POL values were normalised against β 2M values (serving as an internal control) in order to compensate for variations in the quality and quantity of the starting sample. Multiplex PCR was not carried out for quantification of EBV genome copies in viral supernatants.

2.13.2 Preparation of Namalwa Standards

DNA was extracted from test samples and controls using a Qiagen DNeasy[®] Blood and Tissue Kit as described above. DNA from the Namalwa-BL line known to contain two integrated copies of the EBV genome (Lawrence et al.,

1988) was used to generate qPCR standards containing known EBV copy numbers. Namalwa cells were washed, counted, and DNA extracted from pellets containing $3\text{-}5 \times 10^6$ cells. The DNA concentration was measured and adjusted to $132\text{ng}/\mu\text{l}$ (4×10^4 copies/ μl), and serially diluted in PCR-grade water to generate a set of 8 standards ranging from 4×10^4 copies/ μl to 1 copy/ μl . The standards were divided into single-use aliquots and stored at -20°C .

2.13.3 Setting up qPCR Reactions

qPCR reactions were performed essentially as described (Gallagher et al., 1999, Murray et al., 2003). Each $25\mu\text{l}$ reaction contained 1x TaqMan Universal PCR Master Mix (ABI Applied Biosystems), 200nM 5' FAM-labelled POL probe specific for the EBV polymerase (POL) BALF5 gene, $200\mu\text{M}$ forward and reverse POL primers, 100nM 5' VIC-labelled $\beta 2\text{M}$ probe, 60nM $\beta 2\text{M}$ forward and 80nM $\beta 2\text{M}$ reverse primers; note the $\beta 2\text{M}$ reaction is primer-limited so that amplification does not interfere with detection of the weaker POL signal. Primer sequences (Alta Bioscience University of Birmingham) were as follows:- POL forward (5'-AGT CCT TCT TGG CTA GTC TGT TGA C-3'), POL reverse (5'-CTT TGG CGC GGA TCC TC-3'), $\beta 2\text{M}$ forward (5'-GGA ATT GAT TTG GGA GAG CAT C-3') and $\beta 2\text{M}$ reverse (5'CAG GTC CTG GCT CTA CAA TTT ACT AA-3'). Probes (Eurogentec) were as follows:- POL (5'-FAM-CAT CAA GAA GCT GCT GGC GGC C-TAMRA-3') and $\beta 2\text{M}$ (5'-VIC- AGT GTG ACT GGG CAG ATC ATC CAC CTT C-TAMRA-3'). The TaqMan Universal PCR Master Mix contains PCR buffer, AmpliTaq Gold (a modified version of the recombinant AmpliTaq DNA polymerase), MgCl_2 , dNTPs (dUTP replacing dTTP), UNG (uracil N glycosylase, an enzyme that destroys uracil-containing DNA, thereby acting as a carryover prevention step) and ROX (a passive reference dye).

After adding 20µl reaction mix to wells of a 96-well PCR plate, 5µl of test or standard DNA was added to each well. Namalwa standards were loaded in duplicate, and test samples were loaded in triplicate. No template controls were included as negative controls. The wells were sealed with Microamp Optical Caps (Applied Biosystems), and the plate centrifuged at 1000rpm for 1 minute to mix the reagents. The plate was then loaded onto an ABI Prism 7700 Sequence Detection System (Applied Biosystems) machine. The thermal cycling conditions comprised an initial 50°C incubation to activate the UNG, a step 95°C to activate the AmpliTaq Gold and deactivate the UNG, followed by 40 cycles of 95°C for 15 seconds (denaturation) and 60°C for 10 minutes (annealing and extension of primers).

2.13.4 qPCR Data Analysis

Fluorescent signals produced during the qPCR were analysed using SDS software version 1.7 (Applied Biosystems). FAM and VIC fluorescent intensities were plotted against cycle number and amplification curves used to determine Ct values where the fluorescence reaches an arbitrary threshold level. Because the Ct value is inversely proportional to the amount of target DNA in the initial sample, the Namalwa standards could be used to generate POL and β2M calibration curves, from which test sample POL and β2M copy numbers could be deduced. Data are expressed as EBV genome copies (POL) per 10⁶ cells (half of β2M copy number, assuming 2 β2M copies per diploid cell).

2.13.5 Limiting Dilution EBV POL qPCR Assays

Although the quantitative EBV POL assay described above measures the total number of EBV genomes within a sample, it cannot be used to calculate the

number of EBV-positive cells present. In order to estimate the number of infected cells within a population (frequency), limiting dilution PCR assays have been described (Khan et al., 1996). The current protocol was adapted from a published method (Babcock et al., 1998) and was used primarily to examine the frequency of virus-infected cells in both unsorted and sorted tonsillar B cells from IM patients.

The number of cells used in each limiting dilution assay depended upon how many cells were available (if sorted, cell number was often limited), and how many positive cells were expected in the sample based on a previous total EBV load assay carried out on B cells from the same tonsil. For example when analysing B cells from IM donors with high EBV loads, only small numbers of cells are required for a positive signal; in this case the maximum number of cells added per well was 250. In other cases, such as chronic virus carriers, much higher numbers of cells are needed and here the maximum input was 10, 000 – 50, 000 cells per well. The cells to be tested were counted and resuspended in 160µl PBS. Eight replicates of 10µl were added to wells of a 96-well PCR plate. A further 80µl PBS was then added to the remaining cells (two-fold dilution) and the process repeated another 6-7 times. In this way, several 2-fold dilutions were generated with 8 replicates of each dilution. 10ul of 2x lysis buffer(2x PCR buffer, 2% TWEEN[®] 20, and 0.2mg/ml Proteinase K) was added to each well and the plate was covered with a film lid and centrifuged for 1 minute at 1000rpm. The cells were then lysed by incubation at 55°C for 2 hours, followed by 10 minutes at 95°C to inactivate the proteinase K within the lysis buffer. The plates were then stored at -20°C until required.

As the combined volume of cell suspension and lysis buffer was 20 μ l, the PCR reaction volume need to be adjusted to approximately 50 μ l. Each reaction contained:- 25 μ l 2x Taqman reaction mix, 1 μ l POL forward primer (10 μ M), 1 μ l POL reverse primer (10 μ M), 1 μ l POL probe (10 μ M), 1 μ l β 2M forward primer (4 μ M), 1 μ l β 2M reverse primer (4 μ M) and 1 μ l β 2M probe (5 μ M) (see above for primer sequences). 10 μ l Namalwa standard samples (described above) mixed with 10 μ l PCR-grade water were also included as controls. Finally, 30 μ l of PCR mastermix was added to each sample, the wells were sealed with lid strips, and the plate centrifuged at 1000rpm for 1 minute. The PCR conditions were identical to those used for total EBV POL (described above).

For analysis of limiting dilution qPCR assays, each well was scored positive or negative for a detectable POL signal (above the set threshold). The number of positive wells at each dilution, together with the number of replicates (8), and the cell input number was used to estimate the frequency of EBV positive cells by Poisson distribution. The calculation was carried out using software based on (Hu and Smyth, 2009), provided by WEHI Bioinformatics at the following webpage: <http://bioinf.wehi.edu.au/software/elda/index.html>.

2.14 Taqman qPCR to Measure AID Transcripts

In order to study the expression of three AID variants AID-FL, AID- Δ E4 and AID- Δ E3E4 (Figure 10), qPCR assays were designed for each. qPCR can also be used for measuring cellular gene expression with an additional reverse transcription (RT) step (Lossos et al., 2003, Bustin et al., 2005). RT qPCR shares many of the benefits of qPCR (see previous section), however extra attention must be paid when designing primers to avoid amplification of

genomic DNA. Primers that target DNA sequences crossing exon boundaries are less likely to anneal to intronic sequences. The endogenous reference gene used for normalisation must also be carefully selected; human GAPDH RNA was chosen for this study. The multiplex PCR was optimised to prevent the depletion of the reaction by GAPDH amplification, thus minimising interference of detection of the target gene (Bell et al., 2006).

In order to design qPCR assays for the expression of AID-FL, AID- Δ E4 and AID- Δ E3E4, the following steps were taken:- (i) Cloning of the variant transcripts from Akata-BL cells using nested PCR, (ii) ligation of AID variant PCR products into a pGEMT vector and validation of PCR products by sequencing, (iii) design of qPCR primers and probes for each variant and (iv) calculation of copy numbers of AID variant plasmid standards.

2.14.1 Conventional RT-PCR to amplify AID Transcripts in Akata-BL

cDNA Synthesis

RNA extraction from cells was carried out using the Nucleospin kit and protocol. RNA was eluted in 70ul PCR-grade water. RNA concentration was calculated using a nanodrop spectrophotometer, and each sample diluted to 100ng/ul with PCR-grade water.

cDNA reagents were added to a thin-walled PCR tube. A 20ul reaction contained; 5ul RNA at 100ng/ul, 4ul 5x reaction buffer (Roche), 2ul dNTPs at 2mM (Roche), 2ul random hexamers at 50ng/ul (Promega), 6.5ul PCR-grade water and 0.5ul AMV enzyme (Roche). The mix was incubated for 5 minutes at

room temperature, before being placed in a thermocycler for 60 minutes at 42°C, followed by 5 minutes at 90°C. The cDNA samples were stored at -20°C.

PCR to Amplify AID Variant Transcripts

Amplification of AID transcripts AID-FL, AID-ΔE4 and AID-ΔE3E4 from Akata-BL cells was carried out using a nested RT-PCR method (Wu et al., 2008). Both the first and second rounds of the PCR were carried out using primers targeting exon 1 and exon 5 in order to amplifying each of the 3 AID variant transcripts. For the first round PCR, the following primers were used; forward 5'-AGG CAA GAA GAC ACT CTG GAC ACC -3' and reverse 5'-GTG ACA TTC CTG GAA GTT GC -3'. Each PCR reaction contained a final concentration of 1x Expand High Fidelity reaction buffer (with 1.5mM MgCl₂), (Roche), 3.5 units of Expand High Fidelity enzyme mix (Roche), 200μM each of dATP, dGTP, dTTP and dCTP, and 1μM of each primer. The second round PCR was performed using 2μl of the first round PCR product, with the following primers:- forward 5'-GAC AGC CTC TTG ATG AAC CGG-3' and reverse 5'-TCA AAG TCC CAA AGT ACG AAA TGC-3'. The PCR reactions were performed using an Eppendorf™ Thermocycler with the following PCR conditions:- 35 cycles of 95°C for 30 seconds (denaturation), 55°C for 30 seconds (annealing) and 72°C for 30 seconds (extension). To visualise the nested PCR products, electrophoresis was carried out on an acrylamide gel to provide maximal band resolution, and a 1kb ladder was run alongside the samples in order to determine the size of the PCR products.

2.14.2 Sequencing of AID variant transcripts

AID variant PCR products from Akata-BL were cut from an acrylamide gel. The products were cloned and sequenced as described above. Briefly, each PCR product was extracted and ligated into a pGEMT vector. The vector was cloned into competent DH5 α and grown on indicator ampicillin agar plates. Five colonies corresponding to each product were picked and sequenced using the plasmid to profile facility at the Functional Genomics Laboratory, University of Birmingham, UK. AID variant AID-FL, AID- Δ E4 and AID- Δ E3E4 sequences were confirmed using nucleotide blast database.

2.14.3 AID Variant qPCR primer design

The Primer Express program (ABI) was used to design primers and probes to use in Taqman PCR assays to measure AID-FL, AID- Δ E4 and AID- Δ E3E4 transcripts (Figure 12 and Table 2). For the AID-FL assay, a forward primer targeting exon3, a reverse primer targeting exon4, and a Taqman probe targetted to anneal across the exon3-exon4 boundary were designed. For the AID- Δ E4 assay, a forward primer targeting exon3, a reverse primer targeting exon5, and a Taqman probe targetted to anneal across the exon3-exon5 boundary were designed, and for the AID- Δ E3E4 assay, a forward primer targeting exon2, a reverse primer targeting exon5, and a Taqman probe targetted to anneal across the exon2-exon5 boundary were designed.

2.14.4 AID Variant Plasmid Standards

As expression levels of the three AID variants varied significantly, plasmid standards were used to generate standard curves in the qPCR assays (the same plasmids that were generated in order to sequence the nested variant PCR products were used). The advantage of using plasmid standards rather

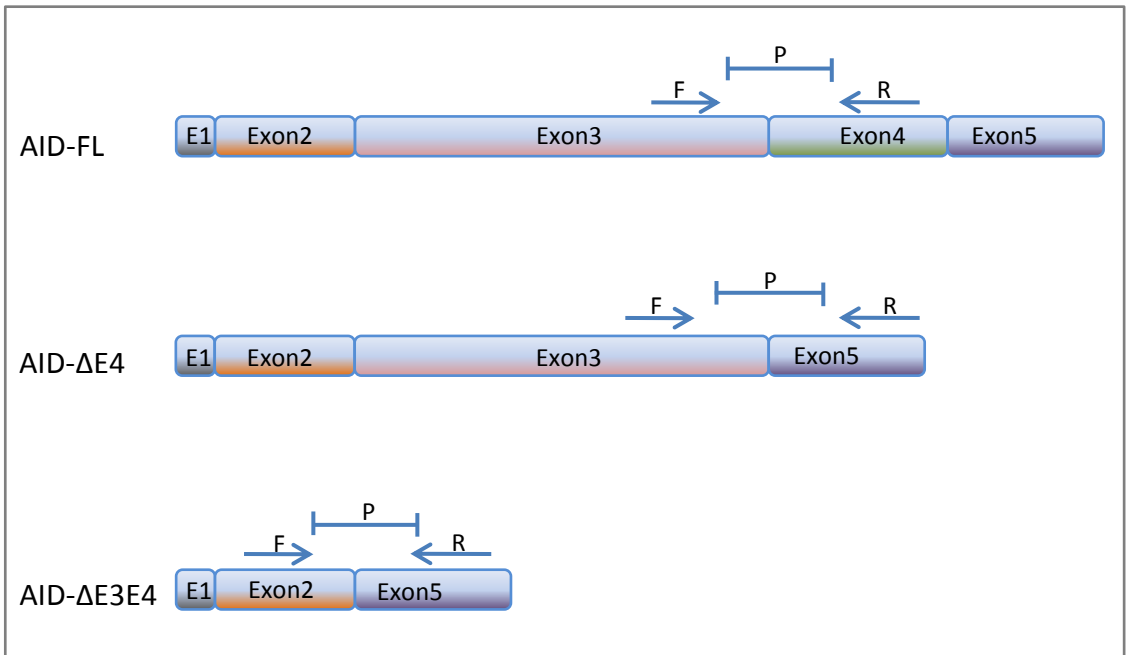


Figure 12 . Taqman primers and probe targets in AID variant qPCRs

AID-FL: the forward primers targets exon3, while the reverse primer targets exon4. The probe was designed to overlap the boundary of exons3 and 4.

AID-ΔE4: forward primer targets exon3, while the reverse primers targets exon5. The probe overlaps the exon3 – exon5 boundary.

AID-ΔE3E4: forward primer targets exon2, while the reverse primers targets exon5. The probe overlaps the exon2 – exon5 boundary.

AID-FL

forward	5'-CGC CGG GGT GCA AAT AG-3'	exon3
reverse	5'-GCC GAA GCT GTC TGG AGA GA-3'	exon4
probe	5'-TAMRA-CAT CAT GAC CTT CAA AGA TTA TTT TTA CTG CTG GAA-FAM-3'	exon3-exon4

AID-ΔE4

forward	5'-CTG AGC CCG AGG GGC T-3'	exon3
reverse	5'-CTA TCA AAG TCC CAA AGT ACG AAA TG-3'	exon5
probe	5'-TAMRA-CAT GAC CTT CAA AGC CCC TGT ATG AGG TTG-FAM-3'	exon3-exon5

AID-ΔE3E4

forward	5'-TAC GTA GTG AAG AGG CGT GAC AGT-3'	exon2
reverse	5'-TGC TAT CAA AGT CCC AAA GTA CGA-3'	exon5
probe	5'-TAMRA-TCT TCG CAA TAA GCC CCT GTA TGA GGT TG-FAM-3'	exon2-exon5

Table 2. AID-FL, AID-ΔE4 and AID-ΔE3E4 qPCR assay primers

than cDNA generated from cell lines is that known plasmid concentrations can be used to calculate gene copy number.

DNA concentrations in each plasmid sample were calculated using a nanodrop spectrophotometer. From the stock concentration, each plasmid was diluted to 5ng/μl using PCR-grade water. From the concentration, the number of plasmid molecules per μl was calculated:

- $(\text{Plasmid} + \text{insert bp}) \times (330 \text{ Da} \times 2 \text{ nucleotide/bp}) = \text{g/mol}$
 - Eg. $(3646\text{bp}) \times (660) = 2.4 \times 10^6 \text{ g/mol}$
- $(\text{g/mol}) / \text{Avogadro's number} (6 \times 10^{23}) = \text{g/molecule}$
 - Eg/ $(2.4 \times 10^6 \text{ g/mol}) / (6 \times 10^{23}) = 4 \times 10^{-18} \text{ g/molecule}$
- $\text{Concentration (g/}\mu\text{l}) / (\text{g/molecule}) = \text{molecules/}\mu\text{l (i.e. copy number)}$
 - Eg. $(5 \times 10^{-9} \text{ g/}\mu\text{l}) / 4 \times 10^{-18} \text{ g/molecule} = 1.2 \times 10^9 \text{ molecules/}\mu\text{l}$

Based on these calculations, the copy numbers of each plasmid at 5ng/μl were:

AID-FL; 1.2×10^9 .

AID--ΔE4; 1.3×10^9 .

AID-ΔE3E4; 1.4×10^9 .

10-fold serial dilutions were then carried out for each plasmid, using PCR-grade water, generating five concentrations for the each standard. Each diluted plasmid was divided into 20ul aliquots and stored at -20°C.

GAPDH qPCR Standards

cDNA prepared from X50-7 cells (see above) was used to generate standard curves for the GAPDH internal control. As described in the cDNA synthesis

section above, 5µl of 100ng/µl RNA was used in each reaction. The cDNA was then diluted in a 5-fold serial dilution using PCR-grade water. Aliquots from each concentration in the series were made and stored at -20°C.

2.14.5 AID variant qPCR Assays

The Taqman assay used for quantifying AID variant transcripts was based on the same principle as that described above for EBV POL quantification. The housekeeping gene GAPDH used as an internal control for RNA input. As previously discussed, plasmids containing the relevant AID variant sequences were used as standards, whereas X50-7 cDNA was used as the GAPDH standard. Each reaction was carried out in duplicate, in a 96-well PCR plate. The reaction mix was assembled and added to the plate in a designated PCR set-up area, as were the cDNA samples. Plasmids were added at the last step in a separate area in order to avoid contamination of the designated PCR area. For each AID variant assay, the following 25µl reaction mix was used; 12.5µl 2x Taqman reaction mix, 2.5µl forward primer at 10µM, 2.5µl reverse primer at 10µM, 1µl probe at 5µM, 0.5µl GAPDH primer mix (ready made), 1µl PCR-grade water and 5µl cDNA sample. Following addition of samples to each row of the plate, the wells were sealed with optical cap lids. When all samples had been loaded, the plate was briefly spun at 1000rpm to ensure all reagents were in the bottom of the wells. The PCR was carried out using an ABI 7500 system, using Sequences Detection System 1.4 Software Prism. Results were normalised to GAPDH expression values.

2.15 Taqman qPCR to Measure UNG and Polη Transcripts

Taqman qPCR assays to measure uracil DNA glycosylase (UNG) and polymerase-eta (Polη) were obtained from. The reagents from each assay included forward and reverse primers, and a FAM-labelled Taqman probe. The housekeeping gene GAPDH used as an internal control for RNA input. Serially diluted Ramos cDNA was used as a standard for UNG, Polη and GAPDH. Each reaction was carried out in duplicate, in a 96-well PCR plate. For each assay, the following 25µl reaction mix was used; 12.5µl 2x Taqman reaction mix, 1.25µl appropriate ready-made primer mix, 0.5µl GAPDH primer mix (ready made), 10.75µl PCR-grade water and 5µl cDNA sample. The PCR plate and PCR reaction was performed as described above. The results were normalised to GAPDH, and values calculated as relative to UNG or Polη expression in the immortalized T cell line, Jurkat.

3 *Ex Vivo* Studies of EBV Colonisation within Distinct B cell Subsets

Both the *ex vivo* and *in vitro* sections of this PhD project involved work that formed a part of ongoing studies carried out within the B cell group. The focus of the *ex vivo* chapter therefore is a continuation of the PhD project previously carried out by Dr Sridhar Chaganti, and as such the initial part of the investigation was carried out in collaboration between myself and Dr Chaganti, and was subsequently published (Chaganti et al., 2009).

In this work, the subject of EBV persistence within the B cell compartment was addressed, with a view to increasing the understanding of the initial cell targets of the virus during primary infection. As discussed previously in the Introduction, the route by which EBV establishes persistence is still a matter of debate. There is evidence suggesting preferential infection and expansion of the switched memory subset, and conversely, other evidence supporting the initial infection of a naive B cell followed by differentiation to a memory B cell via the germinal centre route. The aim of this chapter therefore, is to investigate the distribution of the virus within distinct B cell populations in the peripheral blood (PB) of healthy EBV carriers and the tonsils of chronic carriers and IM patients.

3.1 Isolation of Peripheral Blood B cell Subsets

B cells were routinely isolated from the PB of healthy donors supplied by the National Blood Service (NBS), either in the form of buffy coats or leukocyte cones. The standard method for isolating B cells using magnetic CD19

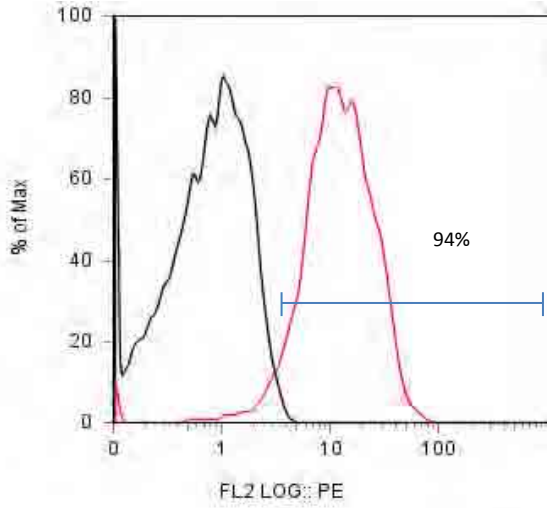
Dynabeads yielded consistently pure populations based on CD20 surface staining, two typical examples of which can be seen in Figure 13.

Purified B cells were further sorted by FACS into three different subgroups based on IgD and CD27 expression. Using this staining protocol, the three different subsets, naive (IgD+CD27-), switched memory (IgD-CD27+) and non-switched memory (IgD+CD27+), are distinguishable within the B cell population (Figure 14). In order to minimise contamination from adjacent populations, appropriately sized sort gates were drawn around the target population, often sacrificing cell numbers for high purity. In each case sorted populations were re-analysed in order to confirm their purity (data from 13 PB sorts is summarised in Table 3). The naive B cell yield was invariably the most pure, in most instances achieving >99% purity and switched memory populations were 96%-100% pure. Since the ease by which the non-switched memory cells could be distinguished from the other two populations often varied between sorts, the purity of this subset was less consistent, but was usually >93% (mean = 92%). Potential contamination of the non-switched memory fraction usually came from the naive B cell population, and specifically in the two sorts (PB6 and PB7) yielding non-switched memory cells of <90% purity, no contamination from the switched memory B cell subset occurred (data not shown). Any source of contamination within the naive or memory B cell subset usually came from the non-switched memory population, but in most cases these levels were <1%.

3.2 Isolation of Tonsillar B cell Populations

Tonsillar UMs were obtained from tonsillar material by Ficoll density gradient centrifugation, and B cells isolated by either positive selection using CD19

Peripheral blood donor 1



Peripheral blood donor 3

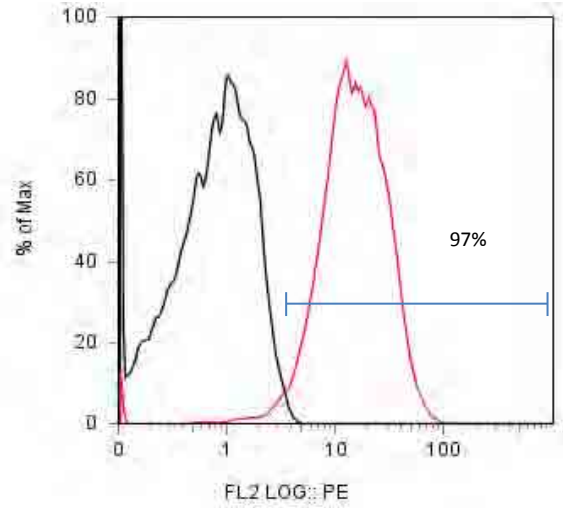


Figure 13. CD20 staining of CD19-selected peripheral blood B cells

Two representative CD19-selected B cell populations stained for surface CD20 expression. CD20+ cells are represented by the pink outlined histogram, whereas the isotype control is represented by the black outlined histogram.

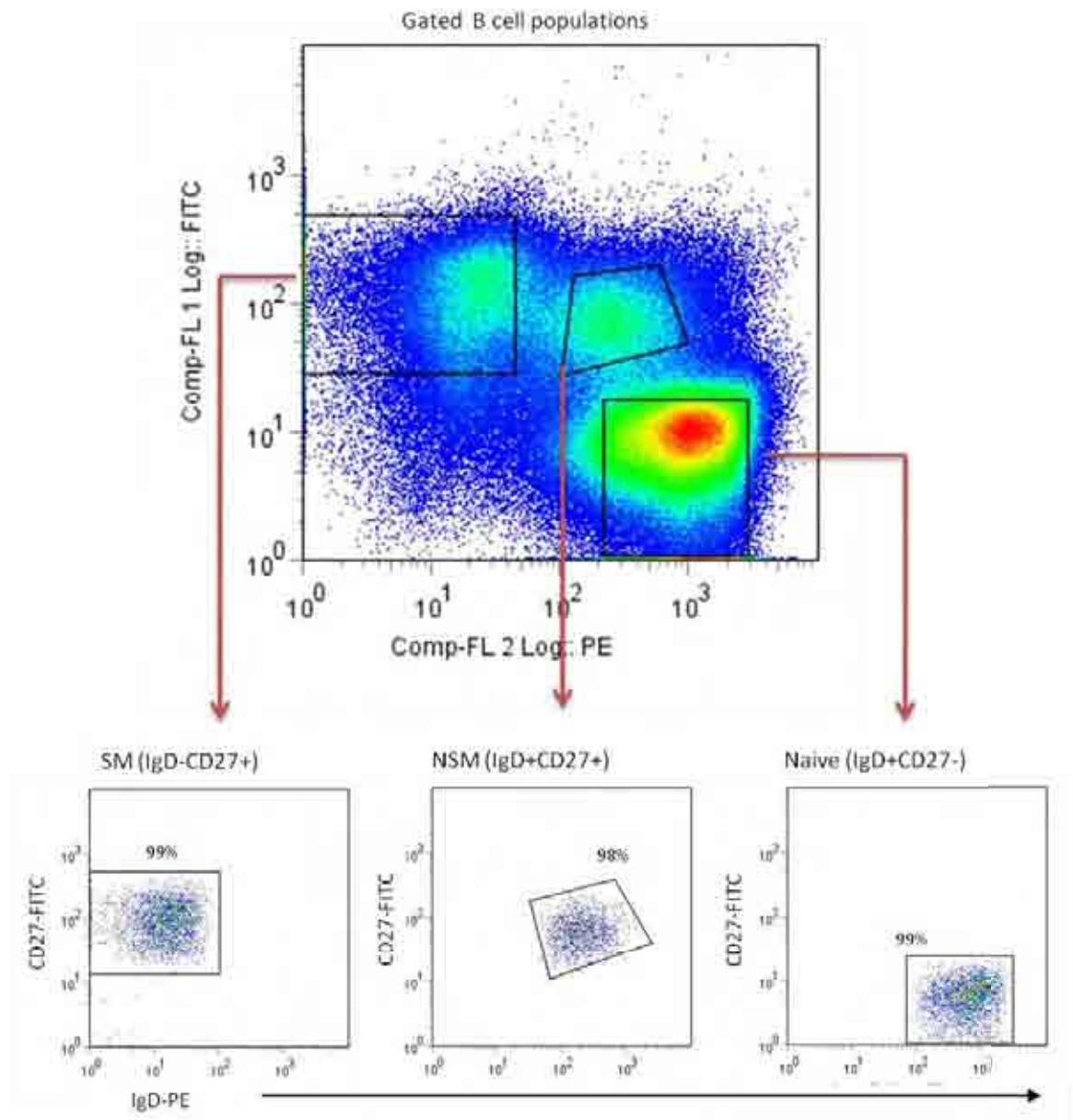


Figure 14. Isolation of peripheral blood B cell subsets

Using IgD-PE and CD27-FITC staining, peripheral blood B cells were sorted into three separate populations; naive (IgD+CD27-), switched memory (IgD-CD27+) and non-switched memory (IgD+CD27+). Three distinct populations can clearly be seen, together with the gates used to select the cells targeted for collection. The three lower panels show reanalysis of each sorted population and the corresponding purities based on analysis of approximately 2000 events. This sort was used to provide cells for experiment 7. Note: the gates drawn around the reanalysed populations are consistently larger than the initial gates due to a shift in fluorescence intensity following sorting.

<i>PB donor</i>	<u>Subset purity (%)</u>		
	naive (IgD+CD27-)	NSM (IgD+CD27+)	SM (IgD-CD27+)
PB 1	99	98	99
PB 2	99	95	99
PB 3	99	91	99
PB 4	99	99	99
PB 5	98	92	97
PB 6	98	85	98
PB 7	92	81	90
PB 8*	n/d	n/d	n/d
PB 9*	99	98	99
PB 10*	99	87	95
PB 11*	99	97	99
PB 12*	99	95	99
PB 13*	99	91	92

Table 3 . Summary of peripheral blood FACS-sorted B cell populations for virus load assays

Summary of re-analysis of peripheral blood (PB) B cell populations sorted by FACS into IgD+CD27- naive, IgD+CD27+ non-switched memory (NSM) and IgD-CD27+ switched memory (SM). n/d = not determined. *B cells used for limiting dilution assays.

Dynabeads, or negative selection using CD3 Dynabeads. B cells were further sorted by FACS based on CD38, IgD and CD27 expression (FACS data from a representative healthy carrier is shown in (Figure 15)). In order to separate GC B cells from those outside GCs, the CD38⁺ and CD38⁻ cell gates were drawn around the two distinct populations. The CD38⁺ GC B cell subset was collected separately, and the CD38⁻ B cells were divided into three further populations; IgD⁺CD27⁻ naive, IgD⁻CD27⁺ switched memory and IgD⁺CD27⁺ non-switched memory. As with the PB B cell isolation, sorted populations were re-analysed in order to confirm their purity (summarised in Table 4). The naive and switched memory B cells were >98% pure in most sorts, and although the non-switched memory populations were less abundant in the tonsil than in blood, it was still possible to sort these cells to between 93-97% purity where analysis was carried out (note, in cases where very small numbers of cells were collected, reanalysis was not possible).

3.3 Total EBV Genome Load in B cell Populations

3.3.1 Healthy Carrier Peripheral Blood B cell Populations

Sorted B cells from the peripheral blood of 13 healthy carriers were examined by qPCR for EBV genome load. Virus loads, expressed as genome number per 10⁶ cells, from naive (IgD⁺CD27⁻), non-switched memory (IgD⁺CD27⁺) and switched memory (IgD⁻CD27⁺) B cell populations are shown in Table 5. The chart depicted in Figure 16 summarises the data from the 13 donors, and shows the median EBV load in each population. The data show that there is considerable variation in EBV load between different donors. The distribution of virus load between the three B cell populations is consistent with published data

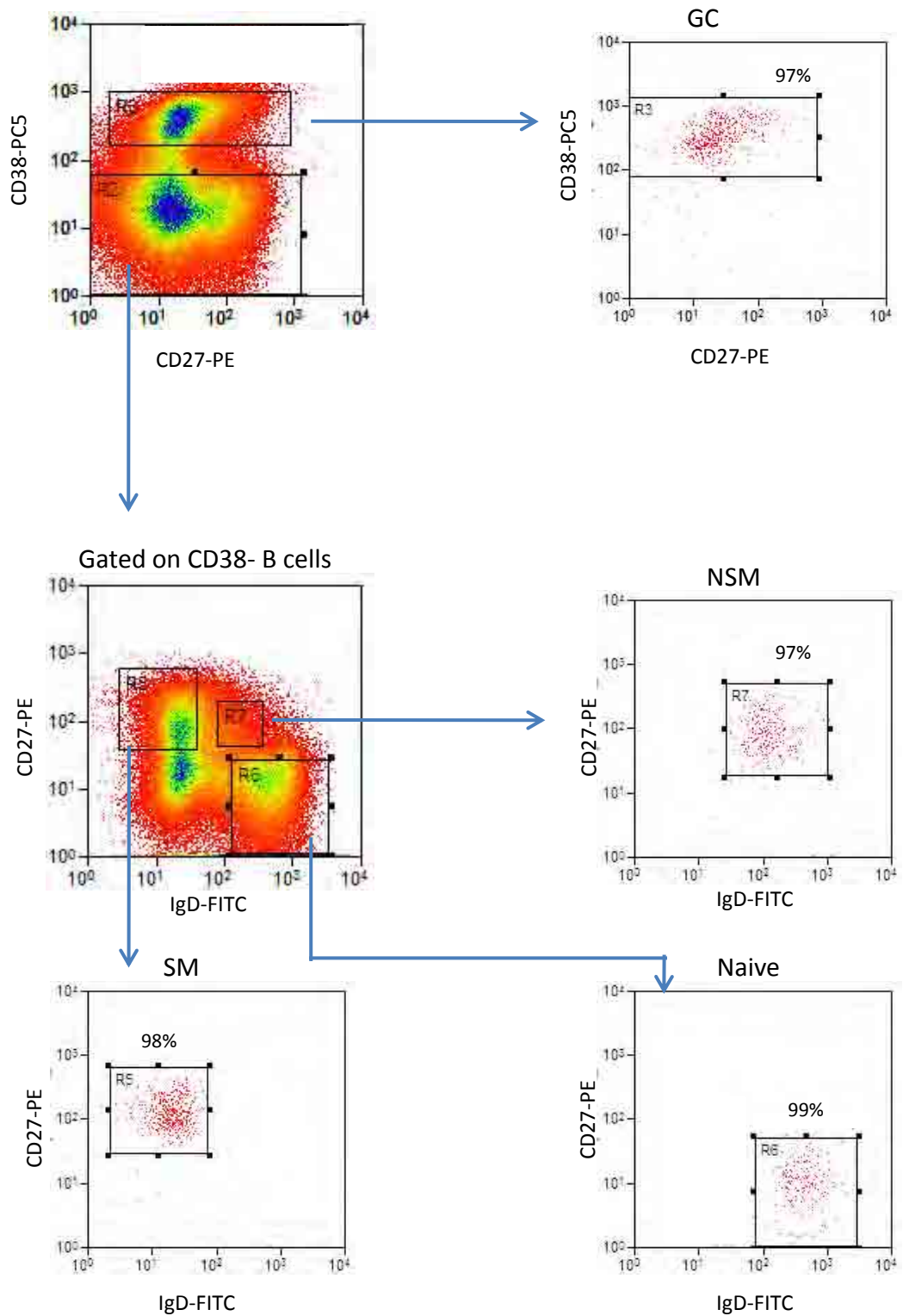


Figure 15. Isolation of tonsillar B cell subsets

A representative sort (tonsil 1) is shown. B cells were first gated according to CD38 expression. CD38+ GC B cells were then collected separately, and CD38- B cells were further divided into switched memory (SM), naive (N) and non-switched memory (NSM).

<i>tonsil</i>	<u>Subset purity (%)</u>			
	naive	NS memory	S memory	GC
	CD38-IgD+CD27-	CD38-IgD+CD27+	CD38-IgD-CD27+	CD38+
T1	99	97	98	97
T2	97	97	99	n/d
T3	n/d	n/d	98	n/d
T4	99	n/d	n/a	98
T5	98	93	90	98
T6	99	94	99	98
IMT3	98	n/d	98	95
IMT5	99	n/d	98	97
IMT6	99	n/d	99	97

Table 4 . Summary of FACS-sorted tonsillar B cell populations for virus load assays

Summary of reanalysis of tonsillar B cells from chronic carriers (T) and IM patients (IMT) sorted by FACS into; CD38-IgD+CD27- naive, CD38-IgD+CD27+ non-switched memory (NSM), CD38-IgD-CD27+ switched memory (SM), and (CD38+) GC B cells. n/d = not determined.

	naive	NSM	SM
PB1	193	1260	770
PB2	0	730	2816
PB3	22	202	2160
PB4	0	15562	4211
PB5	15	55	731
PB6	273	1299	18330
PB7	9	499	1206
PB8	200	1350	5000
PB9	30	1700	28000
PB10	0	250	1000
PB11	44	350	6500
PB12	110	1700	11600
PB13	260	310	6200

Table 5. EBV load distribution in peripheral blood B cell subsets

EBV loads from PB naive, non-switched memory (NSM) and switched memory B cell subsets derived from 13 donors is shown. Values are expressed as EBV genomes per million cells.

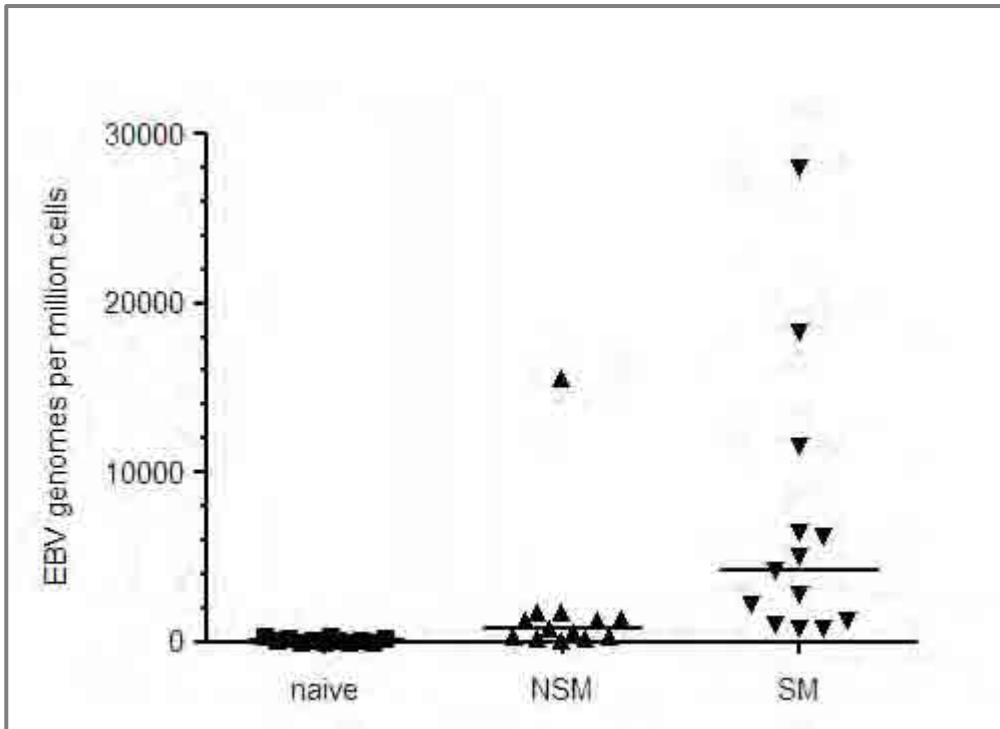


Figure 16. EBV load distribution in peripheral blood B cell subsets

EBV loads from PB naive, non-switched memory (NSM) and switched memory B cell subsets derived from 13 donors is shown. Values are expressed as EBV genomes per million cells. Horizontal lines within data from each subset show the median value.

(Babcock et al., 1998, Chaganti et al., 2009), with the highest viral load (median = 4,210 EBV genomes/ 10^6 cells) observed within the switched memory B cell subset, and only minimal levels (median = 15 EBV genomes/ 10^6 cells) detectable in the naive B cell population. In addition, the non-switched memory population in all 13 donors contained significant levels of viral DNA (median = 730 EBV genomes/ 10^6 cells) that was only ~3-fold lower than that detected in switched memory B cells, and substantially higher than in naive B cells. Note that in 2 out of the 13 donors, the detected load was actually higher in the non-switched memory than in the switched memory B cell subset.

3.3.2 Healthy Carrier Tonsillar B cell Populations

In parallel experiments, sorted tonsillar B cell subsets from 6 healthy carrier individuals were examined for EBV load by qPCR. EBV loads from naive (CD38-IgD+CD27-), non-switched memory (CD38-IgD+CD27+), switched memory (CD38-IgD-CD27+) and GC (CD38+) B cell populations from each tonsil are shown in Table 6 and all the data, together with median values are summarised in Figure 17. In most cases both the naive B cell and GC B cell subsets contained low EBV loads. However, the non-switched and switched memory B cell values consistently gave higher but more varied results.

Collectively the data show that the virus was distributed primarily within the switched memory B cell fraction (median = 5,690 EBV genomes/ 10^6 cells), with minimal loads in both the CD38+ GC (median = 380 EBV genomes/ 10^6 cells) and naive (median = 210 EBV genomes/ 10^6 cells) B cell subsets. As seen in the blood, substantial levels of virus were also detected within the non-switched memory B cell population (median = 3,150 EBV genomes/ 10^6 cells). This median viral load was approximately 15-fold higher than in naive, 8-fold higher

	GC	naive	NSM	SM
Tonsil 1	706	268	1938	843
Tonsil 2	320	2240	6171	13675
Tonsil 3	213	184	4892	10540
Tonsil 4	2651	12	3143	22747
Tonsil 5	444	0	473	618
Tonsil 6	146	232	3162	673
IMT3	1132607	0	n/t	1659062
IMT5	450900	85067	n/t	77079
IMT6	393132	4413	n/t	222165

Table 6. EBV load in tonsillar B cell subsets

EBV load in chronic carrier tonsillar CD38+ germinal centre (GC), naive, non-switched memory (NSM) and switched memory (SM) populations was estimated using qPCR targetting the EBV pol gene. The results were normalised against beta-2-microglobulin (β 2M), and values expressed as number of EBV genomes per million cells. Tonsils derived from IM patients are designated "IM". n/t = not tested.

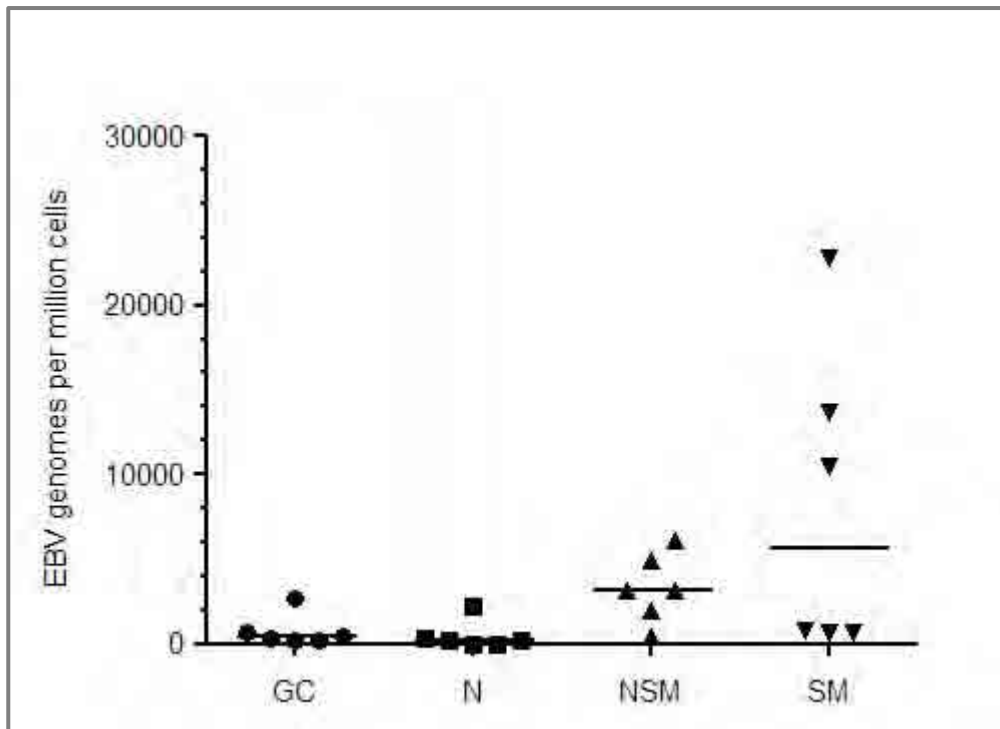


Figure 17 . EBV load distribution in healthy carrier tonsillar B cell subsets

EBV loads from chronic carrier tonsillar germinal centre (GC) naive, non-switched memory (NSM) and switched memory B cell subsets derived from 6 donors. Values are expressed as EBV genomes per million cells. Horizontal lines within data from each subset show the median value.

than in CD38+ GC and only 2–fold lower than in switched memory B cells. In one instance (T6), the load detected in the non-switched memory subset was ~5–fold higher than that in switched memory.

3.3.3 Infectious Mononucleosis Tonsillar B cell Populations

To examine whether a similar distribution of EBV was observed during primary infection, tonsillar B cells from 3 individuals with IM were sorted by FACS into naive (CD38-IgD+CD27-), switched memory (CD38-IgD-CD27+) and GC (CD38+) B cell populations. Note that the non-switched memory (CD38-IgD+CD27+) B cell population was barely detectable from each of these donors and therefore these cells were not available for collection (data not shown).

The results from each tonsil are shown separately in Table 6, and summarised together with median values in Figure 18. The data emphasise that the EBV loads are dramatically higher in IM tonsils compared to chronic carrier tonsils or peripheral blood. The relative distribution of EBV load between the naive and switched memory populations was consistent with previous findings, with the highest load in the memory B cell subset (median = 220,000 EBV genomes/ 10^6 cells) and lowest in the naive B cell fraction (median = 4,000 EBV genomes/ 10^6 cells). In contrast to chronic carrier tonsils, a substantial load was also detected in the CD38+ GC B cell fraction (median = 450,000 EBV genomes/ 10^6 cells). However, in addition to its expression by GC B cells, CD38 is considered to be a marker of activated B cells during IM. The finding of EBV in CD38+ “GC” B cells is therefore open to question (see Discussion).

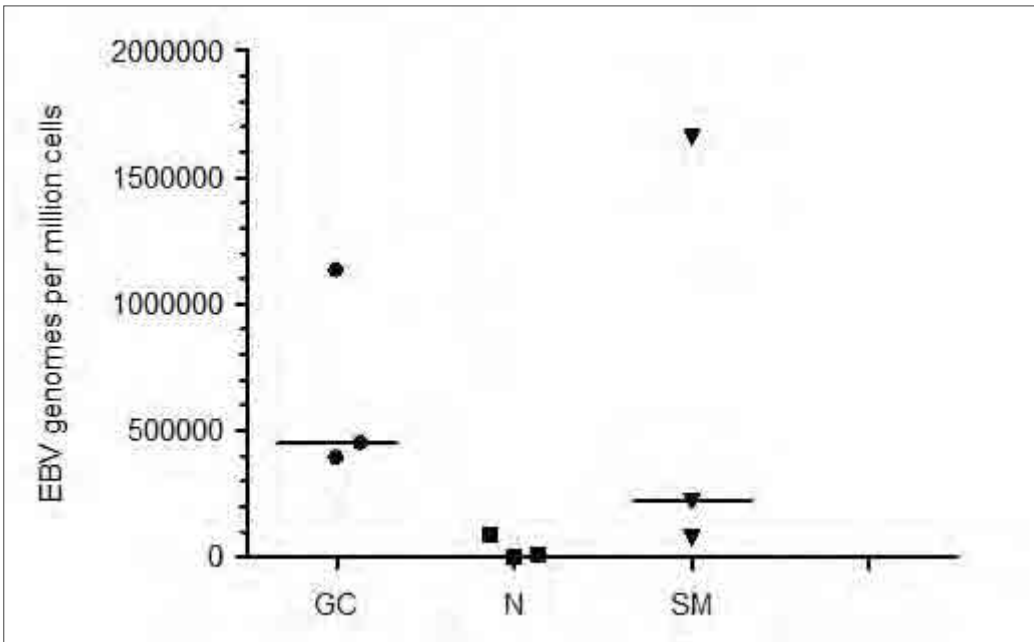


Figure 18 . EBV load distribution in IM tonsillar B cell subsets

EBV loads from IM tonsillar germinal centre (GC) naive and switched memory B cell subsets derived from 3 donors. Values are expressed as EBV genomes per million cells. Horizontal lines within data from each subset show the median value.

3.4 Frequency of EBV-Infected cells

The above method to examine EBV loads in different B cell subsets provides an absolute value of virus genomes within each cell population, but provides no information about the frequency of virus-infected cells. Therefore, it cannot be used to ascertain whether high loads within a cell population reflect increased numbers of infected cells, or higher numbers of EBV genomes per infected cell, or a combination of the two. In order to answer these questions, a limiting dilution PCR approach, based on that first described by Thorley-Lawson and colleagues, was employed to estimate the frequency of infected cells (Khan et al., 1996). Using this limiting dilution method for the analysis of EBV-infected cells, the principle aims were to examine (i) the frequency of infected cells within different B cells subsets from the peripheral blood and tonsil, and (ii) to estimate the number of EBV genomes carried by each infected cell. Data produced using this method therefore supplements the EBV total load data described above.

3.4.1 Validation of the Limiting Dilution Method Using Namalwa-BL Cell Line

Before *ex vivo* samples were used, the limiting dilution method was first validated in a control experiment using the EBV-positive cell line Namalwa-BL (illustrated in Figure 19). EBV+ cells were added to an EBV-negative cell population (DG75) at a known frequency of 1 EBV+ cell to 4,000 EBV- cells. The starting sample, containing a known quantity of cells (eg. 50,000 cells per 50µl), was serially diluted 2-fold until 8 dilutions containing known quantities of cells were acquired. Subsequently 8 replicates from each of the dilutions were

Figure 19 . Validation of limiting dilution analysis using the Namalwa-BL cell line

Cells from the EBV-positive Namalwa-BL cell line were added to an EBV-negative DG75 cell population at a frequency of 1 EBV+ cell per 4000 EBV- cells. **A.** Starting with 50,000 cells per 50µl at the highest concentration, the cell sample was serially diluted 1:2 to the lowest concentration (391 cells per 50ul). 50µl of each dilution was then added to 8 wells of a 96-well plate, the cells lysed and a qPCR assay for EBV pol carried out. **B.** The number of wells containing an EBV pol positive signal was scored at each dilution (total score from the 8 replicates is indicated to the right of the table). **C.** Summary of the data used to calculate the cell frequency. These values are added to the data entry box at the WEHI limiting dilution analysis webpage. The calculation provides an estimated frequency (in this instance 1 positive cell in 4426) together with upper and lower confidence intervals (2799 to 7000). In this control experiment, where a known frequency of 1 EBV+ cell to 4000 EBV- cells was used, the limiting dilution method was validated.

A

	1	2	3	4	5	6	7	8
A	50,000	50,000	50,000	50,000	50,000	50,000	50,000	50,000
B	25,000	25,000	25,000	25,000	25,000	25,000	25,000	25,000
C	12,500	12,500	12,500	12,500	12,500	12,500	12,500	12,500
D	6250	6250	6250	6250	6250	6250	6250	6250
E	3125	3125	3125	3125	3125	3125	3125	3125
F	1563	1563	1563	1563	1563	1563	1563	1563
G	781	781	781	781	781	781	781	781
H	391	391	391	391	391	391	391	391

**B**

	1	2	3	4	5	6	7	8	
A	+	+	+	+	+	+	+	+	8
B	+	+	+	+	+	+	+	+	8
C	+	+	+	+	+	+	+	+	8
D		+	+	+	+	+	+		6
E						+	+		2
F		+							1
G									0
H									0

**C**

cell number	replicates	positive wells
50,000	8	8
25,000	8	8
12,500	8	8
6250	8	7
3125	8	1
1563	8	4
781	8	1
391	8	0



1 out of 4426 cells EBV-positive
(confidence intervals: 2799-7000)

Figure 19. Validation of limiting dilution analysis using the Namalwa-BL cell line

A. Example of cell input in serial dilution series. **B.** Result of qPCR to detect EBV genomes. **C.** Summary of data. (A full description is provided on the opposite page).

placed into a 96-well PCR plate (Figure 19a). The replicate samples were then lysed and subjected to the same EBV load qPCR as described above, and the number of positive wells in each dilution was scored (Figure 19b). Typically all wells containing the highest cell inputs in the series were positive, whilst those at the bottom of the dilution, containing the lowest cell numbers, were negative. The cell input at each dilution, number of replicates and fraction of positive wells were used to estimate the frequency of infected cells (Figure 19c) by a simple Poisson distribution method using software provided by WEHI Institute of Medical Research, Australia (Hu and Smyth, 2009).

In the example shown in Figure 19, the estimated frequency of EBV-infected cells was 1 cell in 4,426 (with confidence intervals of 2,799-7,000). This value is close to the known frequency of 1 cell in 4,000, and therefore validates the limiting dilution method. Note that using this value, the number of genomes per infected cell can also be estimated by dividing the number of genomes per 10^6 cells by the number of infected cells per 10^6 cells (see below).

3.4.2 Frequency of Infected Cells in Peripheral Blood B cell

Subsets Derived from Healthy Carrier Donors

In the first experiment, limiting dilution analysis was carried out on naive, non-switched memory and switched memory B cells from the peripheral blood of 6 healthy carrier donors (shown in Table 7 and Figure 20). In support of the previous section, these results confirm that the highest viral loads were found in switched memory (median = 6,350 EBV genomes/ 10^6 cells), followed by non-switched memory (median = 850 EBV genomes/ 10^6 cells), with minimal loads detected in naive B cells (median = 110 EBV genomes/ 10^6 cells) (Figure 20a).

		Frequency of EBV+ cells	EBV+ cells/10 ⁶	EBV genomes/10 ⁶ cells	EBV genomes/cell (mean)
PB8	naive	1 in 112000 (28000-450000)	8	200	25
	NSM	1 in 36000 (19000-68000)	28	1350	48
	SM	1 in 12000 (7400-19000)	83	5000	60
PB9	naive	1 in 560000 (n/d)	2	30	15
	NSM	1 in 21000 (10000-42000)	48	1700	35
	SM	1 in 730 (450-1200)	1370	28000	20
PB10	naive	nd	nd	nd	nd
	NSM	1 in 44000 (14000-138000)	23	250	11
	SM	1 in 25000 (14000-44000)	40	1000	25
PB11	naive	1 in <90000 (n/d)	<10	44	nd
	NSM	1 in 132000 (43000-405000)	8	350	44
	SM	1 in 6300 (3900-9900)	160	6500	41
PB12	naive	1 in 550000 (n/d)	2	110	55
	NSM	1 in 43000 (19000-95000)	24	1700	71
	SM	1 in 3600 (1400-4100)	410	11600	28
PB13	naive	1 in 54000 (32000-91000)	18	260	14
	NSM	n/d	n/d	310	n/d
	SM	1 in 5800 (3300-10000)	170	6200	36

Table 7. EBV distribution in sorted peripheral blood B cell populations from healthy carriers

Summary of limiting dilution data from naive, non-switched memory (NSM) and switched memory (SM) B cells from the peripheral blood (PB) 6 healthy EBV carrier donors (PB donors 8-13). Also shown are the estimated values for (a) frequency of infected (EBV+) cells calculated using limiting dilution qPCR assay, (b) number of EBV+ cells/10⁶ cells, (c) EBV genomes/10⁶ cells calculated using standard EBV load qPCR assay, with values normalised against β 2M, and (d) mean number of EBV genomes/cell. In cases where too few cells were available, or the virus load was undetectable, values could not be determined (n/d).

Similarly, the frequencies followed the same pattern, with the highest number of EBV-infected cells detected in switched memory (median = 165 EBV+ cells/ 10^6 cells), followed by non-switched memory (median = 24 EBV+ cells/ 10^6 cells), and naive B cells (median = 8 EBV+ cells/ 10^6 cells) (Figure 20b).

Once the the total EBV load (genomes/ 10^6 cells) and the frequency (by limiting dilution) of EBV-positive cells is known, these data can be used to estimate (a) the number of EBV-positive cells per 10^6 cells, and (b) the number of genomes per cell. An example of these calculations, using data from the switched memory population of PB8, is described below:

Frequency of EBV+ cells = 1 in 12,000

EBV+ cells per 10^6 cells = $1,000,000 \div 12,000 = 83$

EBV genomes/ $10^6 = 5,000$

Mean number of genomes per cell = $5,000 \div 83 = 60$

Interestingly, no marked difference in number of EBV genome copies per infected cell were observed in any B cell population (non-switched memory cells median = 44 EBV genomes/cell, switched memory median = 32 EBV genomes/cell and naive median = 20 EBV genomes/cell) (Figure 20c).

3.4.3 Frequency of Infected Cells in *Ex Vivo* IM Tonsillar B cells

In the next experiment, the limiting dilution technique was used to analyse total CD19-selected B cells derived from IM tonsils. These cells were chosen for their higher overall EBV load, and because they were readily available. The frequency of infected tonsillar B cells within the 4 individuals ranged from 6,400

EBV+cells/10⁶ cells to 32,300 EBV+cells/10⁶ cells, with the estimated mean number of EBV genomes per cell ranging from 46 to 343 (median = 128). A summary of the results from 4 IM tonsils (IMT2, IMT3, IMT6 and IMT7) can be seen in Table 8. Due to the small numbers of cells available from these donors, it was not possible to examine specific B cell subsets using the limiting dilution PCR method.

3.4.4 Genome Copies in Lytic and Latent AKBM Cells

From the above experiments an average number of genomes per infected cell can be estimated. However, if the population should contain a small number of lytic cells, the average value may be skewed. In order to estimate how many EBV copies are present in a productively infected cell, the AKBM cell line was used. AKBM is a cell line derived from Akata-BL, which has been stably transfected with a GFP reporter under the control of the lytic BMFR1 promoter. AKBM cells can be induced into lytic cycle following cross-linking with anti-IgG antibody (Ressing et al., 2005), leading to expression of the GFP reporter, which enables the separation of lytically infected cells from latently infected cells by FACS sorting.

Three separate experiments were carried out whereby AKBM cells were induced to undergo lytic replication. In each case, GFP-negative (latent) and GFP-positive (lytic) cells were sorted by FACS (data not shown) directly to individual wells of 96-well PCR plates and viral loads in individual cells were determined by qPCR (data shown in Figure 21 and summarised in Table 9). The results show that in each separate occasion when AKBM cells were induced to go into lytic cycle, individual GFP+ cells appeared to carry 100-fold

Table 8. Frequency of infected cells in unfractionated B cells derived from 4 IM tonsils

Summary of limiting dilution data from 4 IM tonsillar B cell samples. Rows A-H represent limiting dilution qPCR plates, including cell input (cells/well), number of replicate qPCRs (8) and the number wells containing EBV pol amplification (+ve wells). Displayed underneath are the calculated values for (a) EBV genomes/ 10^6 cells calculated using standard EBV load qPCR assay, with values normalised against $\beta 2M$, (b) frequency of infected (EBV+) cells calculated using limiting dilution qPCR assay, (c) number of EBV+ cells/ 10^6 cells, and (d) number of EBV genomes/cell. Numbers in brackets represent lower and upper confidence intervals.

row	IMT3			IMT2			IMT6			IMT7		
	cells/well	replicates	+ve wells									
A	250	8	8	32	8	6	250	8	7	250	8	4
B	125	8	8	16	8	3	125	8	7	125	8	5
C	63	8	8	8	8	0	63	8	6	63	8	4
D	31	8	6	4	8	1	31	8	2	31	8	2
E	16	8	2	2	8	1	16	8	2	16	8	2
F	8	8	1	1	8	0	8	8	5	8	8	1
G	4	8	0	0.5	8	0	4	8	1	4	8	0
H	2	8	0	0.25	8	0	2	8	0	2	8	0
EBV genomes/10 ⁶ cells	1.5 x 10 ⁶			4.3 x 10 ⁶			2.0 x 10 ⁶			2.2 x 10 ⁶		
Frequency of EBV+ cells	1 in 31 (19-48)			1 in 34 (19-61)			1 in 58 (37-92)			1 in 157 (94-260)		
EBV+ cells/10 ⁶ cells	32,300			29,400			17,200			6,400		
EBV genomes/cell	46			145			110			343		

Table 8. Frequency of infected cells in unfractionated B cells derived from 4 IM tonsils

	GFP+ AKBM Cells			GFP- AKBM Cells		
	<u>1</u>	<u>2</u>	<u>3</u>	<u>1</u>	<u>2</u>	<u>3</u>
experiment number						
no. of PCR reactions	68	61	44	82	40	70
median no. EBV genomes per cell	24394	13245	2906	161	36	97

Table 9. EBV genome copies in individual GFP+ and GFP- AKBM cells

Populations of AKBM cells where induced to go into lytic cycle on 3 separate occasions. Single GFP+ (lytic) and GFP- (latent) cells were then sorted directly into 96-well PCR plates and EBV pol qPCR carried out. In most instances levels of the β 2M were undetectable, therefore EBV pol values were not normalised a cellular gene. Median numbers of EBV genome copy number per cell from each sort are shown.

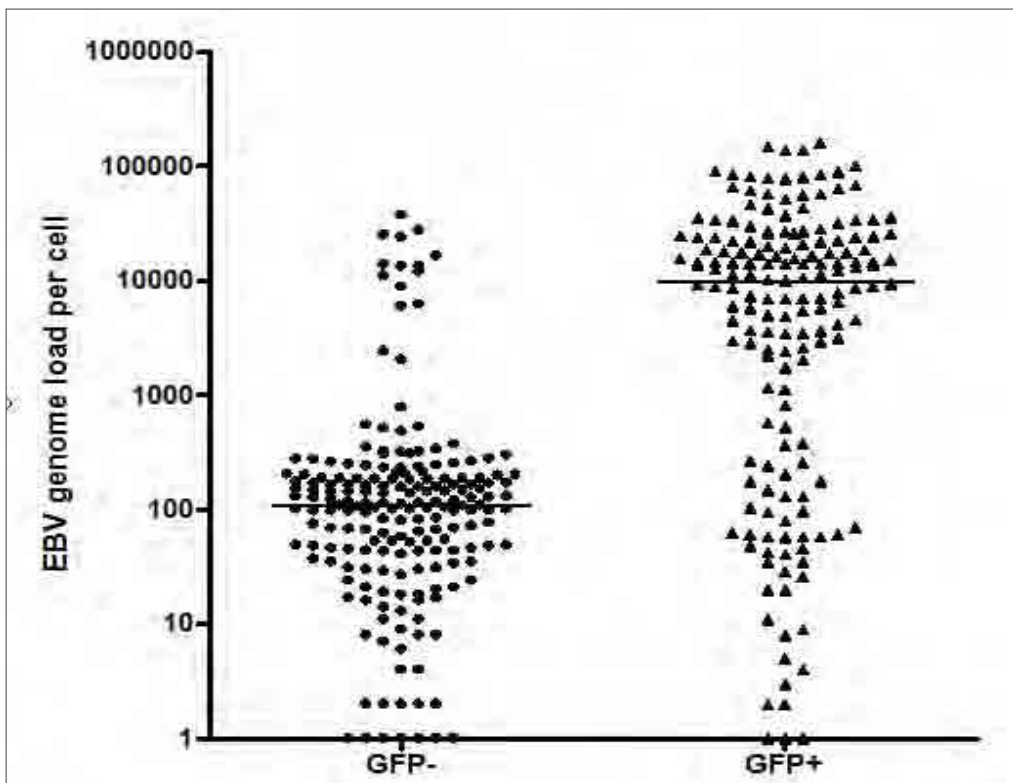


Figure 21. EBV genome copies in individual GFP+ and GFP- AKBM cells

All qPCR values (EBV genome copy number per cell) from single GFP+ and GFP- cells from each of the 3 experiments are shown. The majority of GFP- cells are latently infected, whereas the majority of GFP+ cells were induced into lytic cycle. Median values from each population are highlighted by horizontal lines. The data are presented using a log scale.

higher (median = 9770) numbers of EBV genomes than GFP- cells (median = 109). These values, based on the number of genomes per latently infected AKBM cell, are similar to those seen in infected B cells *ex vivo*.

3.5 Discussion

EBV establishes persistence in the human host by long-term latent infection of circulating memory B cells. Since it has been reported that both naive and memory B cells appear equally infectable *in vitro* (Ehlin-Henriksson et al., 2003), the mechanism by which the virus selectively colonises memory B cells *in vivo* remains unclear. Two models have been suggested to explain this process; the initial targeting of naive B cells during infection, which drives them to differentiate into memory B cells via a physiological GC reaction (Thorley-Lawson, 2001), or the GC-independent targeting of both cell types, followed by the preferential outgrowth of infected memory B cells due to an as yet unidentified survival advantage (Kuppers, 2003). In light of these hypotheses, we proposed that the central question arising from this debate is whether or not GC transit is a prerequisite for the colonisation of the memory B cell compartment by EBV. To address this issue, the current study aimed to examine EBV colonisation of PB B cell subsets from chronic carrier individuals, and in tonsillar B cell subsets from both chronic carriers and IM patients by sorting *ex vivo* cell suspensions, followed by qPCR assays to determine EBV load in each population. Two subsets in particular were focussed upon; (i) non-switched memory B cells, which as suggested by several studies (see Introduction for alternative developmental pathways) develop in a GC-independent manner, and (ii) germinal centre B cells.

3.5.1 EBV Colonisation of Non-Switched Memory B cells

Three major B cell subsets are found in the peripheral blood of healthy individuals (Klein et al., 1998); naive (IgD+CD27-), switched memory (IgD-CD27+) and non-switched memory (IgD+CD27+). Whilst convincing evidence has been put forward for the preferential colonisation of EBV within the switched memory B cell population of chronic carriers (Babcock et al., 1998, Joseph et al., 2000b), prior to the current study, EBV infection of the non-switched memory B cell fraction was not well documented in healthy individuals. EBV colonisation of the non-switched memory subset has, however, been described in the context of immunodeficiency (Chaganti et al., 2008). Specifically, Chaganti et al. showed that in XLP patients, who due to an inherited deficiency that prevents GC formation, lack switched memory B cells (Ma et al., 2006, Ma et al., 2007), but who still possess a circulating non-switched memory B cell population (Ma et al., 2006), EBV is able to establish persistence within the latter cell type. In order to explore whether this subset could also harbour EBV in immunocompetent individuals, B cell subsets were sorted from the peripheral blood of 13 healthy carrier donors and from 6 chronic carrier tonsils.

We first confirmed published findings (Babcock et al., 1998), showing that in healthy carriers a much higher viral load can be found in switched memory than in naive B cells. In addition however, a substantial EBV load was detected in the non-switched memory B cell fraction in all 13 donors, which although in most cases was not as high as that in switched memory, was notably higher than in the naive B cells. It is unlikely that this result is the product of contamination with infected switched memory B cells since the non-switched memory B cell populations were sorted to high purity (mean = 92%), with

contaminating cells being of a naive (IgD+CD27-) phenotype, rather than of a switched memory (IgD-CD27+) phenotype. Indeed given the switched memory B cell population median value (4200 genomes per 10^6 cells), 10% contamination with this subset would produce a value of ~ 420 genomes per 10^6 cells, which is almost 2-fold lower than the median EBV load from the non-switched memory population (730 genomes per 10^6 cells). Interestingly, in 2 of the 13 donors, higher loads were detected in the non-switched memory than in the switched memory fraction. Whereas this is an unexpected result, a similar finding was also observed in the published portion of this study (data generated by Dr Chaganti), where 1 out of 9 donors tested possessed detectable virus exclusively in the non-switched memory population (Chaganti et al., 2009). Following the examination of three B cell populations within peripheral blood, the larger range of phenotypically distinct subsets in tonsillar B cell preparations was then examined. In agreement with a separate study (Babcock et al., 2000), the viral load detected in the switched memory B cell population was substantially higher than in either the naive (CD38-IgD+CD27-) subset or the CD38+ GC subset, both of which contained either undetectable or extremely low levels of virus. Although the non-switched memory (CD38-IgD+CD27+) B cell subset was less abundant in tonsil populations than in the blood, it was still possible to sort these cells to high purity (mean = 95%). In 4 of 6 donors, a robust load was detected in the non-switched memory subset, with an overall median value which was only 2-fold lower than that of the switched memory B cell population. In one case (T6), the load in the non-switched memory population was markedly higher (~ 5 -fold) than in the isotype-switched population. As before, these results are unlikely to represent contaminating

switched memory cells within the non-switched memory B cell populations since the latter cells were sorted to high purity.

Taken together, the results from both the healthy carrier peripheral blood and chronic carrier tonsil donors indicate that EBV can colonise the non-switched memory B cell subset in a substantial number of individuals, albeit not as efficiently as the switched memory B cell population. This observation is in agreement with data from a larger cohort of donors that was generated by Dr Chaganti and subsequently published (Chaganti et al., 2009). Our findings, however, contradict several other studies. One earlier study reported no evidence of EBV infection within peripheral blood IgD+CD27+ B cells from healthy carriers, although only 3 donors were examined (Joseph et al., 2000b). Since 2 of 9 donors were found to have no detectable virus load in our published work (Chaganti et al., 2009), it is not unfeasible that by chance three such individuals were tested in the study by Joseph et al. The original study, which first suggested selective colonisation of the switched memory subset (Babcock et al., 1998), compared EBV infection in CD27+ B cells to CD27- B cells from IM patients. The author reported that the virus was concentrated primarily within the CD27+ subset, which includes both IgD-CD27+ switched memory and IgD+CD27+ non-switched memory B cells. In the same investigation, IgD+ and IgD- B cells were also compared. Whilst virus was found primarily within the IgD- subset, rather than in the IgD+ population, it is possible that infection of the non-switched memory population may have been masked by IgD+ naive cells, which constitute a much larger proportion of the blood B cell compartment (Klein et al., 1998). More recent studies have used RT-PCR single cell analysis of EBV-infected cells within sorted B cell

populations of blood from IM patients (Souza et al., 2005, Souza et al., 2007). In one such study, each of the small number of cells examined per patient carried mutated Ig genes (Souza et al., 2005). However, whilst most of these cells expressed either $\text{Ig}\gamma$ or α transcripts (corresponding to IgG and IgA, respectively), cells expressing mutated $\text{Ig}\mu$ (IgM) transcripts were detected in 3 out of the 6 donors examined. In a similar investigation, EBV-positive cells expressing $\text{Ig}\mu$ were also detected within CD27+ populations (Souza et al., 2007).

If $\text{IgD}^+\text{CD27}^+$ non-switched memory B cell development is GC-independent, our findings suggest that EBV is able to establish persistence in at least one memory B cell subset without the obligation to drive the cell through a GC reaction.

3.5.2 EBV Colonisation of Germinal Centre B cells

One popular model describing selective EBV colonisation of switched memory B cells is based on GC transit of the infected cell (Thorley-Lawson, 2001, Thorley-Lawson and Allday, 2008, Thorley-Lawson and Gross, 2004). It is proposed that following initial infection of naive B cells, the virus mimics physiologic antigen-driven B cell activation via expression of Latency III antigens, LMP1 and LMP2. Using this mechanism, the virus then drives the infected cell to form and participate in a GC reaction, thereby differentiating into a switched memory B cell, in which viral proteins are no longer expressed. Although this theory is supported by evidence of Latency III expression in tonsillar naive B cells (Babcock et al., 2000, Joseph et al., 2000a), up until recently little evidence for EBV infection of GC B cells has been presented. The

second aim of these experiments therefore was to find out whether EBV infection could be detected in GC B cells from chronic carrier and IM tonsils. Examination of sorted B cell subsets from 6 carrier tonsils revealed that B cells expressing the GC marker CD38 consistently contained extremely low levels of detectable virus, which were comparable to those found in the non-GC naive B cell population. These findings were in agreement with results previously generated by our laboratory (Chaganti et al., 2009).

The examination of IM tonsillar B cell subsets revealed firstly that, as expected, viral loads were up to 100-fold higher in IM tonsils than in chronic carriers. Secondly, we noted a different distribution of EBV load between the chronic and IM tonsil suspensions. While higher loads were found in the switched memory than in the naive B cell populations in both situations, high viral loads were also detected within the CD38+ B cells from IM tonsils and were similar, overall, to the loads seen in switched memory. Whilst only 3 IM donors were included in the current study, these findings are consistent with published data using a larger panel of material (Chaganti et al., 2009).

To address this difference in virus distribution, Chaganti et al. adopted a different B cell staining strategy to sort CD77+ centroblasts and CD10+ centrocytes, together with two subsets of CD77-CD10- (non-GC) cells; IgD+ (mainly naive) and IgD- (mainly switched memory). Using this technique, the virus was found to be concentrated within the non-GC, primarily IgD- B cell populations. This latter result raises doubt as to whether in an IM setting EBV is genuinely found in the GC cell fraction. Indeed, although CD38 is considered to be a useful marker of GC B cells in the setting of non-IM tonsils (Pascual et al., 1994, Klein et al., 2003), there is evidence to suggest that *in vitro* transformation

of B cells by EBV induces upregulation of this molecule (Rochford et al., 1993, O'Nions and Allday, 2004). It is possible, therefore, that in the context of primary EBV infection, where the latency III program may be expressed in newly infected cells, CD38 is primarily a marker for EBV-driven activation of infected cells, rather than of GC B cells.

Our findings contradict work that has recently been published. In one study EBV infection was analysed in chronic carrier tonsillar B cells which were co-stained for CD10 expression together with classical GC B cell markers Bcl6 or AID. The similar frequency of EBV-infected cells in tonsillar B cells before and after separation based on GC markers was put forward as evidence of GC B cell colonisation by EBV. Furthermore the expression of AID and Bcl6 in CD10+ B cell populations that contained EBV-positive cells (detected by PCR) was taken as proof that the EBV-infected cells were undergoing a GC reaction (Roughan and Thorley-Lawson, 2009). In a very recent investigation by the same authors, only ~45% of GCs in chronic carrier tonsils were found to contain EBV-infected cells, which were present in very small numbers (~3-4 cells per GC) (Roughan et al., 2010). Although these studies claim to provide confirmation of the existence of EBV-infected GC B cells, immunohistochemical examination of tonsil sections in many other studies has failed to find convincing evidence that EBV-infected cells are situated in the GC (Anagnostopoulos et al., 1995, Niedobitek et al., 1997, Kurth et al., 2000, Kurth et al., 2003). Whilst very small numbers of EBER-positive GC cells were detected in these investigations, Ig gene analysis of such rare cells suggested it was unlikely that they were participating in the local germinal centre reaction, but instead represented members of stable memory B cell clones derived from adjacent lymphoid tissue

(Kurth et al., 2003). In conclusion, therefore our results are consistent with these latter observations that EBV colonisation is not strictly dependent on GC transit.

3.5.3 Frequency of EBV-Infected Cells and Genome Copies in Individual Cells

In a series of parallel experiments, the frequency of infected cells was estimated via limiting dilution PCR in order to verify that virus loads reflected absolute numbers of infected cells in the different B cell subsets (rather than being skewed by differences in mean genome load per infected cell).

In agreement with earlier data, the virus load values were primarily concentrated within the switched memory B cell population, which also yielded the highest frequency of infected cells, while the lowest loads and frequencies were consistently detected in the naive B cell subset. We noted that the load and frequency values from the non-switched population were substantially higher than naive values. Importantly, no consistent difference in average EBV genome copies per infected cell was identified between the 3 distinct B cell subsets. These results therefore confirmed that EBV load values reflected the frequency of infected cells in each B cell population, rather than being skewed by differences in the number of genomes per cell between the 3 subsets.

One limitation of the qPCR method used to estimate the number of EBV genomes per cell in the *ex vivo* populations is that these values are an average calculated from the whole population, rather than an absolute value from each individual cell. Such information would be particularly useful in order to rule out the possibility that lytically infected cells, carrying high numbers of genomes,

may exist within the sample and skew the average value. Although this remains a possibility, it is highly unlikely that lytically infected cells were present in our data since (i) the high genomes numbers in lytically infected AKBM cells (median genomes = >9000 per cell) suggest that even if 1% of the population were lytic, the apparent average values may be substantially increased, (ii) lytic replication has been shown to be absent from peripheral blood B cells (Miyashita et al., 1995), and (iii) examination of lytic cycle transcripts in tonsillar B cells in our own laboratory revealed that only trace signals of immediate early transcripts and no late signal transcripts were detected (Chaganti et al., 2009).

Our estimates of average genomes per cell in latently infected PB B cell populations derived from healthy carriers (non-switched memory median = 44, switched memory median = 32) are consistent with those reported by others in both *in vitro* and *ex vivo* studies. *In vitro* analyses of genome copies in individual latently infected cells have shown that a range of values exist, depending on the cell line and the methods used. Early studies measuring viral DNA using non-PCR methods such as DNA reassociation kinetics have reported that the cell line Raji reportedly carries 50 to 60 EBV genomes per cell (Pritchett et al., 1976, Nonoyama and Pagano, 1973), whereas LCLs may carry 5-800 genomes per individual cell (Sugden et al., 1979). More recently, however, the LCL X50-7 was found to carry a median of 7 (range 2-18) EBV genomes per cell using fluorescent in situ hybridisation (FISH) targeting EBV DNA (Calattini et al., 2010). FISH has also been used to investigate genome copies in individual *ex vivo* B cells derived from PTLD patients (Rose et al., 2002). In this study, analysis of infected cells from both low load (1-20 EBV genomes/ 10^6 cells) and high load (>20 EBV genomes/ 10^6 cells) patients

revealed that both carrier types harboured cells containing 1-2 genomes per cell, but that an additional subset of cells carrying 20-50 genomes per cell was also detected in high load carriers. In a separate, very recent study, EBV genomes in individual *ex vivo* B cells were examined using peripheral blood derived from patients with high EBV loads. Individuals included in the study suffered from a range of disorders including HIV, IM, PTLD and severe primary EBV infection. Remarkably, the numbers of EBV genomes in single B cells from each patient were similar, with an overall median of 13.9 (range 1-40). Although the subject material and techniques used in both these recent studies differed from the current qPCR-based work, which focussed on fractionated B cell populations from healthy carriers, the values are comparable to our own estimations. Furthermore, in agreement with our findings, Calattini et al. also show that total EBV loads did not correlate with numbers of genomes in individual cells.

These results raise the question of how genome amplification within infected cells occurs. Particularly in light of the early study carried out by Sugden et al., which showed that following the infection of peripheral blood lymphocytes *in vitro* with only ~1 EBV particle per cell, after 30 generations in cell culture the number of EBV genomes had amplified 15-20-fold. Exactly how, and at what stage this amplification occurs both *in vitro*, and potentially *in vivo* is unclear, however, and may prove to be an interesting matter for future research.

In conclusion, we therefore propose that EBV is able to establish persistence in at least one memory B cell subset *in vivo* in a GC-independent manner. This hypothesis is explored further in the next chapter, where the ability of EBV infection to impose GC-associated genotypic and phenotypic changes to naive

B cells *in vitro*, and therefore outside a germinal centre environment, is examined in depth.

4 EBV Infection of B cell Subsets *in vitro*: Effects on IgH Genotype and Cellular Phenotype

The work presented in this chapter builds upon previous studies carried out by two former PhD students in the B Cell Group; Dr Sridhar Chaganti, and Dr Noelia Begue Pastor, in which peripheral blood B cells were sorted into naïve (IgD+CD27-), switched memory (IgD-CD27+) and non-switched memory (IgD+CD27+) subpopulations and then infected with EBV *in vitro*. In this EBV infection procedure, a limiting dilution technique was employed in order to generate predominantly monoclonal or biclonal LCL cultures. The effect of EBV infection upon cell genotype, specifically mutations in the IgH variable region, and phenotype, focusing on immunoglobulin (Ig) isotype expression, were then examined. The results from these experiments showed that approximately one quarter of LCL cultures derived from naïve B cells had acquired Ig variable region mutations by approximately 10 weeks post-infection. However, naïve LCLs did not isotype-switch and remained IgD+IgM+ regardless of whether they had accrued mutations. These findings imply a role for EBV in the induction of somatic hypermutation *in vitro*.

The potential to confer a mutated IgH genotype, typically associated with a memory B cell, upon a naïve B cell in the absence of germinal centre transit is an important finding, which is relevant to current theories surrounding EBV persistence *in vivo*. Although a widely accepted hypothesis suggests EBV drives infected naïve B cells to differentiate into memory B cells via a germinal centre reaction, in the previous chapter we challenged the necessity of germinal

centre involvement in EBV persistence. Furthermore the ability of EBV to induce mutation processes which inflict genomic instability upon the cell could have important implications to the oncogenic potential of the virus.

The initial stages of my own project extended these earlier studies. A very small number of these experiments were collaborations between myself and Dr Chaganti (highlighted where appropriate in this chapter). The aim of my investigation was to examine further the phenomenon of *in vitro* somatic hypermutation in naïve LCLs following EBV infection. In addition to carrying out EBV transformation experiments under limiting dilution conditions using small numbers of naïve B cells, bulk LCL cultures were also produced by infecting larger numbers of cells. Whereas limiting dilution assays tended to generate monoclonal cultures that needed to be expanded for ten weeks before enough cells were available for analysis, the establishment of bulk LCLs provided the opportunity to harvest cells at multiple time points. This had the advantage that the appearance of IgH mutations could be followed over time in the culture. Following on from earlier genotypic and phenotypic analyses, several other investigations were also carried out including; (i) transformation efficiency assays comparing transformability of naïve B cells and non-switched memory B cells, (ii) measuring the relative amounts of three distinct AID transcripts by qPCR, (iii) experiments using *in vitro* cytokine stimulation of naïve LCLs in order to ascertain whether naïve B cells were capable of CSR following EBV-driven transformation.

4.1 Isolation of Peripheral Blood B cell Subsets

Highly pure populations of peripheral blood B cell subsets were collected by FACS after staining for IgD and CD27, as described in the previous chapter. Re-analysis data of naïve, non-switched and switched memory B cell purities from 11 sorts are summarised in Table 10. Note that although all three subsets were collected in each sort, only naïve B cells were used from sorts 1-6, whereas naïve B cells plus non-switched memory B cells were used from sorts 7-11.

4.2 Establishment and Analysis of EBV-Infected Naïve LCLs and CD40L/IL-4 B Blasts

4.2.1 Experimental Outline

Although previous findings by Dr Chaganti suggested a link between EBV infection of naïve B cells and the accrual of somatic hypermutations in naïve LCLs, the possibility that this phenomenon was an artifact of *in vitro* cell culture, rather than a direct effect of EBV infection, had not been excluded. Therefore in the first series of experiments we looked for evidence of IgH mutations in naïve B blasts activated to proliferate *in vitro*, in the absence of EBV. To this end, bulk populations of naïve B cells were stimulated with CD40 ligand (CD40L) and IL-4, and maintained as CD40 blasts (BN-blasts) for up to nine weeks after establishment. In parallel, resting naïve B cells from different donors (except in the case of donor 4 where a CD40 blast and an LCL were produced from the same starting population) were infected with EBV to produce bulk naïve LCLs

<i>sort</i>	<u>Subset purity (%)</u>			<i>alias</i>	<i>experiment summary</i>
	naive (IgD+CD27-)	NS memory (IgD+CD27+)	S memory (IgD-CD27+)		
1	99	94	98	BN-blast 1	CD40L/IL-4 stimulation
2	99	94	96	BN-blast 2	CD40L/IL-4 stimulation
3	99	97	98	BN-LCL 1	bulk infection
4	99	80	99	BN-blast 3 + BN-LCL 3	bulk infection + CD40L/IL-4 stimulation
5	99	93	99	BN-LCL 4a, b and c	bulk infection
6	99	95	99	BN-LCL5 + CN-LCL5	limiting dilution + bulk infection
7	99	98	99	BN-LCL6 + CN-LCL6 + TA-1	limiting dilution + bulk infection + transformation assay + isotype switch experiment
8	99	98	99	TA-2	transformation assay
9	99	98	99	TA-3	transformation assay
10	99	95	99	BN-LCL7 + TA-4	transformation assay + isotype switch experiment
11	99	97	99	TA-5	transformation assay + isotype switch experiment

Table 10. Summary of peripheral blood FACS–sorted B cell populations used in *in vitro* experiments

Naive B cells were consistently the most pure sorted populations (>99%). Switched memory sorted populations were also highly pure (96-100%), whereas the purity of sorted non-switched memory cells varied between experiments from 80% to 98%. BN-blast = bulk naive blast, BN-LCL = bulk naive LCL, CN-LCL clonal naive LCL (established by limiting dilution), TA = transformation assay. In experiments 1-6, all 3 populations were sorted, but only naive were used, whereas in experiments 7-11 naive and non-switched memory were used.

(BN-LCLs). Cells were harvested for analysis at regular time points from both BN-blasts and BN-LCLs.

In order to examine IgVH sequences, genomic DNA was extracted from cell pellets, and PCR carried out to amplify the target VDJ sequences. The PCR products were then inserted into pGEMT vectors, and transformed into competent *E.coli*. Each *E.coli* colony represented a cloned IgH product, which in turn represented a single cell within the culture; therefore, each sequence shown in the following results represents the IgH sequence derived from a single B cell. Colonies were picked and grown up into small cultures, plasmid DNA extracted using standard methods and the PCR-generated inserts were sequenced. The IgH mutations were identified by aligning the sequences to published V, D and J germline segments using Vbase (Retter et al., 2005), and where appropriate confirmed using IGMT/V-QUEST (Giudicelli et al., 1998) (see Appendix for correlated V, D and J nomenclature). Mutations were defined as individual nucleotide changes compared to the nearest matched germline sequence. Sequences carrying more than two mutations were classified as “mutated”, whereas those with two or fewer mutations were deemed to be “unmutated”. A schematic outline of these experiments is shown in Figure 22.

For each sequence analysed, several characteristics were recorded. As an example of how individual sequences will be presented in this chapter, two representative sequences (1 and 12) from the BN-blast1 resting cell data are shown in Figure 23. The following features are highlighted; (i) the germline sequence on the top row, (ii) the locations of the V region up to codon 94, (iii) the first ten amino acids of the VDJ junction translation as provided by Vbase, typically including the last 3 codons of the V region sequence and the first 7

Figure 22. Generation of bulk naive CD40 blasts and LCLs

B cells were isolated from peripheral blood using anti-CD19 Dynabeads. IgD⁺CD27⁻ Naïve B cells were then sorted by FACS. Naïve B cells were either infected with EBV to produce a naïve LCL (N-LCL), or cultured with CD40L⁺ mouse L-cells and IL-4 to generate naïve CD40 B blasts (N-blasts). At various time points, cell pellets were collected and IgH PCR carried out on extracted genomic DNA. IgH PCR products were then cloned into competent E.coli and colonies (representing individual cell sequences) were picked to undergo DNA sequencing. The VDJ and CDR3 sequences in each sample were identified using V base, a database containing published germline VDJ segments. Nucleotide differences to published germline sequence were classed as mutations, and any sequence with >2 mutations was considered mutated.

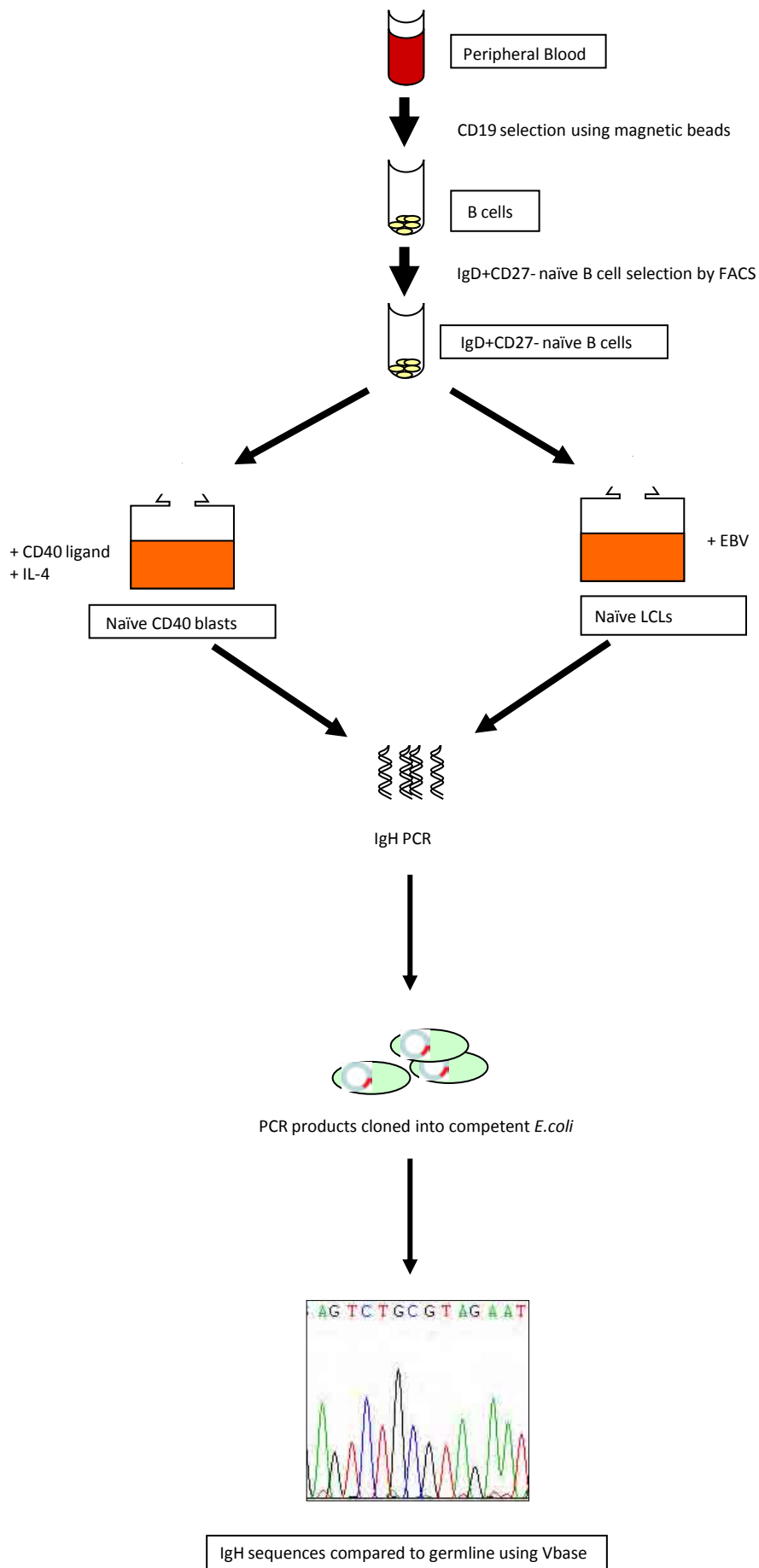


Figure 22. Generation of bulk naïve CD40 blasts and LCLs

Unmutated sequence



Mutated sequence

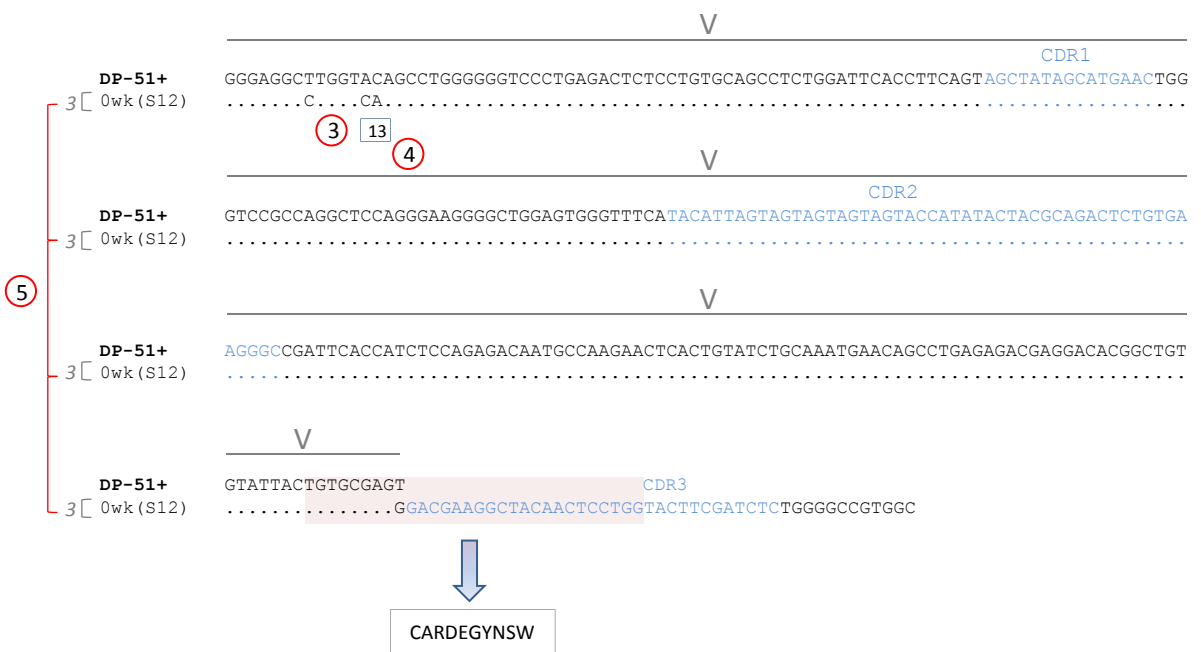


Figure 23. Examples of mutated and unmutated IgH sequences

Data shown are sequences 1 and 12 from BN-blast 1 (0 week) experiment.

Legend

1. V region location.
2. The first 30 bases, corresponding to the first 10 amino acids of the VDJ junction translation provided by Vbase, which also includes the first 7 amino acids of the CDR3 (the sequence between codon 94 and a conserved Trp residue in the J region was deemed to constitute the CDR3 region).
3. Mutations, which are identifiable as nucleotide changes from the germline sequence.
4. Where specific mutation locations are referred to in the text, the codon position may also be indicated.
5. Total number of mutations in the sequence may be shown if multiple mutated sequences are presented together.

Note: sequences shown exclude the FR1c and JH primers sequences since they may not reflect the true sequence of the IgH allele. The V region alignment therefore begins at codon 9.

codons of the CDR3 sequence (highlighted by a lilac box), (iv) sequence changes relative to the germline sequence, (v) where relevant, the codon locations of specific mutations, (vi) where more than one clonal sequence is shown, the individual sequence identity plus number of mutations are highlighted to the left of the figure. CDR1, CDR2 and CDR3 IgH sequences are highlighted in blue text. The CDR3 region was estimated to be between codon 94 (in the V segment) and a conserved Trptophan (Trp) residue in the J segment at approximately codon 102 (Raaphorst et al., 1997).

Since it was not feasible to display all sequence data individually, most of the results are presented as summary tables showing the identification of V, D and J segments and the total number of V region mutations between codons 9 and 91 for each sequence. As individual B cells harbour unique CDR3 region sequences, clonally related cells were identified by the first 10 translated amino acids of the VDJ junction.

4.2.2 IgH Analysis of Bulk Naive CD40 Blasts

In this first experiment, two bulk naive cultures of CD40L/IL-4-stimulated blasts (BN-blasts 1 and 2) were established using PB naive B cells from separate donors. IgH sequences from the starting naïve B cell populations were examined, together with sequences amplified from the bulk cultures at six and nine weeks post-stimulation (Table 11 and Table 12).

The resting naive B cell sorted population used to generate BN-blast1 was estimated to be 99% pure (Table 10). Examination of IgVH sequences from this starting population revealed 11 out of 12 sequences analysed were unmutated (based on the assumption that 0-2 mutations are classified as germline),

Resting naive B cells

sequence	V	D	J	junction translation	mutations
1	DP-71/3d197d...+	D3	JH2	RAREHIKGYF	0
2	DP-10/hv1051...+	D3-10/DXP'1	JH6b	RAITYYYGSG	0
3	DP-54/V3-7...+	D4	JH6c	CARPRHLGLG	0
4	DP-71/3d197d...+	Not found	JH6c	CARTEEGYDS	0
5	DP-73/V5-51...+	D2-21	JH4b	CARSYCGGDC	0
6	DP-49/1.9III...+	D1-26	JH6c	CAKDKKAALG	0
7	DP-75/VI-2...+	D4	JH6b	CARAFRPGY	0
8	DP-15/VI-8+	D1-26	JH6c	CARGGRVTIF	0
9	DP-73/V5-51...+	D7-27/DHQ52	JH4b	CARLGSSVGG	1
10	DP-14/VI-18+	D2-8/DLR1	JH6b	CARGMHYGM	1
11	V3-48/hv3d1...+	D7-27/DHQ52	JH6b	CAKDWGYGM	2
12	DP-51+	D5-24	JH2	CARDEGYNSW	3

6 weeks

sequence	V	D	J	junction translation	mutations
1	DP-71/3d197d...+	D5-5/DK4	JH5b	CARSPRGYSY	0
2	DP-73/V5-51...+	not found	JH4b	CARAGRDDL	0
3	DP-71/3d197d...+	D6-19	JH6b	CARDQGGIAY	0
4	VI-4.1b+	not found	JH5b	CARDRSKRDR	0
5	DP-15/VI-8+	D4	JH6c	CARGGYCSST	0
6	DP-71/3d197d...+	D1-7/DM1	JH3b	CAREKNDIPG	0
7	DP-71/3d197d...+	D2-15/D2	JH6c	CASRFVGYCS	0
8	DP-15/VI-8+	D5-12/DK1	JH6b	CARGVVDIVA	0
9	VIV-4/4.35+	D2-15/D2	JH2	CARDPGYCSSL	0
10	DP-35/V3-11...+	D6-13/DN1	JH4b	CARDHSIAAAA	0
11	DP-78/3d230d...+	D2-15/D2	JH4b	CASSAYCSGG	0
12	DP-54/V3-7...+	D7-27/DHQ52	JH4b	CARTTGEFIP	0
13	DP-47/V3-23...+	D4	JH4b	CAKGGLAGGL	0
14	DP-66/V71-2...+	D3-3/DXP4	JH4b	CARVDVDFWS	1
15	DP-10/hv1051...+	D6-19	JH4b	CARSSYSGGW	1
16	DP-71/3d197d...+	D6-19	JH4b	CARLRGWHIA	1
17	DP-79/4d154...+	D4-17	JH6c	CARHPHIEND	1
18	DP-75/VI-2...+	D1-7/DM1	JH5b	CARKEIVELG	1
19	DP-75/VI-2...+	D1-26	JH4b	CASFFWEGVS	1
20	VIV-4/4.35+	D5-12/DK1	JH6c	CARVAYRRYY	1
21	VI-4.1b+	D3-10/DXP'1	JH6c	CARVWAPLLW	1
22	VHGL1.2	D2-15/D2	JH3b	CAREEDIVVV	2

9 weeks

sequence	V	D	J	junction translation	mutations
1	DP-2/V71-5+	D3-3/DXP4	JH6b	CAAEHDFWSSG	0
2	DP-65/3d75d...+	D5-24	JH6c	CARSLGDYHY	0
3	DP-71/3d197d...+	D6-13/DN1	JH6c	CARSVVYANT	0
4	DP-79/4d154...+	D1-7/DM1	JH6c	CARLPNWNVYV	0
5	DP-10/hv1051...+	not found	JH6c	CARSLIDYVP	0
6	DP-77/WHG16+	D6-13/DN1	JH5a	CAAVYIQQVK	0
7	DP-10/hv1051...+	not found	JH3b	CARGGGAFDI	0
8	DP-48/13-2+	not found	JH6b	CARESRRGGGG	0
9	DP-14/VI-18+	D3-10/DXP'1	JH4b	CARDRILWFR	0
10	DP-15/VI-8+	D5-5/DK4	JH2	CARELWLSLNW	1

Table 11. BN-blast 1

Table summarises the matched V, D and J alignments for each IgH sequence analysed at 0, 6 and 9 weeks post-establishment, the first 10 amino acids of the VDJ junction translation, and the number of mutations detected in the V region.

Resting naive B cells

sequence	V	D	J	junction translation	mutations
1	DP-35/V3-11...+	D1-26	JH4b	CARDLVGGPT	0
2	V3-53+	D5-5/DK4	JH2	CARDRRDTAI	0
3	DP-49/1.9III...+	D5-5/DK4	JH4b	CAKNHVDTAM	0
4	DP-31/V3-9P...+	D4-17	JH2	CAKVGTVTTL	0
5	DP-2/V71-5+	D5-24	JH6b	CAADYLTGIR	0
6	DP-79/4d154...+	D7-27/DHQ52	JH4b	CARRWLTGDL	0
7	DP-49/1.9III...+	D4-17	JH4b	CAKDLGTTVT	0
8	DP-49/1.9III...+	D1-26	JH1	CASTASSSLE	0
9	DP-10/hv1051...+	D7-27/DHQ52	JH5b	CARGGGPYGD	0
10	DP-73/V5-51...+	D6-13/DN1	JH6b	CARRYSSSWY	0
11	3d279d+	D1-1	JH4b	CAREVWDFS	0
12	YAC-5+	D6-13/DN1	JH4b	CARATGIAAA	0
13	DP-65/3d75d...+	D2-15/D2	JH4b	CARAGFGYCS	0
14	DP-14/V1-18+	D2-2	JH5b	CARGLGHCSS	0
15	DP-77/WHG16+	D4-11/DA1	JH6b	CARLRTTVD	0
16	DP-65/3d75d...+	D6-13/DN1	JH6b	CARFWGSSPL	1
17	DP-54/V3-7...+	D6-19	JH4b	CAKTGEVAVA	2

6 weeks

sequence	V	D	J	junction translation	mutations
1	DP-65/3d76d...+	D6-6/DN4	JH4b	CAREASSFGG	0
2	DP-46/3d216...+	D6-13/DN1	JH6b	CARDSYFPGI	0
3	DP-54/V3-7...+	D5-5/DK4	JH6b	CARGFSYPPY	0
4	DP-47/V3-23...+	D6-19	JH6b	CAKDPGVAGT	0
5	DP-31/V3-9P...+	D1-7/DM1	JH6b	CAKEFGLRYS	0
6	DP-35/V3-11...+	D5-24	JH6b	CARVLVEMAT	0
7	DP-79/4d154...+	D2-2	JH5b	CASTKVPAAI	0
8	DP-14/V1-18+	D4	JH6b	CARVYGYCSS	0
9	DP-79/4d154...+	D1-7/DM1	JH4b	CASFRPLIT	0
10	DP-79/4d154...+	not found	JH4b	CARQIGRGxE	0
11	DP-54/V3-7...+	D5-12/DK1	JH4b	CARPVPTVQA	0
12	DP-7/21-2...+	D4-11/DA1	JH6b	CARENYSIHY	0
13	DP-35/V3-11...+	D6-19	JH2	CARNLAVADY	1
14	DP-75/V1-2...+	D3-10/DXP ¹	JH5b	CAREENIGD	1
15	DP-10/hv1051...+	D24-23	JH6b	CARGILSTVV	1
16	DP-46/3d216...+	D4-17	JH6b	CARDPPYGDS	1
17	DP-25/V1-3b+	D3-16	JH4b	CARDGSVITF	1
18	DP-63/VH4.21...+	D3-16	JH6b	CxREISGWGP	2

9 weeks

sequence	V	D	J	junction translation	mutations
1	DP-70/4d68...+	D3	JH4b	CARDLVVIAR	0
2	DP-77/WHG16+	D6-19	JH6b	CARATGAVAG	0
3	DP-10/hv1051...+	D3-3/DXP4	JH4b	CARSPDYDFW	0
4	DP-46/3d216...+	D6-13/DN1	JH4b	CAVGGPEQQL	0
5	DP-10/hv1051...+	D6-6/DN4	JH6b	CARASWDSSS	0
6	V3-53+	not found	JH6b	CARQKSSYYY	0
7	DP-54/V3-7...+	D4	JH6b	CARENCISTS	0
8	DP-49/1.9III...+	D6-6/DN4	JH4b	CARRKQLAEI	0
9	DP-15/V1-8+	D4-11/DA1	JH4b	CARGVAVTNN	0
10	DP-48/13-2+	not found	JH6b	CARGGGGFWS	0
11	DP-35/V3-11...+	D6-19	JH2	CARGIGYSSG	0
12	DP-75/V1-2...+	D2-15/D2	JH4b	CARGRMLVV	1
13	COS-6/DA-8...+	D4	JH4b	CARGLRLVPA	1
14	DP-54/V3-7...+	D6-6/DN4	JH4b	CARARRGWSA	1
15	DP-71/3d197d...+	D2-15/D2	JH4b	CARIVGEYCS	2
16	DP-78/3d230d...+	D3-16	JH4b	CARHGDRRLM	2
17	DP-46/3d216...+	D3	JH3b	CARDPPSAVW	3
18	DP-47/V3-23...+	D6-19	JH6b	CAKDGSSGW*	4

Table 12. BN-blast 2

The table summarises the matched V, D and J alignments for each IgH sequence analysed at 0, 6 and 9 weeks post-establishment, the first 10 amino acids of the VDJ junction translation, and the number of mutations detected in the V region.

confirming the purity of the isolated naive B cells (Table 11). As expected the VDJ rearrangement of each sequence, together with the junction translation, was unique, indicating that each sequence represented a different unrelated B cell.

When the same BN-blast 1 culture was screened after six weeks in culture, 22 of 22 sequences analysed were unmutated. Similar to the resting cells, the IgH sequences contained unrelated VDJ rearrangements and junction translations, signifying a polyclonal culture. Likewise IgH analysis of BN-blast 1 at nine weeks yielded 10 out of 10 unmutated and clonally independent sequences (Table 11).

To confirm these observations, the analysis was repeated with a second CD40 blast culture (BN-blast 2). The results from BN-blast 2 were comparable to those from BN-blast1. All 17 IgH sequences obtained from the isolated naive B cells and all 18 sequences examined in the six week old culture were scored as unmutated (Table 12). Nine weeks after establishment, two mutated IgH sequences out of 18 were identified (sequence 17 and sequence 18, Table 12), accounting for 11% of the total sequences at this time point. The VDJ rearrangements and junction translation combinations of each sequence revealed a polyclonal population of cells prior to stimulation, which remained polyclonal at six and nine weeks (Table 12).

Taken together the results from BN-blast 1 and BN-blast 2 suggest that naive B cell cultures stimulated with CD40L and IL-4 *in vitro* remain polyclonal and show no evidence of SHM for up to nine weeks in culture.

4.2.3 IgH Analysis of Bulk Naive LCL1

In the next experiment, the effect of EBV infection on IgH genotype was determined following transformation of naive B cells *in vitro*. The starting naive B cell population was processed and sorted as before to a purity of 99%. Each of 16 IgH sequences examined in the starting population was unique, based on VDJ analysis and CDR3 sequences, reflecting a polyclonal population. Fifteen of 16 IgH sequences analysed were unmutated. The single mutated IgH sequence carried 12 mutations, and may represent a contaminating memory B cell.

Resting naive B cells were then infected with EBV *in vitro* and expanded in culture, with cells harvested for analysis at six, nine and twelve weeks post-infection. In contrast to the B blast cultures, clonally related IgH sequences were detected in the BN-LCL 1 culture at six weeks post-infection. These sequences (which will be referred to as clonal families) share VDJ rearrangements, junction translations and CDR3 sequences. As shown in Table 13, in order to make the families easily distinguishable, the IgH sequences are grouped together and highlighted in a specific colour (e.g. family1 in each experiment is always yellow). IgH sequences only detected once within a set of data are not colour highlighted and are displayed underneath any clonal families in ascending order according to number of mutations.

By six weeks post-infection, 16 out of 20 sequences were clonally related (referred to as family 1), and the remaining 4 were all unique. At nine weeks, a small proportion of individual sequences were still present, but family 1 still

Resting naive B cells

sequence	V	D	J	junction translation	mutations
1	DP-88/hv1051K...+	D6-13/DN1	JH4b	CARGYSSSWH	0
2	DP-32/V3-20+	not found	JH6b	CARDSWWGGN	0
3	DP-73/V5-51...+	D4	JH5b	CARGAIVVVP	0
4	DP-10/hv1051...+	D4-17	JH4b	CAKMGGGYGQ	0
5	DP-79/4d154...+	D2-21	JH2	CARTAMTWYF	0
6	DP-70/4d68...+	D6-13/DN1	JH4b	CARHSGIAAV	0
7	DP-47/V3-23...+	D4-11/DA1	JH6b	CAKQYSLDY	0
8	DP-8+	D6-6/DN4	JH6b	CARVL*VGQL	0
9	DP-88/hv1051K...+	D3-10/DXP*1	JH6b	CARGLGNYYY	0
10	DP-71/3d197d...+	D2-15/D2	JH6b	CARYHCSSGS	0
11	DP-47/V3-23...+	not found	JH3b	CAKAGYLDGQ	0
12	DP-49/1.9III...+	D3-22/D21-9	JH6b	CAKVGGIKAV	1
13	7A.4	not found	JH6b	TVWTSGAKGP	1
14	VHVCW/COS-24+	D5-12/DK1	JH4b	CARSGYSYV	1
15	V3-48/hv3d1...+	not found	JH4b	CARVARxxFD	2
16	DP-8+	D3	JH6b	CARESHSRPY	12

6 weeks

sequence	V	D	J	junction translation	mutations
1	DP-88/hv1051K...+	D5-12/DK1	JH6b	CARSERSGWE	0
2	DP-88/hv1051K...+	D5-12/DK1	JH6b	CARSERSGWE	0
3	DP-88/hv1051K...+	D5-12/DK1	JH6b	CARSERSGWE	0
4	DP-88/hv1051K...+	D5-12/DK1	JH6b	CARSERSGWE	0
5	DP-88/hv1051K...+	D5-12/DK1	JH6b	CARSERSGWE	0
6	DP-88/hv1051K...+	D5-12/DK1	JH6b	CARSERSGWE	0
7	DP-88/hv1051K...+	D5-12/DK1	JH6b	CARSERSGWE	0
8	DP-88/hv1051K...+	D5-12/DK1	JH6b	CARSERSGWE	0
9	DP-88/hv1051K...+	D5-12/DK2	JH6b	CARSERSGWE	0
10	DP-88/hv1051K...+	D5-12/DK1	JH6b	CARSERSGWE	0
11	DP-88/hv1051K...+	D5-12/DK1	JH6b	CARSERSGWE	1
12	DP-88/hv1051K...+	D5-12/DK1	JH6b	CARSERSGWE	1
13	DP-88/hv1051K...+	D5-12/DK1	JH6b	CARSERSGWE	1
14	DP-88/hv1051K...+	D5-12/DK1	JH6b	CARSERSGWE	1
15	DP-88/hv1051K...+	D5-12/DK1	JH6b	CARSERSGWE	1
16	DP-88/hv1051K...+	D5-12/DK1	JH6b	CARSERSGWE	4
17	DP-78/3d230d...+	D6-25	JH4b	CARGAEDSSG	0
18	DP-10/hv1051...+	D4	JH6b	CARAGGYCSS	1
19	DP-65/3d75d...+	D1-26	JH4b	CARVKGIGGD	5
20	COS-16+	D2-8/DLR1	JH4b	CAKVVHTAPA	21

 Family 1

 Family 2

Table 13. BN-LCL1

Table summarises the matched V, D and J alignments for each IgH sequence analysed at 0 and 6 weeks post-establishment (9 and 12 weeks shown on next page), the first 10 amino acids of VDJ junction translation, and the number of mutations detected in the V region. IgH sequences identified as clonal family 1 are highlighted in yellow, family 2 highlighted in blue and IgH sequences only detected once are not colour-highlighted.

9 weeks

sequence	V	D	J	junction translation	mutations
1	DP-88/hv1051K...+	D5-12/DK1	JH6b	CARSERSGWGE	0
2	DP-88/hv1051K...+	D5-12/DK1	JH6b	CARSERSGWGE	0
3	DP-88/hv1051K...+	D5-12/DK1	JH6b	CARSERSGWGE	0
4	DP-88/hv1051K...+	D5-12/DK1	JH6b	CARSERSGWGE	0
5	DP-88/hv1051K...+	D5-12/DK1	JH6b	CARSERSGWGE	0
6	DP-10/hv1051...+	D5-12/DK1	JH6b	CATSERSGWGE	0
7	DP-88/hv1051K...+	D5-12/DK1	JH6b	CARSERSGWGE	1
8	DP-88/hv1051K...+	D5-12/DK1	JH6b	CARSERSGWGE	1
9	DP-88/hv1051K...+	D5-12/DK1	JH6b	CARSERSGWGE	1
10	DP-88/hv1051K...+	D5-12/DK1	JH6b	CARSERSGWGE	1
11	DP-88/hv1051K...+	D5-12/DK1	JH6b	CARSERSGWGE	1
12	DP-88/hv1051K...+	D5-12/DK1	JH6b	CVRERSGWGE	1
13	DP-88/hv1051K...+	D5-12/DK1	JH6b	CARSERSGWGE	1
14	DP-88/hv1051K...+	D3	JH6b	CARSERSGWGE	1
15	DP-88/hv1051K...+	D5-12/DK1	JH6b	CARSERSGWGE	1
16	DP-88/hv1051K...+	D5-12/DK1	JH6b	CARSERSGWGE	3
17	DP-65/3d75d...+	D2-15/D2	JH5b	CARDQLAYCS	0
18	DP-65/3d75d...+	D2-15/D2	JH5b	CARDQLAYCS	1
19	DP-88/hv1051K...+	not found	JH6b	CARDSRVWLL	1
20	DP-70/4d68...+	not found	JH6b	CAAFNTGFGT	3
21	DP-49/1.9III...+	D2-2	JH4b	CARTRGATHP	3

12 weeks

sequence	V	D	J	junction translation	mutations
1	DP-88/hv1051k...+	D5-12/DK1	JH6b	CARSERSGWGE	0
2	DP-88/hv1051k...+	D5-12/DK1	JH6b	CARSERSGWGE	0
3	DP-88/hv1051k...+	D5-12/DK1	JH6b	CARSERSGWGE	0
4	DP-88/hv1051k...+	D5-12/DK1	JH6b	CARSERSGWGE	0
5	DP-88/hv1051k...+	D5-12/DK1	JH6b	CARSERSGWGE	0
6	DP-88/hv1051k...+	D5-12/DK1	JH6b	CARSERSGWGE	0
7	DP-88/hv1051k...+	D3	JH6b	CARSERSGRE	0
8	DP-88/hv1051k...+	D5-12/DK1	JH6b	CARSERSGWGE	1
9	DP-88/hv1051k...+	D5-12/DK1	JH6b	CARSERSGWGE	1
10	DP-88/hv1051k...+	D5-12/DK1	JH6b	CARSERSGWGE	1
11	DP-88/hv1051k...+	D5-12/DK1	JH6b	CARSERSGWGE	1
12	DP-88/hv1051k...+	D5-12/DK1	JH6b	CARSERSGWGE	1
13	DP-88/hv1051k...+	D5-12/DK1	JH6b	CARSERSGWGE	1
14	DP-88/hv1051k...+	D5-12/DK1	JH6b	CARSERSGWGE	2
15	DP-65/3d75d...+	D2-15/D2	JH5b	CARDQLVYCS	0
16	DP-65/3d75d...+	D2-15/D2	JH5b	CARDQLAYCS	0
17	DP-65/3d75d...+	D2-15/D2	JH5b	CARDQLAYCS	0
18	DP-65/3d75d...+	D2-15/D2	JH5b	CARDQLAYCS	0
19	DP-65/3d75d...+	D2-15/D2	JH5b	CARDQLAYCS	0
20	DP-65/3d75d...+	D2-15/D2	JH5b	CARDQLAYCS	0
21	DP-65/3d75d...+	D2-15/D2	JH5b	CARDQLAYCS	0
22	DP-65/3d75d...+	D2-15/D2	JH5b	CARDQLAYCS	1
23	DP-65/3d75d...+	D2-15/D2	JH5b	CARDQLAYCS	4
24	DP-49/1.9III...+	D6-25	JH4b	YARTRGATHP	1

 Family 1

 Family 2

Table 13. BN-LCL1

The table summarises the matched V, D and J alignments for each IgH sequence analysed at 9 and 12 weeks post-establishment (0 and 6 weeks shown on the previous page), the first 10 amino acids of the VDJ junction translation, and the number of mutations detected in the V region. IgH sequences identified as clonal family 1 are highlighted in yellow, family 2 highlighted in blue and IgH sequences only detected once are not colour-highlighted.

dominated the culture with 16 out of 21 related sequences. At this time point, two sequences from a second clone (family 2) were also detected. Finally, at twelve weeks post-infection, the culture consisted mainly of family 1 and family 2, with only 1 unique sequence. Interestingly the culture contained an increasing proportion of family 2 sequences over time, suggesting initial outgrowth of clones belonging to this family was slower than family 1.

Although a few instances of mutated IgH sequences arose in the BN-LCL1 culture, the majority of IgH sequences obtained were unmutated, regardless of time following infection. Examples of germline sequences from family 1 are shown in Figure 24. Where IgH mutations were identified in either family, they were for the most part situated at distinct V region locations; however, there was one example of a single mutation at codon 32 that was shared by several sequences in family 1 (Figure 25). The recurrence of this mutation within the data suggests it is the result of a genuine mutation event, rather than the product of PCR error. Furthermore, the isolation of a sequence (6wk(s16)) harbouring 3 mutations in addition to the common one, is suggestive of ongoing SHM within this cell clone.

4.2.4 IgH Analysis of Bulk CD40 Blast and Bulk LCL Cultures

Established from a Single Donor

The first three experiments clearly showed preferential outgrowth of clonal cell lines following EBV transformation, whereas BN-blasts remained polyclonal. Since all three cultures were generated from different B cell preparations, it is possible that these differences were a result of variation between individual donors. In order to resolve this issue, a BN-blast (BN-blast 3) and a BN-LCL

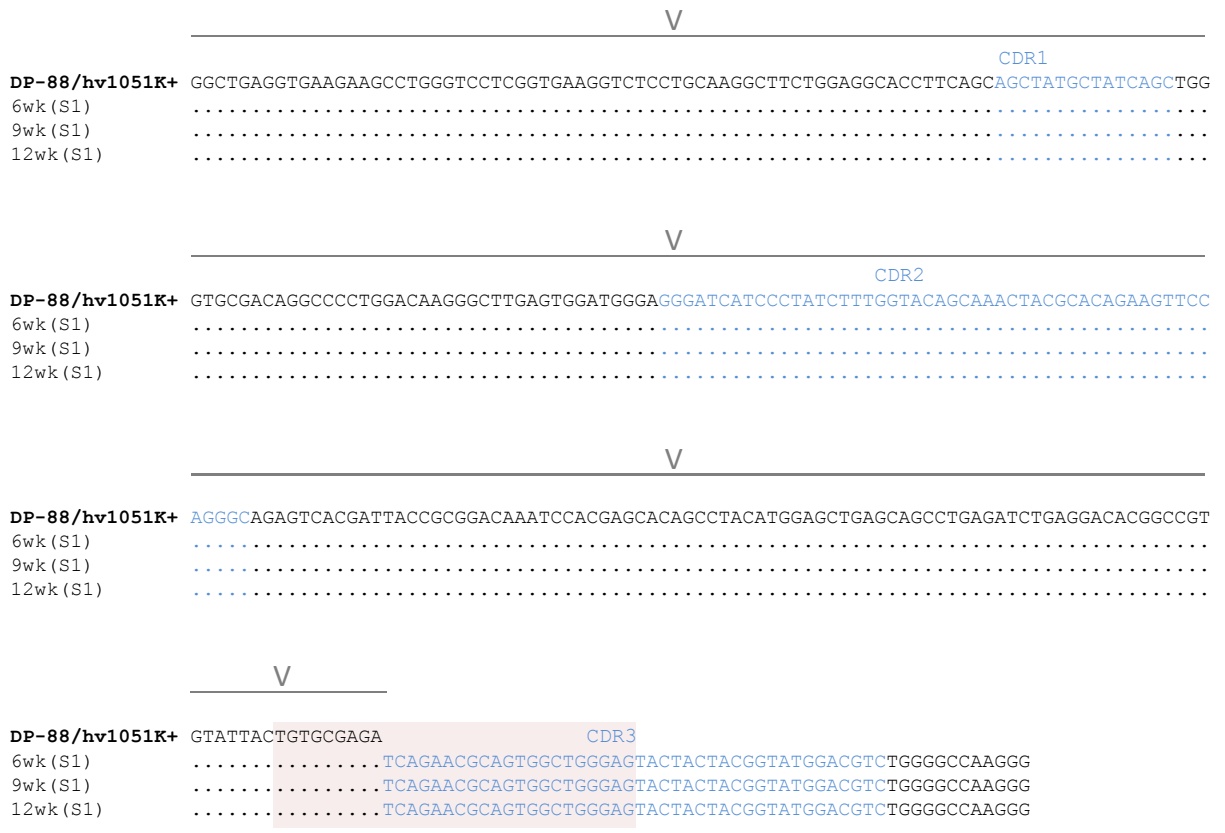


Figure 24. BN-LCL1 family 1 germline sequences were detected at 6, 9 and 12 weeks

BN-LCL1 family 1 sequences are aligned relative to the matched germline V region sequence (top row). The location of the V region is indicated and the CDRs (1, 2 and 3) are highlighted in blue text. A box is drawn around the first 30 nucleotides of the VDJ junction translation. Examples of unmutated IgH sequences from family 1. No changes from the germline IgH sequence (top line) were detected in the V region. Identical CDR3 sequences signify the clonal relationship between the sequences.

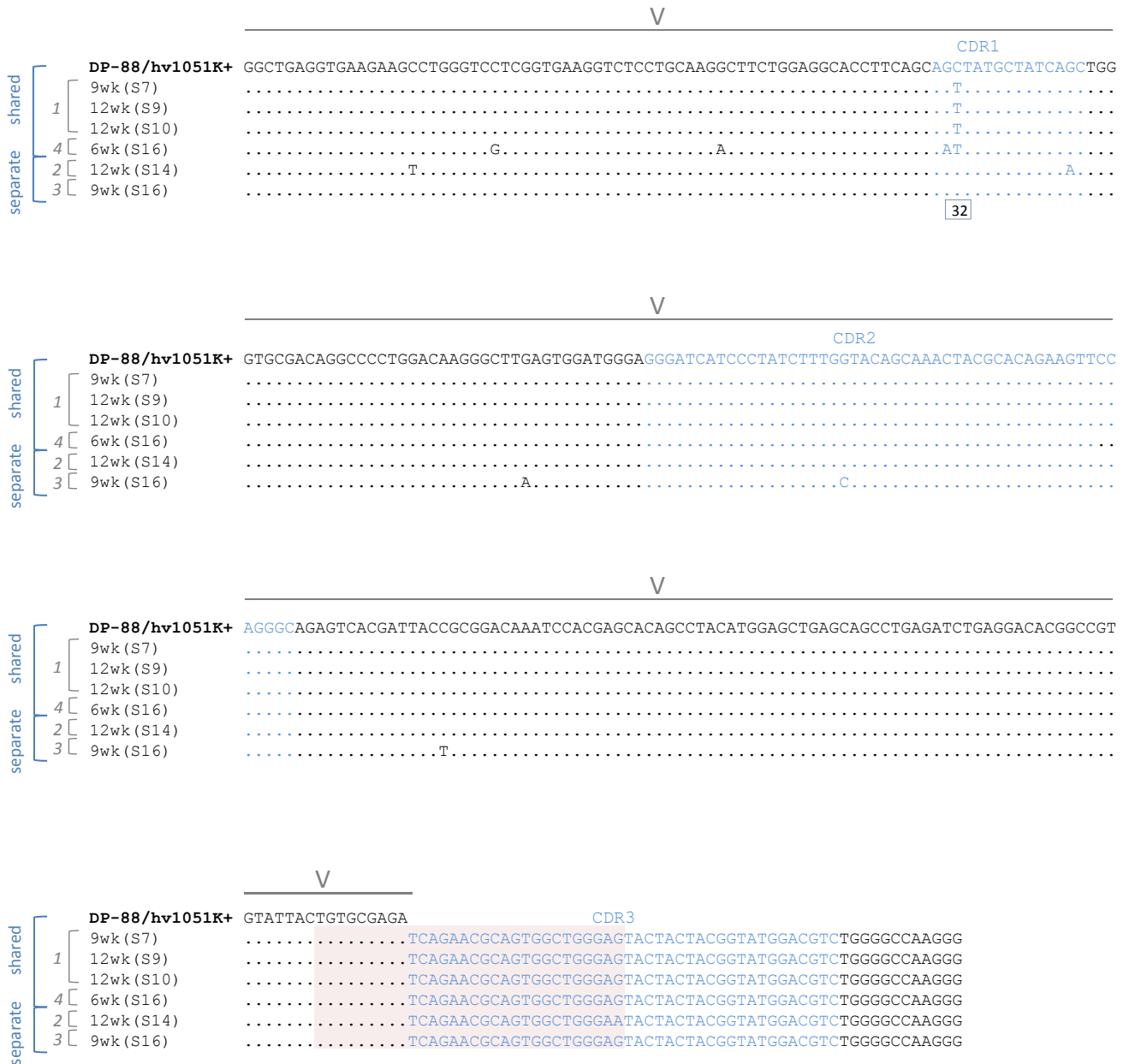


Figure 25. BN-LCL1 family 1 related and unrelated mutations

BN-LCL1 family 1 sequences are aligned relative to the matched germline V region sequence (top row). The location of the V region is indicated and the CDRs (1, 2 and 3) are highlighted in blue text. A box is drawn around the first 30 nucleotides of the VDJ junction translation.

Shared: 4 clonally related IgH sequences shared a common C→T mutation. Sequence 6wk(S16) carries an additional 3 changes.

Separate: 2 clonally related IgH sequences with distinct V region mutations.

(BN-LCL3) were established in parallel from sorted resting naive B cells derived from the same donor. The two cultures were established and grown in parallel, and IgVH sequences from both were studied after for up to twelve weeks.

The IgH sequences amplified from sorted naive B cells from donor 3 showed a polyclonal population of cells, with 17 out of 18 unmutated IgH sequences tested, indicating good sort purity (Table 14). Consistent with previous data, the sequencing results from BN-blast 3 at six and nine weeks revealed minimal IgH changes compared to the resting cells, and the culture was polyclonal at all three time points. Two of 23 IgH sequences were mutated at six weeks, however the absence of mutated IgH sequences at nine weeks suggests there was no accumulation of such sequences over time (Table 15). BN-blast 3 stopped proliferating after this point and no further time points were analysed.

The BN-LCL3 sequence data was clearly different to the BN-blast 3 data, most notably due to the outgrowth of clonally related families in the LCL culture.

Whereas BN-blast 3 remained polyclonal at all time points, BN-LCL3 contained 5 clonally related families by six weeks, 4 of which were also found at nine and twelve weeks (Table 16).

In order to confirm these observations, CDR3 spectratyping was also carried out on the same samples. This method, similar to IgH sequencing, involves the PCR amplification of the IgH region, generating products of varying sizes due to differences in the lengths of CDR3 regions. Consequently, a polyclonal population will produce a spectratype with a broad range of peaks corresponding to different sizes of amplified IgH products, whereas a monoclonal population yields only one peak. Figure 26 shows the CDR3

Resting naive B cells

sequence	V	D	J	junction translation	mutations
1	DP-49/1.9III...+	D6-6/DN4	JH3b	CAKDRAHCTV	0
2	V3-48/hv3d1...+	D1-26	JH6b	CARARHRWFG	0
3	VH32Sanz+	D6-19	JH4b	CARPDGAAA	0
4	DP-77/WHG16+	D3-10/DXP'1	JH6b	CARDPTVWFG	0
5	DP-47/V3-23...+	D2-15/D2	JH3b	CAKDRGYCSG	0
6	DP-71/3d197d...+	D2-21	JH4b	CARGGAGYFD	0
7	DP-73/V5-51...+	not found	JH6b	CARHFTTGY	0
8	DP-5/VI-24P+	not found	JH6b	CATPWGWGIF	0
9	DP-73/V5-51...+	D5-24	JH4b	CARHASIVDY	0
10	DP-73/V5-51...+	not found	JH4b	CARAGRDDFL	0
11	DP-47/V3-23...+	D3-3/DXP4	JH4b	CANLGAYDFW	0
12	DP-71/3d197d...+	D3-22/D21-9	JH5a	CARASSGYR	0
13	DP-79/4d154...+	D3-22/D21-9	JH4b	CARHQDYVC	0
14	DP-51+	D4	JH6b	CASKVVPAAI	0
15	DP-65/3d75d...+	D5-12/DK1	JH6b	CARGLWWLQY	0
16	DP-54/V3-7...+	D2-15/D2	JH6b	CARDDAGMGC	1
17	DP-65/3d75d...+	D4-17	JH5b	CASSSTVTMG	1
18	VH3-8	D6-19	JH6b	CARDLRVDSS	4

Table 14. Resting naive B cells used for BN-blast 3 and BN-LCL3

The table summarises the matched V, D and J alignments for each IgH sequence analysed at in the resting naive B cells used to generate both BN-blast 3 and BN-LCL3, the first 10 amino acids of the VDJ junction translation, and the number of mutations detected in the V region.

6 weeks

sequence	V	D	J	junction translation	mutations
1	DP-47/V3-23...+	D3-22/D21-9	JH4b	CEGWLLLHRV	0
2	DP-79/4d154...+	D2-21	JH4b	CARLLSGYHS	0
3	DP-77/WHG16+	D6-6/DN4	JH4b	CARDKGHIAA	0
4	DP-75/VI-2...+	D5-5/DK4	JH6b	CARDQKYRYS	0
5	DP-10/hv1051...+	D5-5/DK4	JH4b	CARSLSGYSY	0
6	DP-65/3d75d...+	D5-5/DK4	JH4b	CAREGDSAMV	0
7	DP-79/4d154...+	D4-23	JH3b	CARRPMTTVV	0
8	DP-10/hv1051...+	D3-22/D21-9	JH5b	CAIMYYYDSS	0
9	DP-77/WHG16+	D6-6/DN4	JH6b	CARGHSSSSH	0
10	DP-77/WHG16+	D1-26	JH6b	CARASISDYY	0
11	DP-10/hv1051...+	D2-8/DLR1	JH4b	CARVLLSTAV	0
12	DP-75/VI-2...+	D3-10/DXP'1	JH5b	CARDQYYGLG	0
13	DP-79/4d154...+	D6-19	JH4b	CARSGYSSGW	0
14	YAC-9/COS-27...+	D4	JH5b	CTRLSWFDPW	0
15	DP-47/V3-23...+	not found	JH4b	CAKDYFTKRM	0
16	V3-53+	D6-19	JH6b	CARESQRQLV	1
17	DP-75/VI-2...+	not found	JH4b	CARDQSWLDF	1
18	DP-79/4d154...+	D6-19	JH1	CARHVLAVAV	1
19	DP-54/V3-7...+	D4	JH6b	CARVAIPAAI	1
20	DP-48/13-2+	D2-2	JH2	CARSPSYCSS	1
21	DP-54/V3-7...+	D1-26	JH6b	CASRYRKPTD	2
22	DP-79/4d154...+	D4-23	JH4b	CARQFVGYYL	5
23	H9	D3-10/DXP'1	JH4b	CARVGRRGYY	5

9 weeks

sequence	V	D	J	junction translation	mutations
1	LSG6.1	D1-26	JH6b	CTTEGKPVAA	0
2	DP-7/21-2...+	D1-26	JH6b	CAGSTLVGAP	0
3	DP-65/3d76d...+	D2-21	JH5b	CARGYCGGDC	0
4	DP-47/V3-23...+	D4-23	JH4b	CAKEEWTTVV	0
5	VH32Sanz+	D6-19	JH4b	CARPPKNSIA	0
6	DP-77/WHG16+	D5-5/DK4	JH6b	CARDRAIDTA	0
7	DP-65/3d76d...+	D5-24	JH2	CARDGNQWET	0
8	V3-53+	D2-8/DLR1	JH6b	CARAGVGHHY	0
9	DP-75/VI-2...+	D1-26	JH5b	CARDLEWEPR	0
10	DP-77/WHG16+	D4-17	JH4b	CARDQGDYVV	0
11	DP-77/WHG16+	D3-22/D21-9	JH4b	CARDPGQPKD	0
12	DP-74/VH-VI...+	D6-6/DN4	JH4b	CASSFGVGLN	0
13	DP-66/V71-2...+	D3-22/D21-9	JH5b	CASLSITMIV	1
14	DP-47/V3-23...+	D3-22/D21-9	JH4b	CAKVGKCRIT	1
15	LSG6.1	D6-13/DN1	JH6b	CTRPPSGMDV	1
16	VIV-4/4.35+	D2-15/D2	JH6b	CVGEVVVVA	1
17	DP-65/3d76d...+	D5-24	JH5b	CARDGVEMAT	1
18	4M28	D5-5/DK4	JH6b	CARPPGGGAR	1
19	DP-47/V3-23...+	D3-16	JH4b	CAKDPPPPAM	1

Table 15. BN-blast 3

The table summarises the matched V, D and J alignments for each IgH sequence analysed at 6 and 9 weeks post-establishment, the first 10 amino acids of the VDJ junction translation, and the number of mutations detected in the V region.

6 weeks	sequence	V	D	J	junction translation	mutations
	1	DP-2/V71-5+	D3-16	JH6b	CAADFTFGGV	0
	2	DP-2/V71-5+	D3-16	JH6b	CAADFTFGGV	0
	3	DP-2/V71-5+	D3-16	JH6b	CAADFTFGGV	0
	4	DP-2/V71-5+	D3-16	JH6b	CAADFTFGGV	0
	5	DP-2/V71-5+	D3-16	JH6b	CAADFTFGGV	0
	6	DP-2/V71-5+	D3-16	JH6b	CAADFTFGGV	0
	7	DP-2/V71-5+	D3-16	JH6b	CAADFTFGGV	0
	8	DP-75/V1-2...+	D3-3/DXP4	JH4b	CASSRVLRF	0
	9	DP-75/V1-2...+	D3-3/DXP4	JH4b	CASSRVLRF	1
	10	DP-79/4d154...+	D3-22/D21-9	JH3b	CARPIVLL**	0
	11	DP-79/4d154...+	D3-22/D21-9	JH3b	CARPIVLL**	0
	12	DP-79/4d154...+	D3-22/D21-9	JH3b	CARPIVLL**	0
	13	DP-79/4d154...+	D3-22/D21-9	JH3b	CARPIVLL**	0
	14	DP-79/4d154...+	D3-22/D21-9	JH3b	CARPIVLL**	0
	15	DP-79/4d154...+	D3-22/D21-9	JH3b	CARPIVLL**	1
	16	DP-54/V3-7...+	D6-13/DN1	JH4b	CALRIAAAGT	3
	17	DP-54/V3-7...+	D6-13/DN1	JH4b	CALRIAAAGT	3
	18	VIV-4/4.35+	D3-22/D21-9	JH4b	CARASQGYDS	3
	19	VIV-4/4.35+	D3-22/D21-9	JH4b	CARASQGYDS	3
	20	YAC-9/COS-27...+	D2-8/DLR1	JH6b	CTVYVYYYG	0
	21	DP-50/hv3019b9...+	D3-3/DXP4	JH4b	CAREWLLDYW	1
9 weeks	sequence	V	D	J	junction translation	mutations
	1	DP-2/V71-5+	D3-16	JH6b	CAADFTFGGV	0
	2	DP-2/V71-5+	D3-16	JH6b	CAADFTFGGV	0
	3	DP-2/V71-5+	D3-16	JH6b	CAADFTFGGV	0
	4	DP-2/V71-5+	D3-16	JH6b	CAADFTFGGV	0
	5	DP-2/V71-5+	D3-16	JH6b	CAADFTFGGV	0
	6	DP-2/V71-5+	D3-16	JH6b	CAADFTFGGV	0
	7	DP-2/V71-5+	D3-16	JH6b	CAADFTFGGV	0
	8	DP-2/V71-5+	D3-16	JH6b	CAADFTFGGV	0
	9	DP-2/V71-5+	D3-16	JH6b	CAADFTFGGV	0
	10	DP-2/V71-5+	D3-16	JH6b	CAADFTFGGV	0
	11	DP-2/V71-5+	D3-16	JH6b	CAADFTFGGV	0
	12	DP-2/V71-5+	D3-16	JH6b	CAADFTFGGV	0
	13	DP-2/V71-5+	D3-16	JH6b	CAADFTFGGV	1
	14	DP-79/4d154...+	D3-22/D21-9	JH3b	CARPIVLL**	0
	15	DP-79/4d154...+	D3-22/D21-9	JH3b	CARPIVLL**	0
	16	DP-79/4d154...+	D3-22/D21-9	JH3b	CARPIVLL**	0
	17	DP-79/4d154...+	D3-22/D21-9	JH3b	CARPIVLL**	1
	18	DP-54/V3-7...+	D6-13/DN1	JH4b	CALRIAAAGT	4
	19	VIV-4/4.35+	D3-22/D21-9	JH4b	CARASQGYDS	3
	20	VIV-4/4.35+	D3-22/D21-9	JH4b	CARASQGYDS	4
	21	DP-65/3d75d...+	D6-19	JH5b	CARVRPRIAV	0
12 weeks	sequence	V	D	J	junction translation	mutations
	1	DP-2/V71-5+	D3-16	JH6b	CAADFTFGGV	0
	2	DP-2/V71-5+	D3-16	JH6b	CAADFTFGGV	0
	3	DP-2/V71-5+	D3-16	JH6b	CAADFTFGGV	0
	4	DP-2/V71-5+	D3-16	JH6b	CAADFTFGGV	0
	5	DP-2/V71-5+	D3-16	JH6b	CAADFTFGGV	0
	6	DP-2/V71-5+	D3-16	JH6b	CAADFTFGGV	0
	7	DP-2/V71-5+	D3-16	JH6b	CAADFTFGGV	0
	8	DP-2/V71-5+	D3-16	JH6b	CAADFTFGGV	0
	9	DP-2/V71-5+	D3-16	JH6b	CAADFTFGGV	0
	10	DP-2/V71-5+	D3-16	JH6b	CAADFTFGGV	0
	11	DP-2/V71-5+	D3-16	JH6b	CAADFTFGGV	0
	12	DP-2/V71-5+	D3-16	JH6b	CAADFTFGGV	0
	13	DP-79/4d154...+	D3-22/D21-9	JH3b	CARPIVLL***	0
	14	DP-79/4d154...+	D3-22/D21-9	JH3b	CARPIVLL***	0
	15	DP-54/V3-7...+	D6-13/DN1	JH4b	CALRIAAAGT	3
	16	DP-54/V3-7...+	D6-13/DN1	JH4b	CALRIAAAGT	4
	17	DP-54/V3-7...+	D6-13/DN1	JH4b	CALRIAAAGT	4
	18	VIV-4/4.35+	D3-22/D21-9	JH4b	CARASQGYDS	3
	19	VIV-4/4.35+	D3-22/D21-9	JH4b	CARASQGYDS	3
	20	DP-49/1.9III...+	D5-24	JH4b	CAKTPRVATI	5

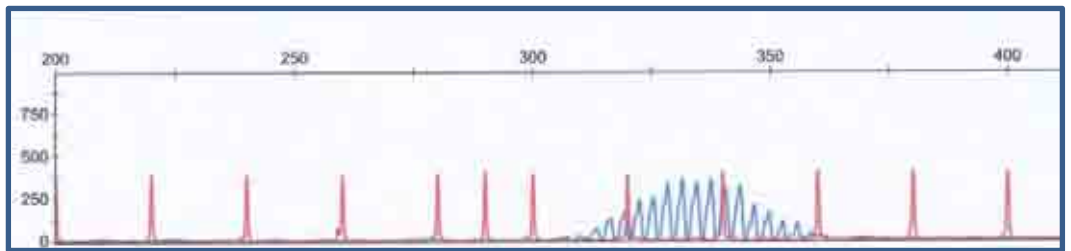
Legend

- Family 1
- Family 2
- Family 3
- Family 4
- Family 5

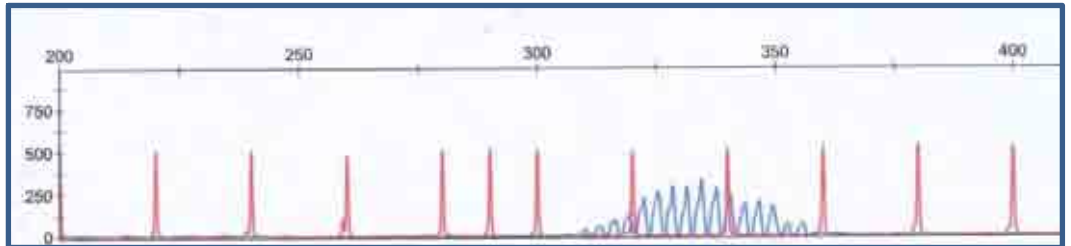
Table 16. BN-LCL3

Summary of matched V, D and J alignments for each IgH sequence analysed at 9 and 12 weeks post-establishment (0 and 6 weeks shown on the previous page), the first 10 amino acids of VDJ junction translation, and the number of mutations detected in the V region. Clonally related IgH sequences are colour highlighted (see legend). Note; family 3 sequences reflect a non-functional Ig rearrangement.

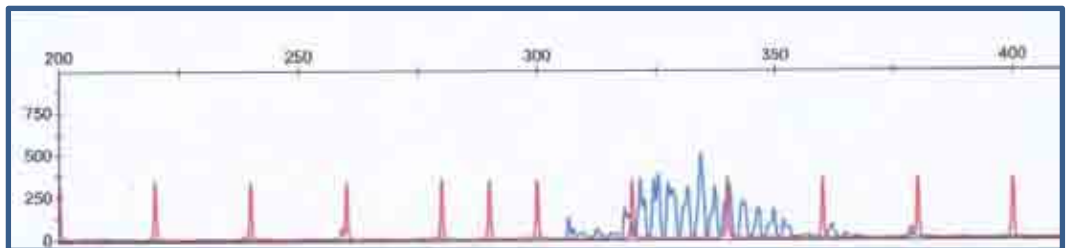
resting
naive B
cells



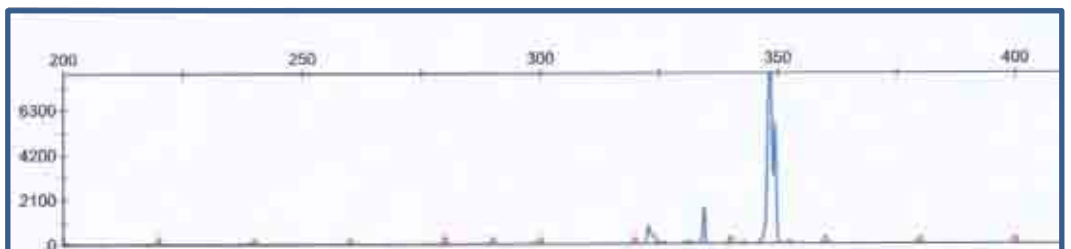
BN-blast3
6 weeks



BN-blast3
9 weeks



BN-LCL3
6 weeks



BN-LCL3
9 weeks

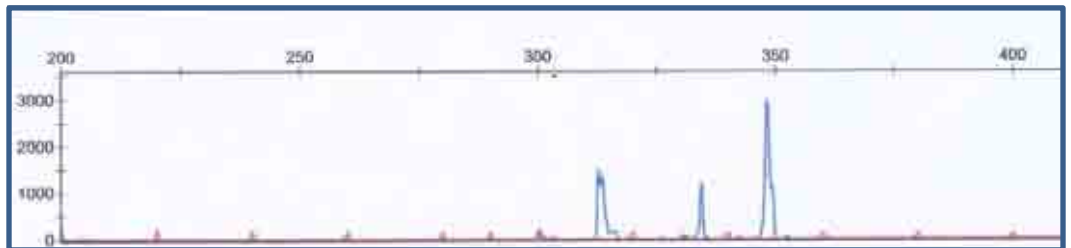


Figure 26. CDR3 spectratyping analysis of BN-blast 3 and BN-LCL3

In-frame rearranged VDJ gene fragments of various sizes are represented by blue peaks. The top axis represents a size ladder in base pairs. The red peaks represent a control sample containing template sequences of known size.

spectratypes from the resting naive B cells and from both BN-blast 3 and BN-LCL3 cultures at six and nine weeks. This data clearly shows that the B blast culture remained polyclonal at six and nine weeks post-establishment, with a spectratype which was unchanged from the resting population. In contrast, the limited number of peaks in the LCL data reflects a cell culture that was oligoclonal at these time points. Taken together these results confirm that expansion of EBV-transformed naive B cells *in vitro* yields selective outgrowth of a limited number of B cell clones, whereas induction of the same cells to proliferate *in vitro* in the absence of EBV does not cause this effect.

Closer inspection of the IgH data from BN-LCL3 showed that three families contained germline IgH sequences, whereas two families harboured mutated IgH sequences (Table 16). In Family 1, which was the dominant clonal family within the culture at six, nine and twelve weeks post-infection, unmutated IgH sequences were consistently detected at each time point post-infection. Similarly the two related IgH sequences at week six that made up family 2 were both germline. Although family 3 was also detected at six, nine and twelve weeks, it is worth noting that these sequences carry stop codons (represented by asterisks) within their CDR3 regions, and as such are not able to express functional BCRs. It is unknown how this family of cells was able to persist for up to twelve weeks in culture, but it is possible that the sequences represent PCR amplification of a non-functional allele which was dismissed prior to successful rearrangement of the alternative allele during allelic exclusion (see Introduction). For the purposes of scoring IgH mutations, however, such non-functional sequences were disregarded. By contrast, IgH sequences from families 4 and 5 were detected at six, nine and twelve weeks post-infection, and

were all mutated. In family 4, each sequence harboured 3 identical V region mutations at codons 31, 60 and 88 (Figure 27). In addition to these shared mutations, three sequences (6wk(18), 12wk(16) and 12wk(17)) had each acquired an additional independent mutation, which could reflect ongoing SHM. Similarly, the IgH sequences analysed from family 5 also shared 3 mutations, at codons 60, 71 and 91 (Figure 28).

In summary, the analysis of IgH sequences in this experiment has revealed the presence of multiple mutated sequences from six weeks onwards within the BN-LCL3 culture. This is in contrast to the almost exclusively germline sequences found in the BN-blast 3 culture. These findings thus strengthen the correlation between EBV infection and the accumulation of IgV mutations within cells seen in earlier experiments.

4.2.5 Detailed Studies of Clonal Evolution in Three LCLs

Established from a Single Donor

The above results suggest differences between the evolution of CD40L/IL-4 – stimulated B blasts and EBV-infected LCLs in terms of clonality and appearance of IgH mutations. To further study this phenomenon, a more detailed experiment was carried out in which three separate BN-LCLs were established from a single donor.

In this experiment, an outline of which is shown in Figure 29, B cells were FACS sorted and naive B cells were collected as previously described. Approximately 0.5×10^6 naive B cells were infected with EBV, and the following day the culture was split evenly into three separate wells of a 96 well plate. The cells were

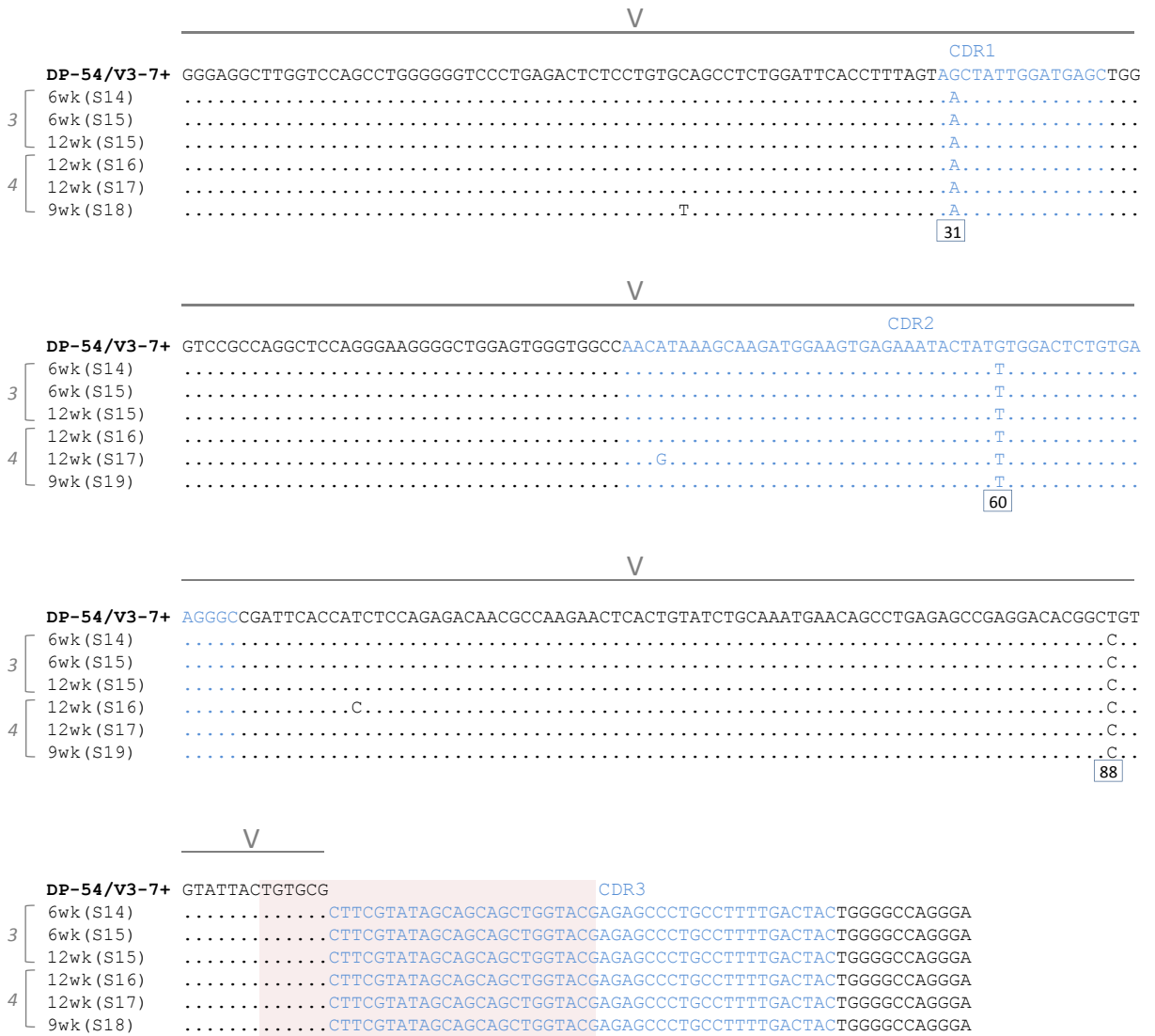


Figure 27. BN-LCL3 family 4

BN-LCL3 family 4 sequences are aligned relative to the matched germline V region sequence (top row). The location of the V region is indicated and the CDRs (1, 2 and 3) are highlighted in blue text. A box is drawn around the first 30 nucleotides of the VDJ junction translation.

5 sequences harboured 3 identical mutations. Extra mutations acquired by sequences “12wks(16)”, “12wks(17)” and “9wks(18)” were distinct from one another.

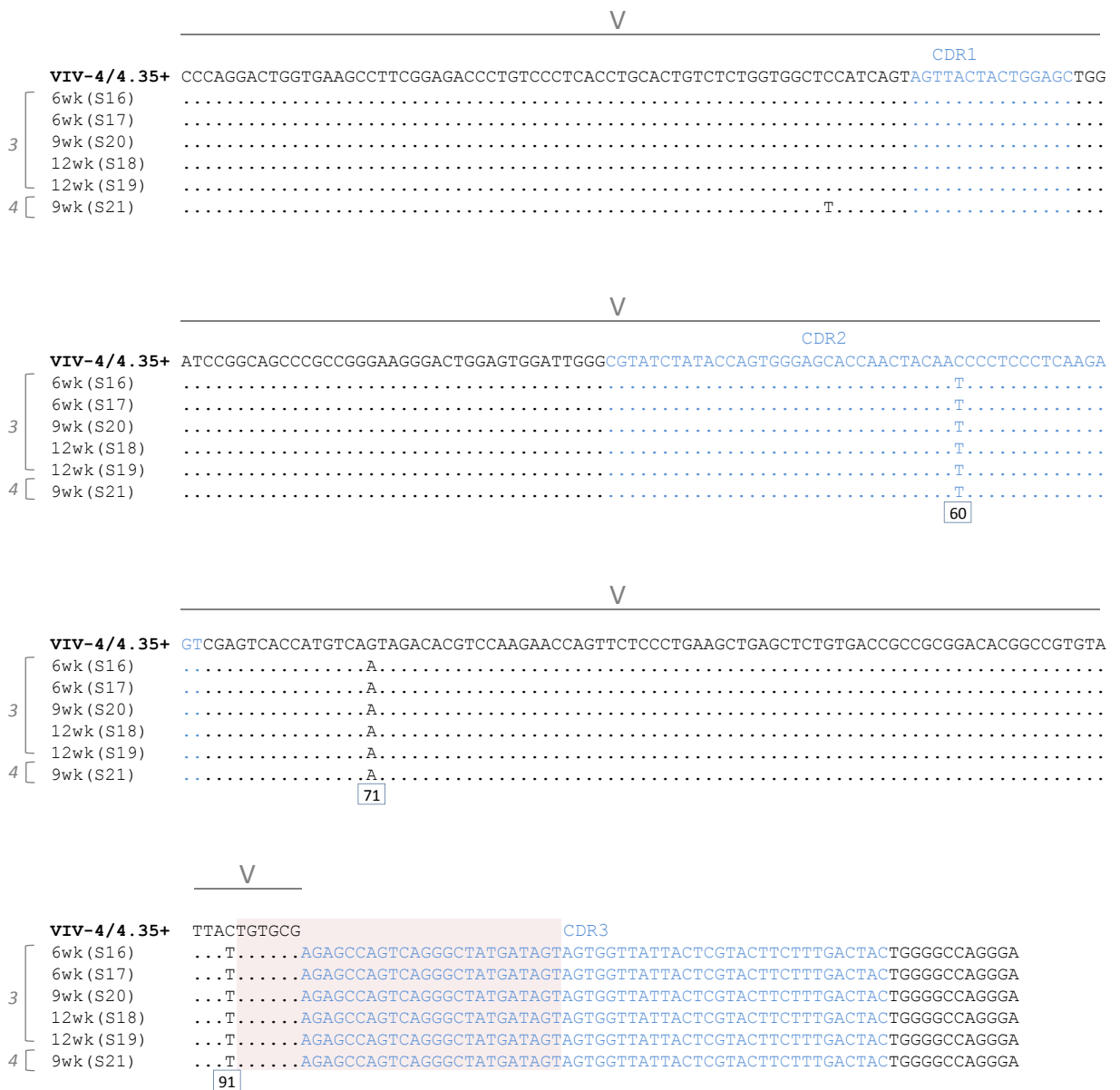


Figure 28. BN-LCL3 family 5

BN-LCL3 family 5 sequences are aligned relative to the matched germline V region sequence (top row). The location of the V region is indicated and the CDRs (1, 2 and 3) are highlighted in blue text. A box is drawn around the first 30 nucleotides of the VDJ junction translation. 6 sequences harboured 3 identical mutations. An extra mutation was acquired by sequences “9wks(20)”.

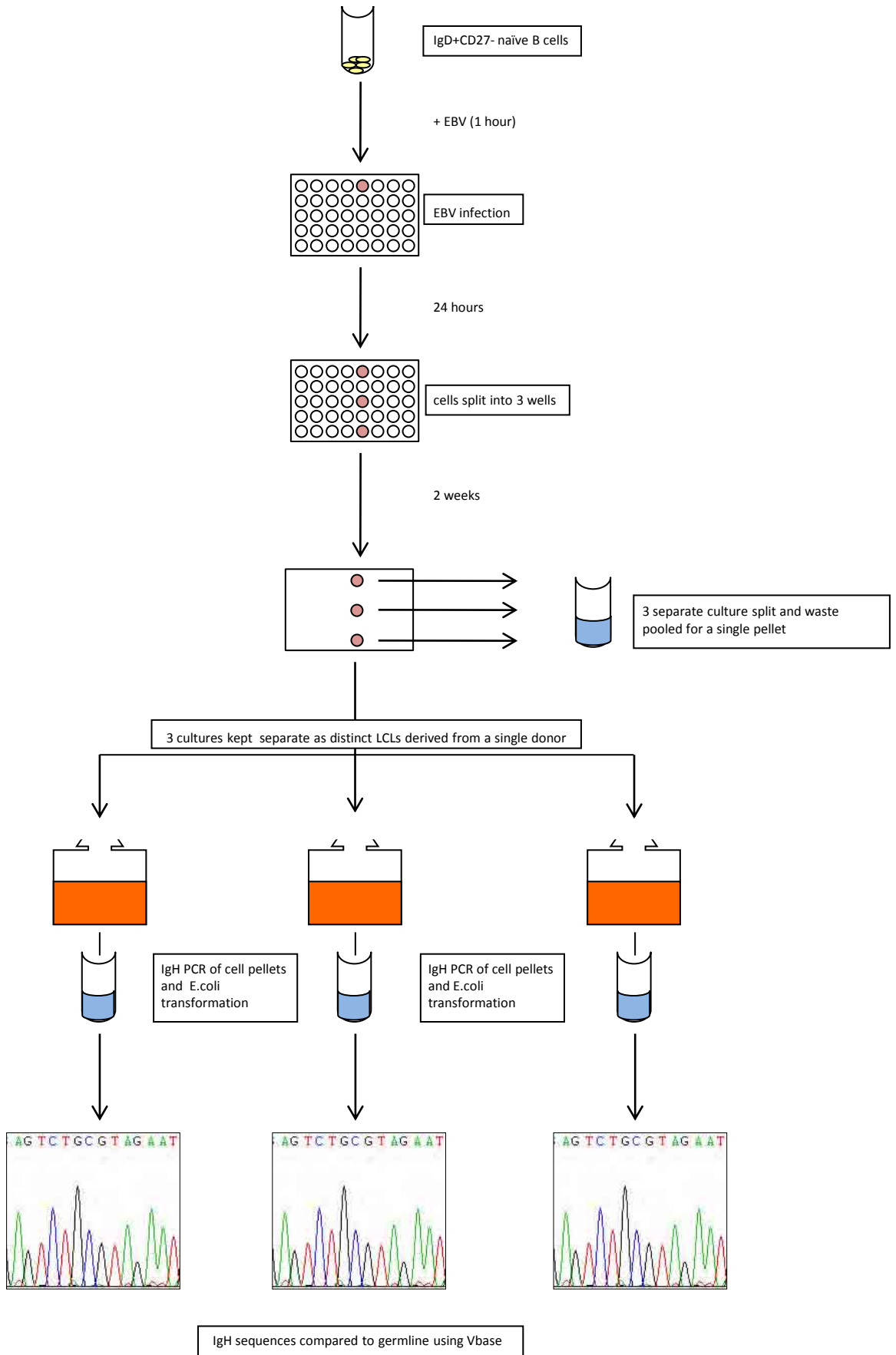


Figure 29. Establishment of three separate LCLs from one donor (BN-LCL4a, b and c)

thereafter cultured and expanded separately and three distinct BN-LCLs (BN-LCL4a, BN-LCL4b and BN-LCL4c) were established.

Since all the naive B cells collected during the cell sort were used to generate the BN-LCL cultures, the first time point analysed was at two weeks post-infection, when a cell sample was obtained by pooling aliquots from each of the three BN-LCLs. Analysis of 33 sequences generated at this two week time point revealed that the cultures were typical of resting naive B cells, containing a polyclonal mixture, of which all 33 sequences were unmutated (Table 17). Cells continued to be harvested from each LCL at regular time points up until twelve weeks post-infection and IgH sequences examined as before.

Clonal Dynamics of BN-LCL4 Cultures

As early as four weeks post-infection, distinct clonal families were identified in the BN-LCL4a culture (Table 18). At this time there was still a significant proportion of clonally independent IgH sequences (9 out of 32), but from six weeks onwards this proportion continued to diminish. Interestingly, whilst family 2 was clearly the predominant clone at four and six weeks post-infection, member of this family vastly declined by week nine, and at week twelve no sequences belonging to this clone were detected. Conversely, only 2 IgH sequences (at week four) from family 1 were observed prior to twelve weeks, at which point this clone not only reappeared in the culture, but became the dominant clonal family. A similar pattern was observed in family 3, in which substantial numbers of IgH sequences were not detected until nine weeks post-infection when they made up the largest proportion of clonally related sequences in the culture. Taken together, these results highlight the shifts in

2 weeks

sequence	V	D	J	junction translation	mutations
1	DP-71/3d197d	D3-10/DXP'1	JH6b	CARHSGITM	0
2	DP-7/21-2	D1-26	JH4b	CARDGGFVGA	0
3	DP-14/V1-18+	D3-9/DXP1	JH4b	CARSTGGYDI	0
4	DP-2/V71-5+	D4	JH6b	CAAQNDIVVV	0
5	DP-66/V71-2	D3-22/D21-9	JH5b	CARYEYYDS	0
6	DP-71/3d197d	D1-26	JH1	CARETIVGAT	0
7	DP-10/hv1051	D3-22/D21-9	JH2	CASSSGYPDW	0
8	VH32sanz+	D6-19	JH4b	CARLSGWYSE	0
9	LSG6.1	D6-19	JH4b	CTTGIRIAVA	0
10	DP-65/3d75d	D1-26	JH4b	CARENNEGSP	0
11	3d277d+	D4-17	JH4b	CARSPRLRGP	0
12	DP-14/V1-18+	D3-3/DXP4	JH6b	CARGSYDFWS	0
13	DP-7/21-2	D3-22/D21-9	JH5b	CVTDSSGFHW	0
14	DP-73/V5-51	D5-5/DK4	JH4b	CARHVTAMAD	0
15	DP-58/hv3d1EG	D4	JH6b	CARDGVPAAM	0
16	hv3005/b1..m..+	D2-8/DLR1	JH6b	CARDPGVTTY	0
17	DP-47/V3-23	D3-10/DXP'1	JH4b	CAKLFHR*ED	0
18	DP-65/3d75d	not found	not found	CARQVAAVD	0
19	DP-25/V1-3b+	not found	JH4b	CARGPTDYWG	0
20	COS-6/DA-8	D2-15/D2	JH6b	CARRGGSDIY	0
21	DP-8+	D7-27	JH3b	CARDGNLGRG	0
22	DP-58/hv3d1EG	D4-11/DA1	JH6b	CARDYSNYDY	0
23	DP-47/V3-23	D3-22/D21-9	JH4b	CAKSSNYYS	0
24	DP-17/3d197d	D1-26	JH4b	CARSPPLN	0
25	DP-73/V5-51	D3-10/DXP'1	JH6b	CARLYYGSGP	0
26	DP-49/1.9III	D6-13/DN1	JH6b	CARAGTRYYY	0
27	DP-70/4d68	D2-15/D2	JH3b	CARDMGKDIV	1
28	DP-17/3d197d	D2-8/DLR1	JH4b	CAKKRxLY*W	1
29	DP-88/hv1051K	D2-2	JH6b	CASSNTVLGG	1
30	DP-73/V5-51	D5-5/DK4	JH6b	CARLGAAMVF	1
31	DP-79/4d154	D3-9/DXP1	JH5b	CARPRHDITM	1
32	DP-5/V1-24P+	D3-10/DXP'1	JH6b	CACCSRSEDIY	2
33	DP-5/V1-24P+	not found	not found	CATVEF	2

Table 17. Two week IgH data from BN-LCL4a, b and c

Summary table of IgH sequences from cells harvested and pooled from all three LCLs (BN-LCL2a, b and c) at 2 weeks post-EBV infection. Data contain matched V, D and J alignments for each IgH sequence, the first 10 amino acids of the VDJ junction translation, and the number of mutations detected in the V region.

4 weeks

sequence	V	D	J	junction translation	mutations
1	DP-73/V5-51...+	D3-10/DXP1	JH4b	CARRWFGELW	1
2	DP-73/V5-51...+	D3-10/DXP1	JH4b	CARRWFGELW	3
3	DP-71/3d197d...+	D1-7/DM1	JH6b	CASGTTVRY	0
4	DP-71/3d197d...+	D1-7/DM1	JH6	CASGTTVRY	1
5	DP-71/3d197d...+	D1-7/DM1	JH6b	CASGTTVRY	2
6	DP-71/3d197d...+	D1-7/DM1	JH6b	CASGTTVRY	3
7	DP-71/3d197d...+	D1-7/DM1	JH6b	CASGTTVRY	4
8	DP-71/3d197d...+	D1-7/DM1	JH6b	CASGTTVRY	4
9	DP-71/3d197d...+	D1-7/DM1	JH6b	CASGTTVRY	4
10	DP-71/3d197d...+	D1-7/DM1	JH6b	CASGTTVRY	4
11	DP-71/3d197d...+	D1-7/DM1	JH6b	CASGTTVRY	4
12	DP-71/3d197d...+	D1-7/DM1	JH6b	CASGTTVRY	4
13	DP-71/3d197d...+	D1-7/DM1	JH6b	CASGTTVRY	4
14	DP-71/3d197d...+	D1-7/DM1	JH6b	CASGTTVRY	4
15	DP-71/3d197d...+	D1-7/DM1	JH6b	CASGTTVRY	4
16	DP-71/3d197d...+	D1-7/DM1	JH6b	CASGTTVRY	4
17	DP-71/3d197d...+	D1-7/DM1	JH6b	CASGTTVRY	5
18	DP-71/3d197d...+	D1-7/DM1	JH6b	CASGTTVRY	5
19	DP-71/3d197d...+	D1-7/DM1	JH6b	CASGTTVRY	5
20	DP-71/3d197d...+	D1-7/DM1	JH6b	CASGTTVRY	5
21	DP-71/3d197d...+	D1-7/DM2	JH6b	CASGTTVRY	5
22	DP-7/21-2...+	D6-6/DN4	JH4b	CAREYSGSSN	13
23	DP-7/21-2...+	D6-6/DN4	JH4b	CAREYSGSSN	14
24	DP-73/V5-51...+	D6-13/DN1	JH4b	CARPYRDSS	0
25	DP-58/hv3d1EG	not found	JH4b	xAxDLDYWGQ	1
26	hv3005/b1...m...+	D6-13/DN1	JH4b	CARALIAAAG	3
27	DP-73/V5-51...+	D4-17	JH4b	CARRTDYGDY	3
28	DP-10/hv1051...+	D4	JH4b	CAKGYCSSTS	4
29	DP-65/3d75d...+	D1-14/DM2	JH4b	CARVSRYSDD	6
30	DP-88/hv1051K...+	D6-6/DN4	JH4b	CARDGGIAAL	7
31	DP-8+	D6-6/DN4	JH5b	CARASPYSSS	12
32	DP-7/21-2...+	D1-1	JH5b	CARVVGRRF	13

6 weeks

sequence	V	D	J	junction translation	mutations
1	DP-71/3d197d...+	D1-7/DM1	JH6b	CASGTTVRY	2
2	DP-71/3d197d...+	D1-7/DM1	JH6b	CASGTTVRY	2
3	DP-71/3d197d...+	D1-7/DM1	JH6b	CASGTTVRY	4
4	DP-71/3d197d...+	D1-7/DM1	JH6b	CASGTTVRY	4
5	DP-71/3d197d...+	D1-7/DM1	JH6b	CASGTTVRY	4
6	DP-71/3d197d...+	D1-7/DM1	JH6b	CASGTTVRY	4
7	DP-71/3d197d...+	D1-7/DM1	JH6b	CASGTTVRY	4
8	DP-71/3d197d...+	D1-7/DM1	JH6b	CASGTTVRY	4
9	DP-71/3d197d...+	D1-7/DM1	JH6b	CASGTTVRY	4
10	DP-71/3d197d...+	D1-7/DM1	JH6b	CASGTTVRY	4
11	DP-71/3d197d...+	D1-7/DM1	JH6b	CASGTTVRY	4
12	DP-71/3d197d...+	D1-7/DM1	JH6b	CASGTTVRY	4
13	DP-71/3d197d...+	D1-7/DM1	JH6b	CASGTTVRY	4
14	DP-71/3d197d...+	D1-7/DM1	JH6b	CASGTTVRY	5
15	DP-71/3d197d...+	D1-7/DM1	JH6b	CASGTTVRY	5
16	DP-71/3d197d...+	D1-7/DM1	JH6b	CASGTTVRY	5
17	DP-71/3d197d...+	D1-7/DM1	JH6b	CASGTTVRY	5
18	DP-71/3d197d...+	D1-7/DM1	JH6b	CASGTTVRY	5
19	DP-71/3d197d...+	D1-7/DM1	JH6b	CTSGTTVRY	6
20	DP-7/21-2...+	D6-6/DN4	JH4b	CAREYSGSSN	13

Legend

- Family 1
- Family 2
- Family 3
- Family 4
- Family 5
- Family 6

Table 18. BN-LCL4a

Summary of matched V, D and J alignments for each IgH sequence analysed at 4 and 6 weeks post-establishment (9 and 12 weeks shown on the next page), the first 10 amino acids of the VDJ junction translation, and the number of mutations detected in the V region. Clonally related IgH sequences are colour highlighted (see legend).

9 weeks

sequence	V	D	J	junction translation	mutations
1	DP-71/3d197d...+	D3-22/D21-9	JH6b	CARGRDDSSG	0
2	DP-71/3d197d...+	D3-22/D21-9	JH6b	CARGRDDSSG	2
3	DP-71/3d197d...+	D1-7/DM1	JH6b	CASGTTVRYY	1
4	DP-71/3d197d...+	D1-7/DM1	JH6b	CASGTTVRYY	3
5	DP-71/3d197d...+	D1-7/DM1	JH6b	CASGTTVRYY	3
6	DP-71/3d197d...+	D1-7/DM1	JH6b	CASGTTVRYY	4
7	DP-71/3d197d...+	D1-7/DM1	JH6b	CASGTTVRYY	4
8	DP-70/4d68...+	D6-6/DN4	JH4b	CARLEAMTSF	5
9	hv3005/b1...m...+	D3-10/DXP'	JH6b	CARDFIHDYY	8
10	hv3005/b1...m...+	D3-10/DXP'	JH6b	CARDFIHDYY	9
11	DP-7/21-2...+	D6-6/DN4	JH4b	CAREYSGSSN	13
12	DP-7/21-2...+	D6-6/DN4	JH4b	CAREYSGSSN	13
13	DP-7/21-2...+	D6-6/DN4	JH4b	CAREYSGSSN	13
14	DP-7/21-2...+	D6-6/DN4	JH4b	CAREYSGSSN	13
15	DP-7/21-2...+	D6-6/DN4	JH4b	CAREYSGSSN	14
16	DP-7/21-2...+	D6-6/DN4	JH4b	CAREYSGSSN	15
17	hv3005/b1...m...+	D1-20	JH6b	CAREVVREGS	3
18	DP-71/3d197d...+	D5-12/DK1	JH6b	CARGGFRGYE	4
19	hv3005/b1...m...+	D5-5/DK4	JH5a	CARDQQTWIQ	9

12 weeks

sequence	V	D	J	junction translation	mutations
1	DP-73/V5-51...+	D3-10/DXP'1	JH4b	CARRWFGELW	3
2	DP-73/V5-51...+	D3-10/DXP'1	JH4b	CARRWFGELW	3
3	DP-73/V5-51...+	D3-10/DXP'1	JH4b	CARRWFGELW	3
4	DP-73/V5-51...+	D3-10/DXP'1	JH4b	CARRWFGELW	3
5	DP-73/V5-51...+	D3-10/DXP'1	JH4b	CARRWFGELW	3
6	DP-73/V5-51...+	D3-10/DXP'1	JH4b	CARRWFGELW	4
7	DP-73/V5-51...+	D3-10/DXP'1	JH4b	CARRWFGELW	4
8	DP-73/V5-51...+	D3-10/DXP'1	JH4b	CARRWFGELW	6
9	DP-73/V5-51...+	D3-10/DXP'1	JH4b	CARRWFGELW	6
10	DP-73/V5-51...+	D3-10/DXP'1	JH4b	CARRWFGELW	7
11	DP-73/V5-51...+	D3-10/DXP'1	JH4b	CARRWFGELW	7
12	DP-70/4d68...+	D6-6/DN4	JH4b	CARLEAMTSF	4
13	DP-70/4d68...+	D6-6/DN4	JH4b	CARLEAMTSF	4
14	hv3005/b1...m...+	D3-10/DXP'1	JH6b	CARDFIHDYY	8
15	DP-73/V5-51...+	D3-10/DXP'1	JH4b	CARTSTLLRG	10
16	DP-49/1.9III...+	D3-22/D21-9	JH4b	CAKDSHSSA	12

Legend

	Family 1
	Family 2
	Family 3
	Family 4
	Family 5
	Family 6

Table 18. BN-LCL4a

Summary of matched V, D and J alignments for each IgH sequence analysed at 9 and 12 weeks post-establishment (4 and 6 weeks shown on the previous page), the first 10 amino acids of the VDJ junction translation, and the number of mutations detected in the V region. Clonally related IgH sequences are colour highlighted (see legend).

the dynamics of clonal dominance within the BN-LCL4a culture, suggesting variability in the relative capacity of each family to thrive or compete as the culture progressed. It is possible that although IgH sequences such as those from family 1 were not detected at six and nine weeks, they were in fact still present in small numbers.

In contrast to BN-LCL4a, the IgH sequencing data from BN-LCL4b reflected a culture that was polyclonal at four weeks post-infection (Table 19). However, by six weeks post-infection three clonally related families (1, 2 and 3) were detected, although half the amplified IgH sequences were still clonally unique. After nine weeks the culture was dominated by two clonal families, with the largest proportion of sequences belonging to family 3. At twelve weeks post-infection, 11 of 11 IgH sequences analysed were derived from family 3 (Table 19).

In the case of LCL4b, the CDR3 spectratyping technique was also used to confirm the evolution of dominant clones in the culture. Figure 30 shows the spectratypes from BN-LCL4b at four, six, nine and twelve weeks post-infection. These data confirm that whilst the culture was still polyclonal at four weeks, fewer peaks were seen at six weeks reflecting an oligoclonal culture, and only 2 peaks were seen at nine weeks. These peaks presumably correspond to the 2 clonal families detected in the IgH sequencing data. A single peak was observed at twelve weeks, in agreement with the IgH data from that time point.

From previous data it was apparent that in some instances clonal families dominating the culture at twelve weeks were detectable in smaller proportions as early as four weeks post-infection. We therefore investigated whether B cell

4 weeks

sequence	V	D	J	junction translation	mutations
1	DP-47/V3-23...+	D6-19	JH4b	CARFSSGWWG	2
2	DP-66/V71-2...+	D6-6/DN4	JH4b	CARDSSAARP	0
3	DP-79/4d154...+	not found	JH3b	CARAGGKLVA	0
4	DP-71/3d197d...+	D7-27/DHQ52	JH5b	CARSGQVRFG	0
5	DP-10/hv1051...+	D6-13/DN1	JH6b	CARAGGRDPP	0
6	DP-71/3d197d...+	D3-22/D21-9	JH4b	CARAVGGPPF	0
7	DP-65/3d75d...+	D3	JH4b	CARDGYGLDY	0
8	DP-73/V5-51...+	D1-26	JH4b	CARLQDSPPD	0
9	DP-7/21-2...+	D5-5/DK4	JH4b	CAREAVRYSY	0
10	DP-3+	D4-b	JH4b	CATARSTGYL	0
11	DP-73/V5-51...+	D1-26	JH6b	CARYGSYPY	0
12	DP-54/V3-7...+	D1-1	JH3b	CARDTNWNGA	1
13	DP-77/VHG16+	D6-13/DN1	JH6b	CARDVGSSSW	1
14	b54.../hv3005f3...+	D3-22/D21-9	JH4b	CAKSRYYYYS	2
15	DP-79/4d154...+	D1-26	JH4b	CARAASGSLD	2
16	DP-88/hv1051K...+	not found	not found	CARVARYDIL	2
17	DP-71/3d197d...+	D3-3/DXP4	JH4b	CARVRLSGWY	3
18	DP-70/4d68...+	D1-26	JH4b	CARDQGSYYG	5
19	DP-67/VH4-4B+	D1-14/DM2	JH4b	CARVSLAVX	5
20	DP-7/21-2...+	D6-19	JH6b	CARDSSGWYS	6

6 weeks

sequence	V	D	J	junction translation	mutations
1	DP-47/V3...+	D6-19	JH4b	CARGSSGWWG	2
2	DP-47/V3-23...+	D6-19	JH4b	CARGSSGWWG	5
3	DP-51+	not found	JH6b	CARVRGWTTY	2
4	DP-51+	not found	JH6b	CARVRGWTTY	5
5	DP-51+	not found	JH6b	CARVRGWTTY	5
6	DP-51+	not found	JH6b	CARVRGWTTY	6
7	DP-47/V3-23...+	D3-10/DXP'1	JH6b	CAKDRGFGE	2
8	DP-47/V3-23...+	D3-10/DXP'1	JH6b	CAKDRGFGE	7
9	DP-47/V3-23...+	D3-10/DXP'1	JH6b	CAKDRGFGE	7
10	DP-47/V3-23...+	D3-D10/DXP'1	JH6b	CAKDRGFGE	7
11	DP-10/hv1051...+	not found	JH6b	CARESTGDYY	0
12	DP-65/3d75d...+	D5-24	JH6b	CARELKRWLQ	0
13	VHSP/VH4.2...+	not found	JH6b	CARDTYYDSN	0
14	DP-71/3d197d...+	D1-26	JH5b	CARDLGSQWE	0
15	DP-73/V5-51...+	D4-23	JH6b	CARHGGGNSR	0
16	DP-79/4d154...+	D3-10/DXP'1	JH3b	CLGGNDAFDI	1
17	DP-73/V5-51...+	D3-22/D21-9	JH4b	CARQTDDSSG	1
18	DP-71/3d197d...+	D6-19	JH6b	CASMP5IAVA	1
19	p1	D3-D21-9	JH6b	CVKEGSSYYY	2

- family 1
- family 2
- family 3

Table 19. BN-LCL4b

Summary of matched V, D and J alignments for each IgH sequence analysed at 4 and 6 weeks post-establishment (9 and 12 weeks shown on the next page), the first 10 amino acids of the VDJ junction translation, and the number of mutations detected in the V region. Clonally related IgH sequences are colour highlighted (see legend).

9 weeks

sequence	V	D	J	junction translation	mutations
1	DP-47/V3-23...+	D6-19	JH4b	CARGSSGWWG	2
2	DP-47/V3-23...+	D6-19	JH4b	CARGSSGWWG	2
3	DP-47/V3-23...+	D6-19	JH4b	CARGSSGWWG	3
4	DP-47/V3-23...+	D3-10/DXP ¹	JH6b	CAKDRGFGEL	7
5	DP-47/V3-23...+	D3-10/DXP ¹	JH6b	CAKDRGFGEL	7
6	DP-47/V3-23...+	D3-10/DXP ¹	JH6b	CAKDRGFGEL	7
7	DP-47/V3-23...+	D3-10/DXP ¹	JH6b	CAKDRGFGEL	7
8	DP-47/V3-23...+	D3-10/DXP ¹	JH6b	CAKDRGFGEL	7
9	DP-47/V3-23...+	D3-10/DXP ¹	JH6b	CAKDRGFGEL	7
10	DP-47/V3-23...+	D3-10/DXP ¹	JH6b	CAKDRGFGEL	7
11	DP-47/V3-23...+	D3-10/DXP ¹	JH6b	CAKDRGFGEL	7
12	DP-47/V3-23...+	D3-10/DXP ¹	JH6b	CAKDRGFGEL	7
13	DP-47/V3-23...+	D3-10/DXP ¹	JH6b	CAKDRGFGEL	7
14	DP-47/V3-23...+	D3-10/DXP ¹	JH6b	CAKDRGFGEL	7
15	DP-47/V3-23...+	D3-10/DXP ¹	JH6b	CAKDRGFGEL	7
16	DP-47/V3-23...+	D3-10/DXP ¹	JH6b	CAKDRGFGEL	8
17	DP-47/V3-23...+	D3-10/DXP ¹	JH6b	CAKDRGFGEL	8
18	DP-47/V3-23...+	D3-10/DXP ¹	JH6b	CAKDRGFGEL	8
19	DP-47/V3-23...+	D3-10/DXP ¹	JH6b	CAKDRGFGEL	8

12 weeks

sequence	V	D	J	junction translation	mutations
1	DP-47/V3-23...+	D3-10/DXP ¹	JH6b	CAKDRGFGEL	4
2	DP-47/V3-23...+	D3-10/DXP ¹	JH6b	CAKDRGFGEL	7
3	DP-47/V3-23...+	D3-10/DXP ¹	JH6b	CAKDRGFGEL	7
4	DP-47/V3-23...+	D3-10/DXP ¹	JH6b	CAKDRGFGEL	7
5	DP-47/V3-23...+	D3-10/DXP ¹	JH6b	CAKDRGFGEL	7
6	DP-47/V3-23...+	D3-10/DXP ¹	JH6b	CAKDRGFGEL	7
7	DP-47/V3-23...+	D3-10/DXP ¹	JH6b	CAKDRGFGEL	7
8	DP-47/V3-23...+	D3-10/DXP ¹	JH6b	CAKDRGFGEL	7
9	DP-47/V3-23...+	D3-10/DXP ²	JH6b	CAKDRGFGEL	7
10	DP-47/V3-23...+	D3-10/DXP ¹	JH6b	CAKDRGFGEL	7
11	DP-47/V3-23...+	D3-10/DXP ¹	JH6b	CAKDRGFGEL	8

- family 1
- family 2
- family 3

Table 19. BN-LCL4b

Summary of matched V, D and J alignments for each IgH sequence analysed at 9 and 12 weeks post-establishment (4 and 6 weeks shown on the previous page), the first 10 amino acids of the VDJ junction translation, and the number of mutations detected in the V region. Clonally related IgH sequences are colour highlighted (see legend).

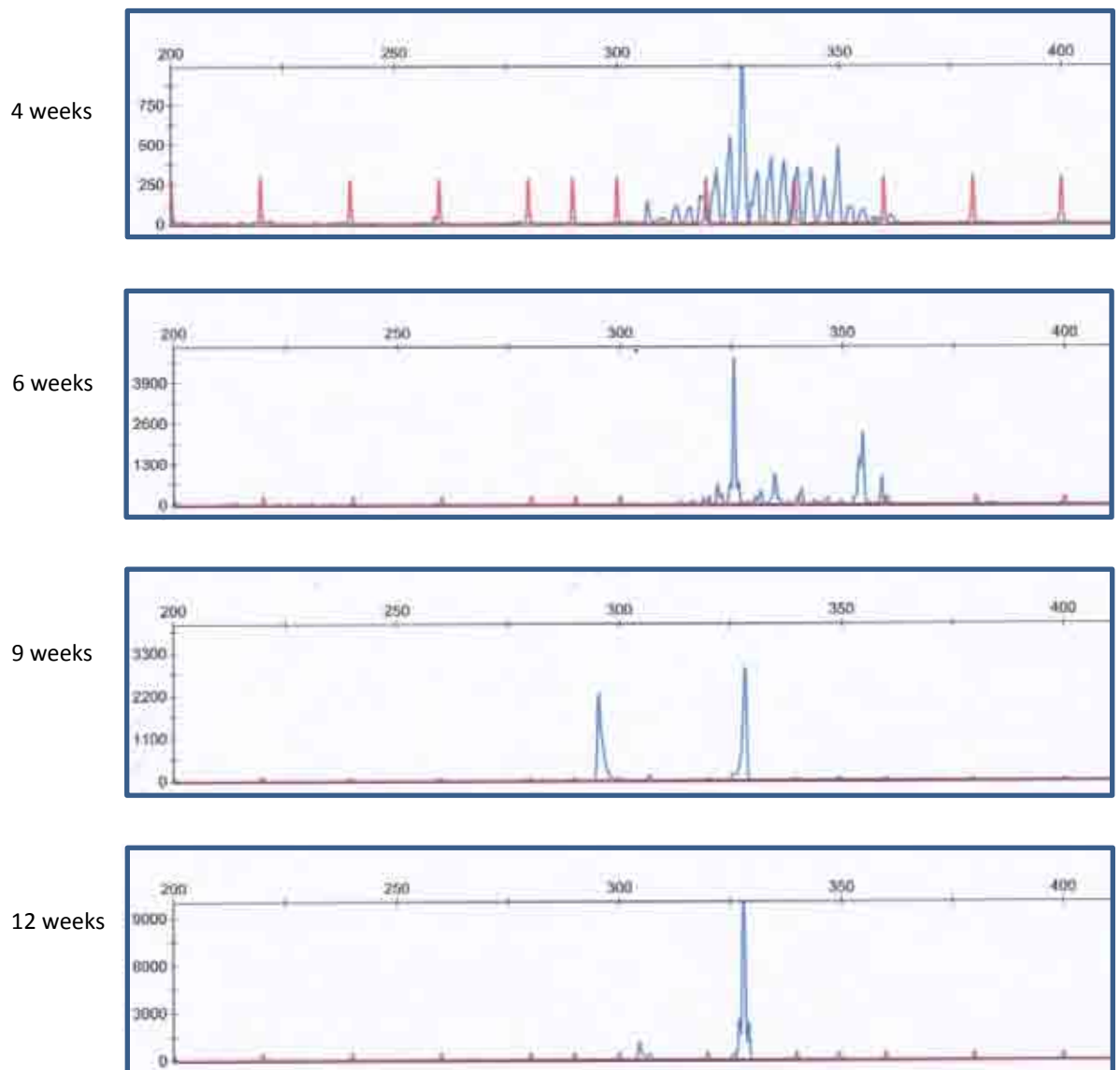


Figure 30. CDR3 spectratyping analysis of BN-LCL4b

In-frame rearranged VDJ gene fragments of various sizes are represented by blue peaks. The top axis represents a size ladder in base pairs. The red peaks represent a control sample containing template sequences of known size. BN-LCL4b was still polyclonal at 4 weeks, but fewer clones were detected over time until one clone dominated the culture at 12 weeks post-infection.

clones from family 3, detectable at six, nine and twelve weeks by sequencing of the bulk IgH PCR products could also be detected at 4 weeks. To address this issue, an Ig V region-alignment/CDR3-specific PCR technique was employed to probe the BN-LCL4b four week DNA sample. Using this approach, 12 sequences from family 3 were isolated, indicating that expansion was clearly occurring at this early stage albeit not to a degree significant enough to be detected by the global IgH PCR method (data not shown).

In the third LCL (BN-LCL4c) established from this donor, IgH sequences at six weeks post-infection reflected an almost monoclonal culture (Table 20). Family 1 was by far the predominant clonal group at six weeks, comprising 13 of 15 IgH sequences amplified. Similar results were found at weeks nine and twelve, reflecting that family 1 largely dominated the culture (Table 20).

During the analysis of BN-LCL4c, no viable sequencing data could be obtained from the four week time point using the standard IgH PCR method. Therefore family 1 CDR3-specific primers were used to amplify DNA from this timepoint. As shown in Table 20, B cells carrying this same CDR3 sequence were present at four weeks, but it is not known if they represented the dominant clone at this time (data not shown).

Somatic Hypermutation within BN-LCL4 Cultures

Having examined the clonal relationships within the BN-LCL4a, -b and -c cultures, we next looked in detail at the patterns of SHM seen in some of the clones. Within all three cultures, most clonal families showed evidence of mutated IgH sequences from four weeks post-infection. Closer examination revealed that IgH sequences in some clonal families shared identical mutation

6 weeks

sequence	V	D	J	junction translation	mutations
1	DP-47/V3-23...+	not found	JH4b	CAKGCGGVKT	5
2	DP-47/V3-23...+	not found	JH4b	CAKGCGGVKT	5
3	DP-47/V3-23...+	not found	JH4b	CAKGCGGVKT	5
4	DP-47/V3-23...+	not found	JH4b	CAKGCGGVKT	5
5	DP-47/V3-23...+	not found	JH4b	CAKGCGGVKT	5
6	DP-47/V3-23...+	not found	JH4b	CAKGCGGVKT	5
7	DP-47/V3-23...+	not found	JH4b	CAKGCGGVKT	5
8	DP-47/V3-23...+	not found	JH4b	CAKGCGGVKT	5
9	DP-47/V3-23...+	not found	JH4b	CAKGCGGVKT	5
10	DP-47/V3-23...+	not found	JH4b	CAKGCGGVKT	5
11	DP-47/V3-23...+	not found	JH4b	CAKGCGGVKT	5
12	DP-47/V3-23...+	not found	JH4b	CAKGCGGVKT	12
13	DP-88/hv1051k...+	D6-19	JH5b	CARGIAVPGG	1
14	DP-88/hv1051k...+	D6-19	JH5b	CARGIAVPGG	1
15	DP-79/4d154...+	D6-25	JH4b	CARQVAAAVD	3

9 weeks

sequence	V	D	J	junction translation	mutations
1	DP-47/V3-23...+	not found	JH4b	CAKGCGGVKT	5
2	DP-47/V3-23...+	not found	JH4b	CAKGCGGVKT	5
3	DP-47/V3-23...+	not found	JH4b	CAKGCGGVKT	5
4	DP-47/V3-23...+	not found	JH4b	CAKGCGGVKT	5
5	DP-47/V3-23...+	not found	JH4b	CAKGCGGVKT	5
6	DP-47/V3-23...+	not found	JH4b	CAKGCGGVKT	5
7	DP-47/V3-23...+	not found	JH4b	CAKGCGGVKT	5
8	DP-47/V3-23...+	not found	JH4b	CAKGCGGVKT	5
9	DP-47/V3-23...+	not found	JH4b	CAKGCGGVKT	5
10	DP-47/V3-23...+	not found	JH4b	CAKGCGGVKT	5
11	DP-47/V3-23...+	not found	JH4b	CAKGCGGVKT	5
12	DP-47/V3-23...+	not found	JH4b	CAKGCGGVKT	5
13	DP-47/V3-23...+	not found	JH4b	CAKGCGGVKT	5
14	DP-47/V3-23...+	not found	JH4b	CAKGCGGVKT	5
15	DP-47/V3-23...+	not found	JH4b	CAKGCGGVKT	5
16	DP-47/V3-23...+	not found	JH4b	CAKGCGGVKT	5
17	DP-47/V3-23...+	not found	JH4b	CAKGCGGVKT	6
18	DP-47/V3-23...+	not found	JH4b	CAKGCGGVKT	6
19	DP-47/V3-23...+	not found	JH4b	CAKGCGGVKT	6
20	DP-47/V3-23...+	not found	JH4b	CAKGCGGVKT	7
21	DP-47/V3-23...+	not found	JH4b	CAKGCGGVKT	8
22	DP-51+	D7-27/DHQ52	JH4b	CARDPGRPQQ	3

12 weeks

sequence	V	D	J	junction translation	mutations
1	DP-47/V3-23...+	not found	JH4b	CAKGCGGVKT	5
2	DP-47/V3-23...+	not found	JH4b	CAKGCGGVKT	5
3	DP-47/V3-23...+	not found	JH4b	CAKGCGGVKT	5
4	DP-47/V3-23...+	not found	JH4b	CAKGCGGVKT	5
5	DP-47/V3-23...+	not found	JH4b	CAKGCGGVKT	5
6	DP-47/V3-23...+	not found	JH4b	CAKGCGGVKT	5
7	DP-47/V3-23...+	not found	JH4b	CAKGCGGVKT	5
8	DP-47/V3-23...+	not found	JH4b	CAKGCGGVKT	5
9	DP-47/V3-23...+	not found	JH4b	CAKGCGGVKT	5
10	DP-47/V3-23...+	not found	JH4b	CAKGCGGVKT	5
11	DP-47/V3-23...+	not found	JH4b	CAKGCGGVKT	5
12	DP-47/V3-23...+	not found	JH4b	CAKGCGGVKT	5
13	DP-47/V3-23...+	not found	JH4b	CAKGCGGVKT	5
14	DP-47/V3-23...+	not found	JH4b	CAKGCGGVKT	5
15	DP-47/V3-23...+	not found	JH4b	CAKGCGGVKT	5
16	DP-47/V3-23...+	not found	JH4b	CAKGCGGVKT	5
17	DP-47/V3-23...+	not found	JH4b	CAKGCGGVKT	5
18	DP-47/V3-23...+	not found	JH4b	CAKGCGGVKT	6
19	DP-47/V3-23...+	not found	JH4b	CAKGCGGVKT	6
20	DP-51+	D7-27/DHQ52	JH4b	CARDPGRPQQ	3
21	DP-51+	D7-27/DHQ52	JH4b	CARDPGRPQQ	3

Legend

	Family 1
	Family 2
	Family 3

Table 20. BN-LCL4c

Summary of matched V, D and J alignments for each IgH sequence analysed at 6, 9 and 12 weeks post-establishment, the first 10 amino acids of the VDJ junction translation, and the number of mutations detected in the V region. Clonally related IgH sequences are colour highlighted (see legend).

patterns (BN-LCL 4a/family 3 and BN-LCL4c/family 3) with little or no deviation detected between sequences. On the other hand, several families contained IgH sequences which although related to one another, varied significantly in the number and location of mutations. Generally, such clonal families contained a mixture of (i) multiple sequences harbouring a pattern of shared, family-specific mutations, (ii) sequences containing the family-specific mutation pattern, plus additional mutations, which may represent ongoing mutation in the culture, (iii) sequences containing some but not all of the shared mutation pattern, possibly representing ancestors, (iv) sequences carrying mutations that were not shared by any other sequence. Indeed in several of these clonal families, detailed analysis of the IgH mutations revealed complex relationships between the sequences, in which mutations appeared to accumulate in a successive fashion in consecutive generations of cell progeny. As these mutations were suggestive of “clonal evolution” within the families, hypothetical family trees were constructed based on the relationships between IgH sequences identified within the cultures.

The first LCL clonal family tree presented in this thesis will be discussed in the greatest detail in order to illustrate how the data was interpreted.

BN-LCL 4a/*Family 2*

Using the sequence information (summarised in Table 18), a family tree was drawn to show the relationship between members of the clonally related family 2 from BN-LCL4a. Cell clones are represented by a circle, inside which is shown the number of IgH mutations. Ancestor cell clones are positioned on the top row, with arrows leading to descendents on the row below, and so on.

Specific IgH sequences representing cells/clones in which the mutations were identified are indicated underneath the circles. Where multiple sequences harbouring the same mutations were found, the identity of an example sequence is provided, and the number of identical sequences detected is shown in brackets inside the circle. Circles with dashed lines represent putative intermediates that were not identified within the cultures. Divergent branches of the family trees are indicated where appropriate, and IgH sequence alignments from distinct branches are presented in separate figures.

Multiple sequences carrying the same 4 mutations (at codons 29, 35, 62 and 70) were identified in family 2; therefore this mutation pattern could be described as family-specific. Importantly, a germline sequence with the same CDR3 region, but carrying 0 mutations was also identified, confirming that the common ancestor in this case was a naive B cell. Several distinct progeny cell lineages can be seen, with additional mutations arising along successive generations (Figure 31). The most striking example of this can be seen in branch 1, where a germline clone with 0 mutations gave rise to a cell that acquired 1 mutation (at codon 70), which was succeeded by a cell acquiring a further mutation (at codon 29), followed by a clone acquiring 2 additional mutations (at codons 35 and 62). Subsequent multiple progeny presumably then went on to acquire additional mutations independently of one another (Figure 32).

Similar lines of succession can be seen in branch 2 (Figure 33) and branch 3 (Figure 34).

Figure 31. BN-LCL4a family 2 tree

Cell clones are represented by a circle, inside which is shown the number of IgH mutations. Ancestor cell clones are positioned on the top row, with arrows leading to descendents on the row below. Specific IgH sequences representing cells/clones in which the mutations were identified are indicated underneath the circles. Where multiple sequences harbouring the same mutations were found, the identity of an example sequence is provided, and the number of identical sequences detected is shown in brackets inside the circle. Circles with dashed lines represent intermediates that were not identified within the cultures. Arrows signify the proposed order of mutation accumulation. Different trees branches are indicated where appropriate.

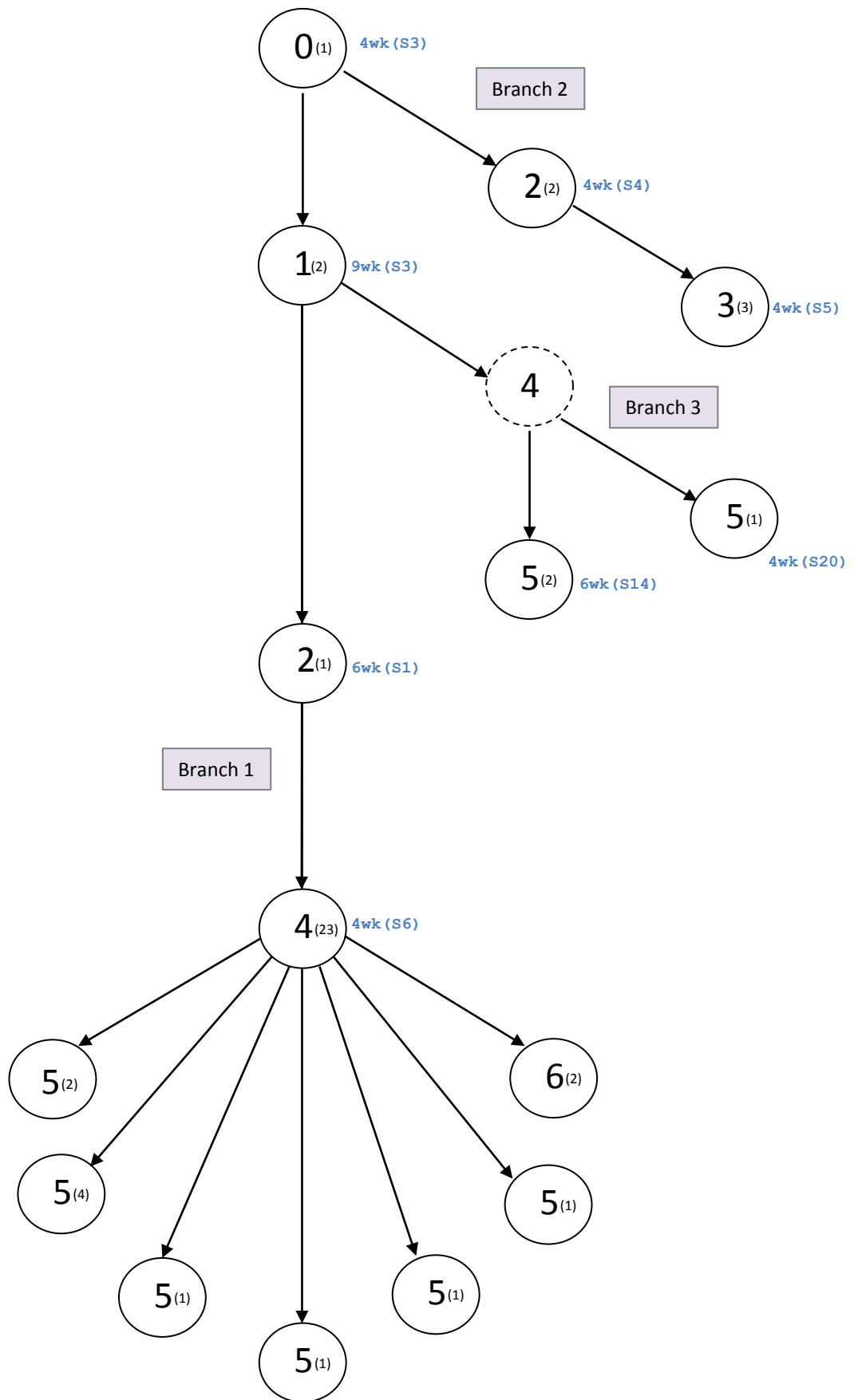


Figure 31. BN-LCL4a family 2 tree

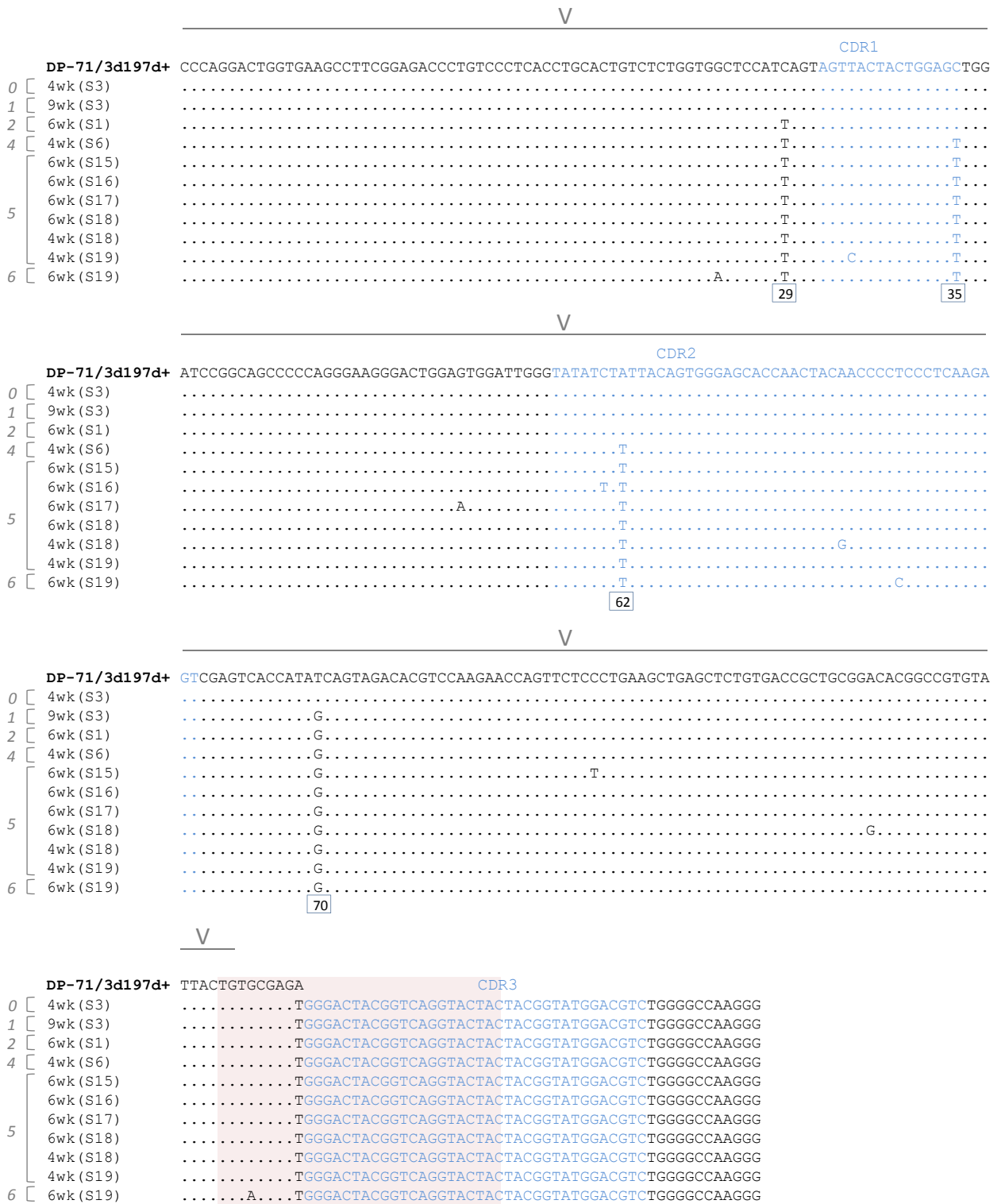


Figure 32. BN-LCL4a family 2 – branch 1

BN-LCL4a family 2 sequences are aligned relative to the matched germline V region sequence (top row). The location of the V region is indicated and the CDRs (1, 2 and 3) are highlighted in blue text. A box is drawn around the first 30 nucleotides of the VDJ junction translation.

The ancestral cell carrying 0 mutations gave rise to progeny harbouring a single mutation at codon 70, followed by a daughter cell which gained an extra mutation at codon 29 and so on. The branch of the family 2 tree shown in this alignment highlights the accumulation of mutations in a stepwise fashion, along with successive generations of cell progeny.

BN-LCL 4b/Family 3

The tree constructed for family 3 (Figure 35) contains one main branch (branch 1), plus a subsidiary branch (branch 2) in which only one IgH sequence (“12wk(S1)”) was detected, harbouring the same 2 mutations (at codons 56 and 81) carried by all sequences belonging to branch 1. Indeed an IgH sequence carrying just these 2 mutations was also present in the data, which not only represents the common ancestor between the two branches, but by the criteria used in this study is also genotypically a naive cell (Figure 36).

As with the BN-LCL4a/family 2 tree, branch 1 is a good example of successive accumulation of mutations within a clonal family. The detection of multiple sequences carrying the family-specific set of 7 mutations at codons 29, 30, 31 (x2), 35, 56 and 81 is particularly interesting as this suggests preferential expansion of the clone at this stage. This analysis strongly suggests that mutated IgH sequences arise from naive B cell infection, rather than PCR error or contamination with memory B cells.

4.2.6 Analysis of IgH Mutations in Bulk LCLs and LCLs

Established by Limiting Dilution

In work performed by Dr Sridhar Chaganti prior to the current study, the effect of EBV infection and transformation on naive B cells was studied using LCLs established under the conditions of limiting dilution. Such experiments mainly yielded monoclonal cultures, of which approximately one quarter contained mutated IgH sequences after ten-twelve weeks of growth. Since this method involved the infection of small numbers of B cells (typically 50-200 per well), sufficient cell numbers were not available to harvest until approximately 10

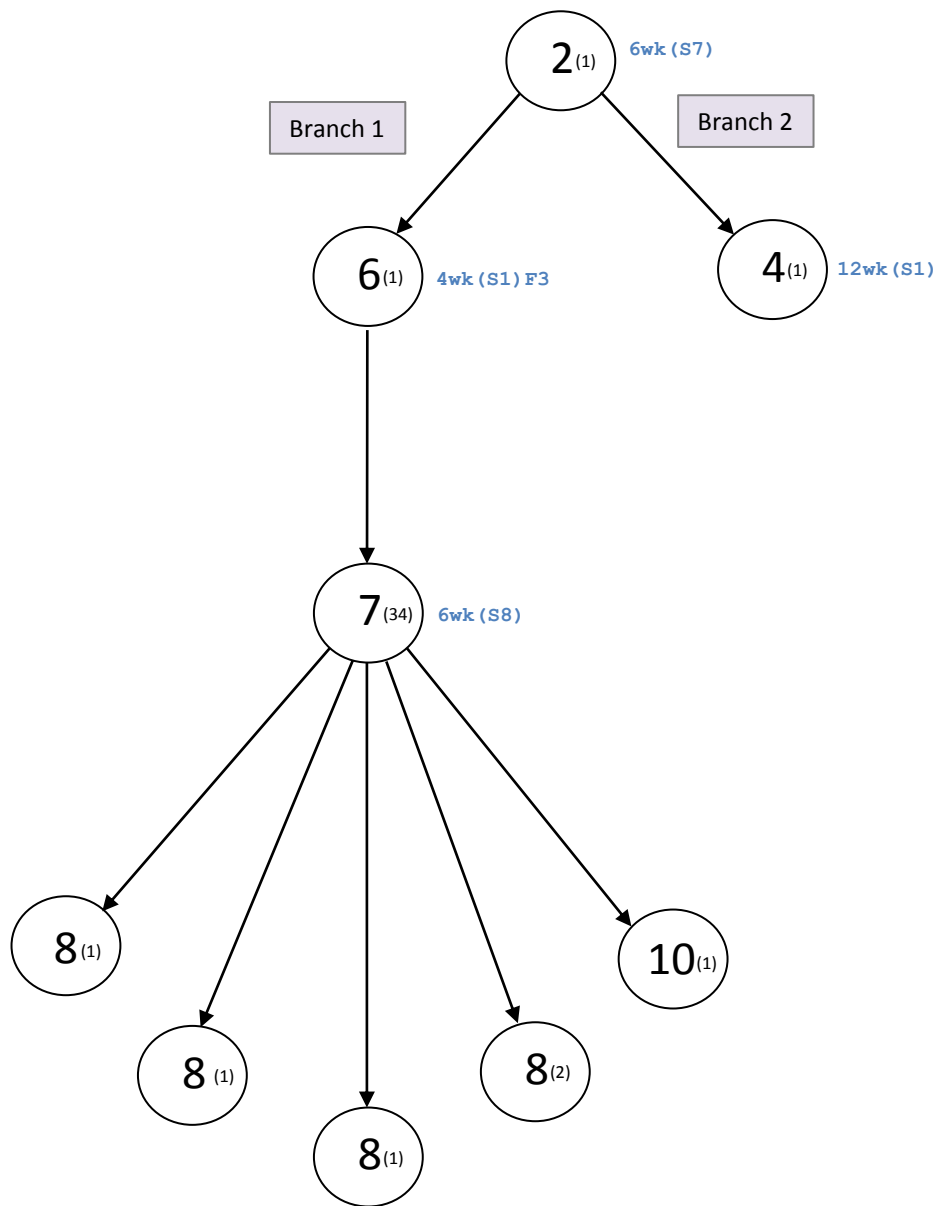


Figure 35. BN-LCL4b family 3 tree

Cell clones are represented by a circle, inside which is shown the number of IgH mutations. Ancestor cell clones are positioned on the top row, with arrows leading to descendants on the row below. Specific IgH sequences representing cells/clones in which the mutations were identified are indicated underneath the circles. Where multiple sequences harbouring the same mutations were found, the identity of an example sequence is provided, and the number of identical sequences detected is shown in brackets inside the circle. Arrows signify the proposed order of mutation accumulation. Separate lineage branches are indicated.

weeks post-infection, thus preventing analysis of the cultures at earlier time points. We therefore aimed to compare this limiting dilution method with the bulk LCL method used in the current work, in order to examine whether both techniques could generate LCLs with mutated IgH genes. To this end, we carried out two experiments in which we established both limiting dilution clonal cultures and a bulk LCL from the same population of purified naive B cells, originating from a single donor (Figure 37).

Naive B cells from a single peripheral blood donor were purified as previously described, and exposed *in vitro* to EBV supernatant taken from a single batch. Cells were seeded into three separate 96-well plates at densities of 1000, 500 or 200 cells per well to generate limiting dilution clones, or into a single well of a 96-well plate at a density of 0.5×10^6 to produce a bulk LCL. The bulk naive LCLs (BN-LCL5 and BN-LCL6), were harvested at six, nine and twelve weeks post-infection. The corresponding clonal naive LCL cultures (CN-LCL5 and CN-LCL6) were expanded and harvested at twelve weeks post infection.

IgH Analysis of Bulk Naive LCL5

The pre-infection IgH sequencing data for both BN-LCL5 and CN-LCL5, reflected a polyclonal population of naive B cells, with all 14 IgH sequences tested being unmutated (Table 21). Consistent with previous results, clonal outgrowth was observed at six weeks post-infection, and thereafter variations in clonal dominance could be seen (Table 21). The proportion of family 1, which was dominant at six weeks (11 out of 18 IgH sequences) declined by twelve weeks (4 out of 26 IgH sequences). By contrast, family 2, which was barely

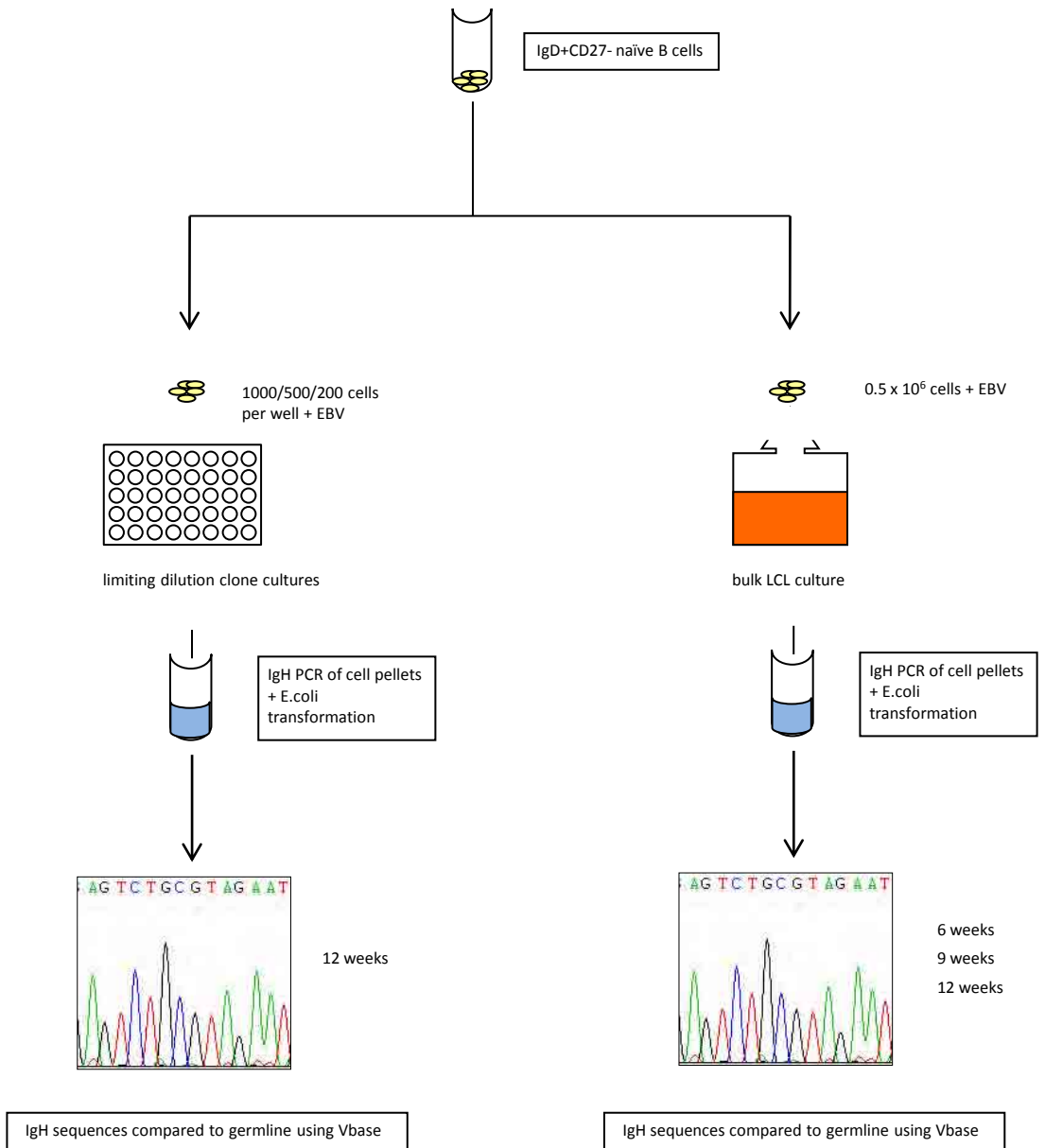


Figure 38. Establishment of limiting dilution naive LCL clones and bulk naive LCLs from one donor

pre-infection

sequence	V	D	J	junction translation	mutations
1	DP-79/4d154...+	D3-22/D21-9	JH3b	CARLYYYDSS	0
2	DP-75/V1-2...+	not found	JH4b	CARLEEEAVT	0
3	V3-53+	D1-7/DM1	JH6b	CARSPRVGDG	0
4	DP-31/V3-9P...+	D2-15/D2	JH6c	CAKDGGGSSY	0
5	DP-31/V3-9P...+	D2-2	JH6c	CAKDSS*YCS	0
6	DP-66/V71-2...+	D4-23	JH5b	CARESGGGWY	0
7	DP-47/V3-23...+	D5-5/DK4	JH6b	CARGVGEIQL	0
8	DP-73/V5-51...+	D1-26	JH3b	CARHGMYSGS	1
9	DP-10/Hv1051...+	D6-6/DN4	JH4b	RALSEARSWY	1
10	DP-75/V1-2...+	D6-13/DN1	JH6b	CARGSQEYSS	1
11	DP-31/V3-9P...+	D4-17	JH4b	CAKDRLPYGD	1
12	DP-7/21-2...+	D3-22/D21-9	JH4b	CARIPTYDSS	1
13	DP-73/V5-51...+	D5-24	JH6c	CARHGAGYMA	1
14	V3-49+	not found	JH6b	CTRELSWVPR	2

6 weeks

sequence	V	D	J	junction translation	mutations
1	DP-65/3d75d...+	D6-6/DN4	JH6b	CARVRLAGPL	0
2	DP-65/3d75d...+	D6-6/DN4	JH6b	CARVRLAGPL	0
3	DP-65/3d75d...+	D6-6/DN4	JH6b	CARVRLAGPL	0
4	DP-65/3d75d...+	D6-6/DN4	JH6b	CARVRLAGPL	0
5	DP-65/3d75d...+	D6-6/DN4	JH6b	CARVRLAGPL	0
6	DP-65/3d75d...+	D6-6/DN4	JH6b	CARVRLAGPL	0
7	DP-65/3d75d...+	D6-6/DN4	JH6b	CARVRLAGPL	1
8	DP-65/3d75d...+	D6-6/DN4	JH6b	CARVRLAGPL	1
9	DP-65/3d75d...+	D6-6/DN4	JH6b	CARVRLAGPL	1
10	DP-65/3d75d...+	D6-6/DN4	JH6b	CARVRLAGPL	1
11	DP-65/3d75d...+	D6-6/DN4	JH6b	CARVRLAGPL	3
12	DP-38/9-1...+	D1-14/DM2	JH6b	CTTYNRIRGS	21
13	DP-31/V3	D4-17	JH4b	CAVGYGDYHS	0
14	DP-31/V3-9P...+	D3-22/D21-9	JH5b	CAKGMMAMY	0
15	DP-50/hv3019b9...+	D3-22/D21-9	JH3b	CAREGYYYDS	0
16	DP-47/V3-23...+	not found	JH4b	CAKEMRLGSR	0
17	DP-58/hv3d1EG	not found	JH5b	CASVRWLTW	1
18	DP-31/V3-9P...+	D4-11/DA1	JH6b	CAKDSPLYG	3

Legend

- Family 1
- Family 2
- Family 3
- Family 4

Table 21. BN-LCL5

Summary of matched V, D and J alignments for each IgH sequence analysed at 0 and 6 weeks post-establishment (9 and 12 weeks shown on next page), the first 10 amino acids of the VDJ junction translation, and the number of mutations detected in the V region. Clonally related IgH sequences are colour highlighted (see legend).

9 weeks

sequence	V	D	J	junction translation	mutations
1	DP-65/3d75d...+	D6-6/DN4	JH6b	CARVRLAGPL	0
2	DP-65/3d75d...+	D6-6/DN4	JH6b	CARVRLAGPL	0
3	DP-65/3d75d...+	D6-6/DN4	JH6b	CARVRLAGPL	0
4	DP-65/3d75d...+	D6-6/DN4	JH6b	CARVRLAGPL	0
5	DP-65/3d75d...+	D6-6/DN4	JH6b	CARVRLAGPL	1
6	DP-65/3d75d...+	D6-6/DN4	JH6b	CARVRLAGPL	1
7	DP-65/3d75d...+	D6-6/DN4	JH6b	CARVRLAGPL	1
8	DP-65/3d75d...+	D6-6/DN4	JH6b	CARVRLAGPL	1
9	DP-65/3d75d...+	D6-6/DN4	JH6b	CARVRLAGPL	1
10	DP-65/3d75d...+	D6-6/DN4	JH6b	CARVRLAGPL	5
11	DP-38/9-1...+	D1-14/DM2	JH6b	CTTYNRIRGS	20
12	DP-38/9-1...+	D1-14/DM2	JH6b	CTTYNRIRGS	21
13	VIV-4/4.35+	not found	JH4b	CARDSSVGWD	11
14	DP-47/V/3-23...+	not found	JH5b	CARDRSGNWF	0
15	DP-38/9-1...+	D3-22/D21-9	JH4b	CTSPL*KRIT	0
16	DP-88/hv1051K...+	D1-26	JH4b	CARDSSAIVG	1

12 weeks

sequence	V	D	J	junction translation	mutations
1	DP-65/3d75d...+	D6-6/DN4	JH6b	CARVRLAGPL	0
2	DP-65/3d75d...+	D6-6/DN4	JH6b	CARVRLAGPL	1
3	DP-65/3d75d...+	D6-6/DN4	JH6b	CARVRLAGPL	2
4	DP-65/3d75d...+	D6-6/DN4	JH6b	CARVRLAGPL	3
5	DP-38/9-1...+	D1-14/DM2	JH6b	CTTYNRIRGS	20
6	DP-38/9-1...+	D1-14/DM2	JH6b	CTTYNRIRGS	20
7	DP-38/9-1...+	D1-14/DM2	JH6b	CTTYNRIRGS	20
8	DP-38/9-1...+	D1-14/DM2	JH6b	CTTYNRIRGS	20
9	DP-38/9-1...+	D1-14/DM2	JH6b	CTTYNRIRGS	20
10	DP-38/9-1...+	D1-14/DM2	JH6b	CTTYNRIRGS	20
11	DP-38/9-1...+	D1-14/DM3	JH6b	CTTYNRIRGS	20
12	DP-38/9-1...+	D1-14/DM2	JH6b	CTTYNRIRGS	20
13	DP-38/9-1...+	D1-14/DM2	JH6b	CTTYNRIRGS	20
14	DP-38/9-1...+	D1-14/DM2	JH6b	CTTYNRIRGS	21
15	DP-38/9-1...+	D1-14/DM2	JH6b	CTTYNRIRGS	21
16	VIV-4/4.35+	not found	JH4b	CARDSSVGWD	11
17	VIV-4/4.35+	not found	JH4b	CARDSSVGWD	11
18	VI-4.1b+	D5-5/DK4	JH5a	CARATQLWTP	6
19	VI-4.1b+	D5-5/DK4	JH5a	CARATQLWTP	6
20	VI-4.1b+	D5-5/DK4	JH5a	CARATQLWTP	6
21	DP-73/V/5-51...+	not found	JH6c	CARCYSMFYY	2
22	DP-71/3d197d...+	D6-25	JH5b	CARSLAAAGW	2
23	DP-32/V/3-20+	D2-15/D2	JH6b	CARDRRFCRG	2
24	DP-65/3d75d...+	D5-12/DK1	JH5b	CARDLVATSFW	3
25	DP-77/WHG16+	D6-6/DN4	JH4b	CARDKGVHAA	15
26	DP-48/13-2+	D4-17	JH6b	CARVRGGHEY	12

Legend

	Family 1
	Family 2
	Family 3
	Family 4

Table 21. BN-LCL5

Summary of matched V, D and J alignments for each IgH sequence analysed at 9 and 12 weeks post-establishment (0 and 6 weeks shown on previous page), the first 10 amino acids of the VDJ junction translation, and the number of mutations detected in the V region. Clonally related IgH sequences are colour highlighted (see legend).

detectable at six weeks (1 out of 18 IgH sequences) became the dominant clone at later time points.

Three out of four families (families 2, 3 and 4) in BN-LCL5 contained mutated IgH sequences. Further analysis revealed that IgH sequences within each of these families shared family-specific mutations. IgH sequences within family 1 carried between 0 and 5 mutations, which was suggestive of *in vitro* mutation, although insufficient sequences were obtained to construct a family tree.

IgH Analysis of Limiting Dilution LCL5 Naive Clones

In parallel to the bulk culture of BN-LCL5, a total of 32 cultures were established by limiting dilution, arising from 1000, 500 or 200 cells per well. DNA was isolated from each culture, subjected to IgH DNA amplification and the PCR products cloned. Up to 5 sequences from each of the cultures were then examined. A summary of the IgH sequencing results is displayed in Table 22.

Of the 32 cultures analysed, 24 yielded a single amplified IgH and were deemed to be monoclonal. In cultures where more than one IgH sequence was detected, the dominant one was designated representative of the culture. For example, culture 31 containing 4 unmutated, clonally related sequences plus a unique sequence carrying 10 mutations, was scored as unmutated. In monoclonal cultures where members of the same clonal family carried different numbers of mutations, the mean numbers of mutations per IgH sequences was calculated in order to decide whether to classify the culture as mutated or unmutated. Based on these criteria, 25% of the CN-LCL5 cultures were classified as mutated. Taking into account the inclusion of biclonal and

seeding	culture	sequence	V	D	J	junction translation	mutations	
200 cells/well	1	1	V3-53+	not found	JH6b	CARDSDYGFE	0	
		2	V3-53+	not found	JH6b	CARDSDYGFE	0	
	2	1	DP-70/4d68...+	D6-19	JH4b	CARGGAVAGP	1	
		2	DP-70/4d68...+	D6-19	JH4b	CARGGAVAGP	1	
	3	1	DP-31/V3-9P...+	D1-26	JH4b	CAKGxGLRLD	0	
		2	DP-31/V3-9P...+	D1-26	JH4b	CAKGVGLRLD	0	
	4	1	DP-7/21-2...+	D6-19	JH4b	CARVGGSSGY	0	
		2	DP-7/21-2...+	D6-19	JH4b	CARVGGSSGY	0	
		3	DP-7/21-2...+	D6-19	JH4b	CARVGGSSGY	1	
	500 cells/well	5	1	DP-65/3d75d...+	D4	JH4b	CARTPNYWGQ	2
			2	DP-65/3d75d...+	D4	JH4b	CARTPNYWGQ	2
			3	DP-65/3d75d...+	D4	JH4b	CARTPNYWGQ	3
6		1	DP-47/V3-23...+	D5-24	JH4b	CAKVSVMAT	2	
		2	DP-47/V3-23...+	D5-24	JH4b	CAKVSVMAT	2	
		3	DP-47/V3-23...+	D5-24	JH4b	CAKVSVMAT	2	
7		1	DP-14/V1-18+	D2-21	JH3b	CARDLVVTA	1	
8		1	DP-79/4d154...+	D3-10/DXP'1	JH5b	CARRNDYVWS	0	
		2	DP-79/4d154...+	D3-10/DXP'1	JH5b	CARRNDYVWS	0	
		3	DP-79/4d154...+	D3-10/DXP'1	JH5b	CARRNDYVWS	0	
9		1	DP-75/V1-2...+	D2-15/D2	JH6b	CARGGCGGGR	4	
		2	DP-75/V1-2...+	D2-15/D2	JH6b	CARGGCGGGR	4	
1000 cells/well	10	1	V3-48/hv3d1...+	D2-15/D2	JH5b	CARGAPRYCS	0	
		2	V3-48/hv3d1...+	D2-15/D2	JH5b	CARGAPRYCS	0	
		3	V3-48/hv3d1...+	D2-15/D2	JH5b	CARGAPRYCS	1	
	11	1	DP-47/V3-23...+	D3-10/DXP-1	JH1	CAKDPVLLWF	0	
		2	DP-47/V3-23...+	D3-10/DXP-1	JH1	CAKDPVLLWF	0	
		3	DP-47/V3-23...+	D3-10/DXP-1	JH1	CAKDPVLLWF	0	
	12	1	DP-79/4d154...+	D2-8/DLR1	JH4b	CARRATIPYF	0	
		2	DP-49/I.9III...+	D3-22/D21-9	JH4b	CAKDHYDSSG	0	
	13	1	DP-54/V3-7...+	D2-21	JH6c	CTRNTCDGD	12	
		2	DP-54/V3-7...+	D2-21	JH6c	CTRNTCDGD	12	
	14	1	DP-77/WHG16+	not found	JH5b	CARDLTYGDY	0	
		2	DP-57/hv3003...+	not found	JH4b	CSSGASVLEG	0	
	15	1	DP-79/4d154...+	not found	JH4b	CARQDDYGEG	0	
		2	DP-79/4d154...+	not found	JH4b	CARQDDYGEG	0	
		3	DP-79/4d154...+	D4-17	JH4b	CARQDDYGEG	0	
		4	DP-79/4d154...+	D4-17	JH4b	CARQDDYGEG	0	
		5	DP-75/V1-2...+	not found	JH4b	CARDSWVYSS	1	
16	1	DP-49/I.9111...+	not found	JH4b	CAKDVGKGRG	5		
	2	DP-49/I.9111...+	not found	JH4b	CAKDVGKGRG	5		
	3	DP-49/I.9111...+	not found	JH4b	CAKDVGKGRG	6		
17	1	DP-7/21-2...+	not found	JH4b	CAMPPTVTTG	0		
	2	DP-7/21-2...+	not found	JH4b	CAMPPTVTTG	1		
	3	DP-71/3d197d...+	not found	JH5b	CARFGTEQLL	0		

Table 22. Naive LCL5 limiting dilution cultures

Blocks shaded grey represent unmutated cultures. Blocks shaded green represent mutated cultures. Green frames around grey blocks highlight instances where cultures contain unmutated and mutated sequences of the same CDR3 clonotype. Cultures were deemed mutated if the majority of sequences contained >2 mutations. Where cultures contained more than one distinct CDR3 clonotype, the mutation status of the family comprising the highest proportion of the culture is represented in the table.

seeding	culture	sequence	V	D	J	junction translation	mutations
1000 cells/well	18	1	DP-79/4d154...+	not found	JH5b	CARRSPGAAY	1
		2	DP-79/4d154...+	not found	JH5b	CARRSPGAAY	1
	19	1	DP-49/I.9111...+	not found	JH4b	CANSYSSSWY	4
		2	DP-49/I.9111...+	not found	JH4b	CANSYSSSWY	4
		3	DP-49/I.9111...+	not found	JH4b	CANSYSSSWY	5
	20	1	DP-31/V3-9P	not found	JH4b	CAKDVS RKDY	0
		2	DP-31/V3-9P	not found	JH4b	CAKDVS RKDY	0
		3	DP-31/V3-9P	D3-22/D21-9	JH4b	CAKDVS RKDY	0
		4	DP-31/V3-9P	D3-22/D21-9	JH4b	CAKDVS RKDY	0
	21	1	DP-66/V71-2...+	D5-5/DK4	JH6b	CARLKG TALV	3
		2	DP-66/V71-2...+	D5-5/DK4	JH6b	CARLKG TALV	3
		3	DP-66/V71-2...+	D5-5/DK4	JH6b	CARLKG TALV	4
	22	1	DP-7/21-2...+	D3-22/D21-9	JH6c	CARAP TLYYD	0
		2	DP-7/21-2...+	D3-22/D21-10	JH6c	CARAP TLYYD	0
		3	DP-7/21-2...+	D3-22/D21-9	JH6c	CARAP TLYYD	1
	23	1	DP-77/WHG16+	D6-13/DN1	JH4b	CARDREWEQ	0
		2	DP-77/WHG16+	D6-13/DN1	JH4b	CARDREWEQ	1
		3	DP-77/WHG16+	D6-13/DN1	JH4b	CARDREWEQ	1
	24	1	DP-77/WHG16+	D2-8/DLR1	JH3b	CARGGPEKYC	0
	25	1	DP-35/V3-11...+	D5-24	JH4b	CARV VPRGWL	6
		2	DP-35/V3-11...+	D5-24	JH4b	CARVxPRGWL	6
		3	DP-35/V3-11...+	D5-24	JH4b	CARV VPRGWL	6
	26	1	DP-63/VH4.21...+	D3-9/DXP1...	JH4b	CAKSDILTGY	9
	27	1	DP-15/V1-8+	D7-27/DHQ52	JH6c	CARGEWGALR	9
		2	DP-15/V1-8+	D7-27/DHQ52	JH6c	CARGEWGALR	9
		3	DP-15/V1-8+	D7-27/DHQ52	JH6c	CARGEWGALR	9
	28	1	DP-5/V1-24P+	D3-10/DXP ¹	JH4b	CAPRFGELSR	0
		2	DP-5/V1-24P+	D3-10/DXP ¹	JH4b	CAPRFGELSR	1
	29	1	DP-71/3d197d...+	D6-19	JH5b	CARDAPGGSY	0
		2	DP-71/3d197d...+	D6-19	JH5b	CARDAPGGSY	0
		3	DP-47/V3-23...+	not found	JH6c	CASNKVGSYM	0
		4	DP-74/VH-VI...+	D6-6/DN4	JH3b	WTGSHREPRI	0
30	1	DP-49/1.9III...+	not found	JH2	CAKDPTMYMKD	0	
	2	DP-49/1.9III...+	not found	JH2	CAKDPTMYMKD	0	
	3	V3-64/YAC-6+	D3-16	JH1	CARGTLL*LRL	2	
31	1	DP-77/WHG16+	not found	JH6c	CARGGSDYYY	10	
	2	DP-75/VI-2...+	D5-5/DK4	JH6b	CASRPRHTAM	1	
	3	DP-75/VI-2...+	D5-5/DK4	JH6b	CASRPRHTAM	1	
	4	DP-75/VI-2...+	D5-5/DK4	JH6b	CASRPRHTAM	1	
	5	DP-75/VI-2...+	D5-5/DK4	JH6b	CASRPRHTAM	1	
32	1	DP-78/3d230d...+	D3-22/D21-9	JH6c	CARGGYDSSG	0	
	2	DP-10/hv1051...+	D3-10/DXP ¹	JH4b	CASxRVVRGV	0	

Table 22. Naive LCL5 limiting dilution cultures

Blocks shaded grey represent unmutated cultures. Blocks shaded green represent mutated cultures. Green frames around grey blocks highlight instances where cultures contain unmutated and mutated sequences of the same CDR3 clonotype. Cultures were deemed mutated if the majority of sequences contained >2 mutations. Where cultures contained more than one distinct CDR3 clonotype, the mutation status of the family comprising the highest proportion of the culture is represented in the table.

oligoclonal cultures, the proportion of total mutated families within the experiment as a whole was also calculated at 23%.

Whether considering mutation frequency in terms of either total cultures (25%) or total clonal families (23%), the results show that by twelve weeks post-infection, mutated IgH sequences were present in significant proportions compared to the resting naive B cell pre-infection data (0%). Interestingly, in culture 5, a monoclonal LCL where only 1 clonal family was identified, unmutated sequences were detected alongside a sequence carrying 3 mutations (Figure 38).

IgH Analysis of Bulk Naive LCL6

IgH sequence analysis data derived from the resting naive B cell population prior to EBV infection and on the BN-LCL population twelve weeks post-infection are shown in Table 23. The resting naive B cells were polyclonal, with 13 out of 14 unmutated IgH sequences confirming the purity of the starting population. As seen previously, the LCL culture had become oligoclonal by twelve weeks, with two families (1 and 2) dominating approximately half of the culture. Interestingly, at this time point, the majority of IgH sequences were mutated including those from both clonal families, and 6 out of 9 of the unique IgH sequences.

IgH Analysis of Limiting Dilution LCL6 Naive Clones

As in the previous experiment, LCL cultures were established in parallel by limiting dilution and expanded for analysis. Table 24 shows the IgH sequence data from 25 such LCL cultures. Overall these cultures were very similar to

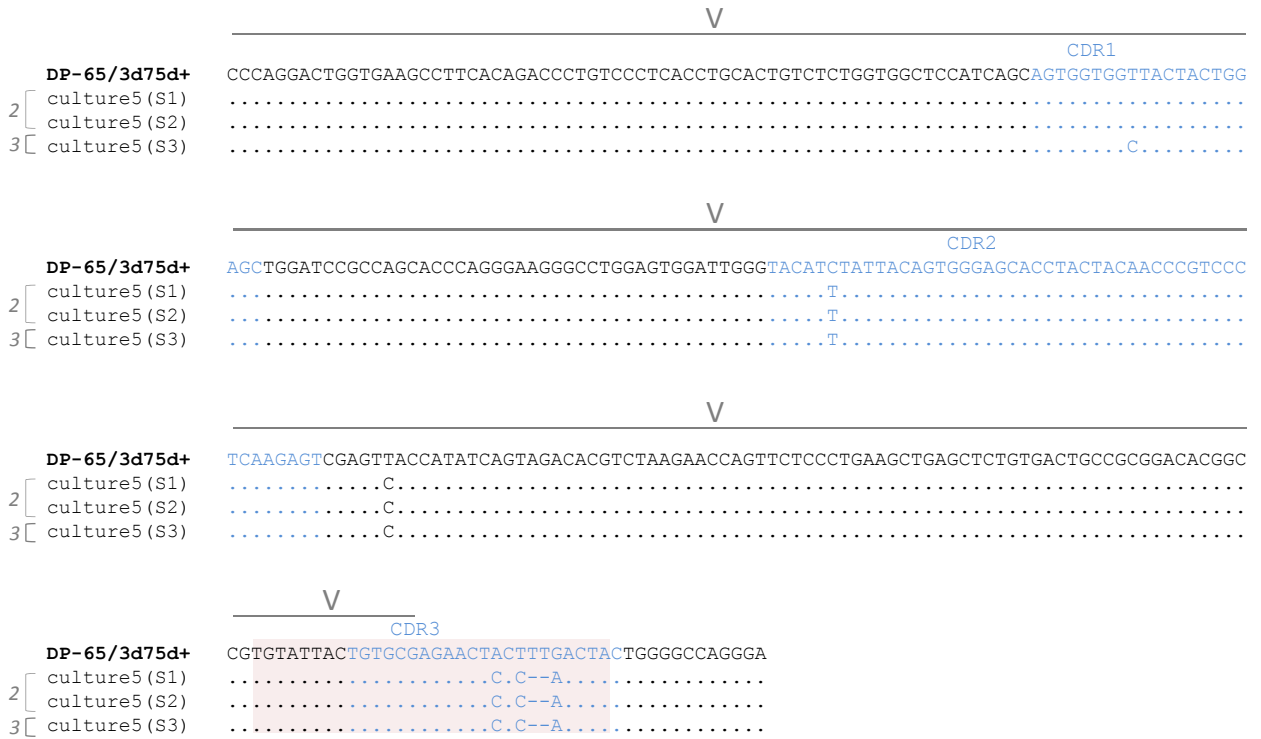


Figure 39. CN-LCL5 culture 5

CN-LCL5/c23 sequences are aligned relative to the matched germline V region sequence (top row). The location of the V region is indicated and the CDRs (1, 2 and 3) are highlighted in blue text. A box is drawn around the first 30 nucleotides of the VDJ junction translation.

CN-LCL5/c23 is an example of a culture containing both unmutated and mutated sequences. Since 2 out of 3 isolated sequences harbour <3 mutations, the culture was deemed unmutated, despite sequence 3 carrying 3 mutations.

pre-infection

sequence	V	D	J	junction translation	mutations
1	3d277d+	D5-5/DK4	JH4b	CAXDPDGYxP	0
2	DP-88/hv1051K...+	D4-17	JH6b	CARSPPGRV	0
3	DP-58/hv3d1EG	D5-12/DK1	JH4b	CAREETVAGV	0
4	DP-71/3d197d...+	D4-17	JH4b	CARAIQKDYG	0
5	DP-73/V5-51...+	D7-27/DHQ52	JH6c	CARWGPWYY	0
6	3-09 DP31/V3-9p	not found	JH4b		0
7	3-74 COS6	not found	JH6b		0
8	V3-49	not found	JH1		0
9	DP-65/3d75d...+	D5-24	JH6b	CARDRGGPNY	1
10	DP-50/hv3019b9	D4-17	JH2	CASNNDYGH	1
11	DP-14/V1-18+	D6-19	JH3b	CARDSHPDSS	1
12	4-31 DP65/3d75d	not found	JH6b		1
13	5-51 DP73/V5-51	not found	JH6b		1
14	b54../hv3005b54	D3-16	JH4b	CARYREGVGA	5

12 weeks

sequence	V	D	J	junction translation	mutations
1	4-b DP67	not found	JH5b	CATSGWYDAK	8
2	4-b DP67	not found	JH5b	CATSGWYDAK	8
3	4-b DP67	not found	JH5b	CATSGWYDAK	8
4	4-b DP67	not found	JH5b	CATSGWYDAK	9
5	4-b DP67	not found	JH5b	CATSGWYDAK	9
6	3-53 V3-53+	not found	JH4b	CARTGEFSFG	7
7	3-33 DP50	not found	JH4b	CARTGEFSFG	8
8	3-33 DP50	not found	JH4b	CARTGEFSFG	8
9	3-33 DP50	not found	JH4b	CARTGEFSFG	8
10	6-01 DP74	not found	JH6b	CARERLSSGW	0
11	3-33 DP50	not found	JH3b	CARDLERYD	1
12	3-74 COS-6	not found	JH6c	CATNLVGVYY	2
13	4-59 DP71	not found	JH6b	CAREAELRQL	4
14	3-21 DP77	not found	JH4b	CARAQDDSSG	6
15	3-21 DP77	not found	JH4b	CARAAGDYAH	8
16	4-59 DP71	not found	JH3b	CARGRITMVR	8
17	4-61 DP66	not found	JH6b	CAREHTVVV	9
18	3-21 DP77	not found	JH5b	CARGRVPAA	10

Table 23. BN-LCL6

Summary of matched V, D and J alignments for each IgH sequence analysed at 9 and 12 weeks post-establishment (0 and 6 weeks shown on previous page), the first 10 amino acids of the VDJ junction translation, and the number of mutations detected in the V region. Clonally related IgH sequences are colour highlighted (see legend).

seeding	culture	sequence	V	D	J	junction translation	mutations
1000 cells/well	1	1	3-11 DP35	not found	JH6b	CAREWGGYKP	0
		2	3-11 DP35	not found	JH6b	CAREWGGYKP	0
	2	1	3-23 DP47	D6-19	JH4b	CAKDR LAVAV	0
		2	3-23 DP47	D6-19	JH4b	CAKDR LAVAV	0
		3	3-23 DP47	not found	JH4b	CAKDR LAVAV	0
		4	3-23 DP47	not found	JH4b	CAKDR LAVAV	0
	3	1	4-59 DP71	not found	JH4b	CASGSSGWLY	7
		2	4-59 DP71	D5-12	JH4b	CASGSSGWLY	7
		3	4-59 DP71	D5-12	JH4b	CASGSSGWLY	7
	4	1	4-04 DP70	not found	JH3b	CARSITIFGV	0
		2	4-04 DP70	not found	JH3b	CARSITIFGV	0
		3	4-04 DP70	not found	JH3b	CARSITIFGV	1
5	1	1-08 DP15	D1-26	JH4b	CARGGYEGF	0	
	2	1-08 DP15	D4-17	JH4b	CARGGYEGF	0	
	3	1-08 DP15	D4-17	JH4b	CARGGYEGF	1	
6	1	1-69 DP10	not found	JH4b	CASASRDSSS	0	
	2	1-69 DP10	not found	JH4b	CASASRDSSS	1	
7	1	3-30 COS-8	D4-23	JH4b	CAREATEVPF	3	
	2	3-30 COS-8	D4-23	JH4b	CAREATEVPF	3	
	3	3-30 COS-8	D4-23	JH4b	CAREATEVPF	3	
8	1	DP58	not found	JH4b	CARDQGGVTT	0	
	2	DP58	not found	JH4b	CARDQGGVTT	0	
	3	DP58	not found	JH4b	CARDQGGVTT	0	
	4	DP58	not found	JH4b	CARDQGGVTT	2	
9	1	3-15 DP38	not found	JH4b	CTTDQWLSWE	0	
	2	3-15 DP38	not found	JH4b	CTTDQWLSWE	0	
	3	1e DP88	not found	JH4b	CARDSSSSWY	1	
10	1	3-23 DP47	not found	JH6c	CAKEWVGSGS	0	
	2	3-23 DP47	not found	JH6c	CAKEWVGSGS	0	
	3	3-23 DP47	not found	JH6c	CAKEWVGSGS	0	
	4	3-23 DP47	not found	JH6c	CAKEWVGSGS	0	
11	1	1-58 DP2	not found	JH5b	CAVELWFGDI	5	
	2	1-58 DP2	not found	JH5b	CAVELWFGDI	5	
	3	1-58 DP2	not found	JH5b	CAVELWFGDI	5	
12	1	DP67	not found	JH4b	CARTLVVVDWG	0	
	2	DP67	not found	JH4b	CARTLVVVDWG	0	
	3	DP67	not found	JH4b	CARTLVVVDWG	0	

Table 24. Naive LCL6 limiting dilution cultures

Blocks shaded grey represent unmutated cultures. Blocks shaded green represent mutated cultures. Green frames around grey blocks highlight instances where cultures contain unmutated and mutated sequences of the same CDR3 clonotype. Cultures were deemed mutated if the majority of sequences contained >2 mutations. Where cultures contained more than one distinct CDR3 clonotype, the mutation status of the family comprising the highest proportion of the culture is represented in the table.

seeding	culture	sequence	V	D	J	junction translation	mutations
1000 cells/well	13	1	1-08 DP15	not found	JH4b	CARGGDYEGF	0
		2	1-08 DP15	not found	JH4b	CARGGDYEGF	1
	14	1	3-74 COS6	not found	JH4b	CARTRITIFG	0
		2	3-74 COS6	not found	JH4b	CARTRITIFG	0
		3	3-74 COS6	not found	JH4b	CARTRITIFG	0
	16	1	5-51 DP73	not found	JH4b	CARQSFSGSYY	1
		2	5-51 DP73	not found	JH4b	CARQSFSGSYY	2
	17	1	4-30 DP65	D2-21	JH6b	CARVRLAGPL	1
		2	5-51 DP73	D6-19	JH5b	CARHEEAGEV	1
	18	1	DP58	D5-5	JH4b	CARDRSRDTA	0
		2	DP58	D5-5	JH4b	CARDRSRDTA	0
	19	1	3-21 DP77	D3-3	JH4b	CARMTTVTRL	0
		2	3-21 DP77	D4-17	JH6b	CVRAPWSGDY	5
	20	1	3-21 DP77	D1-26	JH4b	CAREELRGYWG	0
		2	1-69 DP10	D3-22	JH4b	CARNQDTSGS	3
	21	1	3-11 DP35	D4-17	JH6b	CARDYGDYGA	0
		2	1-08 DP15	D5-12	JH4b	CARVCVGNAA	0
	22	1	3-21 DP77	D5-12	JH4b	CARGDRGDTL	0
		2	3-21 DP77	D5-12	JH4b	CARGDRGDTL	3
	23	1	4-59 DP71	not found	JH4b	CARAPAITMV	0
		2	4-59 DP71	not found	JH4b	CARAPAITMV	0
		3	4-59 DP71	not found	JH4b	CARAPAITMV	1
	24	1	DP58	not found	JH4b	CAVLGSEYSD	9
		2	3-13 DP48	not found	JH6b	CARDNSRGDC	15
		3	3-13 DP48	not found	JH6b	CARDNSRGDC	15
		4	3-13 DP48	not found	JH6b	CARDNSRGDC	16
	25	1	4-04 DP70	not found	JH4b	CARGRFEEDY	4
		2	4-04 DP70	not found	JH4b	CARGRFEEDY	4
3		4-04 DP70	not found	JH4b	CARGRFEEDY	6	

Table 24. Naive LCL6 limiting dilution cultures

Blocks shaded grey represent unmutated cultures. Blocks shaded green represent mutated cultures. Green frames around grey blocks highlight instances where cultures contain unmutated and mutated sequences of the same CDR3 clonotype. Cultures were deemed mutated if the majority of sequences contained >2 mutations. Where cultures contained more than one distinct CDR3 clonotype, the mutation status of the family comprising the highest proportion of the culture is represented in the table.

those generated in the first limiting dilution experiment (CN-LCL5 cultures), both in terms of clonality and proportion of mutated cultures and/or clonal families.

Of the 25 cultures examined (Table 24), 19 were monoclonal and the remaining 6 were presumably biclonal. 24% of the cultures were scored as having mutated IgH sequences. When accounting for the two families detected in the biclonal cultures, it was calculated that 26% of the total number of distinct clonal families identified in the experiment were mutated. In those families that were comprised of mutated IgH sequences, the mutations were shared and “family-specific”. Two instances where 2 or more mutations had been acquired by an IgH sequence in addition to the family-specific mutation pattern were observed in cultures 22 and 25 (data not shown), suggesting ongoing SHM within the culture.

Taken together, the analysis of the limiting dilution LCL cultures from both experiments have confirmed the earlier findings of Dr Pastor and Dr Chaganti that approximately one quarter of established cultures are mutated at twelve weeks post-infection. Furthermore, this observation of IgH mutation in naive B cells is seen in both bulk LCLs and LCLs established by limiting dilution.

4.2.7 Phenotype of Naive LCLs

The data presented so far from the IgH sequence analysis of both bulk and limiting dilution LCL cultures revealed that a substantial proportion of IgH sequences were mutated as early as six weeks post-infection. These results demonstrate that EBV-driven transformation of naive B cells *in vitro* has the capacity to induce a memory IgH genotype within a fraction of the infected cells. In order to find out whether EBV transformation could also induce a memory

phenotype via class switching, selected clonal and bulk LCLs were examined for Ig isotype expression by flow cytometry. Expression of IgM, IgD, IgG, and IgA, together with expression of the memory B cell marker CD27 was analysed.

The staining procedure was first validated using CD19-selected PB B cells (Figure 39a). Using the FIX & PERM[®] (CALTAG) protocol for intracellular and surface Ig staining, 63% of the B cells were IgD⁺ and 68% were IgM⁺, consistent with a naive or non-switched memory B cell phenotype. 16% of the B cells were IgG⁺ and 10% were IgA⁺, both of which represent switched memory B cells. Whereas these percentages are consistent with the expected proportions of B cell subsets within the PB B cell compartments, only 12% of the total B cells stained positive for the memory marker CD27, a result that could reflect weak staining with the anti-CD27 antibody. Ig isotype analysis of 7 bulk naive LCL cultures (BN-LCL1, BN-LCL3, BN-LCL4a-c, BN-LCL5 and BN-LCL6) revealed dual expression of IgD and IgM, with the absence of IgG or IgA, indicating that the cells had not undergone CSR. Two examples (BN-LCL3 and BN-LCL5) of flow cytometry staining analysis can be seen in Figure 39b and c, and results from all 7 bulk LCLs are summarised in Table 25.

We then went on to analyse Ig isotype expression in a selection of limiting dilution LCL cultures with either unmutated or mutated IgH sequences (obtained from CN-LCL5 and CN-LCL6 experiments). As with the bulk cultures, all 37 LCLs tested expressed IgD and IgM in the absence of the memory markers IgG or IgA. CD27 was expressed in either very low cell numbers (1%) or not at all. Staining of representative mutated (CN-LCL5/c13) and unmutated (CN-LCL5/c20) LCL cultures are shown in Figure 40, and all the results are summarised in Table 26.

Figure 39. Phenotypic analysis of BN-LCL3 and BN-LCL5

A. A control for the FIX & PERM[®] intracellular staining protocol was carried out using CD19-selected PB B cells. 63% of the B cells were IgD⁺ and 68% were IgM⁺, consistent with a naive or non-switched memory B cell phenotype. 16% were IgG⁺ and 10% were IgA⁺, consistent with a switched memory phenotype. Only 3% of cells were CD27⁺ using this protocol. **B.** and **C.** Using intracellular staining, both LCLs expressed IgM and IgD, in the absence of IgG, IgA or CD27. Note: for each of the cell populations shown in **A**, **B** and **C**, distinct isotype controls (black outline), using cells from the relevant culture were used to draw gates.

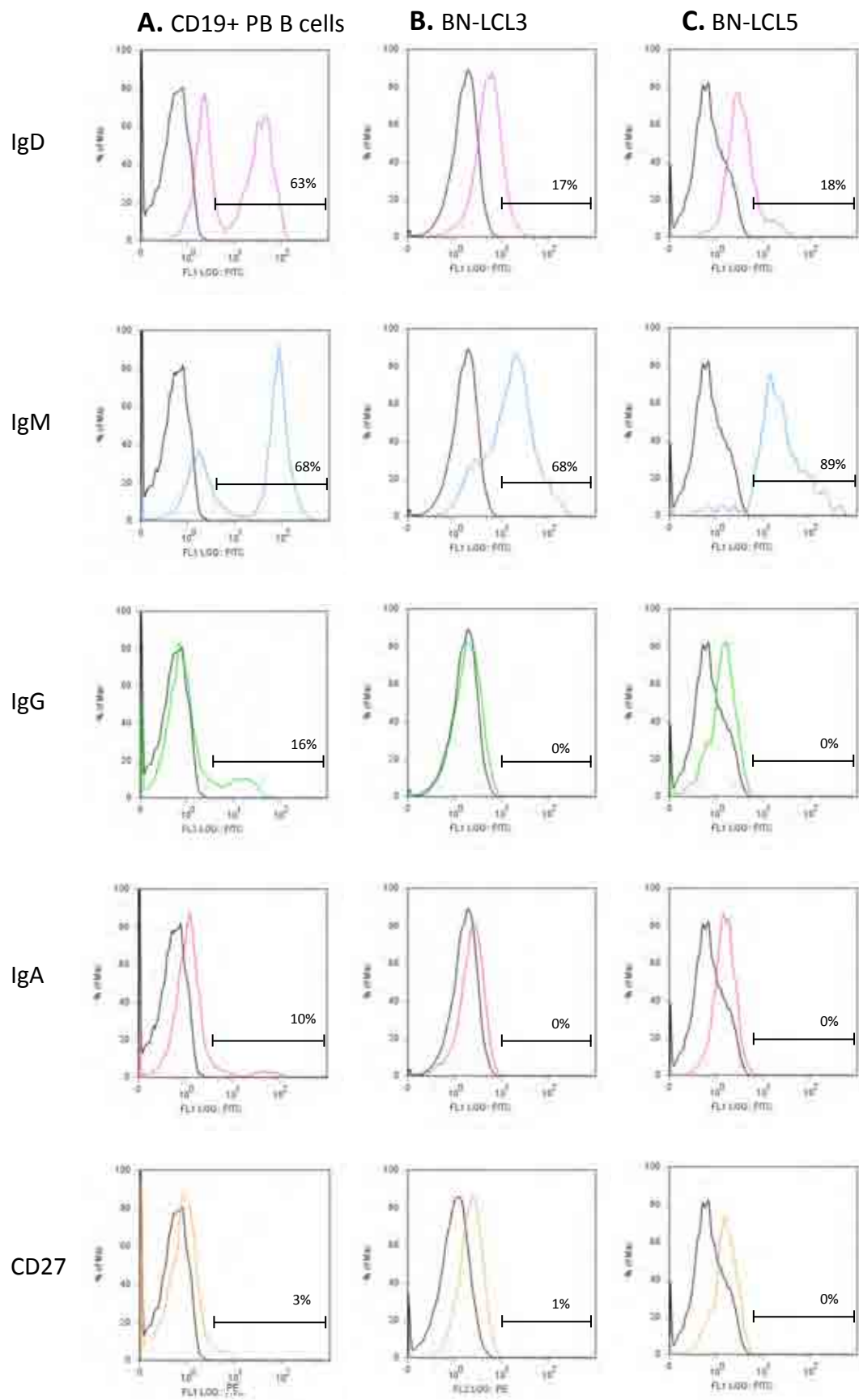


Figure 39. Phenotypic analysis of BN-LCL3 and BN-LCL5

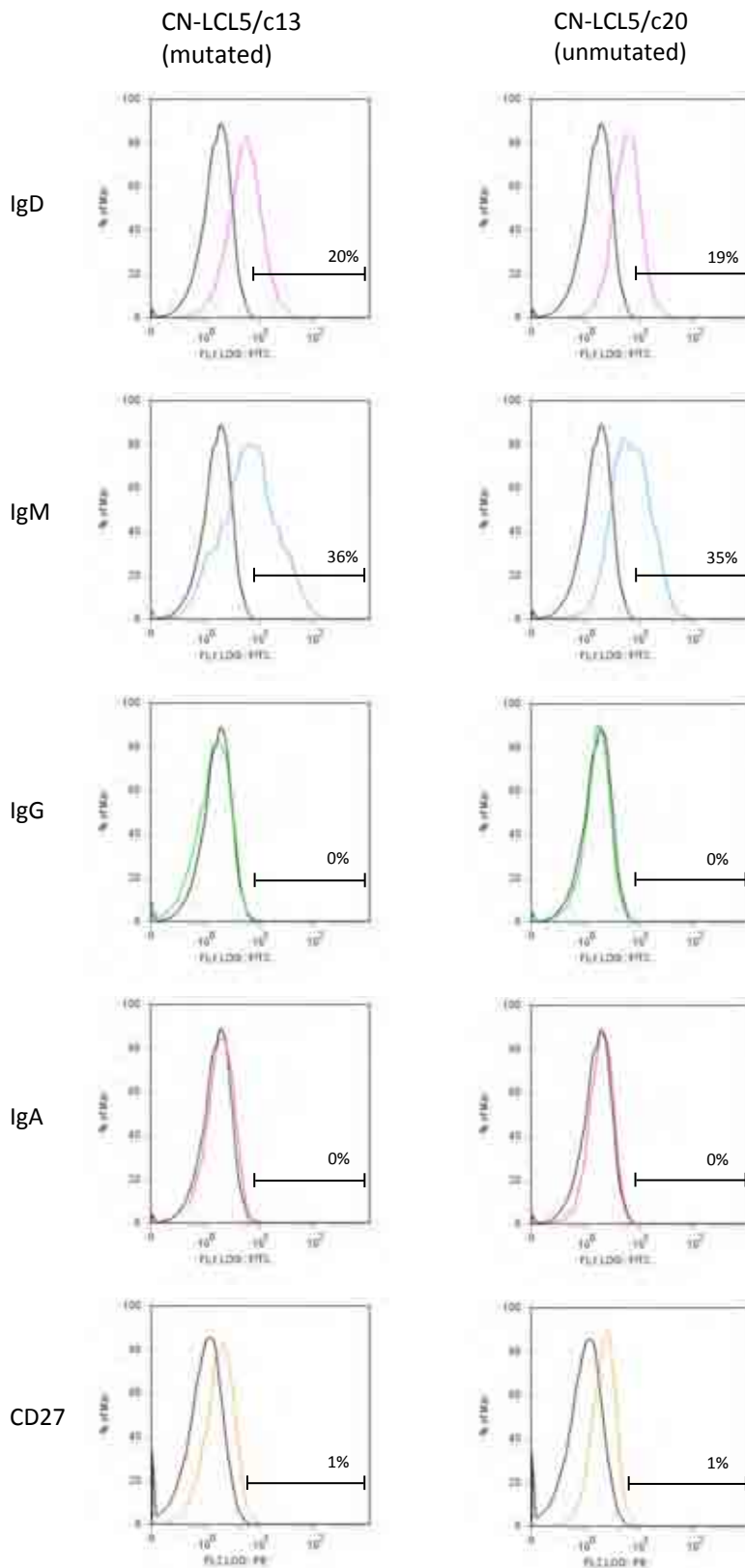


Figure 40. Phenotypic analysis of two representative CN-LCL5 cultures

Shown are examples of fix and perm staining for IgM, IgD, IgG, IgA and CD27 carried out on the CN-LCL5/c13 culture, which carried mutated IgH sequences and the CN-LCL5/c20 culture, which carried unmutated IgH sequences. Both LCL cultures expressed both IgM and IgD in the absence of IgG or IgA. CD27 was expressed by a small percentage of cells.

LCL	Phenotype				
	<u>IgM</u>	<u>IgD</u>	<u>IgG</u>	<u>IgA</u>	<u>CD27</u>
BN-LCL1	+	+	-	-	-
BN-LCL3	+	+	-	-	-
BN-LCL4a	+	+	-	-	-
BN-LCL4b	+	+	-	-	-
BN-LCL4c	+	+	-	-	-
BN-LCL5	+	+	-	-	-
BN-LCL6	+	+	-	-	-

Table 25. Summary of Ig phenotypes of PB bulk naive LCLs

All bulk naive LCLs remained IgM+IgD+IgG-IgA-CD27-, consistent with a naive B cell phenotype.

	IgM	IgD	IgA	IgG	CD27
unmutated LCL cultures	26	26	0	0	0
mutated LCL cultures	11	11	0	0	0

Table 26. Summary of Ig phenotype of PB limiting dilution naive LCLs

All LCL cultures generated by limiting dilution infection remained IgM+IgD+IgG-IgA-CD27-, consistent with a naive B cell phenotype.

Together these findings indicate that although EBV infection of naive B cells *in vitro* can confer genotypic changes consistent with differentiation to memory, no CSR was observed since the cells remained phenotypically naive.

4.3 Transformation Assays Comparing EBV Infection of Peripheral Blood B cell Subsets

Experiments from the previous section strongly suggest that a proportion of naive B cells infected with EBV *in vitro* can acquire IgH mutations in culture. Since mutated IgH genotypes are typically associated with switched or non-switched memory B cells *in vivo*, it was imperative to show that these results did not simply reflect the preferential transformation of small numbers of contaminating memory cells within the initial naive B cell preparations.

The earlier Ig isotype staining data showed that all LCLs derived from naive B cells co-expressed IgM/IgD, consistent with a naive B cell origin. If any of these LCLs had been derived from a switched memory B cell, this would have been identifiable by detection of IgG or IgA expression in the culture. It does, however, remain possible that these mutated IgH sequences were derived from IgM+IgD+ non-switched memory B cells carrying pre-mutated IgH sequences, which grew out preferentially *in vitro* during the transformation. To address this possibility, transformation assays were used to compare the transformation efficiency of naive B cells and non-switched memory B cells *in vitro*. Both subpopulations were sorted to high purity, infected with B95-8 supernatant at various MOIs, and seeded into 96-well plates in equal numbers (800-1000 cells per well). The number of wells showing LCL outgrowth were then counted after six weeks.

Results from five experiments using B cells from different donors are shown in Figure 41. Note that in each transformation assay a range of MOIs was used (between 50 and 1). From this figure, a number of conclusions can be drawn. The most notable observation is that the transformation efficiency of the cells varied greatly between each donor. This can be seen by focussing on the percentage of transformed wells at an MOI of 12.5 in each assay. TA-3 shows the highest proportion of transformed wells (82%), whereas values for the other donors range from 2% to 67%. This large range of values most likely represents variation between different individuals. Nonetheless there were no reproducible differences in transformation efficiency between the two B cell subsets in any of the five donors tested. The most pronounced difference between the two B cell subsets can be seen in TA-1, where the percentage of transformed wells containing naive B cells was more than twice that of non-switched memory B cells at each MOI tested. In the other donors, however, differences in transformation efficiency were less than two-fold (Figure 41).

4.4 Tonsillar Naïve B Cell Transformation

All previous transformation experiments presented so far have used naive B cells isolated from PB. The next two experiments aimed to determine whether similar observations could be found when using B cells from two other sources, namely tonsil and cord blood (see below). First a bulk tonsillar naive B cell infection (BTN-LCL1) was carried out using IgD+CD27- tonsillar B cells purified by FACS using the same method as previously described for the *ex vivo* EBV load experiments (Figure 15).

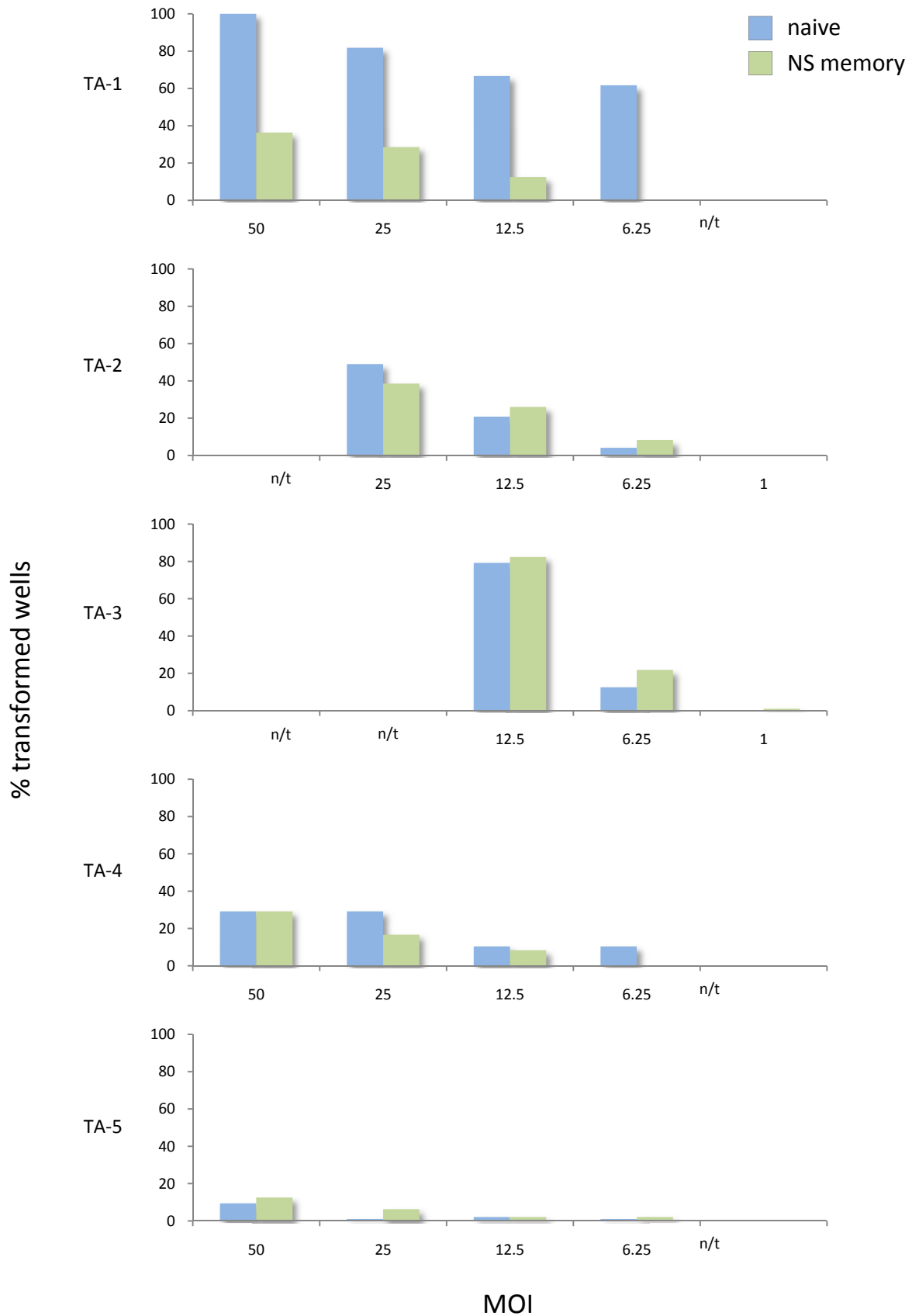


Figure 41. Transformation assays using different B cell subsets

MOI values are shown on the x axis, and the percentage of transformed wells are shown on the y axis (n/t = not tested). Results from 5 separate donors show no consistent difference between naive B cells and non-switched memory B cells in terms of transformation efficiency *in vitro*.

Twenty-four out of 26 IgH sequences analysed from the resting naive B cell sample were unmutated, confirming the purity of the sorted population. All sequences contained individual VDJ recombinations and CDR3 regions, indicating the cell population was polyclonal (Table 27). At six weeks post-infection, most IgH sequences analysed remained clonally unique, although 2 sequences from the same clonal family were detected. At nine and twelve weeks post-infection, small numbers of IgH sequence from multiple clonal families were detected, but the clonally independent sequences persisted in the culture in significant numbers (6 out of 14 IgH sequences at nine weeks, and 7 out of 21 at twelve weeks) (Table 27).

When examining the mutation levels of the IgH sequences generated from the BTN-LCL1 culture, three observations were noted: (i) all sequences isolated from families 1, 3, 4, 7, 8, and 9 were unmutated regardless of time post-infection, (ii) families 5 and 6 were comprised of mutated IgH sequences carrying identical, family-specific mutations, (iii) all sequences identified from family 2 were mutated, carrying 3 family-specific mutations (Figure 42). In addition, increasing numbers of mutated IgH sequences were identified within the clonally unique populations as the culture aged.

The proportion of mutated and non-mutated clonal families detected at each time point is shown in Figure 43. An increase in mutated IgH sequences from 8% prior to infection, to 23% at 6 weeks post-infection, 27% at nine weeks and 37% at twelve weeks was observed. Together these results present a similar scenario to that seen in bulk peripheral blood naive B cell infections, i.e. the outgrowth of clonal families, and an increase in proportion of mutated IgH sequences from six weeks post-infection onwards.

resting tonsillar naive B cells

sequence	V	D	J	junction translation	mutations
1	DP-2/V71-5+	D4-b	JH5b	CARDVDIVVV	0
2	DP-10/hv1051...+	D1-1	JH6c	CARRSPGTTAS	0
3	DP-14/V1-18+	D5-5/DK4	JH6c	CARGPQGYAH	0
4	DP-78/3d230d...+	D5-12/DK1	JH4b	CARWTGYSGY	0
5	DP-31/V3-9P...+	D3-10/DXP'1	JH4b	CAKTYYYGSG	0
6	DP-65/3d75d...+	D4	JH6b	CARVVGICST	0
7	DP-46/3d216...+	D3-22/D21-9	JH6b	CARDYDSSGR	0
8	DP-71/3d197d...+	D5-12/DK1	JH5b	CARADGYLGN	0
9	DP-47/V3-23...+	D2-8/DLR1	JH6c	CAKTPYYMDV	0
10	DP-35/V3-11...+	D2-21	JH6b	CACDWNPHYG	0
11	DP-73/V5-51...+	not found	JH6c	CARRHYYYM	0
12	DP-46/3d216...+	D3-10/DXP'1	JH4b	CAREALWFGE	0
13	DP-54/V3-7...+	D4-17	JH3b	CAKDGPHFGG	0
14	DP-78/3d230d...+	D6-6/DN4	JH2	CAREYSSSEF	0
15	DP-48/13-2+	D1-7/DM1	JH2	CARAIRGTNW	0
16	DP-48/13-2+	D6-6/DN4	JH2	CARVKWLGYF	0
17	DP-46/3d216...+	D5-12/DK1	JH3a	CARGGAILVW	0
18	DP-46/3d216...+	not found	JH6c	CARVTGHYYD	0
19	DP-79/4d154...+	D3-3/DXP4	JH5b	CARRFELNYD	1
20	DP-46/3d216...+	D6-19	JH6b	CAKDQRAAAY	1
21	DP-31/V3-9P...+	not found	JH6c	CSCDMDVWVK	1
22	4.3	D6-19	JH5b	CARDLAVAGV	1
23	DP-70/4d68...+	D6-25	JH4b	CARHLAGGSW	1
24	DP-49/1.9III...+	D5-24	JH4b	CARDRRWLQL	2
25	DP-79/4d154...+	D4-11/DA1	JH5b	CARGDNSNYG	4
26	DP-65/3d75d...+	D4-17	JH6c	CARARQYGDH	15

6 weeks

sequence	V	D	J	junction translation	mutations
1	DP-46/3d216...+	D4-11/DA1	JH4b	CATDFDWSYY	0
2	DP-46/3d216...+	D4-11/DA1	JH4b	CATDFDWSYY	0
3	DP-79/4d154...+	D5-24	JH4b	CARHTRMATI	3
4	DP-71/3d197d...+	D2-15/D2	JH5b	CARERCSGGS	0
5	DP-73/V5-51...+	D3-22/D21-9	JH3b	CARPYDSTV	0
6	DP-78/3d230d...+	D3-22/D21-9	JH6b	CARDGKxYYG	0
7	DP-73/V5-51...+	not found	JH6b	CARRGAESNY	0
8	DP-71/3d197d...+	D1-26	JH4b	CASYSGSYYY	0
9	DP-7/21-2...+	D7-27/DHQ52	JH6b	CARSERRGIS	0
10	DP-73/V5-51...+	D6-6/DN4	JH4b	CARREPYSSS	0
11	DP-46/3d216...+	D2-21	JH6c	CARALTTHSV	2
12	DP-65/3d75d...+	D5-5/DK4	JH2	CASRYNYGYG	2
13	DP-70/4d68...+	D2-15/D2	JH4b	CARFDCSGGS	6
14	DP-77/WHG16+	D1-26	JH6b	CARDRGSHTK	7

- family 1
- family 2
- family 3
- family 4
- family 5
- family 6
- family 7
- family 8
- family 9

Table 27. BTN-LCL1

Summary of matched V, D and J alignments for each IgH sequence analysed at 0 and 6 weeks post-establishment (9 and 12 weeks shown on previous page), the first 10 amino acids of the VDJ junction translation, and the number of mutations detected in the V region. Clonally related IgH sequences are colour highlighted (see legend).

9 weeks

sequence	V	D	J	junction translation	mutations
1	DP-46/3d216...+	D4-11/DA1	JH4b	CATDFDWSYY	0
2	DP-46/3d216...+	D4-11/DA1	JH4b	CATDFDWSYY	0
3	DP50/hv3019b9...+	D3-22/D21-9...+	JH4b	CARDYYDSSG	1
4	DP-50/hv3019b9...+	D3-22/D21-9...+	JH4b	CARDYYDSSG	1
5	DP-50/hv3019b9...+	D3-22/D21-9...+	JH4b	CARDYYDSSG	1
6	DP-78/3d230d...+	D2-2	JH5b	CARGELGYCI	2
7	DP-51+	D6-19	JH2	CAREIGAVAA	6
8	DP-79/4d154...+	D1-7/DM1	JH1	CASSMGRPSI	8
9	DP-31/V3-9P...+	D6-6/DN4	JH4b	CTKARSRTYF	0
10	DP-73/V5-51...+	D2-15/D2	JH4b	CARLGTDPDIV	0
11	DP-15/V1-8+	not found	JH6c	CARGHRLVE	0
12	DP-2/V71-5+	D3-16	JH6b	CAADFTFGGV	0
13	DP-77/WHG16+	D6-19	JH6b	CASSGWYVRY	1
14	b13../hv3019b13	D3-10/DXP'1	JH6c	CAKDGYGSGS	8

12 weeks

sequence	V	D	J	junction translation	mutations
1	DP-10/hv1051...+	D3-22/D21-9...+	JH5b	CAIMYYYDSS	0
2	DP-10/hv1051...+	D3-22/D21-9...+	JH5b	CAIMYYYDSS	0
3	DP-71/3d197d...+	not found	JH4b	CASTRWGVTP	1
4	DP-71/3d197d...+	not found	JH4b	CASTRWGVTP	1
5	DP-64/3d216d+	D6-19	JH2	CARGQAVAGS	1
6	DP-64/3d216d+	D6-19	JH2	CARGQAVAGS	1
7	DP-50/hv3019b9...+	D3-22/D21-9...+	JH4b	CARDYYDSSG	1
8	DP-78/3d230d...+	D2-2	JH5b	CARGELGYCI	2
9	DP-78/3d230d...+	D2-2	JH5b	CARGELGYCI	2
10	DP-79/4d154...+	D5-24	JH4b	CARHTRMATI	3
11	DP-79/4d154...+	D5-24	JH4b	CARHTRMATI	3
12	DP-51+	D6-19	JH2	CAREIGAVAA	6
13	DP-79/4d154...+	D1-7/DM1	JH1	CTSSMGRPSI	8
14	DP-79/4d154...+	D1-7/DM1	JH1	CASSMGRPSI	8
15	DP-79/4d154...+	D6-19	JH4b	CASRGYSSGW	0
16	DP-73/V5-51...+	not found	JH6b	CARAYGDYDY	0
17	DP-54/V3-7...+	D4	JH4b	CARGYCISTS	0
18	DP-46/3d216...+	not found	JH4b	CARDRPSRTL	2
19	DP-78/3d230d...+	D2-21	JH3b	CARHLYYYDA	3
20	DP-51+	D3-10/DXP'1	JH4b	CARVSFNNGY	4
21	DP-46/3d216...+	D6-19	JH4b	CARASSGWYD	5

- family 1
- family 2
- family 3
- family 4
- family 5
- family 6
- family 7
- family 8
- family 9

Table 27. BTN-LCL1

Summary of matched V, D and J alignments for each IgH sequence analysed at 9 and 12 weeks post-establishment (0 and 6 weeks shown on previous page), the first 10 amino acids of the VDJ junction translation, and the number of mutations detected in the V region. Clonally related IgH sequences are colour highlighted (see legend).

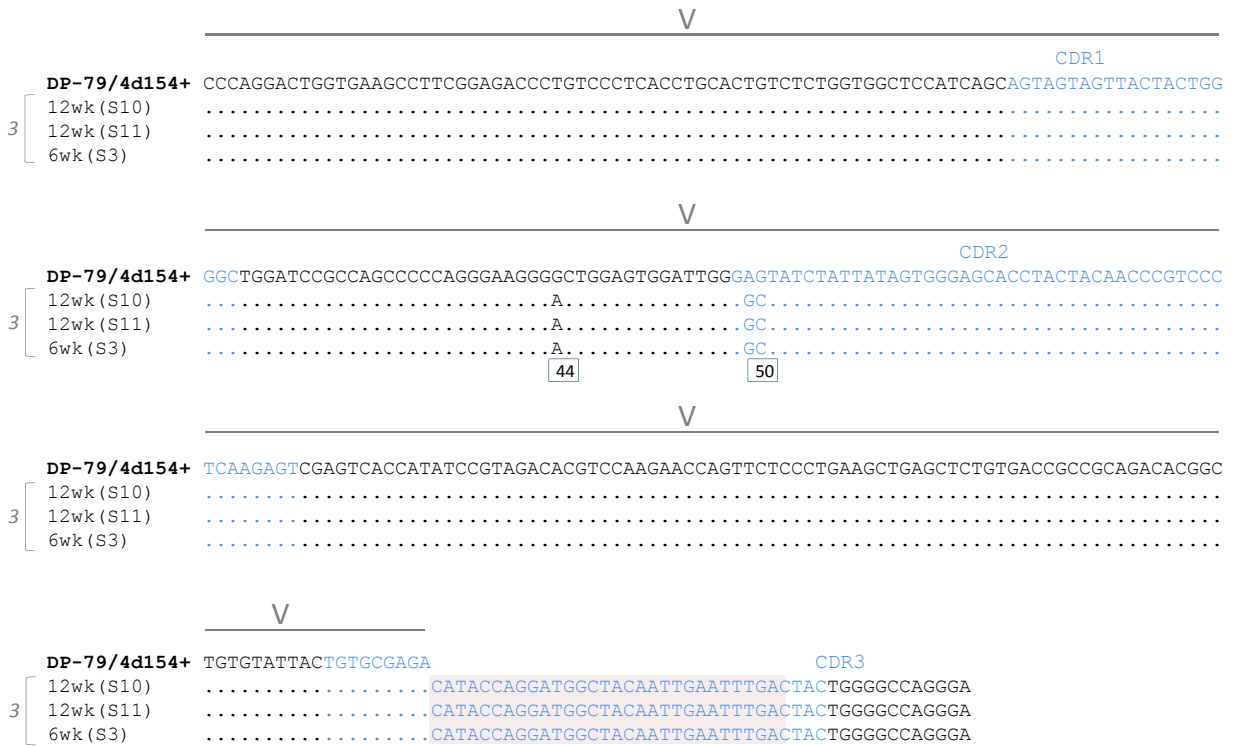


Figure 42. BTN-LCL1 family 2 mutation distribution

BTN-LCL1 family 2 sequences aligned relative to the matched germline V region sequence (top row). The location of the V region is indicated and the CDRs (1, 2 and 3) are highlighted in blue text. A box is drawn around the first 30 nucleotides of the VDJ junction translation. All sequences isolated from family 2 carried 3 identical mutations; 1 at codon 44 and 2 at codon 50.

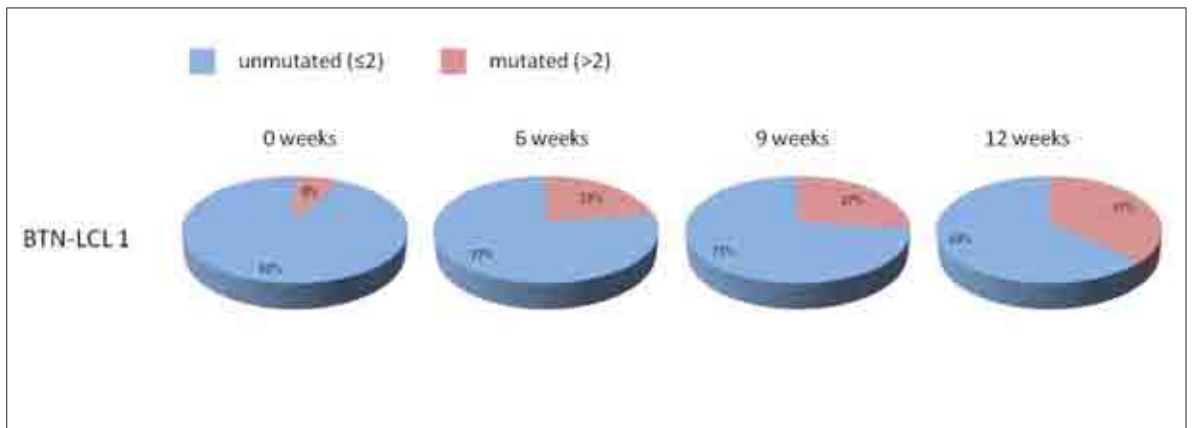


Figure 43. Percentage of mutated and unmutated clonal families in tonsillar naive LCLs over time

The pie charts show the proportion of clonal families yielding predominantly mutated IgH sequences (pink segment) compared to the proportion of clonal families yielding predominantly unmutated IgH sequences (blue segments). Percentage values are indicated within the segments. Data from 0, 6, 9 and 12 weeks are shown. Together these results show an increase in the proportion of clonal families containing IgH mutations over time.

4.4.1 Phenotype of the Bulk Tonsillar Naive LCL

As with the peripheral blood naive LCLs, the LCLs generated from naive tonsillar B cells contained a proportion of IgH sequences (up to 37%) exhibiting a mutated IgV genotype consistent with memory B cells. In order to determine whether EBV infection resulted in Ig class switching, the Ig isotype of the BTN-LCL1 culture was determined using fluorochrome-conjugated antibodies against IgM, IgD, IgG, IgA and CD27. Figure 44 shows that BTN-LCL1 expressed IgM and IgD, but not IgG, IgA or CD27, consistent with a naive B cell phenotype. This data indicates that *in vitro* infection of tonsillar naive B cells with EBV did not induce CSR in the cells, and supports the view that the IgH sequencing results reflect naive B cells that have acquired IgH mutations *in vitro*.

4.5 Umbilical Cord B cell Transformation

In order to examine the effects of *in vitro* EBV transformation in a non-adult B cell population (presumed to contain almost exclusively naive B cells), a final series of transformation experiments, cord blood LCLs (BCB-LCL1 and BCB-LCL2) were established by infecting total cord blood lymphocytes. In this cases, cyclosporine A was added to the culture in order to prevent T cell-mediated B cell killing. Following EBV infection, cells were harvested at various time points for IgH analysis.

4.5.1 Bulk Cord Blood LCL1

Twelve out of 14 IgH sequences generated from the uninfected cord blood lymphocytes were unmutated, and as expected each sequence was clonally unique. Interestingly, 2 mutated IgH sequences were also detected in the resting cell population. It has recently been reported that the majority of CB B

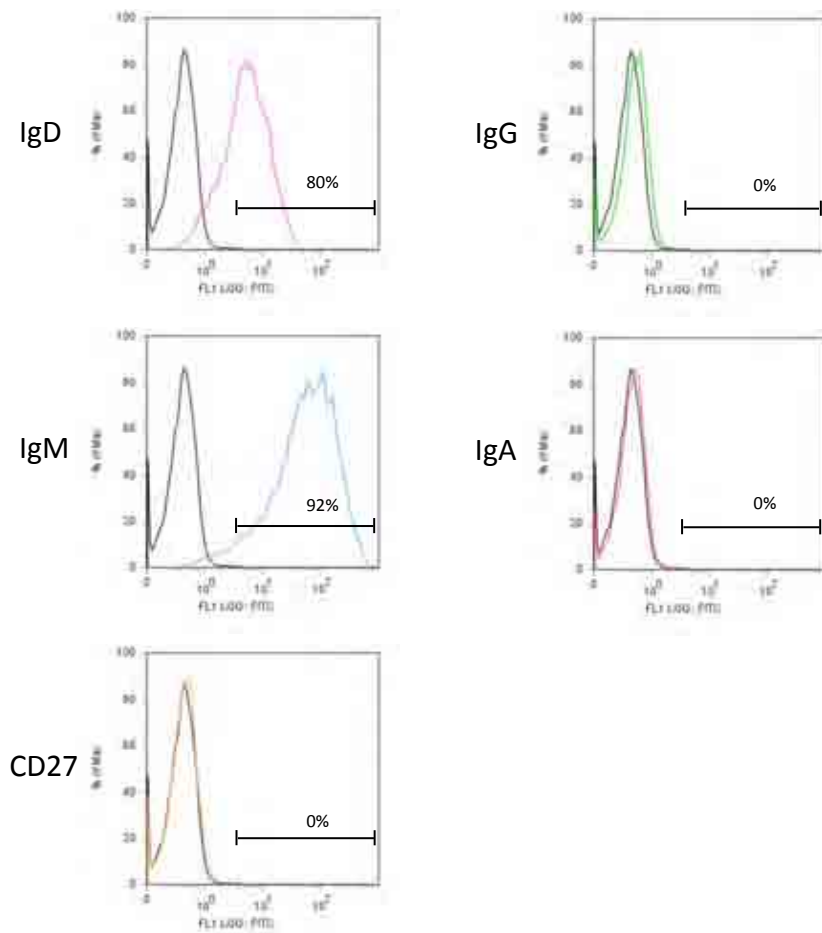


Figure 44. BTN-LCL1 phenotype

Intracellular staining for IgM, IgD, IgG, IgA and CD27 was carried out on BTN-LCL1. The culture expressed both IgM and IgD in the absence of IgG, IgA or CD27.

cells are phenotypically naive (Ha et al., 2008), however in one study a low proportion of CD27+ B cells was described (Ha et al., 2008), and other studies have shown the existence of rare non-switched memory B cells carrying mutated Ig genes (Weill et al., 2009, Scheeren et al., 2008). It is therefore feasible that the 2 mutated IgH sequences are examples of this small proportion of cells. At two weeks post-infection, 2 of 17 IgH sequences were mutated, but the cultures remained polyclonal. At ten weeks, 4 distinct clonal families were detected, yet 16 out of 26 sequences were still unique. All sequences at this last time point were unmutated (Table 28).

4.5.2 Bulk Cord Blood LCL2

The pre-infection data showed that 22 out of 23 IgH sequences analysed were unmutated, and the population was polyclonal (Table 29). By six weeks post-infection, 6 clonal families were detected, and only 3 of 20 IgH sequences were clonally unique. At this time point, all sequences were unmutated except for those identified as family 4, each of which carried the same 3 mutations. At fourteen weeks post-infection, small numbers of sequences from multiple clonal families were identified. The dominant families detected at six weeks (families 1-6) had largely been replaced by different families (7-9), suggesting a shift in outgrowth of distinct clonal families occurred between six and fourteen weeks post-infection. All IgH sequences analysed from the fourteen week time point were unmutated.

Taken together, the data from BCB-LCL1 and BCB-LCL2 show preferential clonal outgrowth within the culture occurring by six weeks post-infection. These results are consistent with EBV infection of both peripheral blood naive B cells

resting CB lymphocytes	sequence	V	D	J	junction translation	mutations
	1	DP-74/VH-V1...+	not found	JH6c	GLLLLLHGRL	0
	2	DP-74/VH-VI...+	not found	not found	CAREF	0
	3	DP-47	D4	JH6c	not found	0
	4	DP-47/V3-23...+	D3-3/DXP4	JH4b	CAKGSYDFW	0
	5	DP-47/V3-23...+	D6-19	JH6c	CAKGQSGYSS	0
	6	DP-65/3d75d	D3-10/DXP1	JH5b	CARVKWFGEL	0
	7	DP-47/V3-3...+		JH6b	CAKGRLLNHG	0
	8	DP-35/V3-11...+	D7-27/DHQ52	JH6b	CAREPLSGSS	1
	9	DP-25/VI-3b+	D3-10/DXP1	JH3b	CATGSGSYD	1
	10	DP-71/3d197d....+	D4	JH6b	CARALGYCSS	1
	11	p1	D4	JH3b	not found	2
	12	DP-48/13-2+	D6-13/DN1	JH4b	CARDSWF*QQ	2
	13	DP-15/VI-8+	D4-23	JH2	CARGREGGNS	3
	14	DP-58/hv3d1EG	D4	JH4b	CARDWGSSSW	4

2 weeks	sequence	V	D	J	junction translation	mutations
	1	DP-10/V1	D6-6	JH6c	CAKAQLLSKI	0
	2	DP-7/V1	D6-13	JH5b	CARAGPDMGW	0
	3	DP-38/V3	not found	not found	CTTVAARGYW	0
	4	hv3005/V3	D4-17	JH3b	CARESEFGDYA	0
	5	V1-4/V7	D1-26	JH6c	CARASTVNY	0
	6	DP-10/V1	D1-26	JH6b	CARDPTVIVG	0
	7	DP-71/V4	D6-6	JH4b	CARLSSSSSN	0
	8	DP-47/V3	D4-11	JH6b	CAKDVWSVTY	1
	9	DP-71/V4	D5-5	JH4b	CARVPRPTGW	1
	10	DP-75/V1	D7-27	JH6c	CARGKGPTRG	1
	11	VH5	D3-10	JH5b	CARLGVVQGV	1
	12	DP-75/V1	D6-6	JH4b	CARDSSSSFD	1
	13	DP-2/V1	not found	JH3b	CAASPQTYKE	1
	14	DP-25/V1	D4-17	JH3b	CARAGSSETT	1
	15	DP-31/V3	D1-26	JH3b	CAKVRGRGH	1
	16	DP-15	D1-26	JH2	CARDLGASNW	2
	17	V3-48	D3-22	JH2	CAKDGYYDSS	3

10 weeks	sequence	V	D	J	junction translation	mutations
	1	DP-58/hv3d1EG	D6-13	JH6c	CARVSAAGHY	0
	2	DP-58/hv3d1EG	D6-13	JH6c	CARVSAAGHY	0
	3	DP-58	D6-13	JH6c	CARVSAAGHY	0
	4	V3-53+	D3-3	JH3b	CARSRRGYA	0
	5	V3-53+	D3-3	JH3b	CARSRRGYA	0
	6	COS-6/DA-8.....+	D6-6/DN4	JH5a	CARVARSSFD	0
	7	COS-6/DA-8.....+	D6-6/DN4	JH4b	CARVARSSFD	0
	8	COS-6/DA-8.....+	D6-6/DN4	JH4b	CARVARSSFD	1
	9	V3-49+	D7-27/DHQ52	JH4b	CTRDTDPVGI	1
	10	V3-49+	D7-27/DHQ52	JH4b	CTRDTDPVGI	1
	11	DP-77/WHG16+	D3-22/D21-9	JH6b	CARDHPYDSS	0
	12	DP-77/WHG16+	not found	JH1	not found	0
	13	DP-10/Hv1051...+	D3-3/DXP4	JH4b	CATGGNITIF	0
	14	COS-6/DA-8.....+	D4	JH4b	CARDGRGIL*	0
	15	DP-77/WHG16+	not found	not found	CARDPVVPA	0
	16	DP-25/VI-3b+	D3-3/DXP4	JH5b	CARVSEGYD	0
	17	DP-71/3d197d....+	D4	JH6c	CARYLNEDIV	0
	18	V3-53+	D4-b	JH6c	AVREFFLH**	0
	19	DP-71/V4	D6-19	JH2	CARDLHSSGW	0
	20	VH32Sanz+	D3-9	JH6c	CARVSEAMT	0
	21	DP-71/V4	D4	JH3b	CARDLGYCSS	0
	22	V3-21+		JH6c	CARGGSDYYY	0
	23	YAC-9/V3	D7-27	JH4b	CTSRILTGDS	0
	24	VI-4.1b+	D7-27	JH6c	CARLPLLNWG	0
	25	DP-73/V5	D6-19	JH4b	CARLEEAVAG	1
	26	DP-15/V1	D2-8	JH4b	CARGLGDFDY	2

	family 1
	family 2
	family 3
	family 4

Table 28. BCB-LCL1

Summary of matched V, D and J alignments for each IgH sequence analysed at 0, 2 and 10 weeks post-establishment, the first 10 amino acids of the VDJ junction translation, and the number of mutations detected in the V region. Clonally related IgH sequences are colour highlighted (see legend).

resting CB lymphocytes	sequence	V	D	J	junction translation	mutations
	1	DP-79/4d154...+	D1-26	JH4b	CARRRSGSYF	0
	2	DP-10/hv1051...+	D5-5/DK4	JH4b	CAGGQSGYSY	0
	3	DP-73/V5-51...+	D3-22/D21-9	JH4b	CARNDSSGYY	0
	4	DP-58/hv3d1EG	D2-15/D2	JH6c	CARDDSSGPY	0
	5	DP-71/3d197d...+	D6-6/DN4	JH4b	CARDGSSSFD	0
	6	VH32Sanz+	D4	JH3a	CARRPVVPA	0
	7	DP-77/WHG16+	D7-27/DHQ52	JH4b	CARGGSFLRG	0
	8	DP-38/9-1...+	D6-13/DN1	JH6b	CTTDPNSSSW	0
	9	DP-71/3d197d...+	D7-27/DHQ52	JH2	CARSTGVYWY	0
	10	DP-75/VI-2...+	not found	JH4b	CARGPITYPE	0
	11	12M28	D1-26	JH6c	CARAGWELL	0
	12	DP-49/1.9III...+	D1-14	JH6b	CAKDRGDHYY	0
	13	DP-75/VI-2...+	D5-5/DK4	JH4b	CARDSGRRGY	0
	14	VH32Sanz+	D5-5/DK4	JH6c	CARGGGWAAM	0
	15	DP-75/VI-2...+	D3-9/DXP1...	JH4b	CALRPEYYDI	0
	16	DP-66/V71-2...+	not found	JH4b	CAGGPGVPPF	1
	17	DP-75/VI-2...+	D6-25	JH4b	CARDSWYSSS	1
	18	DP-71/3d197d...+	D5-12/DK1	JH2	CARGHPGDGY	1
	19	VH32Sanz+	D6-25	JH6b	CATPGIAAWY	1
	20	DP-71/3d197d...+	D6-6/DN4	JH2	CARHGIAARP	2
	21	DP-71/3d197d...+	D1-26	JH4b	CARRDRSSYY	2
	22	DP-71/3d197d...+	D6-6/DN4	JH6c	CARLLAGTWY	2
	23	p1	D3-3/DXP4	JH4b	CVNGGLV*IT	3

6 weeks	sequence	V	D	J	junction translation	mutations
	1	DP-10/hv1051...+	D7-27/DHQ52	JH4b	CAREVPATGD	0
	2	DP-10/hv1051...+	D7-27/DHQ52	JH4b	CAREVPATGD	0
	3	DP-10/hv1051...+	D7-27/DHQ52	JH4b	CAREVPATGD	0
	4	DP-10/hv1051...+	D7-27/DHQ52	JH4b	CAREVPATGD	1
	5	DP-10/hv1051...+	D7-27/DHQ52	JH4b	CAREVPATGD	1
	6	DP-74/VH-VI...+	D6-19	JH4b	CARDRSRGWY	0
	7	DP-74/VH-VI...+	D6-19	JH4b	CARDRSRGWY	0
	8	DP-74/VH-VI...+	D6-19	JH4b	CARDRSRGWY	0
	9	DP-74/VH-VI...+	D6-19	JH4b	CARDRSRGWY	0
	10	V3-53+	D2-21	JH4b	CARASGDFDY	3
	11	V3-53+	D2-21	JH4b	CARASGDFDY	3
	12	V3-53+	D2-21	JH4b	CARASGDFDY	3
	13	12M28	D3-22/D21-9	JH2	CATTYDSSGY	0
	14	12M28	D3-22/D21-9	JH2	CATTYDSSGY	1
	15	4M28	D3-22/D21-9	JH2	CATTYDSSGY	1
	16	DP-79/4d154...+	D1-14/DM2	JH4b	CARHQRSYDP	0
	17	DP-49/1.9III...+	D6-13/DN1	JH4b	CAKVPHSSSW	0
	18	DP-71/3d197d...+	D7-27/DHQ52	JH2	CAREDPTGDW	0
	19	DP-47/V3-23...+	D6-25	JH4b	CAKDLTAAPD	0
	20	DP-58/hv3d1EG	D7-27/DHQ52	JH3b	CARDQMTGDR	0

14 weeks	sequence	V	D	J	junction translation	mutations
	1	DP-10/hv1051...+	D7-27/DHQ52	JH4b	CAREVPATGD	0
	2	DP-74/VH-VI...+	D6-19	JH4b	CARDRSRGWY	0
	3	12M28	D3-22/D21-9	JH2	CATTYDSSGY	0
	4	12M28	D3-22/D21-9	JH2	CATTYDSSGY	1
	5	DP-79/4d154...+	D1-14/DM2	JH4b	CARHQRSYDP	0
	6	DP-49/1.9III...+	D6-13/DN1	JH4b	CAKVPHSSSW	0
	7	4-04 VIV4	not found	JH6c	CARDETLVSS	0
	8	4-04 VIV4	not found	JH6c	CARDETLVSS	0
	9	4-04 VIV4	not found	JH6c	CARDETLVSS	1
	10	4-30.1 DP65	not found	JH3b	CASEFNPSY	0
	11	4-30.1 DP65	not found	JH3b	CASEFNPSY	0
	12	4-59 DP71	not found	JH2	CARQDNWNYW	2
	13	4-59 DP71	not found	JH2	CARQDNWNYW	2
	14	4-59 DP71	not found	JH2	CARQDNWNYW	2
	15	3-30 COS8	not found	JH4b	CARGGSSYYF	0
	16	5-51 DP73	not found	JH5a	CARRGGGGYS	0
	17	3-30 DP49	not found	JH3b	CAKGGYSGS	0
	18	4-59 DP71	not found	JH3b	CARHITGTAF	2

	family 1
	family 2
	family 3
	family 4
	family 5
	family 6
	family 7
	family 8
	family 9

Table 29. BCB-LCL2

Summary of matched V, D and J alignments for each IgH sequence analysed at 0, 2 and 10 weeks post-establishment, the first 10 amino acids of the VDJ junction translation, and the number of mutations detected in the V region. Clonally related IgH sequences are colour highlighted (see legend).

and tonsillar naive B cells. However, in contrast to PB or tonsillar B cells, little evidence of SHM was observed in the cord blood LCLs, suggesting that EBV transformation of cord blood lymphocytes *in vitro* does not induce SHM.

As with the LCL cultures derived from PB and tonsillar naive B cells, the cord blood LCLs were examined for Ig isotype expression. Flow cytometry analysis of Ig and CD27 expression in BCB-LCL1 and BCB-LCL2 revealed that both LCLs expressed IgD and IgM without IgG, IgA or CD27, consistent with a naive B cell phenotype (data not shown).

4.6 *N-LCLs Can be Induced to Undergo Isotype-Switching in Vitro*

Evidence of IgH mutation following EBV transformation of PB and tonsillar naive B cells, suggests the virus is able to induce one of the key processes of an *in vivo* GC reaction in an *in vitro* setting. Although a proportion of the infected naive B cells had acquired memory B cell genotypes, analysis of Ig isotype expression revealed that EBV infection *in vitro* was not able to induce a second hallmark of a GC reaction, CSR. In order to examine whether EBV-transformed naive B cells were capable of undergoing CSR when provided with appropriate B cell-activating signals, a number of experiments were carried out. Based on methods published by others, a combination of CD40L, IL-4 and IL-21 was employed to induce CSR (Avery et al., 2008). A range of LCLs generated from PB naive B cells were used, including recently established (BN-LCLs 6 and 7) and long-established (BN-LCL5) cultures. In addition, a tonsillar naive LCL (BTN-LCL1) and a cord blood LCL (BCB-LCL2), both of which were long-established, were also examined.

For the first experiment (BN-LCL5), purified naive B cells were infected with EBV and cultured for 14 days before being divided into three cultures; the first was left untreated, the second treated with CD40L and IL-4, and the third with CD40L, IL-4 and IL-21. The three cultures were grown for 7 days before being stained for IgD, IgG, IgA and CD27, and analysed by flow cytometry. The results of the three culture conditions are shown in Figure 45. The untreated culture expressed IgD in the absence of IgG, IgA or CD27. The culture treated with CD40L and IL-4 alone showed a slight increase in IgG and IgA expression, with little change in IgD. Exposure to CD40L, IL-4 and IL-21 caused a significant upregulation of IgG and IgA together with a decrease in IgD expression. These findings confirm that EBV infected naive B cells retain their capacity to isotype-switch.

Since the use of CD40L, IL-4 and IL-21 together produced the most potent effect in the first experiment, all three were used in combination for subsequent experiments (summarised in Table 30). A further PB N-LCL (BN-LCL7) was split into two cultures at day 14 post-infection, and either treated with CD40L/IL-4/IL-21, or left untreated. In BN-LCL7, expression of IgG and IgA was upregulated in the CD40L/IL-4/IL-21-treated, but not the untreated culture. The same experiment was carried using the long-established (>12 weeks) BN-LCL5. In this case, IgG expression was upregulated as a result of stimulation, but only a small increase in IgA expression was observed. Similarly examination of a well-established tonsillar naive LCL (BTN-LCL1) and cord blood LCL (BCB-LCL2) revealed selective upregulation of IgG following CD40L/IL-4/IL-21 treatment.

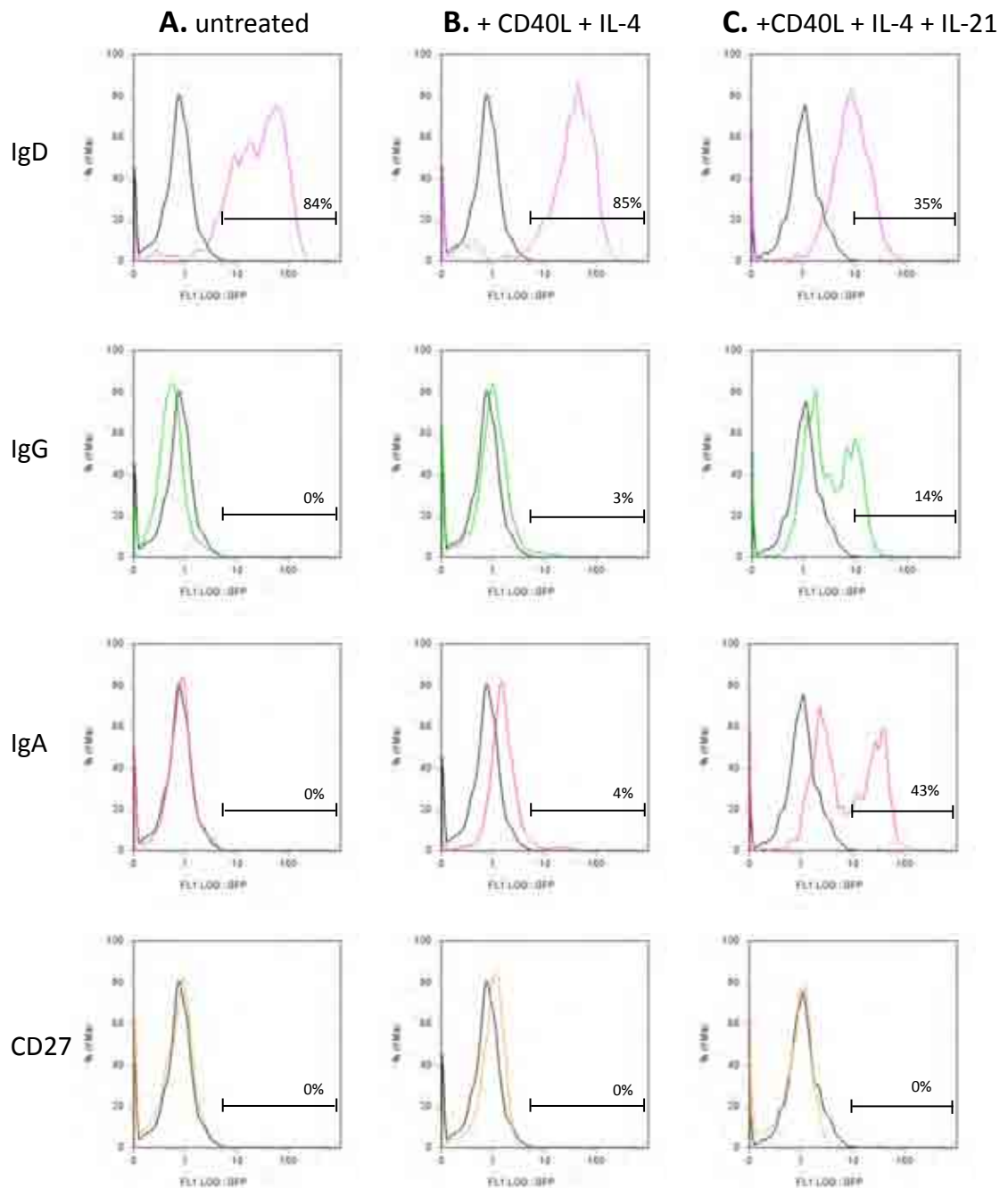


Figure 45. BN-LCL treated with CD40L, IL-4 and IL-21

14 days following in vitro infection, naive B cells were either cultured as before without treatment (A), treated with CD40L and IL-4 (B), or treated with CD40L, IL-4 and IL-21 (C) for 7 days.

Intracellular staining for IgD, IgG, IgA and CD27 was then carried out. The isotype control is shown in black outline, whereas the specific staining is shown in coloured outline (note, the same isotype controls and gates were used in A and B, whereas a separate isotype control and gate was for the staining shown in C.).

A. The untreated LCL culture expressed both IgM and IgD in the absence of IgG, IgA or CD27. **B.** Whilst the majority of cells still expressed IgD, small cells numbers in the CD40L/IL-4-treated LCL switched to IgG or IgA expression. **C.** A decrease in the number of cells expressing IgD was observed in the CD40L/IL-4/IL-21-treated LCL, together with a substantial increase in the number of cells expressing either IgG or IgA. Upregulation of CD27 was not observed in either of the treated cultures.

			<u>Untreated</u> (%)	<u>CD40L IL-4</u> (%)	<u>CD40L IL-4 IL-21</u> (%)
peripheral blood	BN-LCL6 (14 days)	IgD	84	85	35
		IgG	0	3	14
		IgA	0	4	43
		CD27	0	0	0
	BN-LCL7 (14 days)	IgD	45	n/t	49
		IgG	0		53
		IgA	0		15
		CD27	0		0
	BN-LCL5 (>12 weeks)	IgD	85	n/t	58
		IgG	0		42
		IgA	0		2
		CD27	0		0
tonsil	BTN-LCL1 (>12 weeks)	IgD	83	n/t	49
		IgG	0		22
		IgA	0		1
		CD27	0		0
cord blood	BCB-LCL2 (>12 weeks)	IgD	75	n/t	62
		IgG	0		52
		IgA	0		2
		CD27	0		0

Table 30. Summary of isotype-switching experiments

Summary of isotype expression in a range of LCLs treated with CD40L/IL-4/IL-21. All untreated LCLs expressed IgD in the absence of IgG, IgA or CD27. In PB naive B cells treated with CD40L/IL-4/IL-21 at 14 days post-infection, a substantial proportion of cells within both cultures switched to IgG or IgA. In long-established LCLs derived from PB, tonsil and CB, however, whilst class-switching to IgG was clearly observed, only small numbers of cells switched to IgA. CD27 was not upregulated in any of the LCLs treated with CD40L/IL-4/IL-21.

These results show that EBV-transformed naive B cells from PB, tonsil and cord blood are capable of CSR *in vitro*. Whereas each LCL culture retained the capacity to switch to IgG, only those recently established switched to IgA.

4.7 AID Variant Expression in Peripheral Blood B cell Cultures

Activation-induced cytidine deaminase (AID) is essential for the process of both isotype-switching and somatic hypermutation *in vivo* (Muramatsu et al., 2000). In addition to the most abundantly expressed full length AID mRNA transcript, several variants also occur (Figure 10). Significantly, certain AID variants generated by alternative splicing are reportedly deficient in either somatic hypermutation activity (AID- Δ E3E4) or class-switch recombination activity (AID- Δ E4) (Wu et al., 2008). Since EBV infection reportedly upregulates expression of AID *in vitro* (He et al., 2003, Gil et al., 2007, Epeldegui et al., 2007), we designed qPCR assays to determine the relative levels of the full length transcript (AID-FL), the transcript missing exon 4 (AID- Δ E4) and the transcript missing exons 3 and 4 (AID- Δ E3E4). These assays were then used to investigate AID expression in EBV-blasts and CD40-blasts.

Using a nested reverse transcription (RT) PCR approach, we first isolated variant AID cDNA products derived from the Akata-BL cell line by agarose gel electrophoresis (data not shown). These different AID cDNA products were then excised from the gel and cloned into a pGEMT vector system. Following sequence analysis to confirm the identity of the variants, the plasmids were subsequently used as standards in the qPCR reactions.

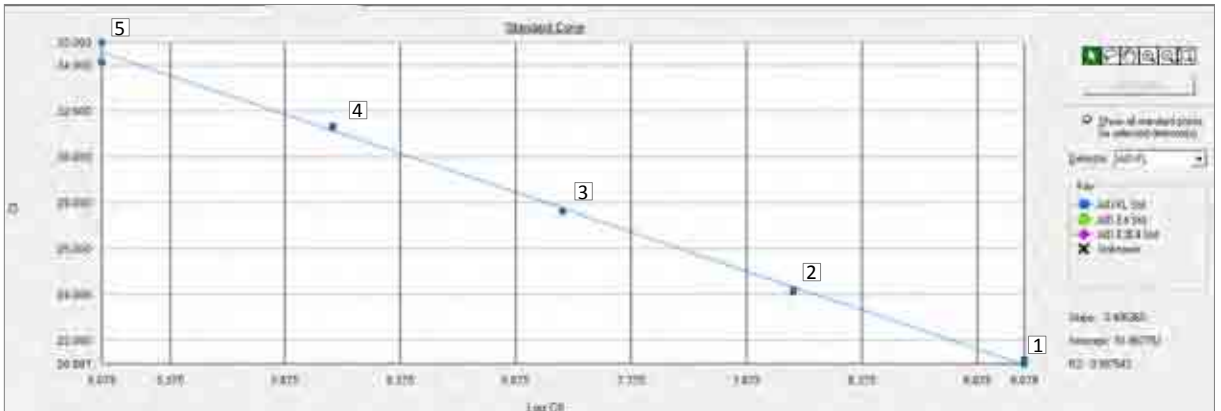
4.7.1 Validation of AID qPCR Assays

Individual qPCR assays were designed to detect each of the three AID isoforms. Each assay was then validated using serial dilutions of each AID variant (Figure 46-a, b and c). The three assays showed similar sensitivities and PCR amplification efficiencies. In addition, each assay was tested against the two other AID variant targets, but no cross-reactivity was detected (data not shown). In conclusion, therefore, these assays were both sensitive and specific.

4.7.2 AID Upregulation in Peripheral Blood B cells Following EBV Infection *in Vitro*

In order to confirm the upregulation of AID expression in B cells following EBV infection, PB B cells were infected with B95.8 virus. In parallel, B cells from the same donor were stimulated with CD40L and IL-4 to generate B blasts. Cells were collected prior to treatment and at various time points up to 35 days following either infection or stimulation. Following RNA isolation and cDNA synthesis, the levels of each AID transcript were then determined by qPCR (Figure 47). Whilst no AID expression was detected in the resting B cells, upregulation of AID-FL and to a lesser degree AID- Δ E4 was detected following both EBV infection and CD40L/IL-4 treatment. A markedly higher level (~ 10-fold) of AID-FL and AID- Δ E4 transcripts was detected in the blast cultures than in the LCL cultures. AID-FL was the most abundantly expressed transcript in both cultures, followed by AID- Δ E4 which was ~10-fold lower; levels of AID- Δ E3E4 were extremely low.

AID-FL standard curve



AID-FL plasmid serial dilution qPCR amplification plots



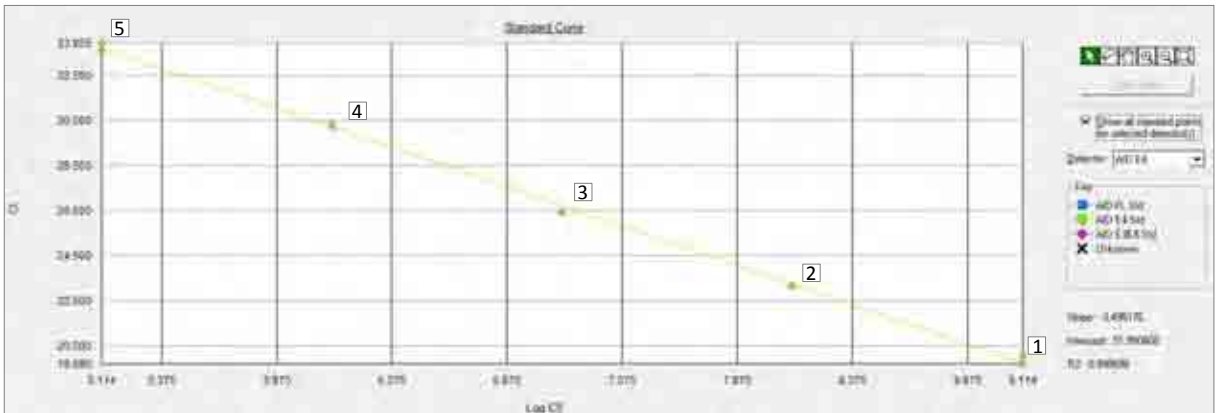
Figure 46a. AID-FL plasmid standards

The plasmid vector containing the AID-FL inserted sequence was serially diluted 1:10 to generate 5 values for a standard curve. Duplicate samples from each concentration were amplified in an AID-FL specific qPCR assay. The upper panel shows a representative AID-FL qPCR standard curve (see legend for plasmid copy numbers). The lower panel shows the corresponding qPCR amplification curves for each point of the standard curve.

Legend

- 1 1.2×10^9 plasmid copies
- 2 1.2×10^8 plasmid copies
- 3 1.2×10^7 plasmid copies
- 4 1.2×10^6 plasmid copies
- 5 1.2×10^5 plasmid copies

AID-ΔE4 standard curve



AID-ΔE4 plasmid serial dilution qPCR amplification plots



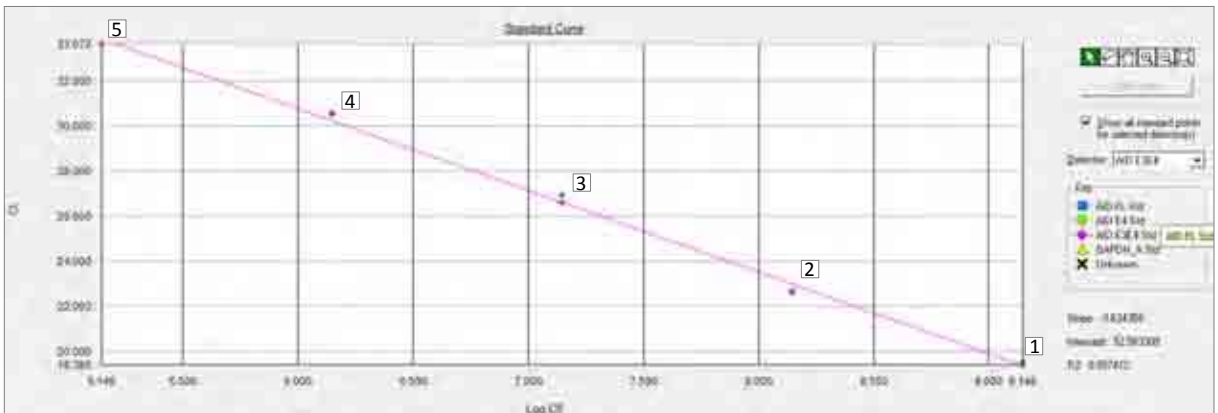
Figure 46b. AID-ΔE4 plasmid standards

The plasmid vector containing the AID-ΔE4 inserted sequence was serially diluted 1:10 to generate 5 values for a standard curve. Duplicate samples from each concentration were amplified in an AID-ΔE4 specific qPCR assay. The upper panel shows a representative AID-ΔE4 qPCR standard curve (see legend for plasmid copy numbers). The lower panel shows the corresponding qPCR amplification curves for each point of the standard curve.

Legend

- 1 1.3 x 10⁹ plasmid copies
- 2 1.3 x 10⁸ plasmid copies
- 3 1.3 x 10⁷ plasmid copies
- 4 1.3 x 10⁶ plasmid copies
- 5 1.3 x 10⁵ plasmid copies

AID- Δ E3 Δ E4 standard curve



AID- Δ E3 Δ E4 plasmid serial dilution qPCR amplification plots

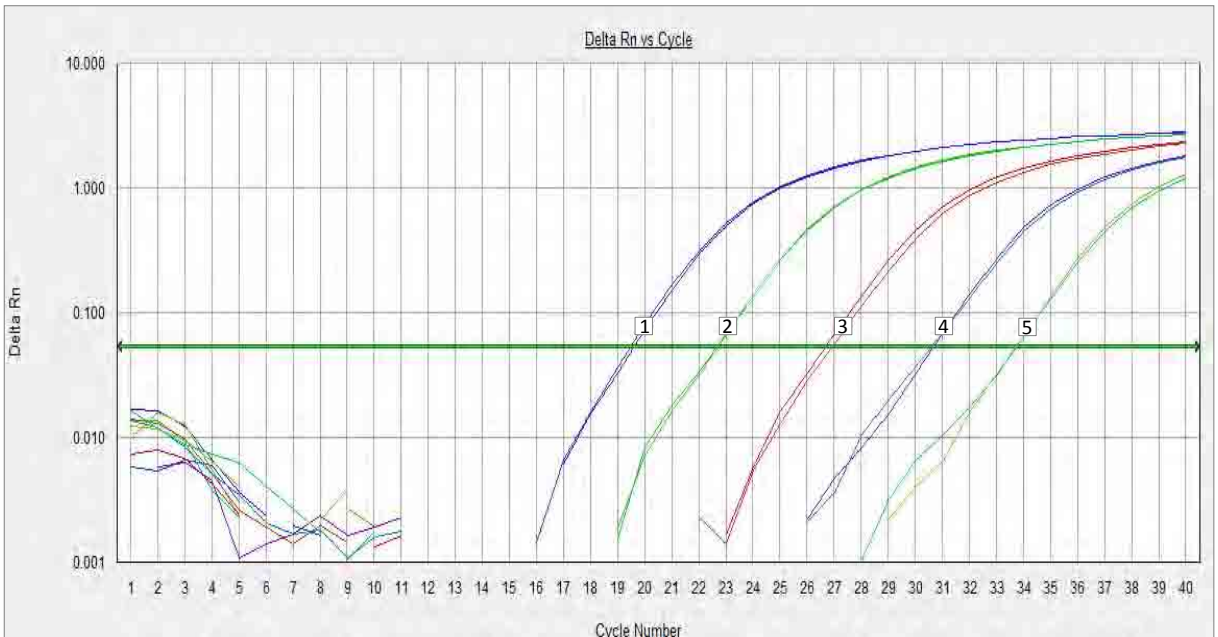


Figure 46c. AID- Δ E3E4 plasmid standards

The plasmid vector containing the AID- Δ E3E4 inserted sequence was serially diluted 1:10 to generate 5 values for a standard curve. Duplicate samples from each concentration were amplified in an AID- Δ E3E4 specific qPCR assay. The upper panel shows a representative AID- Δ E3E4 qPCR standard curve (see legend for plasmid copy numbers). The lower panel shows the corresponding qPCR amplification curves for each point of the standard curve.

Legend

- ① 1.4×10^9 plasmid copies
- ② 1.4×10^8 plasmid copies
- ③ 1.4×10^7 plasmid copies
- ④ 1.4×10^6 plasmid copies
- ⑤ 1.4×10^5 plasmid copies

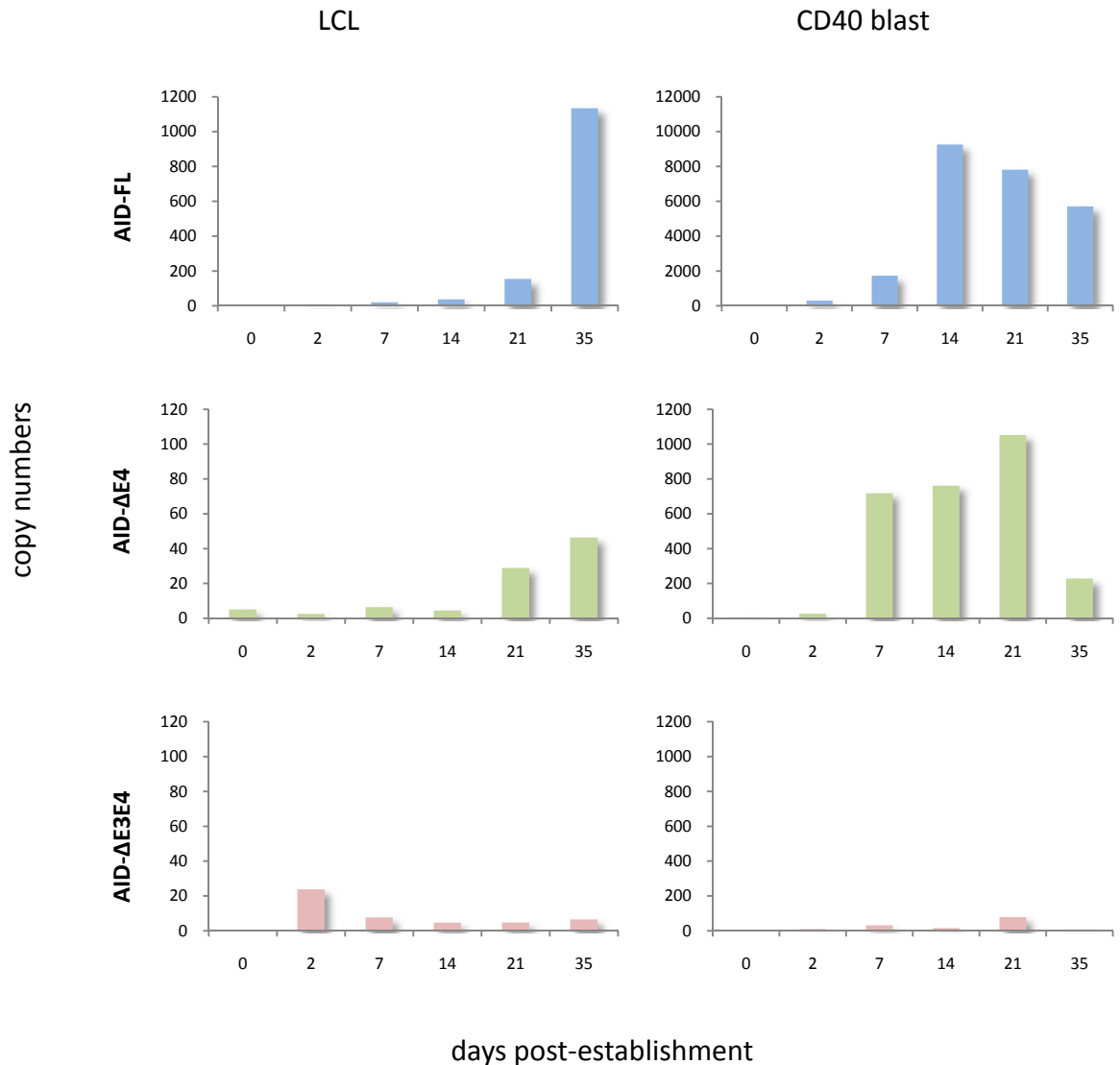


Figure 47. AID upregulation in PB B cells following EBV infection or CD40L/IL-4 stimulation

In order to confirm the induction of AID variant transcription, CD19-selected B cells from a single donor were either infected with EBV, or treated with CD40L/IL-4. Cells were then harvested at various time points, RNA was isolated and expression of AID-FL, AID-ΔE4 and AID-ΔE3E4 measured by qPCR. AID transcript copy numbers were estimated by comparison to plasmid standard curves, and the RNA input was normalised against GAPDH. The values presented are therefore semi-quantitative transcript copy numbers.

Marked upregulation of AID expression was detected at ~21 days post-infection in the LCL , and ~7 days post-establishment of the CD40 blast. Higher levels of all expressed AID transcripts were detected in the CD40 blast than in the LCL. In both cultures, however, AID-FL was expressed ~ 10-fold higher than AID-ΔE4 and AID-ΔE3E4 was expressed in extremely low levels.

4.7.3 AID Expression in Tonsillar B cells

In order to assess whether the levels of AID expression in an LCL were comparable to physiological levels, we compared the levels of AID in the LCL used in the previous experiment, together with *ex vivo* tonsillar B cells and the Ramos-BL cell line, which is known to undergo continuous SHM (Sale and Neuberger, 1998). The primary tonsillar B cells expressed both AID-FL and AID- Δ E4 at similar levels to the LCL and Ramos cells; again levels of AID- Δ E3E4 were extremely low or undetectable (Figure 48). The AID-FL transcript was the most abundantly expressed in each sample, whereas AID- Δ E4 expression was approximately 7-fold lower. The AID- Δ E3E4 transcript expression was a further 10-fold lower, and as such was barely detectable by the assay.

4.7.4 AID expression in Naive LCLs and CD40 blasts

A selection of BN-blast cultures and LCL cultures yielding either predominantly mutated or unmutated IgH sequences were examined for AID variant expression (Figure 49). Consistent with the above findings, all three blast cultures expressed AID transcripts at levels over 10-fold higher than the LCLs, with AID-FL being the most abundantly expressed transcript. Whereas AID-FL and AID- Δ E4 transcripts were detectable in all BN-blast and LCL cultures, the AID- Δ E3E4 was barely detectable (data not shown). No obvious differences in AID transcript expression were detected in the LCLs containing mutated IgH sequences (BN-LCLs3, 4b and 5) compared to those that did not (BN-LCL1 and BCB-LCL1).

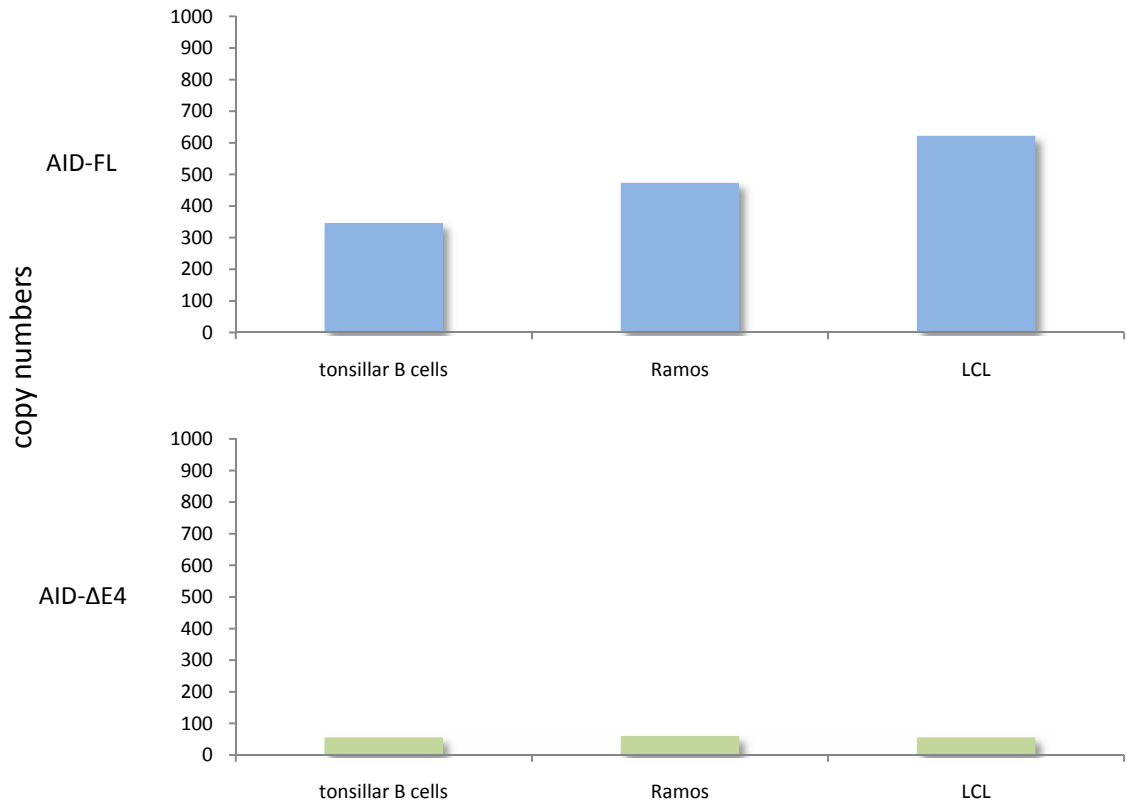


Figure 48. AID expression in tonsillar B cells

AID expression in an LCL derived from PB CD19-selected B cells was compared to that in *ex vivo* tonsillar B cells and the Ramos-BL cell line using qPCR assays. AID transcript copy numbers were estimated by comparison to plasmid standard curves, and the RNA input was normalised against GAPDH. The values presented are therefore semi-quantitative transcript copy numbers. Similar levels of AID-FL and AID-ΔE4 were observed in all 3 cell types, with AID-FL more highly expressed than AID-ΔE4. AID-ΔE3E4 expression was not detected in any of the samples (not shown).

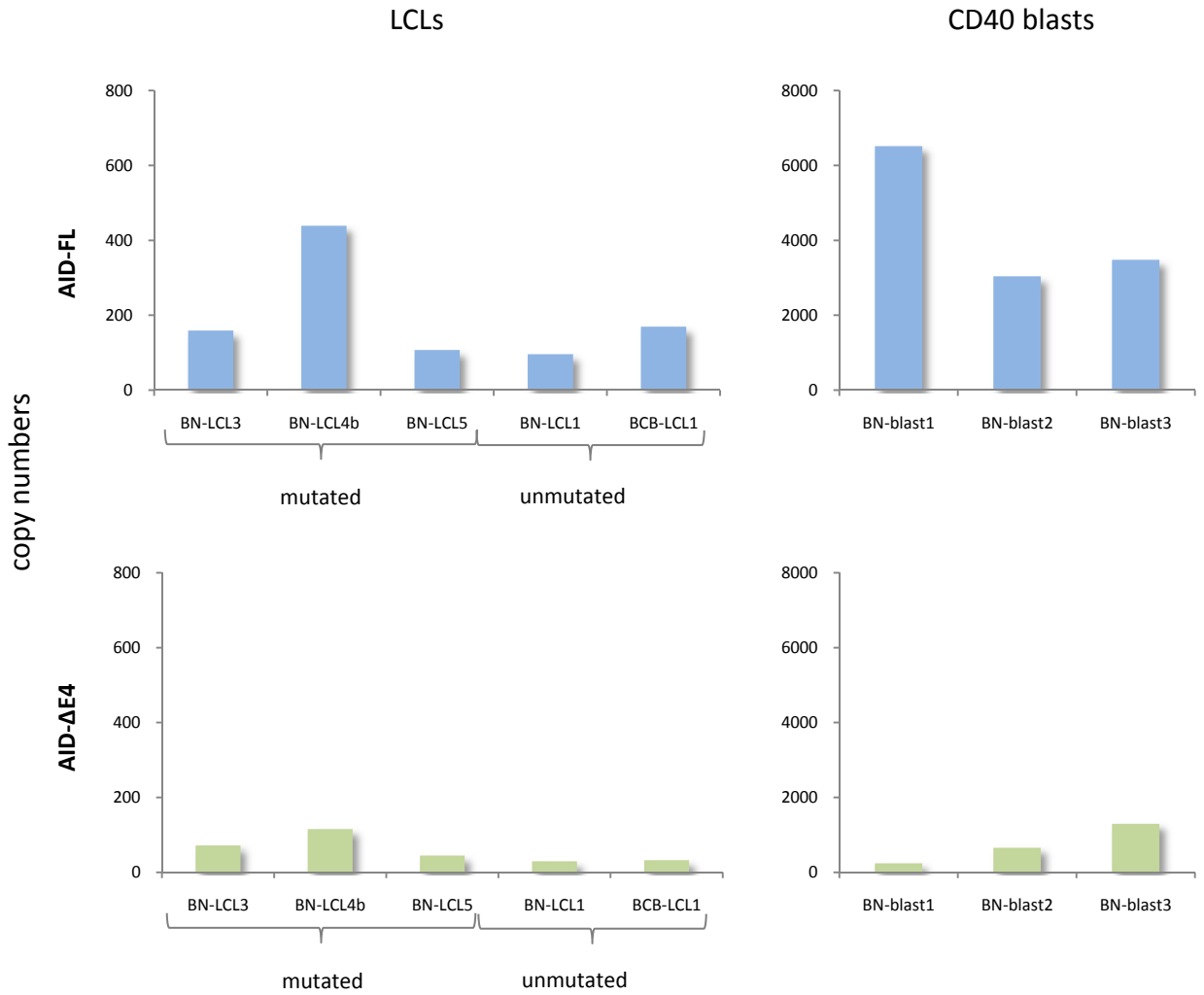


Figure 49. AID expression in established naive LCLs and CD40 blasts

AID variant expression from several of the established LCL and BN-blast cultures featured in this study was evaluated using qPCR. Both AID-FL and AID-ΔE4 were expressed ~10-fold higher in the BN-blasts than in the LCL cultures, however in both cultures AID-FL was expressed more highly than AID-ΔE4. No consistent difference in expression of either AID transcript was observed between LCLs yielding predominantly mutated IgH sequences, and LCLs yielding predominantly unmutated IgH sequences.

4.7.5 Expression of SHM molecules Polymerase- η and Uracil DNA Glycosylase

In the next series of experiments, expression of two further enzymes involved in the SHM process, polymerase- η and uracil DNA glycosylase (UNG) (Peled et al., 2008) were also examined by qRT-PCR. These assays were used to screen a selection of LCLs derived from PB naive B cells (BN-LCL3, BN-LCL4b and BN-LCL5), tonsillar naive B cells (BTN-LCL1) and cord blood (BCB-LCL1), together with two CD40 blasts (BN-blast1 and BN-blast3) (Figure 50). The results show that expression of both Pol- η and UNG was upregulated in all the LCL and CD40 blasts examined, albeit at lower levels than the reference cell line Jurkat. All cultures expressed similar levels of either Pol- η or UNG, with no considerable difference in expression between LCLs or CD40 blasts. As expected, expression of neither Pol- η nor UNG was detected in resting PB B cells (data not shown).

These data confirm that in addition to AID variants AID-FL and AID- Δ E4, expression of two additional components of the SHM process, Pol- η and UNG, were also upregulated in both LCLs of different origin and in CD40-blasts.

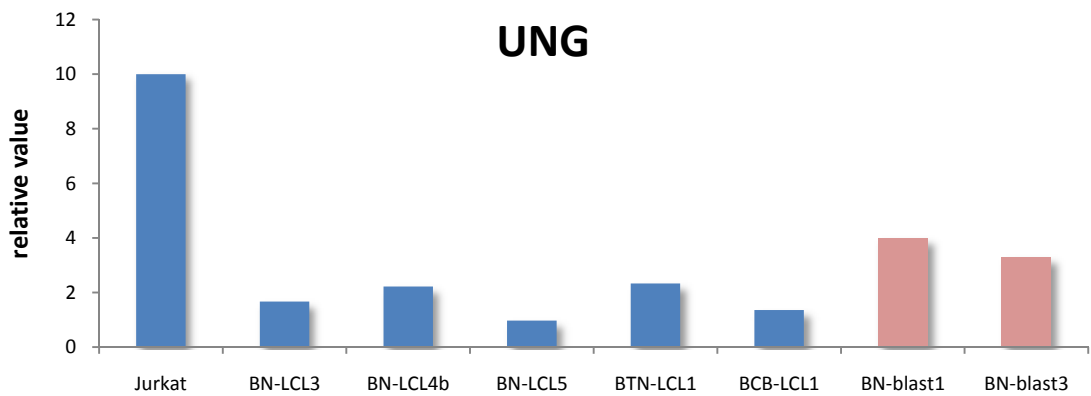
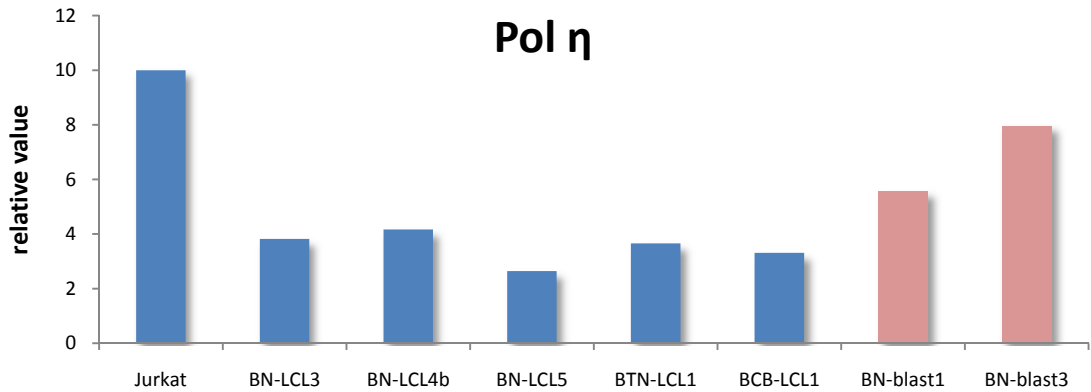


Figure 50. pol- η and UNG expression in established LCLs and CD40 blasts

Relative expression of pol- η and UNG in several established LCL and BN-blast cultures was examined by qPCR. Results were normalised against GAPDH values to control for RNA input. Normalised values are presented relative to the leukemic cell line, Jurkat. The results show that expression of both pol- η and UNG was upregulated in BN-LCLs, BTN-LCL1, BCB-LCL1 and BN-blasts, with no notable difference in expression levels identifiable between the different cultures.

4.8 Discussion

4.8.1 EBV Infection of Naive B cells Induces IgH Mutations *in Vitro*

Previous work carried out by Dr Begue Pastor and Dr Chaganti suggested that *in vitro* transformation of naive B cell populations from PB could yield LCL cultures carrying mutated IgH genes. In the current project, purified naive B cells of PB, tonsil and cord blood B cells were used to generate both bulk and limiting dilution LCL cultures, which were subsequently analysed by IgH sequencing at various time points (up to twelve weeks) post-infection. The present results confirm that following EBV infection of adult PB and tonsillar naive B cells *in vitro*, a subset of cells carrying mutated IgH sequences were detectable from approximately six weeks post-infection, with some evidence of ongoing SHM in some instances. We suggest that these findings do not reflect artifacts of *in vitro* culture or PCR-induced error, since similar results were observed using two different transformation techniques (bulk culture and limiting dilution infections), and from naive B cells derived from both peripheral blood and tonsil.

The simplest explanation for the appearance of LCLs carrying mutated IgH sequences is that the initial naive B cell products were contaminated with memory B cells. However, IgD+CD27- naive B cells derived from adult PB or tonsil were sorted to high purity (~99%) as shown in the reanalysis data summarised in Table 10. In addition, IgH sequence analysis of starting populations from PB or tonsillar naive B cells, and cord blood B cells confirmed that over >95% of the cells carried unmutated IgH genes, confirming the cells

were genotypically naive (summarised in Figure 51). The high purity of the starting populations implies that the vast majority of transformed cells growing out in the LCL cultures should therefore be of naive B cell origin. This was further confirmed by examination of Ig isotype expression in established LCLs, which showed that each culture retained an IgM+IgD+ phenotype, eliminating the possibility that mutated IgH sequences were derived from small numbers of contaminating switched memory B cells. However, such sequences could have arisen from IgM+IgD+CD27+ non-switched memory B cells, which were the most likely source of contamination during FACS sorting. Regarding this issue, expression of the memory marker CD27, which can be used to distinguish IgM+IgD+CD27- naive B cells from IgM+IgD+CD27+ non-switched memory B cells, was consistently undetectable in any of the LCLs, further suggesting that the cultures examined in this study reflected *bone fide* transformed naive B cells. However, the lack of CD27 expression in our established LCLs contradicts a recent report describing upregulation of CD27 in naive LCLs (Siemer et al., 2008).

In order to determine whether non-switched memory B cells were able to transform more efficiently than naive B cells, and therefore may potentially grow out preferentially *in vitro*, we directly compared the transformation efficiency of naive and non-switched memory B cell populations from five separate PB donors. Although a considerable level of variation in transformation efficiency between B cells from separate PB donors was noted, no reproducible difference between the two B cell subsets was detected in these experiments.

The successive accumulation of IgH mutations is a hallmark of SHM within clonal expansions. In order to examine in further detail the development of

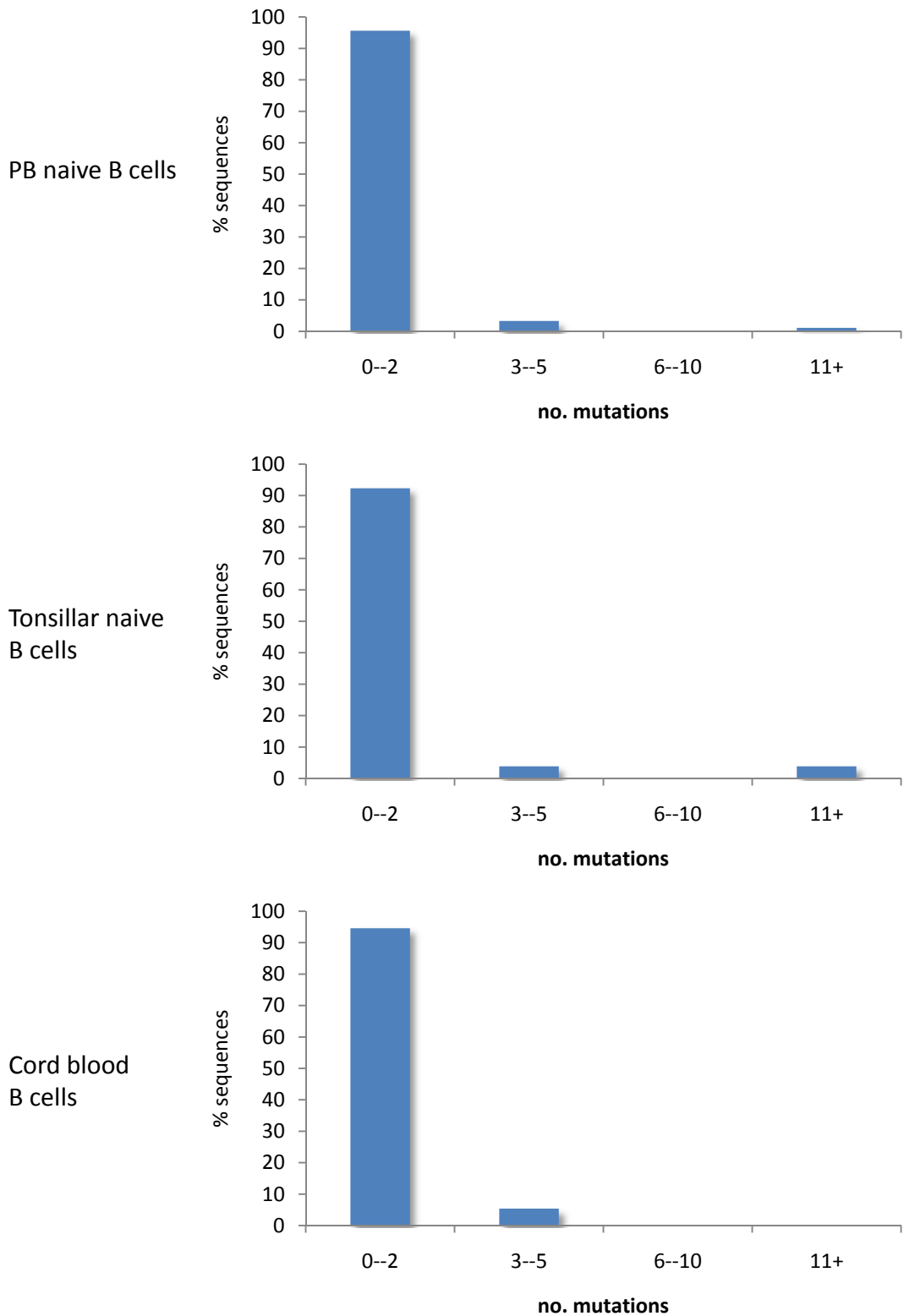


Figure 51. Frequency of mutations in resting B cell populations

IgH mutation frequencies in the resting cell populations used to generate PB N-LCLs, tonsillar N-LCLs and CB-LCLs. IgH analysis revealed >90% of the cells were unmutated.

SHM patterns within IgH genes of EBV-infected cells, three BN-LCLs (BN-LCL4a, -b and -c) were established from a single donor. From mutations identified in IgH sequences within these cultures, clonal family trees were constructed which highlighted the sequential accumulation of mutations along successive generations of cells. Genealogical trees generated by other investigators have described a similar stepwise accumulation of small numbers of mutations *in vitro*, namely in a rheumatoid factor (RF) – producing LCL (Chezar et al., 2008) and in the Ramos BL cell line (Sale and Neuberger, 1998).

In several instances in the current study, cells carrying mutated IgH sequences could be traced back to genotypically naive, germline IgH sequences from the same clone, present within the same culture. Co-existence within the cultures of clonally related cells, each harbouring distinct IgH mutation patterns reflecting different stages of the stepwise accrual of mutations, strongly suggests that this process took place *in vitro*, following EBV infection. Furthermore, it is highly unlikely that these clonal expansions had occurred *in vivo* and were subsequently collected during cell sorting since (i) the cells were derived from PB rather than from lymphoid tissue, (ii) IgH analysis of resting cells in each case revealed polyclonal populations of unmutated cells, and (iii) clonal families containing IgH mutations were not detected until approximately six weeks after infection, suggesting the mutation process occurred over time in culture.

Together these observations suggest that EBV infection of naive B cells can induce IgH mutations in at least a proportion of cells *in vitro*, and support the argument that such sequences do not reflect outgrowth of contaminating memory cells.

EBV Infection of Cord Blood B cells does not Induce IgH Mutation

In contrast to the results seen in transformed naive B cells derived from PB and tonsils, analysis of IgH sequences from two cord blood-derived LCLs did not provide any evidence of IgH mutation. The reason why SHM is induced in adult B cells, but not cord blood B cells is not obvious from these experiments since AID, UNG and Pol- η were also upregulated in the CB-LCL examined.

Nevertheless both phenotypic and functional differences between cord blood and adult PB B cells have been documented. A recent study showed a markedly higher proportional of immature, transitional B cells in cord blood compared to adult PB, together with a deficiency in signaling molecules associated with cell activation such as ERK, p38 and MAP kinases following CD40 stimulation (Ha et al., 2008). Whether or not these discrepancies account for the lack of mutation in the CB-LCLs is unclear, however it is feasible that further unidentified differences exist between cord blood and adult B cells, which render the former subset less susceptible to SHM.

4.8.2 AID is Upregulated Following EBV Infection *in Vitro*

The enzyme AID, whose natural function is to introduce lesions into IgH genes, is critical for the processes of both CSR and SHM (Muramatsu et al., 2000, Revy et al., 2000). Although AID activity is classically refined to the IgH locus, AID is also known to target a range of non-Ig genes within the human genome (Wang et al., 2004), including proto-oncogenes (Liu et al., 2008, Pasqualucci et al., 1998, Shen et al., 1998). Furthermore, ectopic expression of AID is involved in chromosomal translocations (Ramiro et al., 2004, Dorsett et al.,

2007), and has been implicated in malignant transformation of B cells (Okazaki et al., 2007).

Examination of the location of IgH mutations in the PB naive LCLs included in this study revealed a concentration of nucleotide changes at AID hotspots (Dorner et al., 1998) (summarised in Figure 52). Although evidence that this pattern of IgH mutations occurred *in vitro* may be circumstantial, it confirms firstly that the mutations identified in these cultures were AID-mediated, and secondly that PCR error was not responsible. Subsequently, it was also confirmed that whereas no AID expression could be detected in circulating B cells, expression of AID transcripts was upregulated by EBV infection and by CD40L/IL-4 stimulation of B cells *in vitro*, each of which has been reported previously (Pasqualucci et al., 2004, He et al., 2003, Gil et al., 2007, Epeldegui et al., 2007). Although both processes result in the upregulation of AID expression, the means by which this is achieved in CD40 blasts and LCLs is likely to be different. CD40L and IL-4 treatment provides mitogen activation to B cells *in vitro*, similar to those signals provided during T-dependent activation of B cells *in vivo*. In the case of EBV infection, however, components of the latency III program are likely to induce AID expression. Specifically, LMP1 expression has been linked to the upregulation of AID in *ex vivo* PB B cells (He et al., 2003); an observation which is not surprising given the ability of LMP1 to mimic CD40 signalling (Uchida et al., 1999). In the current study, AID expression was detected in all LCL cultures examined by RT-PCR, but SHM was only detected in a fraction of cells. It is unclear why AID expression in some instances lead to SHM, but in others appeared to be inhibited. Studies of AID expression in cases of B cell chronic lymphocytic leukemia B-CLL have

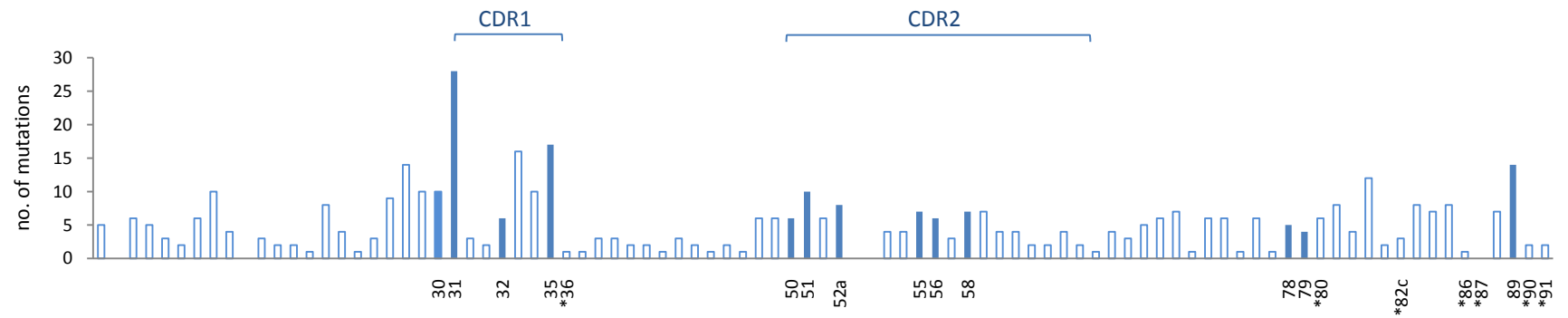


Figure 52. High numbers of mutations in naive LCL cultures accumulate in AID hotspots

The chart shows a summary of mutations identified in each N-LCL culture derived from PB. Identical mutations in clonal families were only counted once. Solid blue bars with above numbered codons represent AID hotspots and asterisks next to numbered codons represent AID coldspots (described by Dorner et al., 1998).

shown that the enzyme is only upregulated in a subset of cells within B-CLL clonal expansions *in vivo* (Albesiano et al., 2003). In the same investigation no differences in levels of overall AID expression were identified when comparing mutated and non-mutated clones. If a similar situation were to take place *in vitro*, whereby only a subset of cells within one population upregulated AID expression, this could lead to SHM within only a fraction of cells in LCL cultures. Indeed, such a phenomenon would be undetectable by RT-PCR, which provides an average expression value across a whole population of cells. This explanation does not, however, account for the finding that no SHM at all was detected in either the BN-blasts or the BCB-LCLs where AID was clearly expressed by some, if not all, of the cells in these cultures. A more likely explanation, therefore, may be that although AID is expressed in each case, in instances where no IgH mutations were found, its capacity to induce SHM was somehow inhibited.

4.8.3 SHM was detected in BN-LCLs but not BN-blasts

In order to carry out EBV-negative control experiments for the *in vitro* activation and cell culture of B cells, three BN-blasts were established using PB naive B cells. Unlike the BN-LCLs, no increase in mutated IgH sequences was detected in any of the BN-blasts after six or nine weeks in culture (the percentage of mutated IgH sequences from all BN-LCLs and BN-blasts at 0, 6 and 9 weeks post-establishment is summarised in Figure 53). To rule out the possibility that these differences merely reflect variations between the naive B cell populations used to generate the separate cultures, a BN-blast (BN-blast 3) and a BN-LCL (BN-LCL3) were established in parallel, using the same collection of naive B cells derived from a single donor. IgH sequence analysis of this experiment

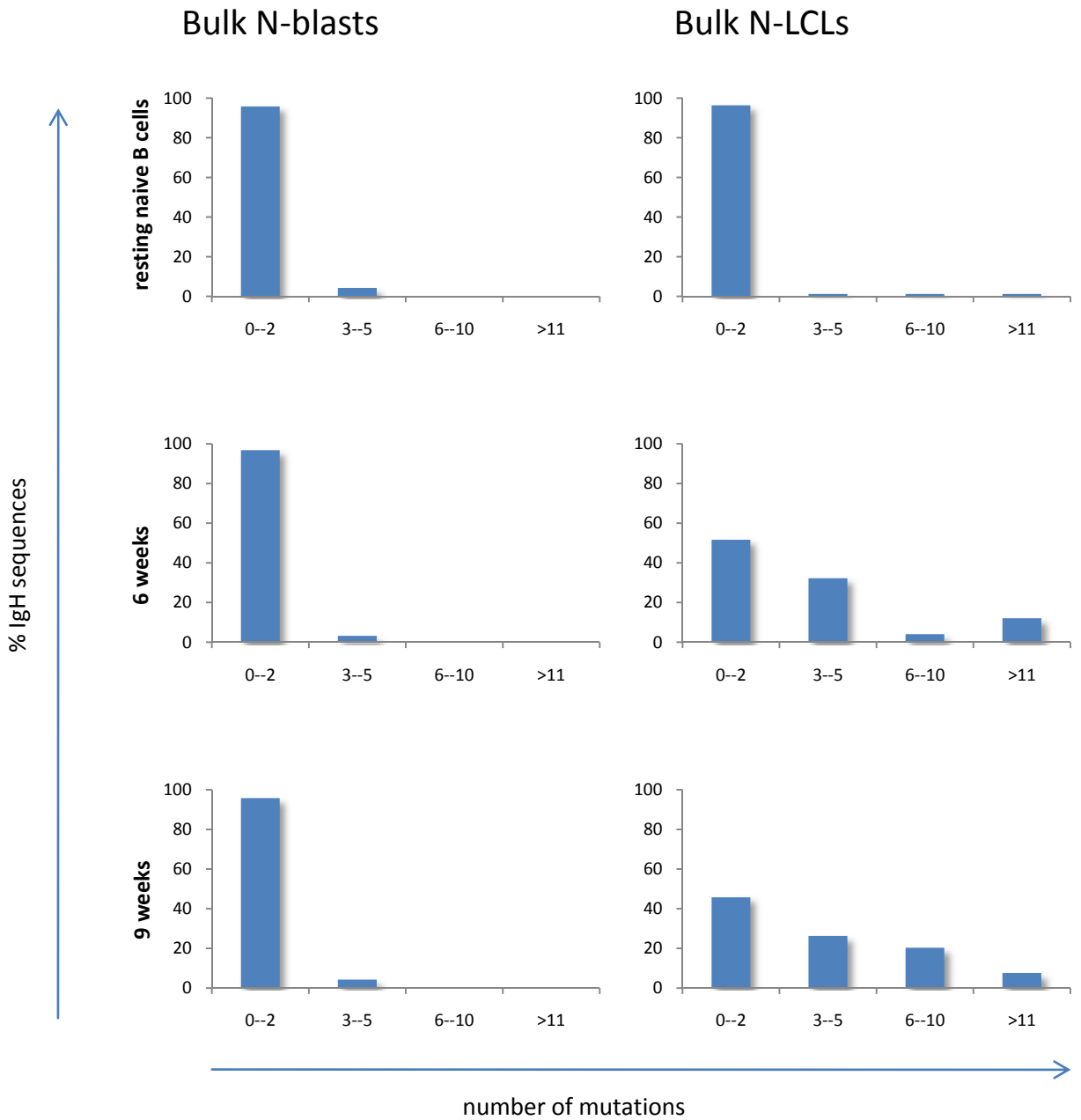


Figure 53. Mutation frequencies in PB BN-blast and BN-LCL cultures over time

IgH sequence data pooled from all BN-blast and BN-LCL cultures. The frequency of IgH mutations in the BN-blasts remained comparable to that of resting naive B cells up to 9 weeks post-establishment. In the BN-LCLs, however, an increase in IgH mutation frequency was observed from 6 weeks post-infection.

revealed that while BN-LCL3 yielded a substantial number of mutated IgH sequences from six weeks onwards, very few IgH sequences from BN-blast 3 were mutated.

The BN-blast IgH data also served to confirm that mutations identified within IgH sequences derived from the LCLs were not merely a reflection of PCR error, since if this were the case, mutations would be expected to arise in IgH sequences from both cultures. Taken together these findings verify that the mutated IgH sequences identified in N-LCL cultures are a result of EBV-driven transformation of naive B cells, rather than an artifact of *in vitro* cell culture or IgH analysis techniques. In order to explore why SHM was detected in a proportion of LCL cultures, but not in BN-blasts, we examined the expression of functionally distinct AID isoforms and of other proteins involved in SHM (UNG and pol- η).

Expression of AID Isoforms

In addition to the fully competent, most abundantly expressed full length AID isoform (AID-FL), AID is known to exist as several other isoforms generated by alternative splicing of the full length transcript. In a recent study, two isoforms in particular were associated with impaired AID function, namely AID- Δ E4, reportedly deficient in CSR, and AID- Δ E3E4, reportedly deficient in both CSR and SHM (Wu et al., 2008). Wu and colleagues further demonstrated that single cells derived from B-CLL were only able to express one given AID isoform, and suggested therefore that the function of the enzyme is regulated by alternative splicing to produce different variants, some of which may be functionally restricted.

Based on the possibility that differentially expressed AID isoforms may be responsible for the presence or absence of mutated IgH sequences, or indeed the lack of CSR observed in cultures included in the present study, qPCR assays were designed to examine the expression of three isoform transcripts in the LCL and BN-blast cultures. The results from these assays showed no preferential expression of AID splice variants associated with CSR or SHM deficiency (AID- Δ E4 or AID- Δ E3E4) in any of the LCLs or BN-blasts. Although upregulation of AID- Δ E4 was detected in most instances, levels of the fully competent AID-FL isoform were consistently approximately 10-fold higher. The lack of SHM observed in the BN-blasts, cord blood LCLs and a proportion of adult LCLs was therefore unlikely to be a result of preferential expression of a functionally defective AID splice variant.

Both AID-FL and AID- Δ E4 transcripts were expressed at consistently higher levels in the BN-blasts than in LCLs, with substantial transcript levels detected at earlier timepoints in the former (~ 3 days) than in the latter (7-14 days). These discrepancies could be a result of the EBNA2-driven inhibitory effect on AID expression that has been described elsewhere (Tobollik et al., 2006). In this study although EBNA2 alone was able to reduce AID expression, subsequent upregulation of other components of the latency III program including LMP1, was able to counterbalance the effects of EBNA2 to a certain degree. Although AID expression was not completely ablated by EBNA2-mediated inhibition, it is possible that the balance between this effect and the LMP1-induced upregulation of AID (He et al., 2003, Tobollik et al., 2006) may contribute to the relatively low levels of AID expression seen in BN-LCLs compared to BN-blasts.

Accessory factors involved in SHM

In normal circumstances, damage introduced to the genome is repaired by high fidelity enzymes, in an error-free manner. During a GC reaction, however, AID-induced DNA damage is repaired in an error-prone fashion, ensuring the accumulation of mutations within the IgH variable region (Peled et al., 2008). Two molecules involved in the repair of AID-mediated damage include; UNG, which is primarily responsible for initiating base excision repair of IgH genes in GC B cells *in vivo* (Di Noia and Neuberger, 2002, Imai et al., 2003), and Pol- η , an error-prone polymerase that has been implicated in the generation of mutations in IgH genes (Kunkel et al., 2003). The present results revealed that both UNG and pol- η were expressed in BN-blasts and LCLs, with no discernable difference in expression levels detected in any particular culture. Thus the expression of these accessory factors is unlikely to account for the lack of SHM seen in a proportion of LCLs and in all BN-blasts.

Regulation of AID Activity

Although we were able to demonstrate that AID transcripts were expressed in LCLs and BN-blasts, it is possible that post-transcriptional modifications of the AID protein may regulate its activity. Due to its potential to induce DNA damage, the expression and function of AID is tightly controlled within healthy individuals. Much research is currently being carried out to decipher the extensive mechanisms that are in place to regulate the activity of the enzyme (Lee-Theilen and Chaudhuri, 2010). Expression of AID has been shown to be regulated by microRNAs such as mir-155 and mir-181b (Teng et al., 2008, Dorsett et al., 2008, de Yebenes et al., 2008), and recent work has also found

evidence that transcription is actively repressed in inactivated B cells and non-B cells by silencer elements which are overcome following activation by CD40L, IL-4 and transforming growth factor- β *in vitro* (Tran et al., 2010).

Post-translational modifications of the AID protein also serve to regulate its activity. Since disruption of phosphorylation sites (such as serine 38) in knock-in mice results in defective CSR and SHM (McBride et al., 2008, Cheng et al., 2009), it has been suggested that phosphorylation of different residues within the AID protein may distinguish between CSR and SHM activity (Delker et al., 2009). Additionally, the subcellular localisation of the AID protein determines the extent to which it is able to come into contact with the genome, and therefore dictates its function. It is known that AID shuttles back and forth between the cytoplasm and nucleus (Ito et al., 2004, McBride et al., 2004, Brar et al., 2004). However whilst it was previously believed that the protein was able to diffuse passively from the one to the other, recent evidence suggests that AID is retained in the cytoplasm or imported to the nucleus in an active manner (McBride et al., 2004, Brar et al., 2004).

Although none of the specific regulatory mechanisms described above can conclusively provide an explanation for the lack of SHM found in some cultures examined in this study, given the myriad of systems in place to regulate AID function, it is not surprising that its activity may be dysregulated in the non-physiological setting of *in vitro* cell culture. Future studies could focus on any one of these regulatory systems in order to determine the discrepancy in SHM activity observed between adult N-LCLs, BCB-LCLs and BN-blasts.

Intriguingly, other viruses including hepatitis C virus (HCV) and Abelson murine leukemia virus (Ab-MLV) have also been shown to upregulate AID expression, together with SHM activity (Sale and Neuberger, 1998, Gourzi et al., 2006, Machida et al., 2004). AID has even been implicated in the host response against Ab-MLV infection since AID-expressing infected cells displayed reduced proliferation with simultaneous upregulation of the immune recognition molecule NKG2DL (Gourzi et al., 2006). Indeed other deaminating enzymes have been shown to act in the defence against retroviral infection by inflicting DNA damage upon the single stranded DNA viral genome. Although any link between EBV-induced AID expression *in vivo* and the host defence against EBV infection remains to be established, it is interesting to speculate that AID may contribute to the elimination of infected cells by instigating genome-wide DNA damage and subsequent cell death.

4.8.4 EBV Infection does not Induce Isotype-Switching in Vitro

The question of whether *in vitro* EBV infection of B cells is able to induce CSR is controversial. While one study described LMP1-induced isotype-switching to IgG (He et al., 2003), others have shown that infection of IgD⁺ PB B cells was unable to induce CSR (Miyawaki et al., 1991). Phenotypic analysis of the LCLs generated in the current study revealed that EBV-transformed PB N-LCLs, tonsillar N-LCLs and cord blood LCLs retained expression of IgM and IgD, and therefore EBV infection *in vitro* did not induce CSR.

In order to determine whether EBV-transformed N-LCLs of PB, tonsil and cord blood origin retained the capacity to undergo CSR, a selection of cultures were provided with various signals known to induce isotype switching *ex vivo*. These

experiments were based on a recent study where PB naive B cells and cord blood B cells were induced to switch to IgG and IgA following the provision of two signals; CD40 ligation and cytokine stimulation (Avery et al., 2008). These authors show that while CD40L plus either IL-4 or IL-21 induced isotype switching to IgG in a proportion of cells, CD40L plus IL-4 with IL-21 produced a synergistic effect, increasing IgG expression 2-fold compared to either cytokine alone. Although IgA expression was induced by treatment with CD40L and IL-21, cells treated with CD40L plus IL-4 with IL-21 did not upregulate IgA expression. Similarly, CD40L with IL-4 alone did not induce isotype-switching to IgA.

Consistent with Avery et al. we found that CD40L treatment with both cytokines (IL-4 and IL-21) had a synergistic effect on the frequency of cells switching to IgG; showing a 5-fold increase compared to CD40L with IL-4 alone. In conflict with Avery et al., however, CD40L/IL-4/IL-21 treatment resulted in a marked increase in IgA+ cells in recently-transformed (~2 weeks) PB N-LCL cultures. Long-established (>3 months) N-LCL cultures derived from PB, tonsil and cord blood, however, were able to switch to IgG, but not IgA. The time spent in culture may therefore have an effect on the capacity to switch to this isotype.

Taken together the results from these experiments suggest that although EBV infection alone is not capable of inducing CSR of B cells *in vitro*, the cells do retain their capacity to switch when provided with the appropriate signals.

4.8.5 LCLs are Characterised by Outgrowth of Dominant Clones

In bulk LCLs examined in the current study, clonal outgrowth was observed primarily by IgH sequence analysis, and confirmed by CDR3 spectratyping.

The tendency of LCL cultures to become monoclonal over time has also been documented by other researchers (Kataoka et al., 1997, Ryan et al., 2006, Lacoste et al., 2010). Such clonal expansions were identified within our LCLs between four and six weeks post-infection, and although the time scale of the progression towards monoclonality varied from culture to culture, dominant families were clearly present in each, with most being either monoclonal or biclonal by twelve weeks post-infection. By this time, each LCL culture had been passaged approximately the same number of times (data not shown), and therefore the variation in time post-infection at which monoclonality was achieved was unlikely to be entirely attributable to proliferation rate. These findings are in agreement with those described by others, whose LCL cultures also reached monoclonality between 8 to 12 weeks post-infection (Ryan et al., 2006, Lacoste et al., 2010). Furthermore, in the study carried out by Ryan et al. the time taken for individual LCL cultures to become monoclonal did not correlate with the rate of cell proliferation.

Clonal Selection in LCL Cultures

In several of the LCLs studied in this investigation the most frequently detected clonal family at early time points was often replaced by a separate clone later on. This switch in dominant clones over time, which was also reported by Lacoste et al, suggests either that a minority of clonally related cells harbour growth advantages enabling their positive selection in the culture, or that the majority of cells are unable to survive due to certain disadvantages, and are essentially negatively selected. Such advantages or disadvantages are unlikely to be a result of IgH mutation since dominant clones carrying unmutated IgH genes were identified in at least one of the LCL cultures. However, while AID is

known to target the IgH locus primarily, its ectopic expression is associated with SHM of non-IgH genes that are undergoing active transcription (Muramatsu et al., 1999, Epeldegui et al., 2007, Liu and Schatz, 2009). There exists, therefore, a possibility that regardless of mutations in the IgH region, AID-induced mutations may have accumulated elsewhere in the genome, and conferred growth advantages to certain cell clones which were positively selected in the culture. This theory may explain the fact that although a broad range of related cells representing various stages of successive SHM were detected within clonal families, multiple IgH sequences derived from dominant families often carried identical, family-specific patterns of mutation. This suggests that during a particular round of SHM, a growth advantage was simultaneously provided to the cell, allowing subsequent clonal expansion in the culture. Although such an advantage is unlikely to be provided by the IgH mutation itself, the introduction of a favourable mutation elsewhere in the genome is a possibility.

Alternatively, Lacoste et al. propose a negative selection process based on evidence that EBV induces genomic instability (in the form of aberrations in chromosome structure) as early as four weeks post-infection. The highest frequency of EBV-induced DNA damage took place at four weeks post-infection, but thereafter declined until six months when the LCL cultures comprised single clones possessing stable karyotypes. The authors therefore suggest that those cells subjected to the most extensive EBV-induced damage died off early on, allowing only healthy cell clones to thrive within the culture.

Taking into consideration the possibility of positive selection via advantageous AID-mediated mutations, or negative selection due to extensive AID-mediated

DNA damage, it is tempting to suggest that either or both of these processes contribute to the outgrowth of certain clones identified within the LCL cultures of this study.

Relevance of EBV-induced Clonal Outgrowth in Vivo

Although clonal outgrowth within EBV-transformed cultures *in vitro* was an interesting observation, it may have little significance to the issue of EBV persistence *in vivo*, since the virus is predominantly found in polyclonal populations of memory B cells in healthy individuals (Souza et al., 2005). The possibility that EBV-induced mutations may confer growth advantages to some cells, resulting in clonal expansion, may be more relevant in post-transplant lymphoproliferations (PTLs). Indeed both PTL tumours and LCLs express the latency III program, and several studies have shown that the majority of EBV-driven post-transplant lymphomas are monoclonal (Gulley et al., 1992, Chadburn et al., 1997, Locker and Nalesnik, 1989). Furthermore, in an *in vitro* examination of LCL cultures generated from total PBMCs, clonal outgrowth correlated with decreasing numbers of T cells in the cultures, the time scale of which, corresponded to the earliest diagnoses of PTL₇ (Ryan et al., 2006).

5 Conclusions and Future Work

It has long been acknowledged that EBV persistently infects circulating IgD-CD27+ switched memory B cells for life in immunocompetent hosts (Babcock et al., 1998). The processes by which this persistence is established during primary infection, however, remain the subject of debate; the central issue of which hinges on whether or not GC-transit of infected cells is necessary. In one model (shown in Figure 54), the virus first targets naive B cells in the oropharyngeal lymphoid tissue, whereby expression of Latency III proteins essentially mimics antigen-driven stimulation of the infected cell, driving it to participate in a GC reaction. After undergoing SHM and CSR, the virus downregulates expression of all viral antigens in order to avoid immune detection and persist in the differentiated memory B cell (Thorley-Lawson, 2001). An alternative model (shown in Figure 54b) challenges the involvement of the GC in this selective colonisation and instead proposes that oropharyngeal memory B cells are either preferentially infected by EBV, or both naive and memory cells are targeted, with the latter cell type possessing a growth advantage following infection (Kurth et al., 2000).

In order to explore this issue in further detail, we carried out a series of *ex vivo* and *in vitro* experiments. In our *ex vivo* investigation, we showed firstly that EBV is capable of colonising a B cell subset (IgD+CD27+ non-switched memory) that most likely develops independently of the GC, and secondly that the virus was rarely detected in CD38+ GC B cells from healthy carrier tonsils. In our *in vitro* infection experiments, we found that in a non-GC environment EBV infection of naive B cells alone is capable of conferring a mutated IgH

Figure 54. Proposed models of selective EBV colonisation of the memory B cell reservoir

A. Shows the current GC-dependent model of EBV persistence in the switched (S) memory B cell compartment (Thorley-Lawson et al., 2001). The virus initially infects naive B cells where Latency III antigens such as LMP1 and LMP2 mimic antigen-driven B cell activation to drive the cell through a GC reaction. The infected cell undergoes SHM and CSR to differentiate into a S memory B cell, whereupon expression of viral antigens are downregulated. **B.** In a second model, which challenges the involvement of GC transit, memory B cells are preferentially infected, or possess a survival advantage post-infection (Kurth et al., 2000). **C.** Depiction of an alternative model of GC-independent memory B cell colonisation based on the *in vitro* results generated in the current study. EBV infection of naive B cells is followed by expression of Latency III antigens and upregulation of AID. EBV infection alone may induce SHM, whereas infection together with the receipt of CSR-inducing signals (CD40-ligation plus cytokines), may induce isotype-switching, producing an infected cell harbouring the genotypic and phenotypic characteristics of a S memory B cell. Our *ex vivo* results show that EBV is able to colonise the NS memory B cell population. Whether this occurs as a result of direct infection, or reflects EBV-induced SHM of infected naive B cells without CSR remains to be resolved. Adapted from Rowe et al. 2009.

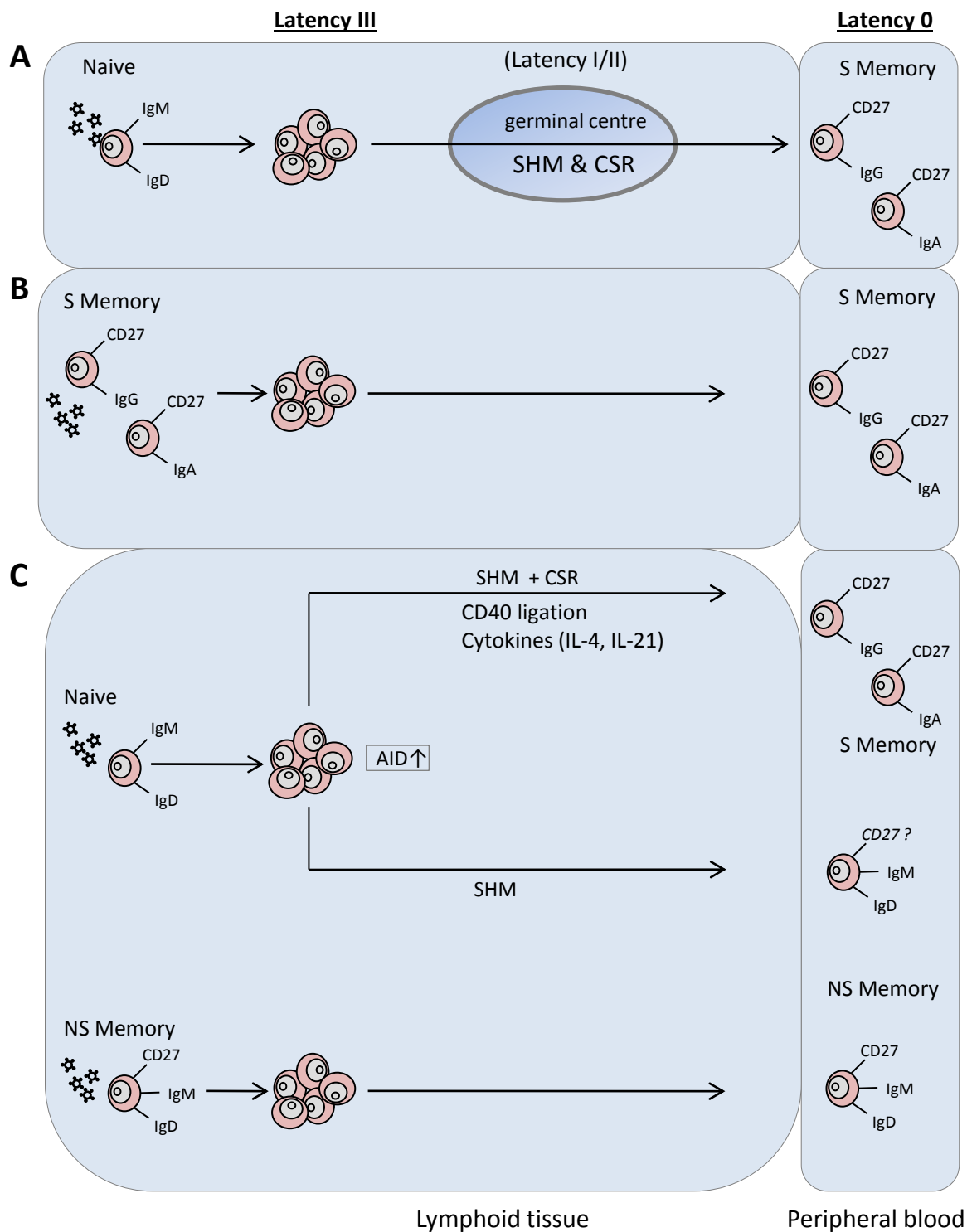


Figure 54. Proposed models of EBV colonisation of the memory B cell reservoir

memory B cell genotype upon a fraction of cells. We further showed that when provided with appropriate stimulation, these EBV-infected cells could be induced to isotype-switch to a memory B cell phenotype. Although these findings were observed in an *in vitro* setting, they raise the possibility that a similar phenomenon may occur *in vivo*. Taken together therefore, these results suggest that EBV is able to establish persistence of both switched and non-switched B cells in a germinal centre-independent manner. A simple diagrammatic depiction of the current models describing selective colonisation of the memory B cell compartment, together with an alternative hypothesis based on the findings of this study is shown in Figure 54.

Future investigations could concentrate on whether EBV directly infects specific tonsillar B cell populations (naive, switched memory and non-switched memory). In light of our observations, it would be particularly useful to examine whether EBV-infected circulating non-switched memory B cells are the result of direct infection, or rather represent naive B cells that have acquired mutated Ig genes, together with CD27 expression, as a result of EBV infection. Further *ex vivo* studies may seek to find evidence of SHM in EBV-positive phenotypically naive tonsillar B cells. To this end, EBER-positive cells could be isolated from both the tonsil and peripheral blood, followed by single cell IgH RT-PCR. It may also be informative to analyse viral load and distribution in individuals who have recently undergone B cell-depleting therapies such as rituximab (Roll et al., 2006, Dorner and Burmester, 2008). Here the central aim would be to follow the re-population of the B cell compartment and in parallel determine the EBV load. A key question would be whether detectable EBV is only seen after memory cells have emerged or whether EBV can colonise the circulating

immature or naive B cells in the absence of switched memory B cells in these patients.

Regarding the *in vitro* study, it is unclear why SHM is seen only in a fraction of EBV-infected cells and not at all in CD40 blasts, despite the observed upregulation of AID in these cultures. Analysis of AID within single cells from LCLs or CD40 blasts may reveal differences in the regulation of AID activity, for example in cellular localisation of the protein, which may be examined microscopically using a fluorescence-labeled antibody for AID. The relationship between EBV infection, AID expression and the emergence of dominant clones within LCL cultures also deserves further investigation, in the context of virus-driven PTLD lesions. Assuming that the functional capacity of AID is comparable in each EBV-infected cell *in vitro*, sequencing the entire genome in representative cells from LCL clonal families may identify other non-IgH genes targeted by AID as a result of EBV transformation. Indeed if such cellular mutations were identified, their potential to confer growth advantages or disadvantages could be explored.

In conclusion, the observations made in this project are important in terms of the controversy surrounding the initial events during EBV primary infection and establishment of persistence. The finding that EBV is capable of inducing SHM via the ectopic expression of AID in infected naive B cells may prove to be of further importance to the oncogenic potential of the virus.

6 References

- ABBOT, S. D., ROWE, M., CADWALLADER, K., RICKSTEN, A., GORDON, J., WANG, F., RYMO, L. & RICKINSON, A. B. 1990. Epstein-Barr virus nuclear antigen 2 induces expression of the virus-encoded latent membrane protein. *J Virol*, 64, 2126-34.
- ADAMS, A. 1987. Replication of latent Epstein-Barr virus genomes in Raji cells. *J Virol*, 61, 1743-6.
- ADEMOKUN, A., WU, Y. C. & DUNN-WALTERS, D. 2010. The ageing B cell population: composition and function. *Biogerontology*, 11, 125-37.
- ADHIKARY, S. & EILERS, M. 2005. Transcriptional regulation and transformation by Myc proteins. *Nat Rev Mol Cell Biol*, 6, 635-45.
- AGEMATSU, K., NAGUMO, H., SHINOZAKI, K., HOKIBARA, S., YASUI, K., TERADA, K., KAWAMURA, N., TOBA, T., NONOYAMA, S., OCHS, H. D. & KOMIYAMA, A. 1998. Absence of IgD-CD27(+) memory B cell population in X-linked hyper-IgM syndrome. *J Clin Invest*, 102, 853-60.
- AITKEN, C., SENGUPTA, S. K., AEDES, C., MOSS, D. J. & SCULLEY, T. B. 1994. Heterogeneity within the Epstein-Barr virus nuclear antigen 2 gene in different strains of Epstein-Barr virus. *J Gen Virol*, 75 (Pt 1), 95-100.
- ALBER, G., KIM, K. M., WEISER, P., RIESTERER, C., CARSETTI, R. & RETH, M. 1993. Molecular mimicry of the antigen receptor signalling motif by transmembrane proteins of the Epstein-Barr virus and the bovine leukaemia virus. *Curr Biol*, 3, 333-9.
- ALBESIANO, E., MESSMER, B. T., DAMLE, R. N., ALLEN, S. L., RAI, K. R. & CHIORAZZI, N. 2003. Activation-induced cytidine deaminase in chronic lymphocytic leukemia B cells: expression as multiple forms in a dynamic, variably sized fraction of the clone. *Blood*, 102, 3333-9.
- ALDINUCCI, D., LORENZON, D., CATTARUZZA, L., PINTO, A., GLOGHINI, A., CARBONE, A. & COLOMBATTI, A. 2008. Expression of CCR5 receptors on Reed-Sternberg cells and Hodgkin lymphoma cell lines: involvement of CCL5/Rantes in tumor cell growth and microenvironmental interactions. *Int J Cancer*, 122, 769-76.

- ALFIERI, C., BIRKENBACH, M. & KIEFF, E. 1991. Early events in Epstein-Barr virus infection of human B lymphocytes. *Virology*, 181, 595-608.
- ALLAN, G. J., INMAN, G. J., PARKER, B. D., ROWE, D. T. & FARRELL, P. J. 1992. Cell growth effects of Epstein-Barr virus leader protein. *J Gen Virol*, 73 (Pt 6), 1547-51.
- ALLMAN, D., JAIN, A., DENT, A., MAILE, R. R., SELVAGGI, T., KEHRY, M. R. & STAUDT, L. M. 1996. BCL-6 expression during B-cell activation. *Blood*, 87, 5257-68.
- ALTMANN, M. & HAMMERSCHMIDT, W. 2005. Epstein-Barr virus provides a new paradigm: a requirement for the immediate inhibition of apoptosis. *PLoS Biol*, 3, e404.
- ALTMANN, M., PICH, D., RUISS, R., WANG, J., SUGDEN, B. & HAMMERSCHMIDT, W. 2006. Transcriptional activation by EBV nuclear antigen 1 is essential for the expression of EBV's transforming genes. *Proc Natl Acad Sci U S A*, 103, 14188-93.
- ANAGNOSTOPOULOS, I., HANSMANN, M. L., FRANSSILA, K., HARRIS, M., HARRIS, N. L., JAFFE, E. S., HAN, J., VAN KRIEKEN, J. M., POPPEMA, S., MARAFIOTI, T., FRANKLIN, J., SEXTRO, M., DIEHL, V. & STEIN, H. 2000. European Task Force on Lymphoma project on lymphocyte predominance Hodgkin disease: histologic and immunohistologic analysis of submitted cases reveals 2 types of Hodgkin disease with a nodular growth pattern and abundant lymphocytes. *Blood*, 96, 1889-99.
- ANAGNOSTOPOULOS, I., HUMMEL, M., KRESCHER, C. & STEIN, H. 1995. Morphology, immunophenotype, and distribution of latently and/or productively Epstein-Barr virus-infected cells in acute infectious mononucleosis: implications for the interindividual infection route of Epstein-Barr virus. *Blood*, 85, 744-50.
- ANNELS, N. E., CALLAN, M. F., TAN, L. & RICKINSON, A. B. 2000. Changing patterns of dominant TCR usage with maturation of an EBV-specific cytotoxic T cell response. *J Immunol*, 165, 4831-41.
- APOLLONI, A. & SCULLEY, T. B. 1994. Detection of A-type and B-type Epstein-Barr virus in throat washings and lymphocytes. *Virology*, 202, 978-81.

- AUBIN, J., DAVI, F., NGUYEN-SALOMON, F., LEBOEUF, D., DEBERT, C., TAHER, M., VALENSI, F., CANIONI, D., BROUSSE, N., VARET, B. & ET AL. 1995. Description of a novel FR1 IgH PCR strategy and its comparison with three other strategies for the detection of clonality in B cell malignancies. *Leukemia*, 9, 471-9.
- AUSTIN, P. J., FLEMINGTON, E., YANDAVA, C. N., STROMINGER, J. L. & SPECK, S. H. 1988. Complex transcription of the Epstein-Barr virus BamHI fragment H rightward open reading frame 1 (BHRF1) in latently and lytically infected B lymphocytes. *Proc Natl Acad Sci U S A*, 85, 3678-82.
- AVERY, D. T., BRYANT, V. L., MA, C. S., DE WAAL MALEFYT, R. & TANGYE, S. G. 2008. IL-21-induced isotype switching to IgG and IgA by human naive B cells is differentially regulated by IL-4. *J Immunol*, 181, 1767-79.
- BABCOCK, G. J., DECKER, L. L., VOLK, M. & THORLEY-LAWSON, D. A. 1998. EBV persistence in memory B cells in vivo. *Immunity*, 9, 395-404.
- BABCOCK, G. J., HOCHBERG, D. & THORLEY-LAWSON, A. D. 2000. The expression pattern of Epstein-Barr virus latent genes in vivo is dependent upon the differentiation stage of the infected B cell. *Immunity*, 13, 497-506.
- BABCOCK, G. J. & THORLEY-LAWSON, D. A. 2000. Tonsillar memory B cells, latently infected with Epstein-Barr virus, express the restricted pattern of latent genes previously found only in Epstein-Barr virus-associated tumors. *Proc Natl Acad Sci U S A*, 97, 12250-5.
- BAER, R., BANKIER, A. T., BIGGIN, M. D., DEININGER, P. L., FARRELL, P. J., GIBSON, T. J., HATFULL, G., HUDSON, G. S., SATCHWELL, S. C., SEGUIN, C. & ET AL. 1984. DNA sequence and expression of the B95-8 Epstein-Barr virus genome. *Nature*, 310, 207-11.
- BALFOUR, H. H., JR., HOLMAN, C. J., HOKANSON, K. M., LELONEK, M. M., GIESBRECHT, J. E., WHITE, D. R., SCHMELING, D. O., WEBB, C. H., CAVERT, W., WANG, D. H. & BRUNDAGE, R. C. 2005. A prospective clinical study of Epstein-Barr virus and host interactions during acute infectious mononucleosis. *J Infect Dis*, 192, 1505-12.
- BANCHEREAU, J. & ROUSSET, F. 1992. Human B lymphocytes: phenotype, proliferation, and differentiation. *Adv Immunol*, 52, 125-262.

- BAUER, G. 2001. Simplicity through complexity: immunoblot with recombinant antigens as the new gold standard in Epstein-Barr virus serology. *Clin Lab*, 47, 223-30.
- BEARD, W. A. & WILSON, S. H. 2006. Structure and mechanism of DNA polymerase Beta. *Chem Rev*, 106, 361-82.
- BECHTEL, D., KURTH, J., UNKEL, C. & KUPPERS, R. 2005. Transformation of BCR-deficient germinal-center B cells by EBV supports a major role of the virus in the pathogenesis of Hodgkin and posttransplantation lymphomas. *Blood*, 106, 4345-50.
- BELL, A. I., GROVES, K., KELLY, G. L., CROOM-CARTER, D., HUI, E., CHAN, A. T. & RICKINSON, A. B. 2006. Analysis of Epstein-Barr virus latent gene expression in endemic Burkitt's lymphoma and nasopharyngeal carcinoma tumour cells by using quantitative real-time PCR assays. *J Gen Virol*, 87, 2885-90.
- BENNINGER-DORING, G., PEPPERL, S., DEML, L., MODROW, S., WOLF, H. & JILG, W. 1999. Frequency of CD8(+) T lymphocytes specific for lytic and latent antigens of Epstein-Barr virus in healthy virus carriers. *Virology*, 264, 289-97.
- BERGQVIST, P., GARDBY, E., STENSSON, A., BEMARK, M. & LYCKE, N. Y. 2006. Gut IgA class switch recombination in the absence of CD40 does not occur in the lamina propria and is independent of germinal centers. *J Immunol*, 177, 7772-83.
- BIHL, F., FRAHM, N., DI GIAMMARINO, L., SIDNEY, J., JOHN, M., YUSIM, K., WOODBERRY, T., SANGO, K., HEWITT, H. S., HENRY, L., LINDE, C. H., CHISHOLM, J. V., 3RD, ZAMAN, T. M., PAE, E., MALLAL, S., WALKER, B. D., SETTE, A., KORBER, B. T., HECKERMAN, D. & BRANDER, C. 2006. Impact of HLA-B alleles, epitope binding affinity, functional avidity, and viral coinfection on the immunodominance of virus-specific CTL responses. *J Immunol*, 176, 4094-101.
- BINNE, U. K., AMON, W. & FARRELL, P. J. 2002. Promoter sequences required for reactivation of Epstein-Barr virus from latency. *J Virol*, 76, 10282-9.
- BLAKE, J. M., EDWARDS, J. M., FLETCHER, W., MCSWIGGAN, D. A. & PEREIRA, M. S. 1976. Measurement of heterophil antibody and antibodies

- to EB viral capsid antigen IgG and IgM in suspected cases of infectious mononucleosis. *J Clin Pathol*, 29, 841-7.
- BRANSTEITTER, R., PHAM, P., CALABRESE, P. & GOODMAN, M. F. 2004. Biochemical analysis of hypermutational targeting by wild type and mutant activation-induced cytidine deaminase. *J Biol Chem*, 279, 51612-21.
- BRANSTEITTER, R., PHAM, P., SCHARFF, M. D. & GOODMAN, M. F. 2003. Activation-induced cytidine deaminase deaminates deoxycytidine on single-stranded DNA but requires the action of RNase. *Proc Natl Acad Sci U S A*, 100, 4102-7.
- BRAR, S. S., WATSON, M. & DIAZ, M. 2004. Activation-induced cytosine deaminase (AID) is actively exported out of the nucleus but retained by the induction of DNA breaks. *J Biol Chem*, 279, 26395-401.
- BRAUD, V. M., TOMASEC, P. & WILKINSON, G. W. 2002. Viral evasion of natural killer cells during human cytomegalovirus infection. *Curr Top Microbiol Immunol*, 269, 117-29.
- BRAUNINGER, A., SCHMITZ, R., BECHTEL, D., RENNE, C., HANSMANN, M. L. & KUPPERS, R. 2006. Molecular biology of Hodgkin's and Reed/Sternberg cells in Hodgkin's lymphoma. *Int J Cancer*, 118, 1853-61.
- BRAUNINGER, A., WACKER, H. H., RAJEWSKY, K., KUPPERS, R. & HANSMANN, M. L. 2003. Typing the histogenetic origin of the tumor cells of lymphocyte-rich classical Hodgkin's lymphoma in relation to tumor cells of classical and lymphocyte-predominance Hodgkin's lymphoma. *Cancer Res*, 63, 1644-51.
- BRIERE, F., SERVET-DELPRAT, C., BRIDON, J. M., SAINT-REMY, J. M. & BANCHEREAU, J. 1994. Human interleukin 10 induces naive surface immunoglobulin D+ (sIgD+) B cells to secrete IgG1 and IgG3. *J Exp Med*, 179, 757-62.
- BROCHET, X., LEFRANC, M. P. & GIUDICELLI, V. 2008. IMGT/V-QUEST: the highly customized and integrated system for IG and TR standardized V-J and V-D-J sequence analysis. *Nucleic Acids Res*, 36, W503-8.
- BURKITT, D. 1958. A sarcoma involving the jaws in African children. *Br J Surg*, 46, 218-23.
- BURKITT, D. 1962. A children's cancer dependent on climatic factors. *Nature*, 194, 232-4.

- BUSTIN, S. A., BENES, V., NOLAN, T. & PFAFFL, M. W. 2005. Quantitative real-time RT-PCR--a perspective. *J Mol Endocrinol*, 34, 597-601.
- CALATTINI, S., SERETI, I., SCHEINBERG, P., KIMURA, H., CHILDS, R. W. & COHEN, J. I. 2010. Detection of EBV genomes in plasmablasts/plasma cells and non-B cells in the blood of most patients with EBV lymphoproliferative disorders by using Immuno-FISH. *Blood*, 116, 4546-59.
- CALDWELL, R. G., WILSON, J. B., ANDERSON, S. J. & LONGNECKER, R. 1998. Epstein-Barr virus LMP2A drives B cell development and survival in the absence of normal B cell receptor signals. *Immunity*, 9, 405-11.
- CALLAN, M. F., FAZOU, C., YANG, H., ROSTRON, T., POON, K., HATTON, C. & MCMICHAEL, A. J. 2000. CD8(+) T-cell selection, function, and death in the primary immune response in vivo. *J Clin Invest*, 106, 1251-61.
- CALLAN, M. F., TAN, L., ANNELS, N., OGG, G. S., WILSON, J. D., O'CALLAGHAN, C. A., STEVEN, N., MCMICHAEL, A. J. & RICKINSON, A. B. 1998. Direct visualization of antigen-specific CD8+ T cells during the primary immune response to Epstein-Barr virus In vivo. *J Exp Med*, 187, 1395-402.
- CANAAN, A., HAVIV, I., URBAN, A. E., SCHULZ, V. P., HARTMAN, S., ZHANG, Z., PALEJEV, D., DEISSEROTH, A. B., LACY, J., SNYDER, M., GERSTEIN, M. & WEISSMAN, S. M. 2009. EBNA1 regulates cellular gene expression by binding cellular promoters. *Proc Natl Acad Sci U S A*, 106, 22421-6.
- CANNONS, J. L., YU, L. J., JANKOVIC, D., CROTTY, S., HORAI, R., KIRBY, M., ANDERSON, S., CHEEVER, A. W., SHER, A. & SCHWARTZBERG, P. L. 2006. SAP regulates T cell-mediated help for humoral immunity by a mechanism distinct from cytokine regulation. *J Exp Med*, 203, 1551-65.
- CAPELLO, D., CERRI, M., MUTI, G., BERRA, E., ORESTE, P., DEAMBROGI, C., ROSSI, D., DOTTI, G., CONCONI, A., VIGANO, M., MAGRINI, U., IPPOLITI, G., MORRA, E., GLOGHINI, A., RAMBALDI, A., PAULLI, M., CARBONE, A. & GAIDANO, G. 2003. Molecular histogenesis of posttransplantation lymphoproliferative disorders. *Blood*, 102, 3775-85.
- CARBONE, A. 2003. Emerging pathways in the development of AIDS-related lymphomas. *Lancet Oncol*, 4, 22-9.

- CATALINA, M. D., SULLIVAN, J. L., BAK, K. R. & LUZURIAGA, K. 2001. Differential evolution and stability of epitope-specific CD8(+) T cell responses in EBV infection. *J Immunol*, 167, 4450-7.
- CATALINA, M. D., SULLIVAN, J. L., BRODY, R. M. & LUZURIAGA, K. 2002. Phenotypic and functional heterogeneity of EBV epitope-specific CD8+ T cells. *J Immunol*, 168, 4184-91.
- CHADBURN, A., CESARMAN, E. & KNOWLES, D. M. 1997. Molecular pathology of posttransplantation lymphoproliferative disorders. *Semin Diagn Pathol*, 14, 15-26.
- CHAGANTI, S., BELL, A. I., PASTOR, N. B., MILNER, A. E., DRAYSON, M., GORDON, J. & RICKINSON, A. B. 2005. Epstein-Barr virus infection in vitro can rescue germinal center B cells with inactivated immunoglobulin genes. *Blood*, 106, 4249-52.
- CHAGANTI, S., HEATH, E. M., BERGLER, W., KUO, M., BUETTNER, M., NIEDOBITEK, G., RICKINSON, A. B. & BELL, A. I. 2009. Epstein-Barr virus colonization of tonsillar and peripheral blood B-cell subsets in primary infection and persistence. *Blood*, 113, 6372-81.
- CHAGANTI, S., MA, C. S., BELL, A. I., CROOM-CARTER, D., HISLOP, A. D., TANGYE, S. G. & RICKINSON, A. B. 2008. Epstein-Barr virus persistence in the absence of conventional memory B cells: IgM+IgD+CD27+ B cells harbor the virus in X-linked lymphoproliferative disease patients. *Blood*, 112, 672-9.
- CHANG, K. C., KHEN, N. T., JONES, D. & SU, I. J. 2005. Epstein-Barr virus is associated with all histological subtypes of Hodgkin lymphoma in Vietnamese children with special emphasis on the entity of lymphocyte predominance subtype. *Hum Pathol*, 36, 747-55.
- CHEN, A., DIVISCONTE, M., JIANG, X., QUINK, C. & WANG, F. 2005. Epstein-Barr virus with the latent infection nuclear antigen 3B completely deleted is still competent for B-cell growth transformation in vitro. *J Virol*, 79, 4506-9.
- CHEN, H., SMITH, P., AMBINDER, R. F. & HAYWARD, S. D. 1999. Expression of Epstein-Barr virus BamHI-A rightward transcripts in latently infected B cells from peripheral blood. *Blood*, 93, 3026-32.

- CHENE, A., DONATI, D., GUERREIRO-CACAIS, A. O., LEVITSKY, V., CHEN, Q., FALK, K. I., OREM, J., KIRONDE, F., WAHLGREN, M. & BEJARANO, M. T. 2007. A molecular link between malaria and Epstein-Barr virus reactivation. *PLoS Pathog*, 3, e80.
- CHENG, H. L., VUONG, B. Q., BASU, U., FRANKLIN, A., SCHWER, B., ASTARITA, J., PHAN, R. T., DATTA, A., MANIS, J., ALT, F. W. & CHAUDHURI, J. 2009. Integrity of the AID serine-38 phosphorylation site is critical for class switch recombination and somatic hypermutation in mice. *Proc Natl Acad Sci U S A*, 106, 2717-22.
- CHEZAR, I., LOBEL-LAVI, L., STEINITZ, M. & LASKOV, R. 2008. Ongoing somatic hypermutation of the rearranged VH but not of the V-lambda gene in EBV-transformed rheumatoid factor-producing lymphoblastoid cell line. *Mol Immunol*, 46, 80-90.
- CHIANG, A. K., TAO, Q., SRIVASTAVA, G. & HO, F. C. 1996. Nasal NK- and T-cell lymphomas share the same type of Epstein-Barr virus latency as nasopharyngeal carcinoma and Hodgkin's disease. *Int J Cancer*, 68, 285-90.
- CLARKE, P. A., SCHWEMMLE, M., SCHICKINGER, J., HILSE, K. & CLEMENS, M. J. 1991. Binding of Epstein-Barr virus small RNA EBER-1 to the double-stranded RNA-activated protein kinase DAI. *Nucleic Acids Res*, 19, 243-8.
- CLINE, J., BRAMAN, J. C. & HOGREFE, H. H. 1996. PCR fidelity of pfu DNA polymerase and other thermostable DNA polymerases. *Nucleic Acids Res*, 24, 3546-51.
- CLUDTS, I. & FARRELL, P. J. 1998. Multiple functions within the Epstein-Barr virus EBNA-3A protein. *J Virol*, 72, 1862-9.
- CLUTE, S. C., WATKIN, L. B., CORNBERG, M., NAUMOV, Y. N., SULLIVAN, J. L., LUZURIAGA, K., WELSH, R. M. & SELIN, L. K. 2005. Cross-reactive influenza virus-specific CD8+ T cells contribute to lymphoproliferation in Epstein-Barr virus-associated infectious mononucleosis. *J Clin Invest*, 115, 3602-12.
- COFFEY, A. J., BROOKSBANK, R. A., BRANDAU, O., OOHASHI, T., HOWELL, G. R., BYE, J. M., CAHN, A. P., DURHAM, J., HEATH, P., WRAY, P., PAVITT, R., WILKINSON, J., LEVERSHA, M., HUCKLE, E.,

- SHAW-SMITH, C. J., DUNHAM, A., RHODES, S., SCHUSTER, V., PORTA, G., YIN, L., SERAFINI, P., SYLLA, B., ZOLLO, M., FRANCO, B., BOLINO, A., SERI, M., LANYI, A., DAVIS, J. R., WEBSTER, D., HARRIS, A., LENOIR, G., DE ST BASILE, G., JONES, A., BEHLORADSKY, B. H., ACHATZ, H., MURKEN, J., FASSLER, R., SUMEGI, J., ROMEO, G., VAUDIN, M., ROSS, M. T., MEINDL, A. & BENTLEY, D. R. 1998. Host response to EBV infection in X-linked lymphoproliferative disease results from mutations in an SH2-domain encoding gene. *Nat Genet*, 20, 129-35.
- COHEN, J. I., WANG, F., MANNICK, J. & KIEFF, E. 1989. Epstein-Barr virus nuclear protein 2 is a key determinant of lymphocyte transformation. *Proc Natl Acad Sci U S A*, 86, 9558-62.
- CORDIER, M., CALENDER, A., BILLAUD, M., ZIMBER, U., ROUSSELET, G., PAVLISH, O., BANCHEREAU, J., TURSZ, T., BORNKAMM, G. & LENOIR, G. M. 1990. Stable transfection of Epstein-Barr virus (EBV) nuclear antigen 2 in lymphoma cells containing the EBV P3HR1 genome induces expression of B-cell activation molecules CD21 and CD23. *J Virol*, 64, 1002-13.
- COTTER, M. A., 2ND & ROBERTSON, E. S. 2000. Modulation of histone acetyltransferase activity through interaction of epstein-barr nuclear antigen 3C with prothymosin alpha. *Mol Cell Biol*, 20, 5722-35.
- COUTINHO, A. & MOLLER, G. 1975. Thymus-independent B-cell induction and paralysis. *Adv Immunol*, 21, 113-236.
- CRAWFORD, D. H., MACSWEEN, K. F., HIGGINS, C. D., THOMAS, R., MCAULAY, K., WILLIAMS, H., HARRISON, N., REID, S., CONACHER, M., DOUGLAS, J. & SWERDLOW, A. J. 2006. A cohort study among university students: identification of risk factors for Epstein-Barr virus seroconversion and infectious mononucleosis. *Clin Infect Dis*, 43, 276-82.
- CROTTY, S., KERSH, E. N., CANNONS, J., SCHWARTZBERG, P. L. & AHMED, R. 2003. SAP is required for generating long-term humoral immunity. *Nature*, 421, 282-7.
- CROUGH, T., BURROWS, J. M., FAZOU, C., WALKER, S., DAVENPORT, M. P. & KHANNA, R. 2005. Contemporaneous fluctuations in T cell responses to persistent herpes virus infections. *Eur J Immunol*, 35, 139-49.

- CUNNINGHAM, A. F., GASPAL, F., SERRE, K., MOHR, E., HENDERSON, I. R., SCOTT-TUCKER, A., KENNY, S. M., KHAN, M., TOELLNER, K. M., LANE, P. J. & MACLENNAN, I. C. 2007. Salmonella induces a switched antibody response without germinal centers that impedes the extracellular spread of infection. *J Immunol*, 178, 6200-7.
- DALLA-FAVERA, R., BREGNI, M., ERIKSON, J., PATTERSON, D., GALLO, R. C. & CROCE, C. M. 1982. Human c-myc onc gene is located on the region of chromosome 8 that is translocated in Burkitt lymphoma cells. *Proc Natl Acad Sci U S A*, 79, 7824-7.
- DAMBAUGH, T., HENNESSY, K., CHAMNANKIT, L. & KIEFF, E. 1984. U2 region of Epstein-Barr virus DNA may encode Epstein-Barr nuclear antigen 2. *Proc Natl Acad Sci U S A*, 81, 7632-6.
- DAVIS-POYNTER, N. J. & FARRELL, H. E. 1996. Masters of deception: a review of herpesvirus immune evasion strategies. *Immunol Cell Biol*, 74, 513-22.
- DAVISON, A. J., EBERLE, R., EHLERS, B., HAYWARD, G. S., MCGEOCH, D. J., MINSON, A. C., PELLETT, P. E., ROIZMAN, B., STUDDERT, M. J. & THIRY, E. 2009. The order Herpesvirales. *Arch Virol*, 154, 171-7.
- DE VINUESA, C. G., COOK, M. C., BALL, J., DREW, M., SUNNERS, Y., CASCALHO, M., WABL, M., KLAUS, G. G. & MACLENNAN, I. C. 2000. Germinal centers without T cells. *J Exp Med*, 191, 485-94.
- DE YEBENES, V. G., BELVER, L., PISANO, D. G., GONZALEZ, S., VILLASANTE, A., CROCE, C., HE, L. & RAMIRO, A. R. 2008. miR-181b negatively regulates activation-induced cytidine deaminase in B cells. *J Exp Med*, 205, 2199-206.
- DEFRANCE, T., VANBERVLIET, B., BRIERE, F., DURAND, I., ROUSSET, F. & BANCHEREAU, J. 1992. Interleukin 10 and transforming growth factor beta cooperate to induce anti-CD40-activated naive human B cells to secrete immunoglobulin A. *J Exp Med*, 175, 671-82.
- DELBOS, F., AOUFOUCHI, S., FAILI, A., WEILL, J. C. & REYNAUD, C. A. 2007. DNA polymerase eta is the sole contributor of A/T modifications during immunoglobulin gene hypermutation in the mouse. *J Exp Med*, 204, 17-23.

- DELKER, R. K., FUGMANN, S. D. & PAPAVALIIOU, F. N. 2009. A coming-of-age story: activation-induced cytidine deaminase turns 10. *Nat Immunol*, 10, 1147-53.
- DEVERGNE, O., CAHIR MCFARLAND, E. D., MOSIALOS, G., IZUMI, K. M., WARE, C. F. & KIEFF, E. 1998. Role of the TRAF binding site and NF-kappaB activation in Epstein-Barr virus latent membrane protein 1-induced cell gene expression. *J Virol*, 72, 7900-8.
- DI NOIA, J. & NEUBERGER, M. S. 2002. Altering the pathway of immunoglobulin hypermutation by inhibiting uracil-DNA glycosylase. *Nature*, 419, 43-8.
- DI NOIA, J. M. & NEUBERGER, M. S. 2007. Molecular mechanisms of antibody somatic hypermutation. *Annu Rev Biochem*, 76, 1-22.
- DILLNER, J., KALLIN, B., ALEXANDER, H., ERNBERG, I., UNO, M., ONO, Y., KLEIN, G. & LERNER, R. A. 1986. An Epstein-Barr virus (EBV)-determined nuclear antigen (EBNA5) partly encoded by the transformation-associated Bam WYH region of EBV DNA: preferential expression in lymphoblastoid cell lines. *Proc Natl Acad Sci U S A*, 83, 6641-5.
- DOGAN, A., BAGDI, E., MUNSON, P. & ISAACSON, P. G. 2000. CD10 and BCL-6 expression in paraffin sections of normal lymphoid tissue and B-cell lymphomas. *Am J Surg Pathol*, 24, 846-52.
- DOLCETTI, R., BOIOCCHI, M., GLOGHINI, A. & CARBONE, A. 2001. Pathogenetic and histogenetic features of HIV-associated Hodgkin's disease. *Eur J Cancer*, 37, 1276-87.
- DORNER, M., ZUCOL, F., ALESSI, D., HAERLE, S. K., BOSSART, W., WEBER, M., BYLAND, R., BERNASCONI, M., BERGER, C., TUGIZOV, S., SPECK, R. F. & NADAL, D. 2010. beta1 integrin expression increases susceptibility of memory B cells to Epstein-Barr virus infection. *J Virol*, 84, 6667-77.
- DORNER, M., ZUCOL, F., BERGER, C., BYLAND, R., MELROE, G. T., BERNASCONI, M., SPECK, R. F. & NADAL, D. 2008. Distinct ex vivo susceptibility of B-cell subsets to epstein-barr virus infection according to differentiation status and tissue origin. *J Virol*, 82, 4400-12.

- DORNER, T. & BURMESTER, G. R. 2008. New approaches of B-cell-directed therapy: beyond rituximab. *Curr Opin Rheumatol*, 20, 263-8.
- DORNER, T., FOSTER, S. J., BREZINSCHEK, H. P. & LIPSKY, P. E. 1998. Analysis of the targeting of the hypermutational machinery and the impact of subsequent selection on the distribution of nucleotide changes in human VHDJH rearrangements. *Immunol Rev*, 162, 161-71.
- DORSETT, Y., MCBRIDE, K. M., JANKOVIC, M., GAZUMYAN, A., THAI, T. H., ROBBIANI, D. F., DI VIRGILIO, M., SAN-MARTIN, B. R., HEIDKAMP, G., SCHWICKERT, T. A., EISENREICH, T., RAJEWSKY, K. & NUSSENZWEIG, M. C. 2008. MicroRNA-155 suppresses activation-induced cytidine deaminase-mediated Myc-Igh translocation. *Immunity*, 28, 630-8.
- DORSETT, Y., ROBBIANI, D. F., JANKOVIC, M., REINA-SAN-MARTIN, B., EISENREICH, T. R. & NUSSENZWEIG, M. C. 2007. A role for AID in chromosome translocations between c-myc and the IgH variable region. *J Exp Med*, 204, 2225-32.
- DORSHKIND, K. & MONTECINO-RODRIGUEZ, E. 2007. Fetal B-cell lymphopoiesis and the emergence of B-1-cell potential. *Nat Rev Immunol*, 7, 213-9.
- DRESANG, L. R., VEREIDE, D. T. & SUGDEN, B. 2009. Identifying sites bound by Epstein-Barr virus nuclear antigen 1 (EBNA1) in the human genome: defining a position-weighted matrix to predict sites bound by EBNA1 in viral genomes. *J Virol*, 83, 2930-40.
- DREXLER, H. G. 1992. Recent results on the biology of Hodgkin and Reed-Sternberg cells. I. Biopsy material. *Leuk Lymphoma*, 8, 283-313.
- DUKERS, D. F., JASPARS, L. H., VOS, W., OUDEJANS, J. J., HAYES, D., CILLESSEN, S., MIDDELDORP, J. M. & MEIJER, C. J. 2000. Quantitative immunohistochemical analysis of cytokine profiles in Epstein-Barr virus-positive and -negative cases of Hodgkin's disease. *J Pathol*, 190, 143-9.
- DUNNE, P. J., FAINT, J. M., GUDGEON, N. H., FLETCHER, J. M., PLUNKETT, F. J., SOARES, M. V., HISLOP, A. D., ANNELS, N. E., RICKINSON, A. B., SALMON, M. & AKBAR, A. N. 2002. Epstein-Barr virus-specific CD8(+) T cells that re-express CD45RA are apoptosis-resistant memory cells that retain replicative potential. *Blood*, 100, 933-40.

- DUNNICK, W., HERTZ, G. Z., SCAPPINO, L. & GRITZMACHER, C. 1993. DNA sequences at immunoglobulin switch region recombination sites. *Nucleic Acids Res*, 21, 365-72.
- DYKSTRA, M. L., LONGNECKER, R. & PIERCE, S. K. 2001. Epstein-Barr virus coopts lipid rafts to block the signaling and antigen transport functions of the BCR. *Immunity*, 14, 57-67.
- EHLERS, B., SPIESS, K., LEENDERTZ, F., PEETERS, M., BOESCH, C., GATHERER, D. & MCGEOCH, D. J. 2010. Lymphocryptovirus phylogeny and the origins of Epstein-Barr virus. *J Gen Virol*, 91, 630-42.
- EHLIN-HENRIKSSON, B., GORDON, J. & KLEIN, G. 2003. B-lymphocyte subpopulations are equally susceptible to Epstein-Barr virus infection, irrespective of immunoglobulin isotype expression. *Immunology*, 108, 427-30.
- EPELDEGUI, M., HUNG, Y. P., MCQUAY, A., AMBINDER, R. F. & MARTINEZ-MAZA, O. 2007. Infection of human B cells with Epstein-Barr virus results in the expression of somatic hypermutation-inducing molecules and in the accrual of oncogene mutations. *Mol Immunol*, 44, 934-42.
- EPSTEIN, M. A., ACHONG, B. G. & BARR, Y. M. 1964. Virus Particles in Cultured Lymphoblasts from Burkitt's Lymphoma. *Lancet*, 1, 702-3.
- FAFI-KREMER, S., MORAND, P., BRION, J. P., PAVESE, P., BACCARD, M., GERMI, R., GENOULAZ, O., NICOD, S., JOLIVET, M., RUIGROK, R. W., STAHL, J. P. & SEIGNEURIN, J. M. 2005. Long-term shedding of infectious Epstein-Barr virus after infectious mononucleosis. *J Infect Dis*, 191, 985-9.
- FAHRAEUS, R., FU, H. L., ERNBERG, I., FINKE, J., ROWE, M., KLEIN, G., FALK, K., NILSSON, E., YADAV, M., BUSSON, P. & ET AL. 1988. Expression of Epstein-Barr virus-encoded proteins in nasopharyngeal carcinoma. *Int J Cancer*, 42, 329-38.
- FAHRAEUS, R., JANSSON, A., RICKSTEN, A., SJOBLOM, A. & RYMO, L. 1990. Epstein-Barr virus-encoded nuclear antigen 2 activates the viral latent membrane protein promoter by modulating the activity of a negative regulatory element. *Proc Natl Acad Sci U S A*, 87, 7390-4.
- FAULKNER, G. C., BURROWS, S. R., KHANNA, R., MOSS, D. J., BIRD, A. G. & CRAWFORD, D. H. 1999. X-Linked agammaglobulinemia patients are

- not infected with Epstein-Barr virus: implications for the biology of the virus. *J Virol*, 73, 1555-64.
- FAYETTE, J., DUBOIS, B., VANDENABEELE, S., BRIDON, J. M., VANBERVLIET, B., DURAND, I., BANCHEREAU, J., CAUX, C. & BRIERE, F. 1997. Human dendritic cells skew isotype switching of CD40-activated naive B cells towards IgA1 and IgA2. *J Exp Med*, 185, 1909-18.
- FECTEAU, J. F., COTE, G. & NERON, S. 2006. A new memory CD27-IgG+ B cell population in peripheral blood expressing VH genes with low frequency of somatic mutation. *J Immunol*, 177, 3728-36.
- FECTEAU, J. F. & NERON, S. 2003. CD40 stimulation of human peripheral B lymphocytes: distinct response from naive and memory cells. *J Immunol*, 171, 4621-9.
- FINKE, J., ROWE, M., KALLIN, B., ERNBERG, I., ROSEN, A., DILLNER, J. & KLEIN, G. 1987. Monoclonal and polyclonal antibodies against Epstein-Barr virus nuclear antigen 5 (EBNA-5) detect multiple protein species in Burkitt's lymphoma and lymphoblastoid cell lines. *J Virol*, 61, 3870-8.
- FISCHER, M., JUREMALM, M., OLSSON, N., BACKLIN, C., SUNDSTROM, C., NILSSON, K., ENBLAD, G. & NILSSON, G. 2003. Expression of CCL5/RANTES by Hodgkin and Reed-Sternberg cells and its possible role in the recruitment of mast cells into lymphomatous tissue. *Int J Cancer*, 107, 197-201.
- FLAVELL, J. R., BAUMFORTH, K. R., WOOD, V. H., DAVIES, G. L., WEI, W., REYNOLDS, G. M., MORGAN, S., BOYCE, A., KELLY, G. L., YOUNG, L. S. & MURRAY, P. G. 2008. Down-regulation of the TGF-beta target gene, PTPRK, by the Epstein-Barr virus encoded EBNA1 contributes to the growth and survival of Hodgkin lymphoma cells. *Blood*, 111, 292-301.
- FOK, V., MITTON-FRY, R. M., GRECH, A. & STEITZ, J. A. 2006. Multiple domains of EBER 1, an Epstein-Barr virus noncoding RNA, recruit human ribosomal protein L22. *RNA*, 12, 872-82.
- FRANGO, P., BUETTNER, M. & NIEDOBITEK, G. 2005. Epstein-Barr virus (EBV) infection in epithelial cells in vivo: rare detection of EBV replication in tongue mucosa but not in salivary glands. *J Infect Dis*, 191, 238-42.

- GAHN, T. A. & SUGDEN, B. 1995. An EBNA-1-dependent enhancer acts from a distance of 10 kilobase pairs to increase expression of the Epstein-Barr virus LMP gene. *J Virol*, 69, 2633-6.
- GAMADIA, L. E., REMMERSWAAL, E. B., WEEL, J. F., BEMELMAN, F., VAN LIER, R. A. & TEN BERGE, I. J. 2003. Primary immune responses to human CMV: a critical role for IFN-gamma-producing CD4+ T cells in protection against CMV disease. *Blood*, 101, 2686-92.
- GASCAN, H., GAUCHAT, J. F., AVERSA, G., VAN VLASSELAER, P. & DEVRIES, J. E. 1991. Anti-CD40 monoclonal antibodies or CD4+ T cell clones and IL-4 induce IgG4 and IgE switching in purified human B cells via different signaling pathways. *J Immunol*, 147, 8-13.
- GEHA, R. S., JABARA, H. H. & BRODEUR, S. R. 2003. The regulation of immunoglobulin E class-switch recombination. *Nat Rev Immunol*, 3, 721-32.
- GEISBERGER, R., LAMERS, M. & ACHATZ, G. 2006. The riddle of the dual expression of IgM and IgD. *Immunology*, 118, 429-37.
- GERBER, P., LUCAS, S., NONOYAMA, M., PERLIN, E. & GOLDSTEIN, L. I. 1972. Oral excretion of Epstein-Barr virus by healthy subjects and patients with infectious mononucleosis. *Lancet*, 2, 988-9.
- GIL, Y., LEVY-NABOT, S., STEINITZ, M. & LASKOV, R. 2007. Somatic mutations and activation-induced cytidine deaminase (AID) expression in established rheumatoid factor-producing lymphoblastoid cell line. *Mol Immunol*, 44, 494-505.
- GILLIGAN, K., SATO, H., RAJADURAI, P., BUSSON, P., YOUNG, L., RICKINSON, A., TURSZ, T. & RAAB-TRAUB, N. 1990. Novel transcription from the Epstein-Barr virus terminal EcoRI fragment, DJhet, in a nasopharyngeal carcinoma. *J Virol*, 64, 4948-56.
- GIUDICELLI, V., CHAUME, D., MENNESSIER, G., ALTHAUS, H. H., MULLER, W., BODMER, J., MALIK, A. & LEFRANC, M. P. 1998. IMGT, the international ImMunoGeneTics database: a new design for immunogenetics data access. *Stud Health Technol Inform*, 52 Pt 1, 351-5.
- GORDON, M. S., KANEGAI, C. M., DOERR, J. R. & WALL, R. 2003. Somatic hypermutation of the B cell receptor genes B29 (Igbeta, CD79b) and mb1 (Igalpha, CD79a). *Proc Natl Acad Sci U S A*, 100, 4126-31.

- GOURZI, P., LEONOVA, T. & PAPAVALIIOU, F. N. 2006. A role for activation-induced cytidine deaminase in the host response against a transforming retrovirus. *Immunity*, 24, 779-86.
- GRATAMA, J. W., OOSTERVEER, M. A., KLEIN, G. & ERNBERG, I. 1990. EBNA size polymorphism can be used to trace Epstein-Barr virus spread within families. *J Virol*, 64, 4703-8.
- GRATAMA, J. W., OOSTERVEER, M. A., WEIMAR, W., SINTNICOLAAS, K., SIZOO, W., BOLHUIS, R. L. & ERNBERG, I. 1994. Detection of multiple 'Ebnotypes' in individual Epstein-Barr virus carriers following lymphocyte transformation by virus derived from peripheral blood and oropharynx. *J Gen Virol*, 75 (Pt 1), 85-94.
- GRAY, J. J. 1995. Avidity of EBV VCA-specific IgG antibodies: distinction between recent primary infection, past infection and reactivation. *J Virol Methods*, 52, 95-104.
- GREENWOOD, B. M. & VICK, R. M. 1975. Evidence for a malaria mitogen in human malaria. *Nature*, 257, 592-4.
- GREEVE, J., PHILIPSEN, A., KRAUSE, K., KLAPPER, W., HEIDORN, K., CASTLE, B. E., JANDA, J., MARCU, K. B. & PARWARESCH, R. 2003. Expression of activation-induced cytidine deaminase in human B-cell non-Hodgkin lymphomas. *Blood*, 101, 3574-80.
- GREGORY, C. D., EDWARDS, C. F., MILNER, A., WIELS, J., LIPINSKI, M., ROWE, M., TURSZ, T. & RICKINSON, A. B. 1988. Isolation of a normal B cell subset with a Burkitt-like phenotype and transformation in vitro with Epstein-Barr virus. *Int J Cancer*, 42, 213-20.
- GROSSMAN, S. R., JOHANNSEN, E., TONG, X., YALAMANCHILI, R. & KIEFF, E. 1994. The Epstein-Barr virus nuclear antigen 2 transactivator is directed to response elements by the J kappa recombination signal binding protein. *Proc Natl Acad Sci U S A*, 91, 7568-72.
- GULLEY, M. L., RAPHAEL, M., LUTZ, C. T., ROSS, D. W. & RAAB-TRAUB, N. 1992. Epstein-Barr virus integration in human lymphomas and lymphoid cell lines. *Cancer*, 70, 185-91.
- GUPPY, A. E., RAWLINGS, E., MADRIGAL, J. A., AMLLOT, P. L. & BARBER, L. D. 2007. A quantitative assay for Epstein-Barr Virus-specific immunity shows interferon-gamma producing CD8+ T cells increase during

- immunosuppression reduction to treat posttransplant lymphoproliferative disease. *Transplantation*, 84, 1534-9.
- HA, Y. J., MUN, Y. C., SEONG, C. M. & LEE, J. R. 2008. Characterization of phenotypically distinct B-cell subsets and receptor-stimulated mitogen-activated protein kinase activation in human cord blood B cells. *J Leukoc Biol*, 84, 1557-64.
- HAAS, K. M., POE, J. C., STEEBER, D. A. & TEDDER, T. F. 2005. B-1a and B-1b cells exhibit distinct developmental requirements and have unique functional roles in innate and adaptive immunity to *S. pneumoniae*. *Immunity*, 23, 7-18.
- HABESHAW, G., YAO, Q. Y., BELL, A. I., MORTON, D. & RICKINSON, A. B. 1999. Epstein-barr virus nuclear antigen 1 sequences in endemic and sporadic Burkitt's lymphoma reflect virus strains prevalent in different geographic areas. *J Virol*, 73, 965-75.
- HADINOTO, V., SHAPIRO, M., GREENOUGH, T. C., SULLIVAN, J. L., LUZURIAGA, K. & THORLEY-LAWSON, D. A. 2008. On the dynamics of acute EBV infection and the pathogenesis of infectious mononucleosis. *Blood*, 111, 1420-7.
- HADINOTO, V., SHAPIRO, M., SUN, C. C. & THORLEY-LAWSON, D. A. 2009. The dynamics of EBV shedding implicate a central role for epithelial cells in amplifying viral output. *PLoS Pathog*, 5, e1000496.
- HAMMERSCHMIDT, W. & SUGDEN, B. 1989. Genetic analysis of immortalizing functions of Epstein-Barr virus in human B lymphocytes. *Nature*, 340, 393-7.
- HAN, J. H., AKIRA, S., CALAME, K., BEUTLER, B., SELSING, E. & IMANISHI-KARI, T. 2007. Class switch recombination and somatic hypermutation in early mouse B cells are mediated by B cell and Toll-like receptors. *Immunity*, 27, 64-75.
- HARADA, S. & KIEFF, E. 1997. Epstein-Barr virus nuclear protein LP stimulates EBNA-2 acidic domain-mediated transcriptional activation. *J Virol*, 71, 6611-8.
- HARRIS, N. L., JAFFE, E. S., DIEBOLD, J., FLANDRIN, G., MULLER-HERMELINK, H. K., VARDIMAN, J., LISTER, T. A. & BLOOMFIELD, C. D. 2000. The World Health Organization classification of neoplastic diseases

- of the haematopoietic and lymphoid tissues: Report of the Clinical Advisory Committee Meeting, Airlie House, Virginia, November 1997. *Histopathology*, 36, 69-86.
- HE, B., RAAB-TRAUB, N., CASALI, P. & CERUTTI, A. 2003. EBV-encoded latent membrane protein 1 cooperates with BAFF/BLyS and APRIL to induce T cell-independent Ig heavy chain class switching. *J Immunol*, 171, 5215-24.
- HEID, C. A., STEVENS, J., LIVAK, K. J. & WILLIAMS, P. M. 1996. Real time quantitative PCR. *Genome Res*, 6, 986-94.
- HERRMANN, K., FRANGO, P., MIDDELDORP, J. & NIEDOBITEK, G. 2002. Epstein-Barr virus replication in tongue epithelial cells. *J Gen Virol*, 83, 2995-8.
- HICKABOTTOM, M., PARKER, G. A., FREEMONT, P., CROOK, T. & ALLDAY, M. J. 2002. Two nonconsensus sites in the Epstein-Barr virus oncoprotein EBNA3A cooperate to bind the co-repressor carboxyl-terminal-binding protein (CtBP). *J Biol Chem*, 277, 47197-204.
- HISLOP, A. D., GUDGEON, N. H., CALLAN, M. F., FAZOU, C., HASEGAWA, H., SALMON, M. & RICKINSON, A. B. 2001. EBV-specific CD8+ T cell memory: relationships between epitope specificity, cell phenotype, and immediate effector function. *J Immunol*, 167, 2019-29.
- HISLOP, A. D., KUO, M., DRAKE-LEE, A. B., AKBAR, A. N., BERGLER, W., HAMMERSCHMITT, N., KHAN, N., PALENDIRA, U., LEESE, A. M., TIMMS, J. M., BELL, A. I., BUCKLEY, C. D. & RICKINSON, A. B. 2005. Tonsillar homing of Epstein-Barr virus-specific CD8+ T cells and the virus-host balance. *J Clin Invest*, 115, 2546-55.
- HISLOP, A. D., TAYLOR, G. S., SAUCE, D. & RICKINSON, A. B. 2007. Cellular responses to viral infection in humans: lessons from Epstein-Barr virus. *Annu Rev Immunol*, 25, 587-617.
- HJALGRIM, H., ASKLING, J., ROSTGAARD, K., HAMILTON-DUTOIT, S., FRISCH, M., ZHANG, J. S., MADSEN, M., ROSDAHL, N., KONRADSEN, H. B., STORM, H. H. & MELBYE, M. 2003. Characteristics of Hodgkin's lymphoma after infectious mononucleosis. *N Engl J Med*, 349, 1324-32.
- HOCHBERG, D., SOUZA, T., CATALINA, M., SULLIVAN, J. L., LUZURIAGA, K. & THORLEY-LAWSON, D. A. 2004. Acute infection with Epstein-Barr

- virus targets and overwhelms the peripheral memory B-cell compartment with resting, latently infected cells. *J Virol*, 78, 5194-204.
- HODGKIN 1832. On some Morbid Appearances of the Absorbent Glands and Spleen. *Med Chir Trans*, 17, 68-114.
- HOUMANI, J. L., DAVIS, C. I. & RUF, I. K. 2009. Growth-promoting properties of Epstein-Barr virus EBER-1 RNA correlate with ribosomal protein L22 binding. *J Virol*, 83, 9844-53.
- HSIEH, J. J. & HAYWARD, S. D. 1995. Masking of the CBF1/RBPJ kappa transcriptional repression domain by Epstein-Barr virus EBNA2. *Science*, 268, 560-3.
- HU, Y. & SMYTH, G. K. 2009. ELDA: extreme limiting dilution analysis for comparing depleted and enriched populations in stem cell and other assays. *J Immunol Methods*, 347, 70-8.
- HUDNALL, S. D., GE, Y., WEI, L., YANG, N. P., WANG, H. Q. & CHEN, T. 2005. Distribution and phenotype of Epstein-Barr virus-infected cells in human pharyngeal tonsils. *Mod Pathol*, 18, 519-27.
- HUEN, D. S., HENDERSON, S. A., CROOM-CARTER, D. & ROWE, M. 1995. The Epstein-Barr virus latent membrane protein-1 (LMP1) mediates activation of NF-kappa B and cell surface phenotype via two effector regions in its carboxy-terminal cytoplasmic domain. *Oncogene*, 10, 549-60.
- IMAI, K., SLUPPHAUG, G., LEE, W. I., REVY, P., NONOYAMA, S., CATALAN, N., YEL, L., FORVEILLE, M., KAVLI, B., KROKAN, H. E., OCHS, H. D., FISCHER, A. & DURANDY, A. 2003. Human uracil-DNA glycosylase deficiency associated with profoundly impaired immunoglobulin class-switch recombination. *Nat Immunol*, 4, 1023-8.
- IMAI, S., KOIZUMI, S., SUGIURA, M., TOKUNAGA, M., UEMURA, Y., YAMAMOTO, N., TANAKA, S., SATO, E. & OSATO, T. 1994. Gastric carcinoma: monoclonal epithelial malignant cells expressing Epstein-Barr virus latent infection protein. *Proc Natl Acad Sci U S A*, 91, 9131-5.
- INOUE, H., NOJIMA, H. & OKAYAMA, H. 1990. High efficiency transformation of Escherichia coli with plasmids. *Gene*, 96, 23-8.
- IOACHIM, H. L., CRONIN, W., ROY, M. & MAYA, M. 1990. Persistent lymphadenopathies in people at high risk for HIV infection.

- Clinicopathologic correlations and long-term follow-up in 79 cases. *Am J Clin Pathol*, 93, 208-18.
- ITO, S., NAGAOKA, H., SHINKURA, R., BEGUM, N., MURAMATSU, M., NAKATA, M. & HONJO, T. 2004. Activation-induced cytidine deaminase shuttles between nucleus and cytoplasm like apolipoprotein B mRNA editing catalytic polypeptide 1. *Proc Natl Acad Sci U S A*, 101, 1975-80.
- IWAKIRI, D., EIZURU, Y., TOKUNAGA, M. & TAKADA, K. 2003. Autocrine growth of Epstein-Barr virus-positive gastric carcinoma cells mediated by an Epstein-Barr virus-encoded small RNA. *Cancer Res*, 63, 7062-7.
- IWAKIRI, D., SHEEN, T. S., CHEN, J. Y., HUANG, D. P. & TAKADA, K. 2005. Epstein-Barr virus-encoded small RNA induces insulin-like growth factor 1 and supports growth of nasopharyngeal carcinoma-derived cell lines. *Oncogene*, 24, 1767-73.
- IZUMI, K. M. & KIEFF, E. D. 1997. The Epstein-Barr virus oncogene product latent membrane protein 1 engages the tumor necrosis factor receptor-associated death domain protein to mediate B lymphocyte growth transformation and activate NF-kappaB. *Proc Natl Acad Sci U S A*, 94, 12592-7.
- JABARA, H. H., FU, S. M., GEHA, R. S. & VERCELLI, D. 1990. CD40 and IgE: synergism between anti-CD40 monoclonal antibody and interleukin 4 in the induction of IgE synthesis by highly purified human B cells. *J Exp Med*, 172, 1861-4.
- JANEWAY, C. A., JR. & MEDZHITOV, R. 2002. Innate immune recognition. *Annu Rev Immunol*, 20, 197-216.
- JEFFERIS, R. & KUMARARATNE, D. S. 1990. Selective IgG subclass deficiency: quantification and clinical relevance. *Clin Exp Immunol*, 81, 357-67.
- JIANG, H., CHO, Y. G. & WANG, F. 2000. Structural, functional, and genetic comparisons of Epstein-Barr virus nuclear antigen 3A, 3B, and 3C homologues encoded by the rhesus lymphocryptovirus. *J Virol*, 74, 5921-32.
- JOSEPH, A. M., BABCOCK, G. J. & THORLEY-LAWSON, D. A. 2000a. Cells expressing the Epstein-Barr virus growth program are present in and restricted to the naive B-cell subset of healthy tonsils. *J Virol*, 74, 9964-71.

- JOSEPH, A. M., BABCOCK, G. J. & THORLEY-LAWSON, D. A. 2000b. EBV persistence involves strict selection of latently infected B cells. *J Immunol*, 165, 2975-81.
- KAISER, C., LAUX, G., EICK, D., JOCHNER, N., BORNKAMM, G. W. & KEMPKES, B. 1999. The proto-oncogene c-myc is a direct target gene of Epstein-Barr virus nuclear antigen 2. *J Virol*, 73, 4481-4.
- KALLED, S. L., SIVA, N., STEIN, H. & REINHERZ, E. L. 1995. The distribution of CD10 (NEP 24.11, CALLA) in humans and mice is similar in non-lymphoid organs but differs within the hematopoietic system: absence on murine T and B lymphoid progenitors. *Eur J Immunol*, 25, 677-87.
- KANZLER, H., KUPPERS, R., HANSMANN, M. L. & RAJEWSKY, K. 1996. Hodgkin and Reed-Sternberg cells in Hodgkin's disease represent the outgrowth of a dominant tumor clone derived from (crippled) germinal center B cells. *J Exp Med*, 184, 1495-505.
- KAPATAI, G. & MURRAY, P. 2007. Contribution of the Epstein Barr virus to the molecular pathogenesis of Hodgkin lymphoma. *J Clin Pathol*, 60, 1342-9.
- KATAOKA, H., TAHARA, H., WATANABE, T., SUGAWARA, M., IDE, T., GOTO, M., FURUICHI, Y. & SUGIMOTO, M. 1997. immortalization of immunologically committed Epstein-Barr virus-transformed human B-lymphoblastoid cell lines accompanied by a strong telomerase activity. *Differentiation*, 62, 203-11.
- KAYE, K. M., IZUMI, K. M. & KIEFF, E. 1993. Epstein-Barr virus latent membrane protein 1 is essential for B-lymphocyte growth transformation. *Proc Natl Acad Sci U S A*, 90, 9150-4.
- KAYE, K. M., IZUMI, K. M., LI, H., JOHANNSEN, E., DAVIDSON, D., LONGNECKER, R. & KIEFF, E. 1999. An Epstein-Barr virus that expresses only the first 231 LMP1 amino acids efficiently initiates primary B-lymphocyte growth transformation. *J Virol*, 73, 10525-30.
- KAYKAS, A., WORRINGER, K. & SUGDEN, B. 2001. CD40 and LMP-1 both signal from lipid rafts but LMP-1 assembles a distinct, more efficient signaling complex. *EMBO J*, 20, 2641-54.
- KAYKAS, A., WORRINGER, K. & SUGDEN, B. 2002. LMP-1's transmembrane domains encode multiple functions required for LMP-1's efficient signaling. *J Virol*, 76, 11551-60.

- KELLY, G., BELL, A. & RICKINSON, A. 2002. Epstein-Barr virus-associated Burkitt lymphomagenesis selects for downregulation of the nuclear antigen EBNA2. *Nat Med*, 8, 1098-104.
- KELLY, G. L., LONG, H. M., STYLIANOU, J., THOMAS, W. A., LEESE, A., BELL, A. I., BORNKAMM, G. W., MAUTNER, J., RICKINSON, A. B. & ROWE, M. 2009. An Epstein-Barr virus anti-apoptotic protein constitutively expressed in transformed cells and implicated in burkitt lymphomagenesis: the Wp/BHRF1 link. *PLoS Pathog*, 5, e1000341.
- KELLY, G. L., MILNER, A. E., BALDWIN, G. S., BELL, A. I. & RICKINSON, A. B. 2006. Three restricted forms of Epstein-Barr virus latency counteracting apoptosis in c-myc-expressing Burkitt lymphoma cells. *Proc Natl Acad Sci U S A*, 103, 14935-40.
- KELLY, G. L., MILNER, A. E., TIERNEY, R. J., CROOM-CARTER, D. S., ALTMANN, M., HAMMERSCHMIDT, W., BELL, A. I. & RICKINSON, A. B. 2005. Epstein-Barr virus nuclear antigen 2 (EBNA2) gene deletion is consistently linked with EBNA3A, -3B, and -3C expression in Burkitt's lymphoma cells and with increased resistance to apoptosis. *J Virol*, 79, 10709-17.
- KELLY, G. L. & RICKINSON, A. B. 2007. Burkitt lymphoma: revisiting the pathogenesis of a virus-associated malignancy. *Hematology Am Soc Hematol Educ Program*, 277-84.
- KEMPKES, B., SPITKOVSKY, D., JANSEN-DURR, P., ELLWART, J. W., KREMMER, E., DELECLUSE, H. J., ROTTENBERGER, C., BORNKAMM, G. W. & HAMMERSCHMIDT, W. 1995. B-cell proliferation and induction of early G1-regulating proteins by Epstein-Barr virus mutants conditional for EBNA2. *EMBO J*, 14, 88-96.
- KHABIR, A., KARRAY, H., RODRIGUEZ, S., ROSE, M., DAOUD, J., FRIKHA, M., BOUDAWARA, T., MIDDELDORP, J., JLIDI, R. & BUSSON, P. 2005. EBV latent membrane protein 1 abundance correlates with patient age but not with metastatic behavior in north African nasopharyngeal carcinomas. *Virology*, 2, 39.
- KHAN, G., MIYASHITA, E. M., YANG, B., BABCOCK, G. J. & THORLEY-LAWSON, D. A. 1996. Is EBV persistence in vivo a model for B cell homeostasis? *Immunity*, 5, 173-9.

- KHAN, N., HISLOP, A., GUDGEON, N., COBBOLD, M., KHANNA, R., NAYAK, L., RICKINSON, A. B. & MOSS, P. A. 2004. Herpesvirus-specific CD8 T cell immunity in old age: cytomegalovirus impairs the response to a coresident EBV infection. *J Immunol*, 173, 7481-9.
- KILGER, E., KIESER, A., BAUMANN, M. & HAMMERSCHMIDT, W. 1998. Epstein-Barr virus-mediated B-cell proliferation is dependent upon latent membrane protein 1, which simulates an activated CD40 receptor. *EMBO J*, 17, 1700-9.
- KIRCHMAIER, A. L. & SUGDEN, B. 1995. Plasmid maintenance of derivatives of oriP of Epstein-Barr virus. *J Virol*, 69, 1280-3.
- KITAGAWA, N., GOTO, M., KUROZUMI, K., MARUO, S., FUKAYAMA, M., NAOE, T., YASUKAWA, M., HINO, K., SUZUKI, T., TODO, S. & TAKADA, K. 2000. Epstein-Barr virus-encoded poly(A)(-) RNA supports Burkitt's lymphoma growth through interleukin-10 induction. *EMBO J*, 19, 6742-50.
- KITANI, A. & STROBER, W. 1994. Differential regulation of C alpha 1 and C alpha 2 germ-line and mature mRNA transcripts in human peripheral blood B cells. *J Immunol*, 153, 1466-77.
- KLEIN, U., RAJEWSKY, K. & KUPPERS, R. 1998. Human immunoglobulin (Ig)M+IgD+ peripheral blood B cells expressing the CD27 cell surface antigen carry somatically mutated variable region genes: CD27 as a general marker for somatically mutated (memory) B cells. *J Exp Med*, 188, 1679-89.
- KLEIN, U., TU, Y., STOLOVITZKY, G. A., KELLER, J. L., HADDAD, J., JR., MILJKOVIC, V., CATTORETTI, G., CALIFANO, A. & DALLA-FAVERA, R. 2003. Transcriptional analysis of the B cell germinal center reaction. *Proc Natl Acad Sci U S A*, 100, 2639-44.
- KNIGHT, J. S., LAN, K., SUBRAMANIAN, C. & ROBERTSON, E. S. 2003. Epstein-Barr virus nuclear antigen 3C recruits histone deacetylase activity and associates with the corepressors mSin3A and NCoR in human B-cell lines. *J Virol*, 77, 4261-72.
- KRAMS, S. M. & MARTINEZ, O. M. 2008. Epstein-Barr virus, rapamycin, and host immune responses. *Curr Opin Organ Transplant*, 13, 563-8.

- KRAUER, K. G., BURGESS, A., BUCK, M., FLANAGAN, J., SCULLEY, T. B. & GABRIELLI, B. 2004. The EBNA-3 gene family proteins disrupt the G2/M checkpoint. *Oncogene*, 23, 1342-53.
- KRUETZMANN, S., ROSADO, M. M., WEBER, H., GERMING, U., TOURNILHAC, O., PETER, H. H., BERNER, R., PETERS, A., BOEHM, T., PLEBANI, A., QUINTI, I. & CARSETTI, R. 2003. Human immunoglobulin M memory B cells controlling *Streptococcus pneumoniae* infections are generated in the spleen. *J Exp Med*, 197, 939-45.
- KUNKEL, T. A., PAVLOV, Y. I. & BEBENEK, K. 2003. Functions of human DNA polymerases eta, kappa and iota suggested by their properties, including fidelity with undamaged DNA templates. *DNA Repair (Amst)*, 2, 135-49.
- KUPPERS, R. 2003. B cells under influence: transformation of B cells by Epstein-Barr virus. *Nat Rev Immunol*, 3, 801-12.
- KUPPERS, R. 2005. Mechanisms of B-cell lymphoma pathogenesis. *Nat Rev Cancer*, 5, 251-62.
- KUPPERS, R. 2009. The biology of Hodgkin's lymphoma. *Nat Rev Cancer*, 9, 15-27.
- KUPPERS, R., RAJEWSKY, K., ZHAO, M., SIMONS, G., LAUMANN, R., FISCHER, R. & HANSMANN, M. L. 1994. Hodgkin disease: Hodgkin and Reed-Sternberg cells picked from histological sections show clonal immunoglobulin gene rearrangements and appear to be derived from B cells at various stages of development. *Proc Natl Acad Sci U S A*, 91, 10962-6.
- KURAOKA, M., LIAO, D., YANG, K., ALLGOOD, S. D., LEVESQUE, M. C., KELSOE, G. & UEDA, Y. 2009. Activation-induced cytidine deaminase expression and activity in the absence of germinal centers: insights into hyper-IgM syndrome. *J Immunol*, 183, 3237-48.
- KURTH, J., HANSMANN, M. L., RAJEWSKY, K. & KUPPERS, R. 2003. Epstein-Barr virus-infected B cells expanding in germinal centers of infectious mononucleosis patients do not participate in the germinal center reaction. *Proc Natl Acad Sci U S A*, 100, 4730-5.
- KURTH, J., SPIEKER, T., WUSTROW, J., STRICKLER, G. J., HANSMANN, L. M., RAJEWSKY, K. & KUPPERS, R. 2000. EBV-infected B cells in

- infectious mononucleosis: viral strategies for spreading in the B cell compartment and establishing latency. *Immunity*, 13, 485-95.
- KUTOK, J. L. & WANG, F. 2006. Spectrum of Epstein-Barr virus-associated diseases. *Annu Rev Pathol*, 1, 375-404.
- LACOSTE, S., WIECHEC, E., DOS SANTOS SILVA, A. G., GUFFEI, A., WILLIAMS, G., LOWBEER, M., BENEDEK, K., HENRIKSSON, M., KLEIN, G. & MAI, S. 2010. Chromosomal rearrangements after ex vivo Epstein-Barr virus (EBV) infection of human B cells. *Oncogene*, 29, 503-15.
- LAICHALK, L. L., HOCHBERG, D., BABCOCK, G. J., FREEMAN, R. B. & THORLEY-LAWSON, D. A. 2002. The dispersal of mucosal memory B cells: evidence from persistent EBV infection. *Immunity*, 16, 745-54.
- LAICHALK, L. L. & THORLEY-LAWSON, D. A. 2005. Terminal differentiation into plasma cells initiates the replicative cycle of Epstein-Barr virus in vivo. *J Virol*, 79, 1296-307.
- LAWRENCE, J. B., VILLNAVE, C. A. & SINGER, R. H. 1988. Sensitive, high-resolution chromatin and chromosome mapping in situ: presence and orientation of two closely integrated copies of EBV in a lymphoma line. *Cell*, 52, 51-61.
- LEBIEN, T. W. & TEDDER, T. F. 2008. B lymphocytes: how they develop and function. *Blood*, 112, 1570-80.
- LEE-THEILEN, M. & CHAUDHURI, J. 2010. Walking the AID tightrope. *Nat Immunol*, 11, 107-9.
- LEE, M. A., DIAMOND, M. E. & YATES, J. L. 1999. Genetic evidence that EBNA-1 is needed for efficient, stable latent infection by Epstein-Barr virus. *J Virol*, 73, 2974-82.
- LENOIR, G. M., PREUD'HOMME, J. L., BERNHEIM, A. & BERGER, R. 1982. Correlation between immunoglobulin light chain expression and variant translocation in Burkitt's lymphoma. *Nature*, 298, 474-6.
- LERNER, M. R., ANDREWS, N. C., MILLER, G. & STEITZ, J. A. 1981. Two small RNAs encoded by Epstein-Barr virus and complexed with protein are precipitated by antibodies from patients with systemic lupus erythematosus. *Proc Natl Acad Sci U S A*, 78, 805-9.

- LI, Y. S., HAYAKAWA, K. & HARDY, R. R. 1993. The regulated expression of B lineage associated genes during B cell differentiation in bone marrow and fetal liver. *J Exp Med*, 178, 951-60.
- LI, Z., VAN CALCAR, S., QU, C., CAVENEY, W. K., ZHANG, M. Q. & REN, B. 2003. A global transcriptional regulatory role for c-Myc in Burkitt's lymphoma cells. *Proc Natl Acad Sci U S A*, 100, 8164-9.
- LIEBOWITZ, D. 1998. Epstein-Barr virus and a cellular signaling pathway in lymphomas from immunosuppressed patients. *N Engl J Med*, 338, 1413-21.
- LIN, J., JOHANNSEN, E., ROBERTSON, E. & KIEFF, E. 2002. Epstein-Barr virus nuclear antigen 3C putative repression domain mediates coactivation of the LMP1 promoter with EBNA-2. *J Virol*, 76, 232-42.
- LITMAN, G. W., RAST, J. P., SHAMBLOTT, M. J., HAIRE, R. N., HULST, M., ROESS, W., LITMAN, R. T., HINDS-FREY, K. R., ZILCH, A. & AMEMIYA, C. T. 1993. Phylogenetic diversification of immunoglobulin genes and the antibody repertoire. *Mol Biol Evol*, 10, 60-72.
- LIU, A., KLEIN, G., BANDOBASHI, K., KLEIN, E. & NAGY, N. 2002. SH2D1A expression reflects activation of T and NK cells in cord blood lymphocytes infected with EBV and treated with the immunomodulator PSK. *Immunol Lett*, 80, 181-8.
- LIU, M., DUKE, J. L., RICHTER, D. J., VINUESA, C. G., GOODNOW, C. C., KLEINSTEIN, S. H. & SCHATZ, D. G. 2008. Two levels of protection for the B cell genome during somatic hypermutation. *Nature*, 451, 841-5.
- LIU, M. & SCHATZ, D. G. 2009. Balancing AID and DNA repair during somatic hypermutation. *Trends Immunol*, 30, 173-81.
- LIU, Y. J., JOSHUA, D. E., WILLIAMS, G. T., SMITH, C. A., GORDON, J. & MACLENNAN, I. C. 1989. Mechanism of antigen-driven selection in germinal centres. *Nature*, 342, 929-31.
- LOCKER, J. & NALESNIK, M. 1989. Molecular genetic analysis of lymphoid tumors arising after organ transplantation. *Am J Pathol*, 135, 977-87.
- LONGNECKER, R. 2000. Epstein-Barr virus latency: LMP2, a regulator or means for Epstein-Barr virus persistence? *Adv Cancer Res*, 79, 175-200.

- LOSSOS, I. S., CZERWINSKI, D. K., WECHSER, M. A. & LEVY, R. 2003. Optimization of quantitative real-time RT-PCR parameters for the study of lymphoid malignancies. *Leukemia*, 17, 789-95.
- LOTZ, M., TSOUKAS, C. D., FONG, S., CARSON, D. A. & VAUGHAN, J. H. 1985. Regulation of Epstein-Barr virus infection by recombinant interferons. Selected sensitivity to interferon-gamma. *Eur J Immunol*, 15, 520-5.
- LU, F., WIKRAMASINGHE, P., NORSEEN, J., TSAI, K., WANG, P., SHOWE, L., DAVULURI, R. V. & LIEBERMAN, P. M. 2010. Genome-wide analysis of host-chromosome binding sites for Epstein-Barr Virus Nuclear Antigen 1 (EBNA1). *Virology*, 7, 262.
- LUFTIG, M., PRINARAKIS, E., YASUI, T., TSICHRITZIS, T., CAHIR-MCFARLAND, E., INOUE, J., NAKANO, H., MAK, T. W., YEH, W. C., LI, X., AKIRA, S., SUZUKI, N., SUZUKI, S., MOSIALOS, G. & KIEFF, E. 2003. Epstein-Barr virus latent membrane protein 1 activation of NF-kappaB through IRAK1 and TRAF6. *Proc Natl Acad Sci U S A*, 100, 15595-600.
- LUNEMANN, J. D. & MUNZ, C. 2009. EBV in MS: guilty by association? *Trends Immunol*, 30, 243-8.
- LUZURIAGA, K. & SULLIVAN, J. L. 2010. Infectious mononucleosis. *N Engl J Med*, 362, 1993-2000.
- MA, C. & STAUDT, L. M. 2001. Molecular definition of the germinal centre stage of B-cell differentiation. *Philos Trans R Soc Lond B Biol Sci*, 356, 83-9.
- MA, C. S., HARE, N. J., NICHOLS, K. E., DUPRE, L., ANDOLFI, G., RONCAROLO, M. G., ADELSTEIN, S., HODGKIN, P. D. & TANGYE, S. G. 2005. Impaired humoral immunity in X-linked lymphoproliferative disease is associated with defective IL-10 production by CD4+ T cells. *J Clin Invest*, 115, 1049-59.
- MA, C. S., NICHOLS, K. E. & TANGYE, S. G. 2007. Regulation of cellular and humoral immune responses by the SLAM and SAP families of molecules. *Annu Rev Immunol*, 25, 337-79.
- MA, C. S., PITTALUGA, S., AVERY, D. T., HARE, N. J., MARIC, I., KLION, A. D., NICHOLS, K. E. & TANGYE, S. G. 2006. Selective generation of functional somatically mutated IgM+CD27+, but not Ig isotype-switched,

- memory B cells in X-linked lymphoproliferative disease. *J Clin Invest*, 116, 322-33.
- MACEDO, C., DONNENBERG, A., POPESCU, I., REYES, J., ABU-ELMAGD, K., SHAPIRO, R., ZEEVI, A., FUNG, J. J., STORKUS, W. J. & METES, D. 2005. EBV-specific memory CD8+ T cell phenotype and function in stable solid organ transplant patients. *Transpl Immunol*, 14, 109-16.
- MACHIDA, K., CHENG, K. T., SUNG, V. M., SHIMODAIRA, S., LINDSAY, K. L., LEVINE, A. M., LAI, M. Y. & LAI, M. M. 2004. Hepatitis C virus induces a mutator phenotype: enhanced mutations of immunoglobulin and protooncogenes. *Proc Natl Acad Sci U S A*, 101, 4262-7.
- MACKEY, D., MIDDLETON, T. & SUGDEN, B. 1995. Multiple regions within EBNA1 can link DNAs. *J Virol*, 69, 6199-208.
- MACKEY, D. & SUGDEN, B. 1999. The linking regions of EBNA1 are essential for its support of replication and transcription. *Mol Cell Biol*, 19, 3349-59.
- MAINI, M. K., GUDGEON, N., WEDDERBURN, L. R., RICKINSON, A. B. & BEVERLEY, P. C. 2000. Clonal expansions in acute EBV infection are detectable in the CD8 and not the CD4 subset and persist with a variable CD45 phenotype. *J Immunol*, 165, 5729-37.
- MANCAO, C., ALTMANN, M., JUNGNICHEL, B. & HAMMERSCHMIDT, W. 2005. Rescue of "crippled" germinal center B cells from apoptosis by Epstein-Barr virus. *Blood*, 106, 4339-44.
- MANCAO, C. & HAMMERSCHMIDT, W. 2007. Epstein-Barr virus latent membrane protein 2A is a B-cell receptor mimic and essential for B-cell survival. *Blood*, 110, 3715-21.
- MANNICK, J. B., COHEN, J. I., BIRKENBACH, M., MARCHINI, A. & KIEFF, E. 1991. The Epstein-Barr virus nuclear protein encoded by the leader of the EBNA RNAs is important in B-lymphocyte transformation. *J Virol*, 65, 6826-37.
- MARKET, E. & PAPAVALIIOU, F. N. 2003. V(D)J recombination and the evolution of the adaptive immune system. *PLoS Biol*, 1, E16.
- MARSHALL, D. & SAMPLE, C. 1995. Epstein-Barr virus nuclear antigen 3C is a transcriptional regulator. *J Virol*, 69, 3624-30.
- MARTIN, F. & KEARNEY, J. F. 2001. B1 cells: similarities and differences with other B cell subsets. *Curr Opin Immunol*, 13, 195-201.

- MARTIN, F., OLIVER, A. M. & KEARNEY, J. F. 2001. Marginal zone and B1 B cells unite in the early response against T-independent blood-borne particulate antigens. *Immunity*, 14, 617-29.
- MASUCCI, M. G., TORSTEINDOTTIR, S., COLOMBANI, J., BRAUTBAR, C., KLEIN, E. & KLEIN, G. 1987. Down-regulation of class I HLA antigens and of the Epstein-Barr virus-encoded latent membrane protein in Burkitt lymphoma lines. *Proc Natl Acad Sci U S A*, 84, 4567-71.
- MASUDA, K., OUCHIDA, R., TAKEUCHI, A., SAITO, T., KOSEKI, H., KAWAMURA, K., TAGAWA, M., TOKUHISA, T., AZUMA, T. & J, O. W. 2005. DNA polymerase theta contributes to the generation of C/G mutations during somatic hypermutation of Ig genes. *Proc Natl Acad Sci U S A*, 102, 13986-91.
- MATHAS, S., JANZ, M., HUMMEL, F., HUMMEL, M., WOLLERT-WULF, B., LUSATIS, S., ANAGNOSTOPOULOS, I., LIETZ, A., SIGVARDSSON, M., JUNDT, F., JOHRENS, K., BOMMERT, K., STEIN, H. & DORKEN, B. 2006. Intrinsic inhibition of transcription factor E2A by HLH proteins ABF-1 and Id2 mediates reprogramming of neoplastic B cells in Hodgkin lymphoma. *Nat Immunol*, 7, 207-15.
- MCAULAY, K. A., HIGGINS, C. D., MACSWEEN, K. F., LAKE, A., JARRETT, R. F., ROBERTSON, F. L., WILLIAMS, H. & CRAWFORD, D. H. 2007. HLA class I polymorphisms are associated with development of infectious mononucleosis upon primary EBV infection. *J Clin Invest*, 117, 3042-8.
- MCBRIDE, K. M., BARRETO, V., RAMIRO, A. R., STAVROPOULOS, P. & NUSSENZWEIG, M. C. 2004. Somatic hypermutation is limited by CRM1-dependent nuclear export of activation-induced deaminase. *J Exp Med*, 199, 1235-44.
- MCBRIDE, K. M., GAZUMYAN, A., WOO, E. M., SCHWICKERT, T. A., CHAIT, B. T. & NUSSENZWEIG, M. C. 2008. Regulation of class switch recombination and somatic mutation by AID phosphorylation. *J Exp Med*, 205, 2585-94.
- MCCARTHY, H., WIERDA, W. G., BARRON, L. L., CROMWELL, C. C., WANG, J., COOMBES, K. R., RANGEL, R., ELENITOBA-JOHNSON, K. S., KEATING, M. J. & ABRUZZO, L. V. 2003. High expression of activation-induced cytidine deaminase (AID) and splice variants is a distinctive

- feature of poor-prognosis chronic lymphocytic leukemia. *Blood*, 101, 4903-8.
- MCHEYZER-WILLIAMS, L. J. & MCHEYZER-WILLIAMS, M. G. 2005. Antigen-specific memory B cell development. *Annu Rev Immunol*, 23, 487-513.
- MIDDELDORP, J. M. & PEGTEL, D. M. 2008. Multiple roles of LMP1 in Epstein-Barr virus induced immune escape. *Semin Cancer Biol*, 18, 388-96.
- MILLER, W. E., EDWARDS, R. H., WALLING, D. M. & RAAB-TRAUB, N. 1994. Sequence variation in the Epstein-Barr virus latent membrane protein 1. *J Gen Virol*, 75 (Pt 10), 2729-40.
- MIN, I. M., ROTHLEIN, L. R., SCHRADER, C. E., STAVNEZER, J. & SELSING, E. 2005. Shifts in targeting of class switch recombination sites in mice that lack mu switch region tandem repeats or Msh2. *J Exp Med*, 201, 1885-90.
- MIYASHITA, E. M., YANG, B., LAM, K. M., CRAWFORD, D. H. & THORLEY-LAWSON, D. A. 1995. A novel form of Epstein-Barr virus latency in normal B cells in vivo. *Cell*, 80, 593-601.
- MIYAWAKI, T., BUTLER, J. L., RADBRUCH, A., GARTLAND, G. L. & COOPER, M. D. 1991. Isotype commitment of human B cells that are transformed by Epstein-Barr virus. *Eur J Immunol*, 21, 215-20.
- MOORMANN, A. M., CHELIMO, K., SUMBA, O. P., LUTZKE, M. L., PLOUTZ-SNYDER, R., NEWTON, D., KAZURA, J. & ROCHFORD, R. 2005. Exposure to holoendemic malaria results in elevated Epstein-Barr virus loads in children. *J Infect Dis*, 191, 1233-8.
- MOORMANN, A. M., CHELIMO, K., SUMBA, P. O., TISCH, D. J., ROCHFORD, R. & KAZURA, J. W. 2007. Exposure to holoendemic malaria results in suppression of Epstein-Barr virus-specific T cell immunosurveillance in Kenyan children. *J Infect Dis*, 195, 799-808.
- MOSS, D. J., BURROWS, S. R., CASTELINO, D. J., KANE, R. G., POPE, J. H., RICKINSON, A. B., ALPERS, M. P. & HEYWOOD, P. F. 1983. A comparison of Epstein-Barr virus-specific T-cell immunity in malaria-endemic and -nonendemic regions of Papua New Guinea. *Int J Cancer*, 31, 727-32.
- MOSTOSLAVSKY, R., ALT, F. W. & RAJEWSKY, K. 2004. The lingering enigma of the allelic exclusion mechanism. *Cell*, 118, 539-44.

- MOWRY, S. E., STROCKER, A. M., CHAN, J., TAKEHANA, C., KALANTAR, N., BHUTA, S. & SHAPIRO, N. L. 2008. Immunohistochemical analysis and Epstein-Barr virus in the tonsils of transplant recipients and healthy controls. *Arch Otolaryngol Head Neck Surg*, 134, 936-9.
- MURAMATSU, M., KINOSHITA, K., FAGARASAN, S., YAMADA, S., SHINKAI, Y. & HONJO, T. 2000. Class switch recombination and hypermutation require activation-induced cytidine deaminase (AID), a potential RNA editing enzyme. *Cell*, 102, 553-63.
- MURAMATSU, M., SANKARANAND, V. S., ANANT, S., SUGAI, M., KINOSHITA, K., DAVIDSON, N. O. & HONJO, T. 1999. Specific expression of activation-induced cytidine deaminase (AID), a novel member of the RNA-editing deaminase family in germinal center B cells. *J Biol Chem*, 274, 18470-6.
- MUSCHEN, M., RE, D., JUNGNICKEL, B., DIEHL, V., RAJEWSKY, K. & KUPPERS, R. 2000. Somatic mutation of the CD95 gene in human B cells as a side-effect of the germinal center reaction. *J Exp Med*, 192, 1833-40.
- NAGUMO, H., AGEMATSU, K., KOBAYASHI, N., SHINOZAKI, K., HOKIBARA, S., NAGASE, H., TAKAMOTO, M., YASUI, K., SUGANE, K. & KOMIYAMA, A. 2002. The different process of class switching and somatic hypermutation; a novel analysis by CD27(-) naive B cells. *Blood*, 99, 567-75.
- NAGY, N. & KLEIN, E. 2010. Deficiency of the proapoptotic SAP function in X-linked lymphoproliferative disease aggravates Epstein-Barr virus (EBV) induced mononucleosis and promotes lymphoma development. *Immunol Lett*, 130, 13-8.
- NAGY, N., MATSKOVA, L., KIS, L. L., HELLMAN, U., KLEIN, G. & KLEIN, E. 2009. The proapoptotic function of SAP provides a clue to the clinical picture of X-linked lymphoproliferative disease. *Proc Natl Acad Sci U S A*, 106, 11966-71.
- NAGY, N., TAKAHARA, M., NISHIKAWA, J., BOURDON, J. C., KIS, L. L., KLEIN, G. & KLEIN, E. 2004. Wild-type p53 activates SAP expression in lymphoid cells. *Oncogene*, 23, 8563-70.

- NANBO, A., INOUE, K., ADACHI-TAKASAWA, K. & TAKADA, K. 2002. Epstein-Barr virus RNA confers resistance to interferon-alpha-induced apoptosis in Burkitt's lymphoma. *EMBO J*, 21, 954-65.
- NEMAZEE, D., RUSSELL, D., ARNOLD, B., HAEMMERLING, G., ALLISON, J., MILLER, J. F., MORAHAN, G. & BUERKI, K. 1991. Clonal deletion of autospecific B lymphocytes. *Immunol Rev*, 122, 117-32.
- NEMEROW, G. R., MOLD, C., SCHWEND, V. K., TOLLEFSON, V. & COOPER, N. R. 1987. Identification of gp350 as the viral glycoprotein mediating attachment of Epstein-Barr virus (EBV) to the EBV/C3d receptor of B cells: sequence homology of gp350 and C3 complement fragment C3d. *J Virol*, 61, 1416-20.
- NICHOLS, K. E., HARKIN, D. P., LEVITZ, S., KRAINER, M., KOLQUIST, K. A., GENOVESE, C., BERNARD, A., FERGUSON, M., ZUO, L., SNYDER, E., BUCKLER, A. J., WISE, C., ASHLEY, J., LOVETT, M., VALENTINE, M. B., LOOK, A. T., GERALD, W., HOUSMAN, D. E. & HABER, D. A. 1998. Inactivating mutations in an SH2 domain-encoding gene in X-linked lymphoproliferative syndrome. *Proc Natl Acad Sci U S A*, 95, 13765-70.
- NIEDOBITEK, G., AGATHANGGELOU, A., HERBST, H., WHITEHEAD, L., WRIGHT, D. H. & YOUNG, L. S. 1997. Epstein-Barr virus (EBV) infection in infectious mononucleosis: virus latency, replication and phenotype of EBV-infected cells. *J Pathol*, 182, 151-9.
- NIEDOBITEK, G., DEACON, E. M., YOUNG, L. S., HERBST, H., HAMILTON-DUTOIT, S. J. & PALLESEN, G. 1991. Epstein-Barr virus gene expression in Hodgkin's disease. *Blood*, 78, 1628-30.
- NIEDOBITEK, G., HERBST, H., YOUNG, L. S., BROOKS, L., MASUCCI, M. G., CROCKER, J., RICKINSON, A. B. & STEIN, H. 1992. Patterns of Epstein-Barr virus infection in non-neoplastic lymphoid tissue. *Blood*, 79, 2520-6.
- NITSCHKE, F., BELL, A. & RICKINSON, A. 1997. Epstein-Barr virus leader protein enhances EBNA-2-mediated transactivation of latent membrane protein 1 expression: a role for the W1W2 repeat domain. *J Virol*, 71, 6619-28.
- NJIE, R., BELL, A. I., JIA, H., CROOM-CARTER, D., CHAGANTI, S., HISLOP, A. D., WHITTLE, H. & RICKINSON, A. B. 2009. The effects of acute

- malaria on Epstein-Barr virus (EBV) load and EBV-specific T cell immunity in Gambian children. *J Infect Dis*, 199, 31-8.
- NOGUCHI, E., SHIBASAKI, M., INUDOU, M., KAMIOKA, M., YOKOUCHI, Y., YAMAKAWA-KOBAYASHI, K., HAMAGUCHI, H., MATSUI, A. & ARINAMI, T. 2001. Association between a new polymorphism in the activation-induced cytidine deaminase gene and atopic asthma and the regulation of total serum IgE levels. *J Allergy Clin Immunol*, 108, 382-6.
- NONKWELO, C., SKINNER, J., BELL, A., RICKINSON, A. & SAMPLE, J. 1996. Transcription start sites downstream of the Epstein-Barr virus (EBV) Fp promoter in early-passage Burkitt lymphoma cells define a fourth promoter for expression of the EBV EBNA-1 protein. *J Virol*, 70, 623-7.
- NONOYAMA, M. & PAGANO, J. S. 1973. Homology between Epstein-Barr virus DNA and viral DNA from Burkitt's lymphoma and nasopharyngeal carcinoma determined by DNA-DNA reassociation kinetics. *Nature*, 242, 44-7.
- O'NIONS, J. & ALLDAY, M. J. 2004. Proliferation and differentiation in isogenic populations of peripheral B cells activated by Epstein-Barr virus or T cell-derived mitogens. *J Gen Virol*, 85, 881-95.
- O'REILLY, R. J., SMALL, T. N., PAPADOPOULOS, E., LUCAS, K., LACERDA, J. & KOULOVA, L. 1997. Biology and adoptive cell therapy of Epstein-Barr virus-associated lymphoproliferative disorders in recipients of marrow allografts. *Immunol Rev*, 157, 195-216.
- OHNO, S., LUKA, J., LINDAHL, T. & KLEIN, G. 1977. Identification of a purified complement-fixing antigen as the Epstein-Barr-virus determined nuclear antigen (EBNA) by its binding to metaphase chromosomes. *Proc Natl Acad Sci U S A*, 74, 1605-9.
- OKAZAKI, I. M., KOTANI, A. & HONJO, T. 2007. Role of AID in tumorigenesis. *Adv Immunol*, 94, 245-73.
- OPPEZZO, P., DUMAS, G., LALANNE, A. I., PAYELLE-BROGARD, B., MAGNAC, C., PRITSCH, O., DIGHIERO, G. & VUILLIER, F. 2005. Different isoforms of BSAP regulate expression of AID in normal and chronic lymphocytic leukemia B cells. *Blood*, 105, 2495-503.
- OPPEZZO, P., VUILLIER, F., VASCONCELOS, Y., DUMAS, G., MAGNAC, C., PAYELLE-BROGARD, B., PRITSCH, O. & DIGHIERO, G. 2003. Chronic

- lymphocytic leukemia B cells expressing AID display dissociation between class switch recombination and somatic hypermutation. *Blood*, 101, 4029-32.
- OUYANG, Q., WAGNER, W. M., WALTER, S., MULLER, C. A., WIKBY, A., AUBERT, G., KLATT, T., STEVANOVIC, S., DODI, T. & PAWELEC, G. 2003. An age-related increase in the number of CD8+ T cells carrying receptors for an immunodominant Epstein-Barr virus (EBV) epitope is counteracted by a decreased frequency of their antigen-specific responsiveness. *Mech Ageing Dev*, 124, 477-85.
- PAJIC, A., STAEGE, M. S., DUDZIAK, D., SCHUHMACHER, M., SPITKOVSKY, D., EISSNER, G., BRIELMEIER, M., POLACK, A. & BORNKAMM, G. W. 2001. Antagonistic effects of c-myc and Epstein-Barr virus latent genes on the phenotype of human B cells. *Int J Cancer*, 93, 810-6.
- PALLESEN, G., HAMILTON-DUTOIT, S. J., ROWE, M. & YOUNG, L. S. 1991a. Expression of Epstein-Barr virus latent gene products in tumour cells of Hodgkin's disease. *Lancet*, 337, 320-2.
- PALLESEN, G., SANDVEJ, K., HAMILTON-DUTOIT, S. J., ROWE, M. & YOUNG, L. S. 1991b. Activation of Epstein-Barr virus replication in Hodgkin and Reed-Sternberg cells. *Blood*, 78, 1162-5.
- PARHAM, P. 2000. *The Immune System*.
- PARKER, D. C. 1993. T cell-dependent B cell activation. *Annu Rev Immunol*, 11, 331-60.
- PASCUAL, V., LIU, Y. J., MAGALSKI, A., DE BOUTEILLER, O., BANCHEREAU, J. & CAPRA, J. D. 1994. Analysis of somatic mutation in five B cell subsets of human tonsil. *J Exp Med*, 180, 329-39.
- PASQUALUCCI, L., GUGLIELMINO, R., HOULDSWORTH, J., MOHR, J., AOUFOUCHI, S., POLAKIEWICZ, R., CHAGANTI, R. S. & DALLA-FAVERA, R. 2004. Expression of the AID protein in normal and neoplastic B cells. *Blood*, 104, 3318-25.
- PASQUALUCCI, L., MIGLIAZZA, A., FRACCHIOLLA, N., WILLIAM, C., NERI, A., BALDINI, L., CHAGANTI, R. S., KLEIN, U., KUPPERS, R., RAJEWSKY, K. & DALLA-FAVERA, R. 1998. BCL-6 mutations in normal

- germinal center B cells: evidence of somatic hypermutation acting outside Ig loci. *Proc Natl Acad Sci U S A*, 95, 11816-21.
- PASQUALUCCI, L., NEUMEISTER, P., GOOSSENS, T., NANJANGUD, G., CHAGANTI, R. S., KUPPERS, R. & DALLA-FAVERA, R. 2001. Hypermutation of multiple proto-oncogenes in B-cell diffuse large-cell lymphomas. *Nature*, 412, 341-6.
- PEARSON, G. R., LUKA, J., PETTI, L., SAMPLE, J., BIRKENBACH, M., BRAUN, D. & KIEFF, E. 1987. Identification of an Epstein-Barr virus early gene encoding a second component of the restricted early antigen complex. *Virology*, 160, 151-61.
- PELED, J. U., KUANG, F. L., IGLESIAS-USSEL, M. D., ROA, S., KALIS, S. L., GOODMAN, M. F. & SCHARFF, M. D. 2008. The biochemistry of somatic hypermutation. *Annu Rev Immunol*, 26, 481-511.
- PENE, J., GAUCHAT, J. F., LECART, S., DROUET, E., GUGLIELMI, P., BOULAY, V., DELWAIL, A., FOSTER, D., LECRON, J. C. & YSSEL, H. 2004. Cutting edge: IL-21 is a switch factor for the production of IgG1 and IgG3 by human B cells. *J Immunol*, 172, 5154-7.
- PENE, J., ROUSSET, F., BRIERE, F., CHRETIEN, I., BONNEFOY, J. Y., SPITS, H., YOKOTA, T., ARAI, N., ARAI, K., BANCHEREAU, J. & ET AL. 1988. IgE production by normal human lymphocytes is induced by interleukin 4 and suppressed by interferons gamma and alpha and prostaglandin E2. *Proc Natl Acad Sci U S A*, 85, 6880-4.
- PENG, R., MOSES, S. C., TAN, J., KREMMER, E. & LING, P. D. 2005. The Epstein-Barr virus EBNA-LP protein preferentially coactivates EBNA2-mediated stimulation of latent membrane proteins expressed from the viral divergent promoter. *J Virol*, 79, 4492-505.
- PETERSEN, S., CASELLAS, R., REINA-SAN-MARTIN, B., CHEN, H. T., DIFILIPPANTONIO, M. J., WILSON, P. C., HANITSCH, L., CELESTE, A., MURAMATSU, M., PILCH, D. R., REDON, C., RIED, T., BONNER, W. M., HONJO, T., NUSSENZWEIG, M. C. & NUSSENZWEIG, A. 2001. AID is required to initiate Nbs1/gamma-H2AX focus formation and mutations at sites of class switching. *Nature*, 414, 660-5.

- PETTI, L., SAMPLE, C. & KIEFF, E. 1990. Subnuclear localization and phosphorylation of Epstein-Barr virus latent infection nuclear proteins. *Virology*, 176, 563-74.
- PLAZA, G., SANTON, A. & BELLAS, C. 2003. Coinfection by multiple strains of Epstein-Barr virus in infectious mononucleosis in immunocompetent patients. *Acta Otolaryngol*, 123, 543-6.
- PORTIS, T., DYCK, P. & LONGNECKER, R. 2003. Epstein-Barr Virus (EBV) LMP2A induces alterations in gene transcription similar to those observed in Reed-Sternberg cells of Hodgkin lymphoma. *Blood*, 102, 4166-78.
- PRECOPIO, M. L., SULLIVAN, J. L., WILLARD, C., SOMASUNDARAN, M. & LUZURIAGA, K. 2003. Differential kinetics and specificity of EBV-specific CD4+ and CD8+ T cells during primary infection. *J Immunol*, 170, 2590-8.
- PRITCHETT, R., PEDERSEN, M. & KIEFF, E. 1976. Complexity of EBV homologous DNA in continuous lymphoblastoid cell lines. *Virology*, 74, 227-31.
- PUNNONEN, J., AVERSA, G., COCKS, B. G., MCKENZIE, A. N., MENON, S., ZURAWSKI, G., DE WAAL MALEFYT, R. & DE VRIES, J. E. 1993. Interleukin 13 induces interleukin 4-independent IgG4 and IgE synthesis and CD23 expression by human B cells. *Proc Natl Acad Sci U S A*, 90, 3730-4.
- PURTILO, D. T., CASSEL, C. K., YANG, J. P. & HARPER, R. 1975. X-linked recessive progressive combined variable immunodeficiency (Duncan's disease). *Lancet*, 1, 935-40.
- RAAPHORST, F. M., RAMAN, C. S., TAMI, J., FISCHBACH, M. & SANZ, I. 1997. Human Ig heavy chain CDR3 regions in adult bone marrow pre-B cells display an adult phenotype of diversity: evidence for structural selection of DH amino acid sequences. *Int Immunol*, 9, 1503-15.
- RADKOV, S. A., BAIN, M., FARRELL, P. J., WEST, M., ROWE, M. & ALLDAY, M. J. 1997. Epstein-Barr virus EBNA3C represses Cp, the major promoter for EBNA expression, but has no effect on the promoter of the cell gene CD21. *J Virol*, 71, 8552-62.
- RADKOV, S. A., TOUITOU, R., BREHM, A., ROWE, M., WEST, M., KOUZARIDES, T. & ALLDAY, M. J. 1999. Epstein-Barr virus nuclear

- antigen 3C interacts with histone deacetylase to repress transcription. *J Virol*, 73, 5688-97.
- RAJEWSKY, K. 1996. Clonal selection and learning in the antibody system. *Nature*, 381, 751-8.
- RAMIRO, A. R., JANKOVIC, M., EISENREICH, T., DIFILIPPANTONIO, S., CHEN-KIANG, S., MURAMATSU, M., HONJO, T., NUSSENZWEIG, A. & NUSSENZWEIG, M. C. 2004. AID is required for c-myc/IgH chromosome translocations in vivo. *Cell*, 118, 431-8.
- RASTI, N., FALK, K. I., DONATI, D., GYAN, B. A., GOKA, B. Q., TROYE-BLOMBERG, M., AKANMORI, B. D., KURTZHALS, J. A., DODOO, D., CONSOLINI, R., LINDE, A., WAHLGREN, M. & BEJARANO, M. T. 2005. Circulating epstein-barr virus in children living in malaria-endemic areas. *Scand J Immunol*, 61, 461-5.
- RAWLINS, D. R., MILMAN, G., HAYWARD, S. D. & HAYWARD, G. S. 1985. Sequence-specific DNA binding of the Epstein-Barr virus nuclear antigen (EBNA-1) to clustered sites in the plasmid maintenance region. *Cell*, 42, 859-68.
- REEDMAN, B. M. & KLEIN, G. 1973. Cellular localization of an Epstein-Barr virus (EBV)-associated complement-fixing antigen in producer and non-producer lymphoblastoid cell lines. *Int J Cancer*, 11, 499-520.
- RESSING, M. E., KEATING, S. E., VAN LEEUWEN, D., KOPPERS-LALIC, D., PAPPWORTH, I. Y., WIERTZ, E. J. & ROWE, M. 2005. Impaired transporter associated with antigen processing-dependent peptide transport during productive EBV infection. *J Immunol*, 174, 6829-38.
- RETH, M. 1989. Antigen receptor tail clue. *Nature*, 338, 383-4.
- RETTNER, I., ALTHAUS, H. H., MUNCH, R. & MULLER, W. 2005. VBASE2, an integrative V gene database. *Nucleic Acids Res*, 33, D671-4.
- REY, P., MUTO, T., LEVY, Y., GEISSMANN, F., PLEBANI, A., SANAL, O., CATALAN, N., FORVEILLE, M., DUFOURCQ-LABELOUSE, R., GENNERY, A., TEZCAN, I., ERSOY, F., KAYSERILI, H., UGAZIO, A. G., BROUSSE, N., MURAMATSU, M., NOTARANGELO, L. D., KINOSHITA, K., HONJO, T., FISCHER, A. & DURANDY, A. 2000. Activation-induced cytidine deaminase (AID) deficiency causes the autosomal recessive form of the Hyper-IgM syndrome (HIGM2). *Cell*, 102, 565-75.

- RICKINSON, A. B. & KIEFF, E. 2007. *Fields Virology*.
- ROBERTSON, P., BEYNON, S., WHYBIN, R., BRENNAN, C., VOLLMER-CONNA, U., HICKIE, I. & LLOYD, A. 2003. Measurement of EBV-IgG anti-VCA avidity aids the early and reliable diagnosis of primary EBV infection. *J Med Virol*, 70, 617-23.
- ROCHFORD, R., HOBBS, M. V., GARNIER, J. L., COOPER, N. R. & CANNON, M. J. 1993. Plasmacytoid differentiation of Epstein-Barr virus-transformed B cells in vivo is associated with reduced expression of viral latent genes. *Proc Natl Acad Sci U S A*, 90, 352-6.
- ROLL, P., PALANICHAMY, A., KNEITZ, C., DORNER, T. & TONY, H. P. 2006. Regeneration of B cell subsets after transient B cell depletion using anti-CD20 antibodies in rheumatoid arthritis. *Arthritis Rheum*, 54, 2377-86.
- ROONEY, C. M., BRIMMELL, M., BUSCHLE, M., ALLAN, G., FARRELL, P. J. & KOLMAN, J. L. 1992. Host cell and EBNA-2 regulation of Epstein-Barr virus latent-cycle promoter activity in B lymphocytes. *J Virol*, 66, 496-504.
- ROSE, C., GREEN, M., WEBBER, S., KINGSLEY, L., DAY, R., WATKINS, S., REYES, J. & ROWE, D. 2002. Detection of Epstein-Barr virus genomes in peripheral blood B cells from solid-organ transplant recipients by fluorescence in situ hybridization. *J Clin Microbiol*, 40, 2533-44.
- ROUGHAN, J. E. & THORLEY-LAWSON, D. A. 2009. The intersection of Epstein-Barr virus with the germinal center. *J Virol*, 83, 3968-76.
- ROUGHAN, J. E., TORGBOR, C. & THORLEY-LAWSON, D. A. 2010. Germinal center B cells latently infected with Epstein-Barr virus proliferate extensively but do not increase in number. *J Virol*, 84, 1158-68.
- ROWE, D. T., ROWE, M., EVAN, G. I., WALLACE, L. E., FARRELL, P. J. & RICKINSON, A. B. 1986. Restricted expression of EBV latent genes and T-lymphocyte-detected membrane antigen in Burkitt's lymphoma cells. *EMBO J*, 5, 2599-607.
- ROWE, M., KELLY, G. L., BELL, A. I. & RICKINSON, A. B. 2009. Burkitt's lymphoma: the Rosetta Stone deciphering Epstein-Barr virus biology. *Semin Cancer Biol*, 19, 377-88.
- ROWE, M., ROWE, D. T., GREGORY, C. D., YOUNG, L. S., FARRELL, P. J., RUPANI, H. & RICKINSON, A. B. 1987. Differences in B cell growth

- phenotype reflect novel patterns of Epstein-Barr virus latent gene expression in Burkitt's lymphoma cells. *EMBO J*, 6, 2743-51.
- RUF, I. K., RHYNE, P. W., YANG, C., CLEVELAND, J. L. & SAMPLE, J. T. 2000. Epstein-Barr virus small RNAs potentiate tumorigenicity of Burkitt lymphoma cells independently of an effect on apoptosis. *J Virol*, 74, 10223-8.
- RYAN, J. L., KAUFMANN, W. K., RAAB-TRAUB, N., OGLESBEE, S. E., CAREY, L. A. & GULLEY, M. L. 2006. Clonal evolution of lymphoblastoid cell lines. *Lab Invest*, 86, 1193-200.
- SALE, J. E. & NEUBERGER, M. S. 1998. TdT-accessible breaks are scattered over the immunoglobulin V domain in a constitutively hypermutating B cell line. *Immunity*, 9, 859-69.
- SAMPLE, J., HENSON, E. B. & SAMPLE, C. 1992. The Epstein-Barr virus nuclear protein 1 promoter active in type I latency is autoregulated. *J Virol*, 66, 4654-61.
- SAMPLE, J., HUMMEL, M., BRAUN, D., BIRKENBACH, M. & KIEFF, E. 1986. Nucleotide sequences of mRNAs encoding Epstein-Barr virus nuclear proteins: a probable transcriptional initiation site. *Proc Natl Acad Sci U S A*, 83, 5096-100.
- SAMPLE, J., YOUNG, L., MARTIN, B., CHATMAN, T., KIEFF, E. & RICKINSON, A. 1990. Epstein-Barr virus types 1 and 2 differ in their EBNA-3A, EBNA-3B, and EBNA-3C genes. *J Virol*, 64, 4084-92.
- SAULQUIN, X., IBISCH, C., PEYRAT, M. A., SCOTET, E., HOURMANT, M., VIE, H., BONNEVILLE, M. & HOUSSAINT, E. 2000. A global appraisal of immunodominant CD8 T cell responses to Epstein-Barr virus and cytomegalovirus by bulk screening. *Eur J Immunol*, 30, 2531-9.
- SAYOS, J., NGUYEN, K. B., WU, C., STEPP, S. E., HOWIE, D., SCHATZLE, J. D., KUMAR, V., BIRON, C. A. & TERHORST, C. 2000. Potential pathways for regulation of NK and T cell responses: differential X-linked lymphoproliferative syndrome gene product SAP interactions with SLAM and 2B4. *Int Immunol*, 12, 1749-57.
- SAYOS, J., WU, C., MORRA, M., WANG, N., ZHANG, X., ALLEN, D., VAN SCHAİK, S., NOTARANGELO, L., GEHA, R., RONCAROLO, M. G., OETTGEN, H., DE VRIES, J. E., AVERSA, G. & TERHORST, C. 1998.

- The X-linked lymphoproliferative-disease gene product SAP regulates signals induced through the co-receptor SLAM. *Nature*, 395, 462-9.
- SCHAEFER, B. C., STROMINGER, J. L. & SPECK, S. H. 1995. Redefining the Epstein-Barr virus-encoded nuclear antigen EBNA-1 gene promoter and transcription initiation site in group I Burkitt lymphoma cell lines. *Proc Natl Acad Sci U S A*, 92, 10565-9.
- SCHATZ, D. G., OETTINGER, M. A. & BALTIMORE, D. 1989. The V(D)J recombination activating gene, RAG-1. *Cell*, 59, 1035-48.
- SCHEEREN, F. A., NAGASAWA, M., WEIJER, K., CUPEDO, T., KIRBERG, J., LEGRAND, N. & SPITS, H. 2008. T cell-independent development and induction of somatic hypermutation in human IgM+ IgD+ CD27+ B cells. *J Exp Med*, 205, 2033-42.
- SCHNEIDER, F., NEUGEBAUER, J., GRIESE, J., LIEFOLD, N., KUTZ, H., BRISENO, C. & KIESER, A. 2008. The viral oncoprotein LMP1 exploits TRADD for signaling by masking its apoptotic activity. *PLoS Biol*, 6, e8.
- SCHRADER, C. E., LINEHAN, E. K., MOCHEGOVA, S. N., WOODLAND, R. T. & STAVNEZER, J. 2005. Inducible DNA breaks in Ig S regions are dependent on AID and UNG. *J Exp Med*, 202, 561-8.
- SCHUSTER, V., OTT, G., SEIDENSPINNER, S. & KRETH, H. W. 1996. Common Epstein-Barr virus (EBV) type-1 variant strains in both malignant and benign EBV-associated disorders. *Blood*, 87, 1579-85.
- SCHWERING, I., BRAUNINGER, A., KLEIN, U., JUNGNIKEL, B., TINGUELY, M., DIEHL, V., HANSMANN, M. L., DALLA-FAVERA, R., RAJEWSKY, K. & KUPPERS, R. 2003. Loss of the B-lineage-specific gene expression program in Hodgkin and Reed-Sternberg cells of Hodgkin lymphoma. *Blood*, 101, 1505-12.
- SEEMAYER, T. A., GROSS, T. G., EGELER, R. M., PIRRUCCELLO, S. J., DAVIS, J. R., KELLY, C. M., OKANO, M., LANYI, A. & SUMEGI, J. 1995. X-linked lymphoproliferative disease: twenty-five years after the discovery. *Pediatr Res*, 38, 471-8.
- SEIFERT, M. & KUPPERS, R. 2009. Molecular footprints of a germinal center derivation of human IgM+(IgD+)CD27+ B cells and the dynamics of memory B cell generation. *J Exp Med*, 206, 2659-69.

- SERVET-DELPAT, C., BRIDON, J. M., BLANCHARD, D., BANCHEREAU, J. & BRIERE, F. 1995. CD40-activated human naive surface IgD⁺ B cells produce IgG2 in response to activated T-cell supernatant. *Immunology*, 85, 435-41.
- SHAH, K. M. & YOUNG, L. S. 2009. Epstein-Barr virus and carcinogenesis: beyond Burkitt's lymphoma. *Clin Microbiol Infect*, 15, 982-8.
- SHANNON-LOWE, C. D., NEUHIERL, B., BALDWIN, G., RICKINSON, A. B. & DELECLUSE, H. J. 2006. Resting B cells as a transfer vehicle for Epstein-Barr virus infection of epithelial cells. *Proc Natl Acad Sci U S A*, 103, 7065-70.
- SHEN, H. M., MICHAEL, N., KIM, N. & STORB, U. 2000. The TATA binding protein, c-Myc and survivin genes are not somatically hypermutated, while Ig and BCL6 genes are hypermutated in human memory B cells. *Int Immunol*, 12, 1085-93.
- SHEN, H. M., PETERS, A., BARON, B., ZHU, X. & STORB, U. 1998. Mutation of BCL-6 gene in normal B cells by the process of somatic hypermutation of Ig genes. *Science*, 280, 1750-2.
- SHIMAKAGE, M., KURATA, A., INOUE, H., OKAMOTO, Y., YUTSUDO, M. & HAKURA, A. 1995. Tumorigenicity of EBNA2-transfected cells. *FEBS Lett*, 371, 245-8.
- SHIRE, K., CECCARELLI, D. F., AVOLIO-HUNTER, T. M. & FRAPPIER, L. 1999. EBP2, a human protein that interacts with sequences of the Epstein-Barr virus nuclear antigen 1 important for plasmid maintenance. *J Virol*, 73, 2587-95.
- SIEMER, D., KURTH, J., LANG, S., LEHNERDT, G., STANELLE, J. & KUPPERS, R. 2008. EBV transformation overrides gene expression patterns of B cell differentiation stages. *Mol Immunol*, 45, 3133-41.
- SINCLAIR, A. J., PALMERO, I., PETERS, G. & FARRELL, P. J. 1994. EBNA-2 and EBNA-LP cooperate to cause G0 to G1 transition during immortalization of resting human B lymphocytes by Epstein-Barr virus. *EMBO J*, 13, 3321-8.
- SITKI-GREEN, D., COVINGTON, M. & RAAB-TRAUB, N. 2003. Compartmentalization and transmission of multiple Epstein-Barr virus strains in asymptomatic carriers. *J Virol*, 77, 1840-7.

- SITKI-GREEN, D. L., EDWARDS, R. H., COVINGTON, M. M. & RAAB-TRAUB, N. 2004. Biology of Epstein-Barr virus during infectious mononucleosis. *J Infect Dis*, 189, 483-92.
- SIXBEY, J. W., NEDRUD, J. G., RAAB-TRAUB, N., HANES, R. A. & PAGANO, J. S. 1984. Epstein-Barr virus replication in oropharyngeal epithelial cells. *N Engl J Med*, 310, 1225-30.
- SKINNIDER, B. F. & MAK, T. W. 2002. The role of cytokines in classical Hodgkin lymphoma. *Blood*, 99, 4283-97.
- SMITH, T. F. 1992. IgG subclasses. *Adv Pediatr*, 39, 101-26.
- SONI, V., YASUI, T., CAHIR-MCFARLAND, E. & KIEFF, E. 2006. LMP1 transmembrane domain 1 and 2 (TM1-2) FWLY mediates intermolecular interactions with TM3-6 to activate NF-kappaB. *J Virol*, 80, 10787-93.
- SOUZA, T. A., STOLLAR, B. D., SULLIVAN, J. L., LUZURIAGA, K. & THORLEY-LAWSON, D. A. 2005. Peripheral B cells latently infected with Epstein-Barr virus display molecular hallmarks of classical antigen-selected memory B cells. *Proc Natl Acad Sci U S A*, 102, 18093-8.
- SOUZA, T. A., STOLLAR, B. D., SULLIVAN, J. L., LUZURIAGA, K. & THORLEY-LAWSON, D. A. 2007. Influence of EBV on the peripheral blood memory B cell compartment. *J Immunol*, 179, 3153-60.
- STAVNEZER, J., GUIKEMA, J. E. & SCHRADER, C. E. 2008. Mechanism and regulation of class switch recombination. *Annu Rev Immunol*, 26, 261-92.
- SUGDEN, B., PHELPS, M. & DOMORADZKI, J. 1979. Epstein-Barr virus DNA is amplified in transformed lymphocytes. *J Virol*, 31, 590-5.
- SUGIURA, M., IMAI, S., TOKUNAGA, M., KOIZUMI, S., UCHIZAWA, M., OKAMOTO, K. & OSATO, T. 1996. Transcriptional analysis of Epstein-Barr virus gene expression in EBV-positive gastric carcinoma: unique viral latency in the tumour cells. *Br J Cancer*, 74, 625-31.
- SUMAYA, C. V. & ENCH, Y. 1985. Epstein-Barr virus infectious mononucleosis in children. II. Heterophil antibody and viral-specific responses. *Pediatrics*, 75, 1011-9.
- SUNG, N. S., EDWARDS, R. H., SEILLIER-MOISEWITSCH, F., PERKINS, A. G., ZENG, Y. & RAAB-TRAUB, N. 1998. Epstein-Barr virus strain variation in nasopharyngeal carcinoma from the endemic and non-endemic regions of China. *Int J Cancer*, 76, 207-15.

- SUNG, N. S., KENNEY, S., GUTSCH, D. & PAGANO, J. S. 1991. EBNA-2 transactivates a lymphoid-specific enhancer in the BamHI C promoter of Epstein-Barr virus. *J Virol*, 65, 2164-9.
- TAKADA, K. & NANBO, A. 2001. The role of EBERs in oncogenesis. *Semin Cancer Biol*, 11, 461-7.
- TAKAHASHI, H., HIDESHIMA, K., KAWAZOE, K., TSUDA, N., FUJITA, S., SHIBATA, Y., OKABE, H. & YAMABE, S. 1995. Immunophenotypes of Reed-Sternberg cells and their variants: a study of 68 cases of Hodgkin's disease. *Tohoku J Exp Med*, 177, 193-211.
- TAKEUCHI, K., TANAKA-TAYA, K., KAZUYAMA, Y., ITO, Y. M., HASHIMOTO, S., FUKAYAMA, M. & MORI, S. 2006. Prevalence of Epstein-Barr virus in Japan: trends and future prediction. *Pathol Int*, 56, 112-6.
- TAMARU, Y., MIYAWAKI, T., IWAI, K., TSUJI, T., NIBU, R., YACHIE, A., KOIZUMI, S. & TANIGUCHI, N. 1993. Absence of bcl-2 expression by activated CD45RO+ T lymphocytes in acute infectious mononucleosis supporting their susceptibility to programmed cell death. *Blood*, 82, 521-7.
- TANNER, J., WEIS, J., FEARON, D., WHANG, Y. & KIEFF, E. 1987. Epstein-Barr virus gp350/220 binding to the B lymphocyte C3d receptor mediates adsorption, capping, and endocytosis. *Cell*, 50, 203-13.
- TAUB, R., KIRSCH, I., MORTON, C., LENOIR, G., SWAN, D., TRONICK, S., AARONSON, S. & LEDER, P. 1982. Translocation of the c-myc gene into the immunoglobulin heavy chain locus in human Burkitt lymphoma and murine plasmacytoma cells. *Proc Natl Acad Sci U S A*, 79, 7837-41.
- TENG, G., HAKIMPOUR, P., LANDGRAF, P., RICE, A., TUSCHL, T., CASELLAS, R. & PAPAVALIIOU, F. N. 2008. MicroRNA-155 is a negative regulator of activation-induced cytidine deaminase. *Immunity*, 28, 621-9.
- THACKER, E. L., MIRZAEI, F. & ASCHERIO, A. 2006. Infectious mononucleosis and risk for multiple sclerosis: a meta-analysis. *Ann Neurol*, 59, 499-503.
- THOMPSON, M. P. & KURZROCK, R. 2004. Epstein-Barr virus and cancer. *Clin Cancer Res*, 10, 803-21.
- THORLEY-LAWSON, D. A. 2001. Epstein-Barr virus: exploiting the immune system. *Nat Rev Immunol*, 1, 75-82.

- THORLEY-LAWSON, D. A. & ALLDAY, M. J. 2008. The curious case of the tumour virus: 50 years of Burkitt's lymphoma. *Nat Rev Microbiol*, 6, 913-24.
- THORLEY-LAWSON, D. A. & BABCOCK, G. J. 1999. A model for persistent infection with Epstein-Barr virus: the stealth virus of human B cells. *Life Sci*, 65, 1433-53.
- THORLEY-LAWSON, D. A. & GROSS, A. 2004. Persistence of the Epstein-Barr virus and the origins of associated lymphomas. *N Engl J Med*, 350, 1328-37.
- TIERNEY, R. J., EDWARDS, R. H., SITKI-GREEN, D., CROOM-CARTER, D., ROY, S., YAO, Q. Y., RAAB-TRAUB, N. & RICKINSON, A. B. 2006. Multiple Epstein-Barr virus strains in patients with infectious mononucleosis: comparison of ex vivo samples with in vitro isolates by use of heteroduplex tracking assays. *J Infect Dis*, 193, 287-97.
- TIERNEY, R. J., STEVEN, N., YOUNG, L. S. & RICKINSON, A. B. 1994. Epstein-Barr virus latency in blood mononuclear cells: analysis of viral gene transcription during primary infection and in the carrier state. *J Virol*, 68, 7374-85.
- TIMMS, J. M., BELL, A., FLAVELL, J. R., MURRAY, P. G., RICKINSON, A. B., TRAVERSE-GLEHEN, A., BERGER, F. & DELECLUSE, H. J. 2003. Target cells of Epstein-Barr-virus (EBV)-positive post-transplant lymphoproliferative disease: similarities to EBV-positive Hodgkin's lymphoma. *Lancet*, 361, 217-23.
- TOBOLLIK, S., MEYER, L., BUETTNER, M., KLEMMER, S., KEMPKES, B., KREMMER, E., NIEDOBITEK, G. & JUNGNICHEL, B. 2006. Epstein-Barr virus nuclear antigen 2 inhibits AID expression during EBV-driven B-cell growth. *Blood*, 108, 3859-64.
- TOCZYSKI, D. P., MATERA, A. G., WARD, D. C. & STEITZ, J. A. 1994. The Epstein-Barr virus (EBV) small RNA EBER1 binds and relocalizes ribosomal protein L22 in EBV-infected human B lymphocytes. *Proc Natl Acad Sci U S A*, 91, 3463-7.
- TOELLNER, K. M., GULBRANSON-JUDGE, A., TAYLOR, D. R., SZE, D. M. & MACLENNAN, I. C. 1996. Immunoglobulin switch transcript production in

- vivo related to the site and time of antigen-specific B cell activation. *J Exp Med*, 183, 2303-12.
- TOELLNER, K. M., JENKINSON, W. E., TAYLOR, D. R., KHAN, M., SZE, D. M., SANSOM, D. M., VINUESA, C. G. & MACLENNAN, I. C. 2002. Low-level hypermutation in T cell-independent germinal centers compared with high mutation rates associated with T cell-dependent germinal centers. *J Exp Med*, 195, 383-9.
- TOMKINSON, B. & KIEFF, E. 1992. Use of second-site homologous recombination to demonstrate that Epstein-Barr virus nuclear protein 3B is not important for lymphocyte infection or growth transformation in vitro. *J Virol*, 66, 2893-903.
- TOMKINSON, B., ROBERTSON, E. & KIEFF, E. 1993. Epstein-Barr virus nuclear proteins EBNA-3A and EBNA-3C are essential for B-lymphocyte growth transformation. *J Virol*, 67, 2014-25.
- TORNELL, J., FARZAD, S., ESPANDER-JANSSON, A., MATEJKA, G., ISAKSSON, O. & RYMO, L. 1996. Expression of Epstein-Barr nuclear antigen 2 in kidney tubule cells induce tumors in transgenic mice. *Oncogene*, 12, 1521-8.
- TOUITOU, R., HICKABOTTOM, M., PARKER, G., CROOK, T. & ALLDAY, M. J. 2001. Physical and functional interactions between the corepressor CtBP and the Epstein-Barr virus nuclear antigen EBNA3C. *J Virol*, 75, 7749-55.
- TRAN, T. H., NAKATA, M., SUZUKI, K., BEGUM, N. A., SHINKURA, R., FAGARASAN, S., HONJO, T. & NAGAOKA, H. 2010. B cell-specific and stimulation-responsive enhancers derepress Aicda by overcoming the effects of silencers. *Nat Immunol*, 11, 148-54.
- UCHIDA, J., YASUI, T., TAKAOKA-SHICHIJO, Y., MURAOKA, M., KULWICHIT, W., RAAB-TRAUB, N. & KIKUTANI, H. 1999. Mimicry of CD40 signals by Epstein-Barr virus LMP1 in B lymphocyte responses. *Science*, 286, 300-3.
- UEDA, Y., LIAO, D., YANG, K., PATEL, A. & KELSOE, G. 2007. T-independent activation-induced cytidine deaminase expression, class-switch recombination, and antibody production by immature/transitional 1 B cells. *J Immunol*, 178, 3593-601.

- VAN DEN BERG, A., VISSER, L. & POPPEMA, S. 1999. High expression of the CC chemokine TARC in Reed-Sternberg cells. A possible explanation for the characteristic T-cell infiltrate in Hodgkin's lymphoma. *Am J Pathol*, 154, 1685-91.
- VASKOVA, M., FRONKOVA, E., STARKOVA, J., KALINA, T., MEJSTRIKOVA, E. & HRUSAK, O. 2008. CD44 and CD27 delineate B-precursor stages with different recombination status and with an uneven distribution in nonmalignant and malignant hematopoiesis. *Tissue Antigens*, 71, 57-66.
- VAUX, D. L., CORY, S. & ADAMS, J. M. 1988. Bcl-2 gene promotes haemopoietic cell survival and cooperates with c-myc to immortalize pre-B cells. *Nature*, 335, 440-2.
- VEILLETTE, A. 2006. Immune regulation by SLAM family receptors and SAP-related adaptors. *Nat Rev Immunol*, 6, 56-66.
- VIDAL, S. M. & LANIER, L. L. 2006. NK cell recognition of mouse cytomegalovirus-infected cells. *Curr Top Microbiol Immunol*, 298, 183-206.
- VOCKERODT, M., MORGAN, S. L., KUO, M., WEI, W., CHUKWUMA, M. B., ARRAND, J. R., KUBE, D., GORDON, J., YOUNG, L. S., WOODMAN, C. B. & MURRAY, P. G. 2008. The Epstein-Barr virus oncoprotein, latent membrane protein-1, reprograms germinal centre B cells towards a Hodgkin's Reed-Sternberg-like phenotype. *J Pathol*, 216, 83-92.
- WANG, C. L., HARPER, R. A. & WABL, M. 2004. Genome-wide somatic hypermutation. *Proc Natl Acad Sci U S A*, 101, 7352-6.
- WANG, F., GREGORY, C. D., ROWE, M., RICKINSON, A. B., WANG, D., BIRKENBACH, M., KIKUTANI, H., KISHIMOTO, T. & KIEFF, E. 1987. Epstein-Barr virus nuclear antigen 2 specifically induces expression of the B-cell activation antigen CD23. *Proc Natl Acad Sci U S A*, 84, 3452-6.
- WANG, F., TSANG, S. F., KURILLA, M. G., COHEN, J. I. & KIEFF, E. 1990. Epstein-Barr virus nuclear antigen 2 transactivates latent membrane protein LMP1. *J Virol*, 64, 3407-16.
- WANG, Y. H., NOMURA, J., FAYE-PETERSEN, O. M. & COOPER, M. D. 1998. Surrogate light chain production during B cell differentiation: differential intracellular versus cell surface expression. *J Immunol*, 161, 1132-9.
- WEI, C., ANOLIK, J., CAPPIONE, A., ZHENG, B., PUGH-BERNARD, A., BROOKS, J., LEE, E. H., MILNER, E. C. & SANZ, I. 2007. A new

- population of cells lacking expression of CD27 represents a notable component of the B cell memory compartment in systemic lupus erythematosus. *J Immunol*, 178, 6624-33.
- WEILL, J. C., WELLER, S. & REYNAUD, C. A. 2009. Human marginal zone B cells. *Annu Rev Immunol*, 27, 267-85.
- WELLER, S., BRAUN, M. C., TAN, B. K., ROSENWALD, A., CORDIER, C., CONLEY, M. E., PLEBANI, A., KUMARARATNE, D. S., BONNET, D., TOURNILHAC, O., TCHERNIA, G., STEINIGER, B., STAUDT, L. M., CASANOVA, J. L., REYNAUD, C. A. & WEILL, J. C. 2004. Human blood IgM "memory" B cells are circulating splenic marginal zone B cells harboring a prediversified immunoglobulin repertoire. *Blood*, 104, 3647-54.
- WELLER, S., FAILI, A., GARCIA, C., BRAUN, M. C., LE DEIST, F. F., DE SAINT BASILE, G. G., HERMINE, O., FISCHER, A., REYNAUD, C. A. & WEILL, J. C. 2001. CD40-CD40L independent Ig gene hypermutation suggests a second B cell diversification pathway in humans. *Proc Natl Acad Sci U S A*, 98, 1166-70.
- WELLER, S., MAMANI-MATSUDA, M., PICARD, C., CORDIER, C., LECOEUQUE, D., GAUTHIER, F., WEILL, J. C. & REYNAUD, C. A. 2008. Somatic diversification in the absence of antigen-driven responses is the hallmark of the IgM+ IgD+ CD27+ B cell repertoire in infants. *J Exp Med*, 205, 1331-42.
- WELLER, S., REYNAUD, C. A. & WEILL, J. C. 2005. Splenic marginal zone B cells in humans: where do they mutate their Ig receptor? *Eur J Immunol*, 35, 2789-92.
- WHITE, D. O. & FENNER, F. J. 1994. *Medical Virology*.
- WHITTLE, H. C., BROWN, J., MARSH, K., GREENWOOD, B. M., SEIDELIN, P., TIGHE, H. & WEDDERBURN, L. 1984. T-cell control of Epstein-Barr virus-infected B cells is lost during *P. falciparum* malaria. *Nature*, 312, 449-50.
- WILLIAMS, H., MACSWEEN, K., MCAULAY, K., HIGGINS, C., HARRISON, N., SWERDLOW, A., BRITTON, K. & CRAWFORD, D. 2004. Analysis of immune activation and clinical events in acute infectious mononucleosis. *J Infect Dis*, 190, 63-71.

- WILLIAMS, H., MCAULAY, K., MACSWEEN, K. F., GALLACHER, N. J., HIGGINS, C. D., HARRISON, N., SWERDLOW, A. J. & CRAWFORD, D. H. 2005. The immune response to primary EBV infection: a role for natural killer cells. *Br J Haematol*, 129, 266-74.
- WILSON, J. B., BELL, J. L. & LEVINE, A. J. 1996. Expression of Epstein-Barr virus nuclear antigen-1 induces B cell neoplasia in transgenic mice. *EMBO J*, 15, 3117-26.
- WOISETSCHLAEGER, M., JIN, X. W., YANDAVA, C. N., FURMANSKI, L. A., STROMINGER, J. L. & SPECK, S. H. 1991. Role for the Epstein-Barr virus nuclear antigen 2 in viral promoter switching during initial stages of infection. *Proc Natl Acad Sci U S A*, 88, 3942-6.
- WOISETSCHLAEGER, M., STROMINGER, J. L. & SPECK, S. H. 1989. Mutually exclusive use of viral promoters in Epstein-Barr virus latently infected lymphocytes. *Proc Natl Acad Sci U S A*, 86, 6498-502.
- WOISETSCHLAEGER, M., YANDAVA, C. N., FURMANSKI, L. A., STROMINGER, J. L. & SPECK, S. H. 1990. Promoter switching in Epstein-Barr virus during the initial stages of infection of B lymphocytes. *Proc Natl Acad Sci U S A*, 87, 1725-9.
- WONG, H. L., WANG, X., CHANG, R. C., JIN, D. Y., FENG, H., WANG, Q., LO, K. W., HUANG, D. P., YUEN, P. W., TAKADA, K., WONG, Y. C. & TSAO, S. W. 2005. Stable expression of EBERs in immortalized nasopharyngeal epithelial cells confers resistance to apoptotic stress. *Mol Carcinog*, 44, 92-101.
- WOODBERRY, T., SUSCOVICH, T. J., HENRY, L. M., DAVIS, J. K., FRAHM, N., WALKER, B. D., SCADDEN, D. T., WANG, F. & BRANDER, C. 2005. Differential targeting and shifts in the immunodominance of Epstein-Barr virus--specific CD8 and CD4 T cell responses during acute and persistent infection. *J Infect Dis*, 192, 1513-24.
- WRIGHTHAM, M. N., STEWART, J. P., JANJUA, N. J., PEPPER, S. D., SAMPLE, C., ROONEY, C. M. & ARRAND, J. R. 1995. Antigenic and sequence variation in the C-terminal unique domain of the Epstein-Barr virus nuclear antigen EBNA-1. *Virology*, 208, 521-30.
- WU, X., DARCE, J. R., CHANG, S. K., NOWAKOWSKI, G. S. & JELINEK, D. F. 2008. Alternative splicing regulates activation-induced cytidine deaminase

- (AID): implications for suppression of AID mutagenic activity in normal and malignant B cells. *Blood*, 112, 4675-82.
- WU, Y., MARUO, S., YAJIMA, M., KANDA, T. & TAKADA, K. 2007. Epstein-Barr virus (EBV)-encoded RNA 2 (EBER2) but not EBER1 plays a critical role in EBV-induced B-cell growth transformation. *J Virol*, 81, 11236-45.
- WU, Y. C., KIPLING, D., LEONG, H. S., MARTIN, V., ADEMOKUN, A. A. & DUNN-WALTERS, D. K. 2010. High-throughput immunoglobulin repertoire analysis distinguishes between human IgM memory and switched memory B-cell populations. *Blood*, 116, 1070-8.
- YANG, L., AOZASA, K., OSHIMI, K. & TAKADA, K. 2004. Epstein-Barr virus (EBV)-encoded RNA promotes growth of EBV-infected T cells through interleukin-9 induction. *Cancer Res*, 64, 5332-7.
- YAO, Q. Y., RICKINSON, A. B. & EPSTEIN, M. A. 1985. Oropharyngeal shedding of infectious Epstein-Barr virus in healthy virus-immune donors. A prospective study. *Chin Med J (Engl)*, 98, 191-6.
- YAO, Q. Y., ROWE, M., MARTIN, B., YOUNG, L. S. & RICKINSON, A. B. 1991. The Epstein-Barr virus carrier state: dominance of a single growth-transforming isolate in the blood and in the oropharynx of healthy virus carriers. *J Gen Virol*, 72 (Pt 7), 1579-90.
- YASUI, T., LUFTIG, M., SONI, V. & KIEFF, E. 2004. Latent infection membrane protein transmembrane FWLY is critical for intermolecular interaction, raft localization, and signaling. *Proc Natl Acad Sci U S A*, 101, 278-83.
- YATES, J., WARREN, N., REISMAN, D. & SUGDEN, B. 1984. A cis-acting element from the Epstein-Barr viral genome that permits stable replication of recombinant plasmids in latently infected cells. *Proc Natl Acad Sci U S A*, 81, 3806-10.
- YATES, J. L., WARREN, N. & SUGDEN, B. 1985. Stable replication of plasmids derived from Epstein-Barr virus in various mammalian cells. *Nature*, 313, 812-5.
- YONE, C. L., KUBE, D., KREMSNER, P. G. & LUTY, A. J. 2006. Persistent Epstein-Barr viral reactivation in young African children with a history of severe *Plasmodium falciparum* malaria. *Trans R Soc Trop Med Hyg*, 100, 669-76.

- YOUNG, L., ALFIERI, C., HENNESSY, K., EVANS, H., O'HARA, C., ANDERSON, K. C., RITZ, J., SHAPIRO, R. S., RICKINSON, A., KIEFF, E. & ET AL. 1989. Expression of Epstein-Barr virus transformation-associated genes in tissues of patients with EBV lymphoproliferative disease. *N Engl J Med*, 321, 1080-5.
- YOUNG, L. S., DAWSON, C. W., CLARK, D., RUPANI, H., BUSSON, P., TURSZ, T., JOHNSON, A. & RICKINSON, A. B. 1988. Epstein-Barr virus gene expression in nasopharyngeal carcinoma. *J Gen Virol*, 69 (Pt 5), 1051-65.
- YOUNG, L. S. & MURRAY, P. G. 2003. Epstein-Barr virus and oncogenesis: from latent genes to tumours. *Oncogene*, 22, 5108-21.
- YOUNG, L. S. & RICKINSON, A. B. 2004. Epstein-Barr virus: 40 years on. *Nat Rev Cancer*, 4, 757-68.
- ZANDVOORT, A. & TIMENS, W. 2002. The dual function of the splenic marginal zone: essential for initiation of anti-TI-2 responses but also vital in the general first-line defense against blood-borne antigens. *Clin Exp Immunol*, 130, 4-11.
- ZHAO, B. & SAMPLE, C. E. 2000. Epstein-barr virus nuclear antigen 3C activates the latent membrane protein 1 promoter in the presence of Epstein-Barr virus nuclear antigen 2 through sequences encompassing an spi-1/Spi-B binding site. *J Virol*, 74, 5151-60.
- ZHOU, C., SAXON, A. & ZHANG, K. 2003. Human activation-induced cytidine deaminase is induced by IL-4 and negatively regulated by CD45: implication of CD45 as a Janus kinase phosphatase in antibody diversification. *J Immunol*, 170, 1887-93.
- ZIMBER-STROBL, U., SUENTZENICH, K. O., LAUX, G., EICK, D., CORDIER, M., CALENDER, A., BILLAUD, M., LENOIR, G. M. & BORNKAMM, G. W. 1991. Epstein-Barr virus nuclear antigen 2 activates transcription of the terminal protein gene. *J Virol*, 65, 415-23.

Appendix

V region nomenclature (Vbase and IMGT correlation)

	<u>Vbase</u>	<u>IMGT</u>		<u>Vbase</u>	<u>IMGT</u>		<u>Vbase</u>	<u>IMGT</u>
1	1-1+	IGHV1-2*03	41	7A.10	IGHV7-40*03	81	COS-3/BHGH1+	IGHV3-30*02
2	1--17	IGHV3-9*01	42	7A.16	IGHV7-40*03	82	COS-30	IGHV3-15*02
3	1--19	IGHV3-20*01	43	7A.18	IGHV7-40*03	83	COS-4	IGHV1-3*01
4	1--36	IGHV3-23*01	44	7A.4	IGHV7-4-1*03	84	COS-5+	IGHV1-45*03
5	>1-52	IGHV3-9*01	45	7E.2	IGHV7-40*03	85	COS-6/DA-8...+	IGHV3-74*02
6	1-v/CLL-27...+	IGHV5-78*01	46	7R.9	IGHV7-40*03	86	COS-8/hv3005f3...+	IGHV3-30*04
7	12M28	IGHV1-69*10	47	8-1B+	IGHV3-66*01	87	DA-1+	IGHV1-f*02
8	15-1/HC16-3	IGHV1-2*02	48	8M27	IGHV1-69*08	88	DA-2+	IGHV1-69*07
9	1d101/DP-18+	IGHV7-40*03	49	b1..e	IGHV3-30*05	89	DA-3+	IGHV3-72*01
10	>2-2	IGHV3-43*01	50	b13../hv3019b13	IGHV3-30*19	90	DA-4+	IGHV3-49*05
11	2--20	IGHV3-43*01	51	b18../hv3019b18	IGHV3-30*06	91	DA-5+	IGHV3-h*01
12	2.9II/VH4-MC8...+	IGHV4-55*02	52	b25	IGHV3-30*10	92	DP-1/HC15-1	IGHV1-2*02
13	2.9III+	IGHV3-54*02	53	b26	IGHV3-30*12	93	DP-10/hv1051...+	IGHV1-69*01
14	22-1+	IGHV1-2*01	54	b28e	IGHV3-33*05	94	DP-11/8-2+	IGHV1-46*01
15	2M27/11M27...	IGHV1-69*12	55	b28m	IGHV3-33*01	95	DP-12	IGHV1-46*01
16	>3-17	IGHV3-20*01	56	b29e	IGHV3-30*13	96	DP-13+	IGHV7-81*01
17	>3-36	IGHV3-20*01	57	b29m	IGHV3-30*05	97	DP-14/V1-18+	IGHV1-18*01
18	3-49RBe	IGHV3-49*04	58	b30	IGHV3-33*04	98	DP-15/V1-8+	IGHV1-8*01
19	3-49RBm	IGHV3-49*03	59	b32e/b36m	IGHV3-30*14	99	DP-17/HC16-1	IGHV1-46*01
20	3d277d+	IGHV4-31*01	60	b32m	IGHV3-30*05	100	DP-19/HC15-3	IGHV1-3*01
21	3d279d+	IGHV4-61*02	61	b37	IGHV3-30*15	101	DP-2/V71-5+	IGHV1-58*01
22	>4-32	IGHV3-20*01	62	b43	IGHV3-30*16	102	DP-21/4d275a+	IGHV7-4-1*01
23	4.3	IGHV4-39*06	63	b48	IGHV3-30*17	103	DP-22/HC15-2	IGHV1-18*03
24	4.31	IGHV4-30-2*03	64	b52	IGHV3-30*11	104	DP-23/HC15-4	IGHV1-2*02
25	4.32	IGHV4-31*10	65	b54../hv3005b54	IGHV3-30*07	105	DP-24	IGHV1-f*02
26	4.34.2	IGHV4-30-4*02	66	COS-10+	IGHV3-7*01	106	DP-25/VI-3b+	IGHV1-3*01
27	4.36	IGHV4-34*09	67	COS-12+	IGHV3-d*01	107	DP-28/VH2-MC1...+	IGHV2-70*04
28	4.37	IGHV4-34*10	68	COS-13/HC16-14	IGHV3-74*02	108	DP-29/12-2+	IGHV3-72*01
29	4.38	IGHV4-59*10	69	COS-14/HC15-5	IGHV1-46*01	109	DP-3+	IGHV1-f*01
30	4.39	IGHV4-61*03	70	COS-15+	IGHV3-47*01	110	DP-30	IGHV3-72*01
31	4.42/VH4.13...	IGHV4-28*01	71	COS-16+	IGHV3-43*02	111	DP-31/V3-9P...+	IGHV3-9*01
32	4.43.4	IGHV4-55*09	72	COS-18/HC15-6	IGHV1-24*01	112	DP-32/V3-20+	IGHV3-20*01
33	4.43/VH4-MC8...	IGHV4-55*02	73	COS-19+	IGHV1-c*01	113	DP-33/V3-43+	IGHV3-43*01
34	4.44	IGHV4-34*04	74	COS-2+	IGHV3-52*02	114	DP-34/DA-10+	IGHV3-71*01
35	4.44.3	IGHV4-34*05	75	COS-20	IGHV3-15*03	115	DP-35/V3-11...+	IGHV3-11*01
36	4M28	IGHV1-69*09	76	COS-21/DA-12+	IGHV3-30*19	116	DP-36/HC16-6...	IGHV3-15*08
37	65-1/DP-20...	IGHV1-46*01	77	COS-22+	IGHV3-54*02	117	DP-37/HC16-7	IGHV3-15*03
38	65-3/COS-11...	IGHV1-2*02	78	COS-23+	IGHV3-38*02	118	DP-38/9-1...+	IGHV3-15*01
39	6M27	IGHV1-69*11	79	COS-25+	IGHV5-51*05	119	DP-39/HC16-8...	IGHV3-11*03
40	7-2+	IGHV1-45*01	80	COS-28+	IGHV3-62*01	120	DP-4+	IGHV1-45*02

Appendix

V region nomenclature (Vbase and IMGT correlation)

	<u>Vbase</u>	<u>IMGT</u>		<u>Vbase</u>	<u>IMGT</u>		<u>Vbase</u>	<u>IMGT</u>
121	DP-40/HC16-9...	IGHV3-11*03	161	DP-76+	IGHV2-5*10	201	hv4005/3d24d+	IGHV4-28*02
122	DP-41+	IGHV3-21*04	162	DP-77/WHG16+	IGHV3-21*01	202	LSG11.1	IGHV3-15*08
123	DP-42+	IGHV3-53*02	163	DP-78/3d230d...+	IGHV4-30-4*01	203	LSG12.1	IGHV3-49*02
124	DP-43/V3-52P...+	IGHV3-52*01	164	DP-79/4d154...+	IGHV4-39*01	204	LSG2.1	IGHV3-15*04
125	DP-44/HC16-10...	IGHV3-13*01	165	DP-8+	IGHV1-2*04	205	LSG3.1	IGHV3-15*05
126	DP-45	IGHV3-13*01	166	DP-81+	IGHV3-63*02	206	LSG4.1	IGHV3-15*06
127	DP-46/3d216...+	IGHV3-30-3*01	167	DP-84/HC16-12	IGHV3-11*01	207	LSG6.1	IGHV3-15*07
128	DP-47/V3-23...+	IGHV3-23*01	168	DP-85/HC16-11	IGHV3-13*01	208	LSG8.1/LSG9.1...	IGHV3-15*03
129	DP-48/13-2+	IGHV3-13*01	169	DP-86/DA-9+	IGHV3-66*03	209	MTGLa	IGHV3-66*01
130	DP-49/1.9III...+	IGHV3-30*03	170	DP-87/HC16-13	IGHV3-74*02	210	p1	IGHV3-64*05
131	DP-5/V1-24P+	IGHV1-24*01	171	DP-88/hv1051K...+	IGHV1-69*06	211	p2	IGHV3-30-3*02
132	DP-50/hv3019b9...+	IGHV3-33*01	172	DP-9/V1-27P...+	IGHV7-4-1*04	212	p6	IGHV3-33*03
133	DP-51+	IGHV3-48*02	173	E	IGHV3-9*01	213	p9e	IGHV3-30*03
134	DP-52+	IGHV3-47*02	174	F	IGHV3-20*01	214	PS421	IGHV4-34*01
135	DP-53/hvm148...+	IGHV3-74*01	175	f1m/f2e	IGHV3-64*03	215	psiRC	IGHV3-15*08
136	DP-54/V3-7...+	IGHV3-7*01	176	f2m	IGHV3-64*03	216	RR.VH1.1e	IGHV1-69*02
137	DP-55+	IGHV3-25*02	177	f3..e	IGHV3-64*04	217	RR.VH1.2	IGHV1-69*05
138	DP-56+	IGHV3-25*03	178	f7	IGHV3-30*09	218	S12-1	IGHV2-70*09
139	DP-57/hv3003...+	IGHV3-22*02	179	GL-SJ2e	IGHV3-30*08	219	S12-10	IGHV2-70*12
140	DP-58/hv3d1EG	IGHV3-48*03	180	H10	IGHV4-31*04	220	S12-12	IGHV2-5*08
141	DP-59/V3-35...+	IGHV3-35*01	181	H11Rechavi+	IGHV3-74*03	221	S12-14	IGHV2-5*09
142	DP-6+	IGHV1-NL1*01	182	H11vanEs	IGHV4-31*05	222	S12-2	IGHV2-5*04
143	DP-60/V3-6P+	IGHV3-21*02	183	H12	IGHV4-30-2*02	223	S12-4	IGHV2-5*05
144	DP-61+	IGHV3-64*02	184	H16BR+	IGHV3-52*03	224	S12-5	IGHV2-70*10
145	DP-63/VH4.21...+	IGHV4-34*01	185	H3	IGHV4-34*08	225	S12-6	IGHV2-5*06
146	DP-64/3d216d+	IGHV4-30-2*01	186	H4	IGHV4-59*03	226	S12-7	IGHV2-70*11
147	DP-65/3d75d...+	IGHV4-31*03	187	H6	IGHV4-39*05	227	S12-8	IGHV2-5*04
148	DP-66/V71-2...+	IGHV4-61*01	188	H7	IGHV4-59*04	228	S12-9/DP-27...+	IGHV2-70*01
149	DP-67/VH4-4B+	IGHV4-b*01	189	H8	IGHV4-59*05	229	Tou-VH4.21	IGHV4-34*12
150	DP-68/1.9II...+	IGHV4-28*01	190	H9	IGHV4-59*06	230	V1-12P+	IGHV1-2*02
151	DP-69/4d255...	IGHV4-4*02	191	HA2	IGHV1-3*01	231	V1-14P/DP-16+	IGHV1-46*01
152	DP-7/21-2...+	IGHV1-46*01	192	HC15-7	IGHV3-72*01	232	V1-17P+	IGHV1-NL1*01
153	DP-70/4d68...+	IGHV4-4*02	193	HC16-15/VHGL3.4	IGHV3-16*02	233	V1-40P+	IGHV7-4-1*04
154	DP-71/3d197d...+	IGHV4-59*01	194	HC16-16/DP-82	IGHV3-16*02	234	V1-45+	IGHV1-45*01
155	DP-71RBe	IGHV4-59*08	195	HG3+	IGHV1-46*02	235	V1-46+	IGHV1-46*01
156	DP-71RBm	IGHV4-59*08	196	HHG4	IGHV3-21*01	236	V11	IGHV4-4*02
157	DP-72/V4-55P...+	IGHV4-55*01	197	hv1263/3M28...	IGHV1-69*04	237	V13C	IGHV1-46*01
158	DP-73/V5-51...+	IGHV5-51*01	198	hv1f10t	IGHV1-46*01	238	V2-1+	IGHV4-39*02
159	DP-74/VH-VI...+	IGHV6-1*01	199	hv3.3+	IGHV3-11*01	239	V2-10P/COS-1+	IGHV2-10*01
160	DP-75/VI-2...+	IGHV1-2*02	200	hv3005/b1..m...+	IGHV3-30*01	240	V2-26/DP-26+	IGHV2-26*01

Appendix

V region nomenclature (Vbase and IMGT correlation)

	<u>Vbase</u>	<u>IMGT</u>		<u>Vbase</u>	<u>IMGT</u>		<u>Vbase</u>	<u>IMGT</u>
241	V201	IGHV1-NL1*01	281	V79/VIV-4b...+	IGHV4-4*01	321	VHD26	IGHV3-72*01
242	V3-13+	IGHV3-13*02	282	VF2-26/HC16-5...	IGHV2-26*01	322	VHGL1.2	IGHV1-2*02
243	V3-15+	IGHV3-15*02	283	VF3-16P/YAC-2	IGHV3-16*02	323	VHGL1.8	IGHV1-69*13
244	V3-16P+	IGHV3-16*01	284	VH15+	IGHV5-78*01	324	VHGL1.9	IGHV1-69*13
245	V3-19P/COS-26+	IGHV3-19*01	285	VH1GRR	IGHV1-18*02	325	VHGL3.5/DP-82	IGHV3-16*02
246	V3-21+	IGHV3-21*02	286	VH2-MC1a	IGHV2-70*06	326	VHGL3.6	IGHV3-16*02
247	V3-22P+	IGHV3-22*01	287	VH2-MC2b	IGHV2-70*07	327	VHGL3.7/DP-82	IGHV3-16*02
248	V3-25P+	IGHV3-25*01	288	VH2-MC2d	IGHV2-70*08	328	VHGL3.8	IGHV3-23*03
249	V3-30+	IGHV3-30*03	289	VH20	IGHV1-46*01	329	VHGL3.9	IGHV3-16*02
250	V3-32P+	IGHV3-32*01	290	VH251Shen+	IGHV5-51*02	330	VHSP/VH4.22...+	IGHV4-b*02
251	V3-33+	IGHV3-33*02	291	VH26Rabbits+	IGHV3-23*02	331	VHVBK32	IGHV5-a*04
252	V3-36P/DP-83+	IGHV3-h*01	292	VH26-3.7	IGHV3-23*03	332	VHVCW/COS-24+	IGHV5-51*03
253	V3-37P+	IGHV3-48*03	293	VH3-11	IGHV3-7*02	333	VHVJB	IGHV5-51*04
254	V3-38P+	IGHV3-38*01	294	VH3-8	IGHV3-11*03	334	VHVMW/VHVRG	IGHV5-a*03
255	V3-41P+	IGHV3-7*01	295	VH32Humphries+	IGHV5-a*02	335	VI-3+	IGHV1-3*02
256	V3-42P+	IGHV3-72*01	296	VH32Sanz+	IGHV5-a*01	336	VI-4.1b+	IGHV7-4-1*02
257	V3-44P+	IGHV3-73*01	297	VH4-MC3a	IGHV4-61*01	337	VII-5+	IGHV2-5*01
258	V3-47P+	IGHV3-47*03	298	VH4-MC4a	IGHV4-4*04	338	VII-5b+	IGHV2-5*10
259	V3-48/hv3d1...+	IGHV3-48*01	299	VH4-MC4b	IGHV4-4*05	339	VIV-4/4.35+	IGHV4-4*07
260	V3-49+	IGHV3-49*01	300	VH4-MC5a	IGHV4-34*06	340	WAD4GL	IGHV2-5*03
261	V3-50P+	IGHV3-11*01	301	VH4-MC5c	IGHV4-34*07	341	YAC-10/1d37+	IGHV7-81*01
262	V3-53+	IGHV3-53*01	302	VH4-MC7	IGHV4-28*05	342	YAC-11/COS-29+	IGHV3-74*01
263	V3-54P+	IGHV3-54*01	303	VH4-MC8b	IGHV4-55*03	343	YAC-12/V3-29P+	IGHV3-32*01
264	V3-63P+	IGHV3-63*01	304	VH4-MC8d	IGHV4-55*04	344	YAC-3+	IGHV2-70*05
265	V3-64/YAC-6+	IGHV3-64*01	305	VH4-MC8e	IGHV4-55*05	345	YAC-4+	IGHV3-49*05
266	V35/VI-2b+	IGHV1-2*01	306	VH4-MC8f	IGHV4-55*06	346	YAC-5+	IGHV3-66*02
267	V3e	IGHV3-11*03	307	VH4-MC8g	IGHV4-55*07	347	YAC-7/10M28...+	IGHV1-69*02
268	V3m	IGHV3-71*02	308	VH4-MC9a	IGHV4-31*06	348	YAC-8+	IGHV1-46*01
269	V4-31+	IGHV4-31*02	309	VH4-MC9b	IGHV4-31*07	349	YAC-9/COS-27...+	IGHV3-73*01
270	V4-34+	IGHV4-34*02	310	VH4-MC9c	IGHV4-31*08			
271	V54	IGHV1-18*03	311	VH4-MC9d	IGHV4-31*09			
272	V58	IGHV4-34*11	312	VH4-MC9e	IGHV4-30-4*03			
273	V71-1e+	IGHV3-62*01	313	VH4-MC9f	IGHV4-30-4*04			
274	V71-1m/DP-62+	IGHV3-62*01	314	VH4.12	IGHV4-61*05			
275	V71-3e+	IGHV3-62*01	315	VH4.14	IGHV4-28*04			
276	V71-3m/COS-9+	IGHV3-62*01	316	VH4.15m	IGHV4-59*01			
277	V71-4+	IGHV4-59*02	317	VH4.16	IGHV4-59*07			
278	V71-6e+	IGHV3-21*03	318	VH4/COS-7+	IGHV3-21*01			
279	V71-6m+	IGHV3-13*01	319	VH5/4d76...+	IGHV4-34*01			
280	V71-7+	IGHV7-81*01	320	VHBam+	IGHV3-72*01			

Appendix

D region nomenclature (Vbase and IMGT correlation)

	<u>Vbase</u>	<u>IMGT</u>		<u>Vbase</u>	<u>IMGT</u>		<u>Vbase</u>	<u>IMGT</u>
1	D1	IGHD2-8*02	13	D3-16	IGHD3-16*02	25	D5-24	IGHD5-24*01
2	D1-1	IGHD1-1*01	14	D3-22/D21-9	IGHD3-22*01	26	D5-5/DK4	IGHD5-5*01
3	D1-14/DM2	IGHD1-14*01	15	D3-3/DXP4	IGHD3-3*01	27	D6-13/DN1	IGHD6-13*01
4	D1-20	IGHD1-20*01	16	D3-9/DXP1...	IGHD3-9*01	28	D6-19	IGHD6-19*01
5	D1-26	IGHD1-26*01	17	D4	IGHD2-2*01	29	D6-25	IGHD6-25*01
6	D1-7/DM1	IGHD1-7*01	18	D4-11/DA1	IGHD4-11*01	30	D6-6/DN4	IGHD6-6*01
7	D2-15/D2	IGHD2-15*01	19	D4-17	IGHD4-17*01	31	D7-27/DHQ52	IGHD7-27*01
8	D2-2	IGHD2-2*02	20	D4-23	IGHD4-23*01			
9	D2-21	IGHD2-21*02	21	D4-4/DA4	IGHD4-4*01			
10	D2-8/DLR1	IGHD2-8*01	22	D4-b	IGHD2-2*03			
11	D3	IGHD2-21*01	23	D5-12/DK1	IGHD5-12*01			
12	D3-10/DXP'1	IGHD3-10*01	24	D5-18	IGHD5-18*01			

J region nomenclature (Vbase and IMGT correlation)

	<u>Vbase</u>	<u>IMGT</u>		<u>Vbase</u>	<u>IMGT</u>		<u>Vbase</u>	<u>IMGT</u>
1	JH1	IGHJ1*01	13	JHpsi1	IGHJ1P*01			
2	JH2	IGHJ2*01	14	JHpsi3	IGHJ3P*01			
3	JH3a	IGHJ3*01						
4	JH3b	IGHJ3*02						
5	JH4a	IGHJ4*01						
6	JH4b	IGHJ4*02						
7	JH4d	IGHJ4*03						
8	JH5a	IGHJ5*01						
9	JH5b	IGHJ5*02						
10	JH6a	IGHJ6*01						
11	JH6b	IGHJ6*02						
12	JH6c	IGHJ6*03						